frontiers | Research Topics

New-generation vaccines and novel vaccinal strategies against infectious diseases of livestock, wild and companion animals

Edited by
Suresh Kumar Tikoo, Raúl Manzano Román,
Christophe Chevalier, Denis Archambault and Brad Pickering

Published in
Frontiers in Immunology

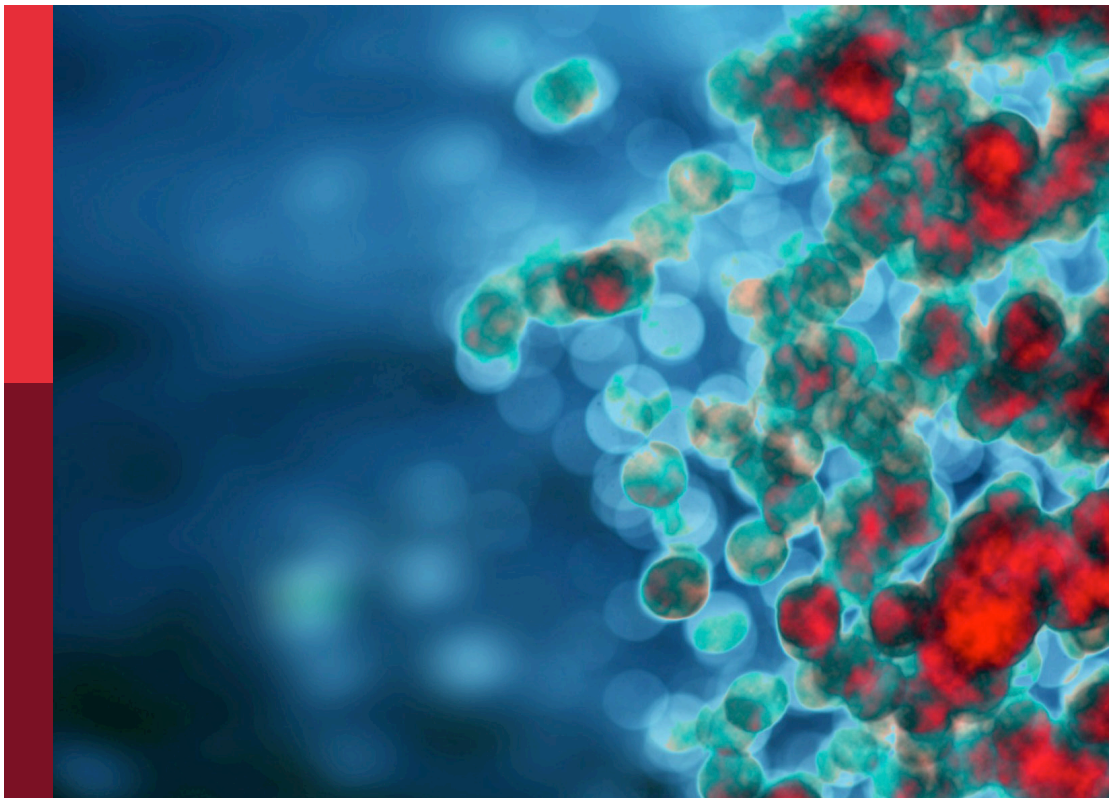

ISSN 1664-8714
ISBN 978-2-8325-3254-6
DOI 10.3389/978-2-8325-3254-6

About Frontiers

Frontiers is more than just an open access publisher of scholarly articles: it is a pioneering approach to the world of academia, radically improving the way scholarly research is managed. The grand vision of Frontiers is a world where all people have an equal opportunity to seek, share and generate knowledge. Frontiers provides immediate and permanent online open access to all its publications, but this alone is not enough to realize our grand goals.

Frontiers journal series

The Frontiers journal series is a multi-tier and interdisciplinary set of open-access, online journals, promising a paradigm shift from the current review, selection and dissemination processes in academic publishing. All Frontiers journals are driven by researchers for researchers; therefore, they constitute a service to the scholarly community. At the same time, the *Frontiers journal series* operates on a revolutionary invention, the tiered publishing system, initially addressing specific communities of scholars, and gradually climbing up to broader public understanding, thus serving the interests of the lay society, too.

Dedication to quality

Each Frontiers article is a landmark of the highest quality, thanks to genuinely collaborative interactions between authors and review editors, who include some of the world's best academicians. Research must be certified by peers before entering a stream of knowledge that may eventually reach the public - and shape society; therefore, Frontiers only applies the most rigorous and unbiased reviews. Frontiers revolutionizes research publishing by freely delivering the most outstanding research, evaluated with no bias from both the academic and social point of view. By applying the most advanced information technologies, Frontiers is catapulting scholarly publishing into a new generation.

What are Frontiers Research Topics?

Frontiers Research Topics are very popular trademarks of the *Frontiers journals series*: they are collections of at least ten articles, all centered on a particular subject. With their unique mix of varied contributions from Original Research to Review Articles, Frontiers Research Topics unify the most influential researchers, the latest key findings and historical advances in a hot research area.

Find out more on how to host your own Frontiers Research Topic or contribute to one as an author by contacting the Frontiers editorial office: frontiersin.org/about/contact

New-generation vaccines and novel vaccinal strategies against infectious diseases of livestock, wild and companion animals

Topic editors

Suresh Kumar Tikoo — University of Saskatchewan, Canada
Raúl Manzano Román — University of Salamanca, Spain
Christophe Chevalier — Institut National de recherche pour l'agriculture, l'alimentation et l'environnement (INRAE), France
Denis Archambault — Université du Québec à Montréal, Canada
Brad Pickering — National Centre for Foreign Animal Disease, Canadian Food Inspection Agency (CFIA), Canada

Citation

Tikoo, S. K., Román, R. M., Chevalier, C., Archambault, D., Pickering, B., eds. (2023). *New-generation vaccines and novel vaccinal strategies against infectious diseases of livestock, wild and companion animals*. Lausanne: Frontiers Media SA. doi: 10.3389/978-2-8325-3254-6

Table of contents

frontiers | Frontiers in Immunology

TYPE Editorial
PUBLISHED 02 August 2023
DOI 10.3389/fimmu.2023.1256363

OPEN ACCESS

EDITED AND REVIEWED BY
Santosh Dhakal,
Kansas State University, United States

*CORRESPONDENCE
Brad Pickering
bradley.pickering@inspection.gc.ca
Denis Archambault
archambault.denis@uqam.ca

RECEIVED 10 July 2023
ACCEPTED 19 July 2023
PUBLISHED 02 August 2023

CITATION
Pickering B, Manzano-Román R, Tikoo SK, Chevalier C and Archambault D (2023) Editorial: New-generation vaccines and novel vaccinal strategies against infectious diseases of livestock, wild and companion animals.
Front. Immunol. 14:1256363.
doi: 10.3389/fimmu.2023.1256363

Editorial: New-generation vaccines and novel vaccinal strategies against infectious diseases of livestock, wild and companion animals

Brad Pickering[1,2]*, Raúl Manzano-Román[3], Suresh Kumar Tikoo[4], Christophe Chevalier[5] and Denis Archambault[6]*

[1]National Centre for Foreign Animal Disease, Canadian Food Inspection Agency, Winnipeg, MB, Canada, [2]Department of Medical Microbiology and Infectious Diseases, College of Medicine, Faculty of Health Sciences, University of Manitoba, Winnipeg, MB, Canada, [3]Infectious and Tropical Diseases Group (e-INTRO), Institute of Biomedical Research of Salamanca-Research Center for Tropical Diseases at the University of Salamanca (IBSAL-CIETUS), Faculty of Pharmacy, University of Salamanca, Salamanca, Spain, [4]Vaccinology & Immunotherapeutics Program School of Public Health, and VIDO, University of Saskatchewan, Saskatoon SK, Canada, [5]INRAE, UVSQ, UMR892 VIM, Equipe Influenza Virus, Université Paris-Saclay, Jouy-en-Josas, France, [6]Department of Biological Sciences, University of Quebec at Montreal, Montreal, QC, Canada

KEYWORDS

infectious disease, fish, animals, vaccines, VLP/RNA/DNA-based vaccines, nanovaccine, immunogens/antigens, adjuvant

Editorial on the Research Topic
New-generation vaccines and novel vaccinal strategies against infectious diseases of livestock, wild and companion animals

Vaccination against infectious disease is an invaluable tool to protect humans against severe morbidity and mortality. For this reason, significant advances in human vaccines have propelled the field of vaccinology forward. Emerging and neglected diseases still pose an important challenge (1); fortunately, the evolution of technology in the vaccinology field is providing modern options to successfully prevent viral and non-viral human infections (2, 3). In contrast, the development of animal vaccines has lagged, although their importance is just as critical to the health and welfare of wild, domestic, and companion animals. In addition to the zoonotic risk it poses to public health, infectious animal diseases have accounted for more than 20 billion euros in direct losses over the last decade, and more than ten times that amount in indirect costs (4). This Research Topic "*New-generation vaccines and novel vaccinal strategies against infectious diseases of livestock, wild and companion animals*" highlights advances and innovations in animal vaccines.

Within this Research Topic, both original research and review articles are presented. The original article "Targeted delivery of oral vaccine antigens to aminopeptidase N (APN) protects pigs against pathogenic *Escherichia coli* challenge infection" describes the complications of oral subunit vaccines and the significant hurdles in overcoming the barriers of the gastrointestinal tract, limiting their development and efficacy. However, by utilizing APN-specific antibody-

antigen fusion constructs, researchers have demonstrated the induction of both mucosal and systemic immune responses in a piglet model of bacterial infection, providing a stepping stone toward the realization of an effective and protective oral subunit vaccine targeting APN. The manuscript by Souto et al. provides data to support the development of a bivalent vaccine candidate to protect fish from viral hemorrhagic septicemia (VHS) and viral encephalopathy and retinopathy (VER), major threats in aquaculture. By modifying the genome of viral hemorrhagic septicemia virus (VHSV) and introducing an expression cassette encoding the protective antigen domain of nervous necrosis virus (NNV) capsid protein, the authors successfully demonstrated the safety, immunogenicity, and protective efficacy of the recombinant VHSVs (rVHSV) in trout and sole. These findings hold promise for the development of a valuable bivalent live attenuated vaccine for commercially valuable fish species. Another study assessed the immune responses in calves to vaccines targeting *Mycobacterium avium* subspecies paratuberculosis (MAP), a cause of chronic enteritis in ruminants. Here, the authors analyzed the immune response induced by truncated MAP antigens as a fusion either on protein particles or as a soluble recombinant MAP (rMAP) fusion protein and compared this to a commercial vaccine. The rMAP fusion protein vaccine displayed the strongest immune response and showed promise in providing protective immunity against MAP infection while avoiding interference with bovine tuberculosis diagnostic tests. In another article, the authors describe a promising vaccination strategy for East Coast fever, a prevalent bovine disease in Africa caused by *Theileria parva*. In this study, using a recombinant lumpy skin disease virus (LSDV), the authors engineered virus-like particles (VLPs) containing a modified form of the *T. parva* p67 surface antigen and the bovine leukemia virus (BLV) gag gene. Studies in mice demonstrated the vaccine's immunogenicity, showing higher antibody titers in the group vaccinated with the recombinant LSDV. This encouraging progress paves the way for further investigations and potential applications of this dual vaccine candidate in cattle. Using recombinant bovine herpesvirus (BHV)-4 expressing nonstructural protein 5 (NSP5) and M fusion protein of porcine reproductive and respiratory syndrome virus (PRRSV), a study suggested that a T cell response induced in recombinant viral vector primed pigs can help in reducing PRRSV-1–associated tissue damage without reducing the viral load. A separate study explored the potential of an adenoviral-vectored Epigraph vaccine as a promising alternative to current Swine Influenza A Virus (IAV-S) vaccines. Their findings demonstrated encouraging results, with the vaccine inducing robust and durable antibody responses in vaccinated pigs, as well as significant protection against viral challenge 6 months after initial vaccination.

To complement the original research outlined above, this Research Topic also delves into important questions regarding new vaccine strategies and considerations for future approaches in detailed reviews. "Recent advances in antigen targeting to antigen-presenting cells in veterinary medicine" outlines the dynamic field of veterinary medicine, where the quest for innovative strategies to combat challenging diseases has gained considerable momentum. Notably, groundbreaking advancements in antigen targeting, with a particular focus on antigen-presenting cells such as dendritic cells, through the use of DC peptides and MHC-II, have emerged as a beacon of hope. Moreover, another review describes the complications of vaccination in wildlife animals. Prion diseases, such as chronic wasting disease (CWD), pose significant challenges due to their unique biology and potential zoonotic risks. Current efforts to manage CWD have been largely ineffective, emphasizing the need for new tools such as vaccines. Despite the hurdles of overcoming immune tolerance and vaccinating wild animals, progress has been made in identifying safe antigens and effective strategies for formulation and delivery, including oral delivery to wild cervids.

The intricate immune system of the upper reproductive tract (URT) serves a remarkable purpose: shielding against sexually transmitted pathogens while simultaneously embracing immune tolerance toward sperm and the developing fetus. The review "Immune responses in the uterine mucosa: clues for vaccine development in pigs" explores the pursuit of effective strategies, with intrauterine immunization emerging as a promising approach, aiming to elicit localized or systemic immunity that safeguards against potential threats. Finally, Type I interferons (IFNs-α/β) are vital components of the innate immune response against viral infections. However, viruses have developed clever strategies to evade the antiviral effects of IFNs, compromising the efficiency of the immune system and vaccines. Understanding these evasion mechanisms can pave the way for the development of innovative vaccines that counteract viral IFN antagonism and induce robust immune responses for enhanced protection against a wide range of pathogens. The review article "Reprogramming viral immune evasion for a rational design of next-generation vaccines for RNA viruses" explores advances in developing IFN antagonism-deficient viruses, their immune evasion, and attenuated phenotypes in natural host animal species.

This Research Topic brings a diverse selection of topics outlining advances in the field of veterinary vaccinology. The importance of generating protective vaccines against disease in animals is critical to ensuring their health and wellness, thus favoring production systems and reducing zoonotic disease risk (5).

Author contributions

BP: Writing – original draft, Writing – review & editing. RM-R: Writing – review & editing. ST: Writing – review & editing. CC: Writing – review & editing. DA: Writing – review & editing.

Acknowledgments

We would like to extend our thanks to all the authors who participated in this Research Topic and our sincere gratitude to all the reviewers and the Frontiers team for their hard work on this compilation.

Conflict of interest

The authors declare that the research was conducted in the absence of any commercial or financial relationships that could be construed as a potential conflict of interest.

Publisher's note

References

1. Vuitika L, Prates-Syed WA, Silva JDQ, Crema KP, Côrtes N, Lira A, et al. Vaccines against Emerging and neglected infectious diseases: an overview. *Vaccines (Basel)* (2022) 10(9):1385. doi: 10.3390/vaccines10091385

2. Brisse M, Vrba SM, Kirk N, Liang Y, Ly H. Emerging concepts and technologies in vaccine development. *Front Immunol* (2020) 11:583077. doi: 10.3389/fimmu.2020.583077

3. Tsakiri M, Naziris N, Demetzos C. Innovative vaccine platforms against infectious diseases: Under the scope of the COVID-19 pandemic. *Int J Pharm* (2021) 610:121212. doi: 10.1016/j.ijpharm.2021.121212

4. Barratt AS, Rich KM, Eze JI, Porphyre T, Gunn GJ, Stott AW. Framework for estimating indirect costs in animal health using time series analysis. *Front Vet Sci* (2019) 6:190. doi: 10.3389/fvets.2019.00190

5. Carpenter A, Waltenburg MA, Hall A, Kile J, Killerby M, Knust B, et al. Vaccine preventable zoonotic diseases: challenges and opportunities for public health progress. *Vaccines (Basel)* (2022) 10(7):993. doi: 10.3390/vaccines10070993

frontiers | Frontiers in Immunology

TYPE Original Research
PUBLISHED 18 January 2023
DOI 10.3389/fimmu.2022.1087015

OPEN ACCESS

EDITED BY
Brad Pickering,
National Centre for Foreign Animal Disease (NCFAD), Canada

REVIEWED BY
Maria Agallou,
Pasteur Hellenic Institute, Greece
John Bannantine,
National Animal Disease Center (USDA), United States

*CORRESPONDENCE
Sandeep K. Gupta
sandeep.gupta@agresearch.co.nz

SPECIALTY SECTION
This article was submitted to Vaccines and Molecular Therapeutics, a section of the journal Frontiers in Immunology

RECEIVED 01 November 2022
ACCEPTED 27 December 2022
PUBLISHED 18 January 2023

CITATION
Gupta SK, Wilson T, Maclean PH, Rehm BHA, Heiser A, Buddle BM and Wedlock DN (2023) *Mycobacterium avium* subsp. *paratuberculosis* antigens induce cellular immune responses in cattle without causing reactivity to tuberculin in the tuberculosis skin test. *Front. Immunol.* 13:1087015. doi: 10.3389/fimmu.2022.1087015

Mycobacterium avium subsp. *paratuberculosis* antigens induce cellular immune responses in cattle without causing reactivity to tuberculin in the tuberculosis skin test

Sandeep K. Gupta[1]*, Tania Wilson[1], Paul H. Maclean[2], Bernd H. A. Rehm[3,4], Axel Heiser[1], Bryce M. Buddle[1] and D. Neil Wedlock[1]

[1]AgResearch, Hopkirk Research Institute, Palmerston North, New Zealand, [2]AgResearch, Grasslands, Palmerston North, New Zealand, [3]Centre for Cell Factories and Biopolymers, Griffith Institute for Drug Discovery, Griffith University, Brisbane, QLD, Australia, [4]Menzies Health Institute Queensland (MHIQ), Griffith University, Gold Coast, QLD, Australia

Mycobacterium avium subspecies *paratuberculosis* (MAP) causes chronic progressive granulomatous enteritis leading to diarrhea, weight-loss, and eventual death in ruminants. Commercially available vaccine provides only partial protection against MAP infection and can interfere with the use of current diagnostic tests for bovine tuberculosis in cattle. Here, we characterized immune responses in calves to vaccines containing four truncated MAP antigens as a fusion (Ag85A$^{202-347}$-SOD$^{1-72}$-Ag85B$^{173-330}$-74F$^{1-148+669-786}$), either displayed on protein particles, or expressed as a soluble recombinant MAP (rMAP) fusion protein as well as to commercially available Silirum® vaccine. The rMAP fusion protein elicited the strongest antigen-specific antibody responses to both PPDA and recombinant antigen and strong and long-lasting T-cell immune responses to these antigens, as indicated by increased production of IFN-γ and IL-17A in antigen-stimulated whole blood cultures. The MAP fusion protein particle vaccine induced minimal antibody responses and weak IFN-γ responses but stimulated IL-17A responses to recombinant antigen. The immune response profile of Silirum® vaccine was characterized by weak antibodies and strong IFN-γ and IL-17A responses to PPDA. Transcription analysis on antigen-stimulated leukocytes from cattle vaccinated with rMAP fusion protein showed differential expression of several immune response genes and genes involved in costimulatory signaling, *TLR4*, *TLR2*, *PTX3*, *PTGS2*, *PD-L1*, *IL1B*, *IL2*, *IL6*, *IL12B*, *IL17A*, *IL22*, *IFNG*, *CD40*, and *CD86*. Moreover, the expression of several genes of immune pathways correlated with cellular immune responses in the rMAP fusion protein vaccinated group. These genes have key roles in pathways of mycobacterial immunity, including autophagy, manipulation of macrophage-mediated killing, Th17- and regulatory T cells- (Treg) mediated responses. Calves vaccinated

with either the rMAP fusion protein or MAP fusion protein particle vaccine did not induce reactivity to PPDA and PPDB in a comparative cervical skin test, whereas Silirum® induced reactivity to these tuberculins in most of the vaccinated animals. Overall, our results suggest that a combination of recombinant MAP antigens in the form of a soluble fusion protein vaccine are capable of inducing strong antigen-specific humoral and a balanced Th1/Th17-cell immune response. These findings, together with the absence of reactivity to tuberculin, suggest this subunit vaccine could provide protective immunity against intracellular MAP infection in cattle without compromising the use of current bovine tuberculosis surveillance test.

KEYWORDS

Mycobacterium avium subspecies *paratuberculosis*, Johne's disease, recombinant MAP fusion protein particle vaccine, IFN-γ, IL-17, nanostring, gene expression, tuberculin skin test

Introduction

Johne's disease (JD) or paratuberculosis is caused by *Mycobacterium avium* subspecies *paratuberculosis* (MAP), and results in chronic progressive granulomatous enteritis affecting ruminants (1, 2). Animals with clinical infection are often culled due to chronic diarrhea, gradual weight loss, and reduced milk production, resulting in considerable economic losses to the livestock industry worldwide (3, 4). The only commercially available vaccine for cattle, Silirum® (Zoetis, NSW, Australia), provides partial protection by reducing bacterial shedding in feces and the severity of JD (5). The vaccine is comprised of heat-killed MAP and interferes with the use of the tuberculin skin test for bovine tuberculosis (6, 7). A more effective vaccine against MAP infection without sensitizing animals to tuberculin is required.

New approaches of developing a vaccine against MAP infection have been proposed including, protein-based subunit vaccines, DNA vaccines and live vector vaccines (8–10). However, the level of protection induced by these types of vaccines has not exceeded the levels conferred by live attenuated or killed MAP vaccines (11). Efficient and targeted delivery of antigens to antigen-presenting cells (APCs) is crucial to induce effective protective immune responses (12–14). Advances in particulate-type vaccines hold promise for improved vaccines due to their efficient uptake by APCs (12–14). A wide range of approaches are being used for enhanced antigen delivery, including formulation of antigens in particulate adjuvants, such as liposomes and microparticles as well as particles displaying antigens such as virus-like particles, bacteria-based vectors, liposomes, immune-stimulating complexes, inclusion bodies, and protein particles (15–17).

Protein particles have several advantages for vaccine antigen delivery. The large surface area of protein particles, along with the co-delivery of multiple antigens on the same particle leads to better activation of APCs (18–20). In addition, their low production cost and ease of manufacture process have made protein particles an attractive choice for use in vaccine formulation (21–23).

Studies have demonstrated that MAP antigens including antigen complex 85A (Ag85A), Ag85B, Ag85C, and superoxide dismutase (SOD) and a polyprotein 74F produced as recombinant soluble proteins in *E. coli* (24, 25) or truncated fusion secretory proteins ($Ag85A^{202-347}$-SOD^{1-72}-$Ag85B^{173-330}$ and $74F^{1-148+669-786}$) in two Salmonella vectors (26) can induce protective immunity against MAP infection in mice. In a previous study, we demonstrated that protein particles displaying different regions of MAP antigens Ag85A, Ag85B, SOD and 74F as well as soluble form of these antigens induced strong antigen-specific T-cell immune responses and provided protection against MAP challenge in mice (27). In the current study in cattle, we investigated the ability of protein particles displaying Ag85A, SOD, Ag85B and 74F to induce antibody and cellular immune responses and compared them to the MAP antigens expressed as a single fusion soluble recombinant protein and the commercial vaccine Silirum®. We also tested the reactivity of the vaccinated animals to bovine purified protein derivatives in the intradermal tuberculin skin test.

Materials and methods

Animals

Thirty-two Holstein-Friesian cattle, 2-3 months old were sourced from a commercial farm with no history of JD. Prior to

the trial, the cattle (n = 32) tested negative for reactivity to protein purified derivative from *Mycobacterum avium* (PPDA) (Prionics, Schlieren-Zurich, Switzerland) in the whole-blood interferon-γ (IFN-γ) assay and were selected from a larger group of animals (n = 45). The cattle were grazed on pasture in a separate paddock during the trial.

Production and purification of protein particle and recombinant protein

Protein particles displaying MAP fusion antigen were produced as described previously (27). The coding sequence for truncated MAP fusion antigens ($Ag85A^{202-347}$-SOD^{1-72}-$Ag85B^{173-330}$-$74F^{1-148+669-786}$) was fused to the N-terminal of PhaC protein coding sequence in pPolyN plasmid using the strategy as described previously (27). The resultant plasmid was transformed into *E. coli* BL21 (DE3) cells (ThermoFisher Scientific, New Zealand) to produce protein particles displaying MAP fusion antigen fused to PhaC. Briefly, transformed *Escherichia coli* BL21 (DE3) cells were grown in Luria Broth supplemented with 75 μg/mL ampicillin (Sigma, St. Louis, MO) in a shaking incubator at 37°C. The cultures were induced with 0.5 mM of isopropyl β-D-1-thiogalactopyranoside (IPTG) (Sigma, St. Louis, MO) until an OD_{600} of 0.5 was reached, and the cultures were further incubated for 48 h at 25°C with shaking at 200 rpm. The cells were lysed using a microfluidizer and the lysate was centrifuged at 8,000 × g for 15 min at 4°C to purify the protein particles. The purified protein particles were treated with 70% ethanol for 1 h to kill any residual bacteria. The protein particles were washed twice in cold phosphate-buffered saline (PBS), 10 mM, pH 7.3 and re-suspended in PBS as a 20% slurry. Sterility of the protein particles was confirmed by plating an aliquot of the slurry onto LB and incubating for 2 days at 37°C.

The coding sequence for the MAP fusion antigen was cloned into the pET151 expression vector and used to produce MAP fusion protein as a recombinant protein with a 6x histidine tag in *E. coli* BL21 (DE3) cells as described previously (27). The his-tagged protein was purified using a gravity flow nickel-chelate (Ni-NTA) column (Takara Bio, CA, USA) and treated with Triton X-114 to reduce endotoxin contamination (28, 29).

Vaccine preparation

Vaccines were prepared as previously reported (27). Briefly, vaccines were prepared by formulating either PBS alone, recombinant MAP (rMAP) fusion protein or protein particles displaying MAP fusion antigen (300 μg per vaccine dose) with Emulsigen-D (20%, vol/vol, MVP Laboratories, Omaha, NE). The concentration of MAP fusion antigen in protein particles was calculated (Table 1 and Figure S1) according to a previously published method (30). Silirum® vaccine containing heat-inactivated MAP strain 316F was purchased from Zoetis, NSW, Australia.

Vaccination

Thirty-two calves were divided randomly into 4 vaccine groups of 8 animals as shown in Table 2. Calves in groups 1, 3 and 4 were vaccinated subcutaneously with 2 mL vaccine in the anterior region of the neck (week 0). Animals were re-vaccinated with the same vaccine 3 weeks after the first vaccination. Calves in group 2 were vaccinated in the same manner as the other groups, but only once with 1 mL Silirum® vaccine.

Blood samples were collected by jugular venipuncture using blood tubes with no anti-coagulant and heparinized blood tubes (Vacutainer, Becton Dickinson, NZ) before vaccination (week 0) and after vaccination at weeks 3, 6, 9, and 12 to measure antibody titers. For serology, blood was centrifuged at 2,500 × g for 10 min at room temperature and serum was aspirated and stored at −20°C. Heparinized blood samples were used to measure IFN-γ, IL-17A and gene expression in antigen-stimulated leukocytes.

Antibody ELISA

Serum IgG antibody responses to PPDA and rMAP fusion protein (referred to as recombinant antigen (RA) when used to measure immune responses) were measured by ELISA using a previously described method with some modifications (27). Briefly, Microlon high-binding capacity 96 well ELISA plates (Greiner Bio-One, Germany) were coated overnight at 4°C with 50 μL/well of PPDA or rMAP fusion protein (4 μg/mL) in 50 mM sodium carbonate buffer, pH 9.6. The following day, the plates were washed with PBS + Tween-20 (0.5%) (PBST) and blocked for 1 h at room temperature with 100 μL/well of blocking buffer (PBS containing 1% (w/v) casein). After incubation, the plates were washed with PBST, and 2-fold serial dilutions of sera (range 1:200 – 1:204,800 diluted in blocking buffer) were added (50 μL/well). The pre-vaccination (week 0) and post-vaccination sera (week 3, 6, 9, and 12) of an animal were tested on the same plate. The plates were incubated for 1 h at room temperature, washed with PBST, then incubated for 1 h at room temperature with HRP-conjugated donkey anti-bovine IgG (BioRad, CA, USA) diluted at 1:6,000 in blocking buffer (50 μL/well). Following washing with PBST, 50 μL/well of 3,3′,5,5′-Tetramethylbenzidine (TMB) substrate (BD Biosciences) was added, and the plates incubated for 20 min at room temperature in the dark. The reactions were stopped with the addition of 50 μL/well of 0.5 M H_2SO_4 and the absorbance read at 450 nm using a microplate reader (VERSAmax, Molecular Devices). For each animal, the antibody titer of

TABLE 1 Concentration of MAP fusion antigen in protein particles.

	Amount of PhaC-MAP antigen fusion/ wet particles (ng protein/mg beads)	µg particles loaded	ng MAP fusion protein per µg particles	total MAP fusion protein weight MW	MAP fusion protein component MW	MW ratio fusion protein to PhaC	ng MAP fusion protein per µg particles	µg MAP fusion protein per mg particles (average)	mg of particles required for 300 µg antigen
PhaC-MAP fusion antigen	219	15	14.60	130	65.7	0.51	7.38	5.96	50.31
	96	7.5	12.80				6.47		
	26	3.25	8.00				4.04		

The concentration of MAP fusion antigen on protein particles was calculated by densitometry analysis on purified PhaC-MAP fusion protein particles separated on SDS-PAGE (Figure S1). Bovine serum albumin was used as a standard to quantify amount of MAP fusion antigen.

each post-vaccination serum was calculated from the reciprocal of the highest dilution showing an OD_{450} value greater than the OD_{450} value of a 1:200 dilution of pre-vaccination serum.

IFN-γ and IL-17 assays

Heparinized blood samples were obtained from the calves and within 6 h of collection, aliquots (1 mL) were dispersed into wells of a 48-well plate and either PBS (negative control), pokeweed mitogen (positive control, 2.5 µg/mL final concentration), PPDA (24 µg/mL final concentration; Prionics, Schlieren-Zurich, Switzerland), or RA (10 µg/mL final concentration) was added for IFN-γ and IL-17A whole blood assays. After incubation at 37°C for 24 h, the plasma supernatants were harvested (400 × g for 10 min). IFN-γ levels were measured using a sandwich ELISA kit (Prionics, Thermo Fisher Scientific) and bovine IFN-γ standard (Kingfisher Biotech, St. Paul, USA) was titrated to calculate the concentration of IFN-γ (pg/mL) in each sample and results were expressed using the standard curve.

An ELISA for bovine-specific IL-17A was developed and optimized in-house using capture, detection antibodies and recombinant bovine IL-17A as standards (Kingfisher Biotech, MN, USA) according to the manufacturer's instructions. The optimized conditions were used to measure IL-17A levels in plasmas from antigen-stimulated whole blood of the animals prior to vaccination (week 0) and at weeks 3, 6, 9, and 12 post-vaccination. Briefly, MaxiSorp high protein-binding capacity 96 well ELISA plates (Nunc™) were coated overnight at room temperature with 50 µL/well of capture antibody (2 µg/mL protein) in PBS. The plates were washed with PBST and blocked for 1 h with 100 µL/well of blocking buffer (PBS containing 4% (w/v) BSA) at 37°C with shaking. Following blocking, the plates were washed again with PBST. Bovine IL-17A standards and undiluted plasma samples (50 µL/well) were added to the plates and the plates were incubated for 1 h at 37°C. Following the incubation, the plates were washed with PBST and incubated for 1 h at 37°C with biotin-conjugated detection antibody (Kingfisher Biotech, MN, USA) diluted at 1:4,000 in blocking buffer (50 µL/well). After incubation, the plates were washed with PBST, and then incubated for 30 min at 37°C with streptavidin-HRP (Kingfisher Biotech, MN, USA) diluted at 1:500 in blocking buffer (50 µL/well). After the incubation, the plates were washed with PBST, and 50 µL/well of TMB substrate (BD Biosciences) was added, and the plates were incubated 20 min at room temperature in the dark. The reactions were stopped by the addition of 50 µL/well of 0.5 M H_2SO_4 and absorbance read at 450 nm using a microplate reader (VERSAmax, Molecular Devices). The concentration of IL-17A (pg/mL) for each sample was calculated from the standard curve.

TABLE 2 Vaccine groups.

Groups	Antigens	Adjuvant
1	PBS	Emulsigen-D
2	Silirum®	–
3	Recombinant MAP fusion protein	Emulsigen-D
4	Protein particle displaying MAP fusion protein	Emulsigen-D

Measurement of gene expression in antigen-stimulated leukocytes

Leukocytes were prepared from heparinized blood samples using a method previously described with some modifications (31). Briefly, 3 mL of blood was transferred into a 50 mL falcon tube and 13.5 mL of chilled water was added (4.5 mL/ml of blood) to lyse the red blood cells. The tubes were quickly mixed for 15 sec, and 1.5 mL of 10X DPBS (500 µL/mL of blood) (Thermo Fisher Scientific, New Zealand) was added to equilibrate the sample. Subsequently, the cells were centrifuged at 250 × g for 10 min at 4°C, washed with PBS (10 mM, pH-7.3) and re-suspended in 0.5 mL of RPMI-1640 containing 10% fetal bovine serum (Thermo Fisher Scientific, New Zealand). Cell

number and viability was measured by trypan blue exclusion method using TC20 cell counter (BioRad). A total of $2x10^6$ cells were added to each well in a U-bottom 96-well tissue culture plate (Nunc™) and stimulated with either media alone (un-stimulated), PPDA (24 μg/mL) or RA (10 μg/mL) at 37°C for 24 h. After incubation, plates were centrifuged in a swing out rotor at 350 × g for 10 min at room temperature. The supernatant was removed and 150 μL of a commercial lysis buffer for RNA preparation was added (RLT buffer, Qiagen, Hilden, Germany) to the samples and the plates were stored at –80°C until RNA isolation. Total RNA was isolated from the samples using RNeasy kit according to the manufacturer's instructions (Qiagen, Hilden, Germany).

nCounter analysis of gene expression

Gene expression analysis was performed using the nCounter Analysis System (Nanostring Technologies Inc., Seattle, WA) as previously described (32). The use of NanoString technology enables RNA expression analysis from either purified RNA or directly from cell lysates without further RNA purification or amplification (33). The method uses molecular barcodes on gene-sequence-specific probes and single molecule imaging to count RNA copies (34). RNA was prepared from the antigen-stimulated leukocytes before vaccination (week 0) and after vaccination (weeks 6, 9 and 12) and analyzed using PlexSet-24 consisting of probes specific to 21 immune response genes and 3 reference genes (Table 3).

A titration was performed using bovine-specific ProbeSets (Supplementary Data Sheet) and a PlexSet-24 titration kit according to the manufacturer's instructions (NanoString Technologies) to optimize the input RNA concentration of each sample in the final PlexSet-24 analyses (data not shown). As a result, a total of 1.1 μg of purified RNA was used to measure the expression of various immune response genes (Table 2) using bovine specific PlexSet-24.

For analysis, background subtraction was performed by subtracting the geometric mean of 8 internal negative controls from each sample. Positive control normalization was performed using the geometric mean of 6 internal positive controls to compute the normalization factor. The normalization factor of all samples was inside the 0.65 to 1.67 range.

The geometric mean of counts of the three reference genes included in the ProbeSet was used for gene normalization. The average of these geometric means across all lanes was used as the reference against which each lane is normalized. A normalization factor was then calculated for each of the lanes based on the geometric mean of counts for the reference genes in each lane relative to the average geometric mean of counts for the reference genes across all lanes. This normalization factor was then used to adjust the counts for each gene target and controls in the associated lane. The normalization factor of all samples was inside the 0.5 to 21 range.

Fold-change was calculated by dividing normalized RNA counts for each gene of antigen-stimulated blood leukocytes over media alone stimulated cells at weeks 0, 6, 9, and 12. Ratios were calculated for each gene at weeks 6, 9, and 12 by dividing fold-change (antigen stimulation/media alone) values at weeks 6, 9, and 12 over fold-change expression at week 0. The data were log2 transformed prior to statistical analysis.

Intradermal tuberculin test

A comparative cervical tuberculin intradermal test was conducted at week 12. For this test, the cattle were inoculated intradermally with 0.1 mL volumes containing either 2,500 IU of PPDA or 5,000 IU of purified protein derivative from *Mycobacterium bovis* (PPDB) (AsureQuality, Upper Hutt, New Zealand) at separate sides on the right side of the neck. The skin fold thicknesses were measured with Calipers prior to and 72 h after injection of the PPDs. Positive skin test responses to PPD were defined as increases in skin thickness prior to injection and 3 days later of ≥ 2 mm and ≥ 4 mm and the differential increase, PPDB-PPDA of ≥ 2 mm and ≥ 4 mm.

Statistical analysis

The statistical analysis of fold-change of antibodies, cytokine responses and gene expression values was performed using R software version 4.1.1 (35). For each gene, permutation ANOVAs as implemented in the lmPerm R package version 2.1.0 (36) were used to evaluate the significance of timepoint and vaccine. *Post-hoc* testing and calculation of predicted means and 95% confidence intervals were calculated using the predictmeans R package version 1.0.6 (37). P-values < 0.05 were considered statistically significant. The "pca" function within the mixOmics R package version 6.12.1 (38) was used to perform PCA on the gene expression values. The mixomics R package was also used to perform canonical correlation analysis with the shrinkage method to account for a large amount of co-correlation between the gene expression and immunology data. The canonical correlation analysis results, along with Pearson correlations were displayed in a network plot were prepared using Cytoscape version 3.8.2 (39).

TABLE 3 List of genes analyzed by nCounter.

Accession Number	Target Gene	Possible function
NM_174093.1:330	*IL1B*	Pro-inflammatory cytokines
NM_173923.2:319	*IL6*	
NM_174356.1:874	*IL12B*	
NM_174445.2:1746	*PTGS2/Cox-2*	
NM_174086.1:502	*IFNG*	Adaptive immunity cytokines
NM_001008412.1:147	*IL17A*	
NM_001098379.1	*IL22*	
NM_001166068.1:961	*TGFB*	
NM_180997.2:217	*IL2*	Anti-inflammatory cytokines
NM_173921.2:335	*IL4*	
NM_174088.1:144	*IL10*	
NM_001076259.1:718	*PTX3*	Innate receptors
NM_174197.2:1497	*TLR2*	
NM_174198.6:2640	*TLR4*	
NM_001105611.2:414	*CD40*	T-cell activation markers
NM_174624.2:608	*CD40LG*	
NM_001038017.2:719	*CD86*	
NM_174297.1:35	*CTLA4*	
NM_001039957.1:1178	*ITGAM*	
NM_001083506.1:320	*PDCD1*	
NM_001163412.1:393	*PDL1*	
NM_001083436.1:1814	*GUSB*	Reference genes
NM_001077866.1:553	*RPL15*	
NM_174814.2:146	*YWHAZ*	

Results

Recombinant MAP fusion protein induces long lasting antibody responses

Serum antibody responses to RA and PPDA were measured in the vaccinated animals. Antibody levels to RA and PPDA were significantly higher in the animals vaccinated with rMAP fusion protein at 3, 6, 9 and 12 weeks compared to animals vaccinated with PBS, Silirum® or the protein particles ($P < 0.05$, Figure 1). The strong antibody responses induced by the rMAP fusion protein vaccine were long-lasting with peak responses at week 6 and antibody responses still higher than the other groups at week 12 ($P < 0.05$). In comparison, calves vaccinated with the protein particles or given Silirum® produced no significant antibody responses to both RA and PPDA.

Recombinant MAP fusion protein induces cell-mediated immune responses

The ability of the vaccines to induce T-cell immune responses was evaluated by measuring antigen-specific IFN-γ and IL-17A responses in the vaccinated animals. Calves vaccinated with rMAP fusion protein vaccine elicited antigen-specific cell-mediated immune responses as indicated by increases in IFN-γ levels in blood stimulated *in vitro* with PPDA or RA (Figures 2A, B). These responses were significantly higher compared to the PBS vaccinated animals after vaccination at weeks 3, 6, 9 and 12 ($P < 0.05$, Figures 2A, B). IL-17A cytokine levels were also increased significantly at weeks 3, 6, 9, and 12 after stimulation with RA and only at week 9 with PPDA stimulation in the blood of the rMAP fusion protein vaccinated animals compared to the PBS group. In comparison,

10.3389/fimmu.2022.1087015

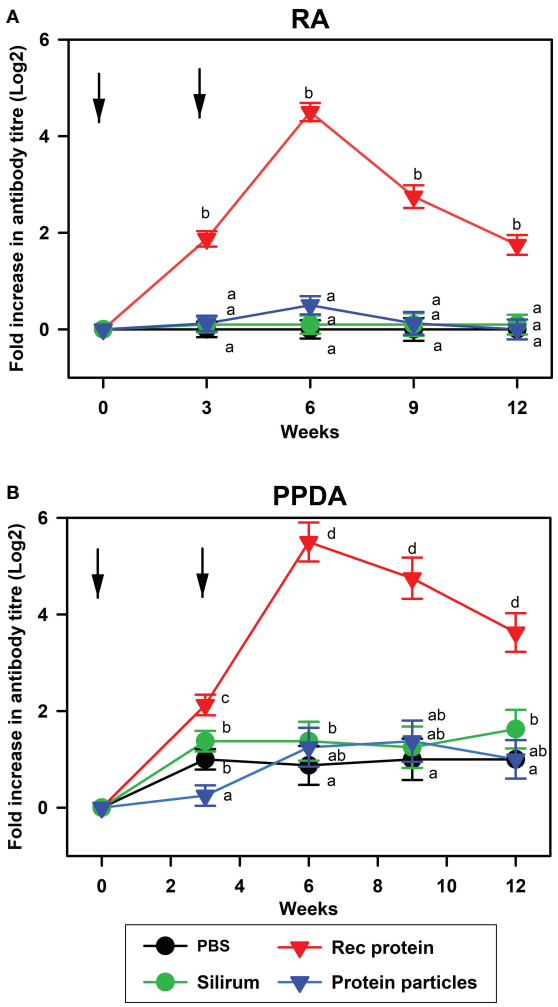

FIGURE 1
Antibody responses to recombinant antigen and PPDA in different vaccine groups. Mean serum antibody responses to **(A)**, recombinant antigen (RA); and **(B)**, PPDA in calves vaccinated with PBS, Silirum®, rMAP fusion protein (Rec protein) and protein particles displaying MAP fusion protein (Protein particles) vaccines at weeks 0 and 3. Timing of vaccinations is indicated by arrows. Antibody titers were measured in sera before vaccination and after vaccination at weeks 3, 6, 9, and 12 using ELISA. Significance differences ($P < 0.05$) in antibody responses between different vaccine groups are indicated by different letters, while the same letter indicates no significant differences.

the MAP fusion protein particle vaccine induced weaker responses with significant increase in IL-17A levels in response to RA observed at weeks 3, 6 and 12 compared to the PBS group ($P < 0.05$, Figure 2B). There were no differences in IFN-γ levels between the MAP fusion protein particle group and the PBS group. The animals vaccinated with Silirum® vaccine also produced significantly higher levels of IFN-γ and IL-17A at weeks 3-12 in response to PPDA but not to RA compared to the PBS group ($P < 0.05$, Figures 2A, B). The range of IFN-γ levels in the pokeweed mitogen stimulated whole blood cells was 1093 pg/mL to 10767 pg/mL indicating responsiveness of the cells (data not shown).

Recombinant MAP fusion protein induces expression of key genes of various immune pathways

The ability of the vaccines to stimulate various immune pathways was evaluated in antigen-stimulated leukocytes prepared from blood of the immunized animals. Purified leukocytes were stimulated *in-vitro* with PPDA or RA for 24 h and expression of immune response genes was measured using NanoString.

Transcription analysis revealed that several immune response genes were significantly upregulated upon re-stimulation of leukocytes from calves vaccinated with rMAP fusion protein compared to animals administered PBS alone. Genes for *TLR4*, *TLR2*, *PTX3*, *PTGS2*, *PDL1*, *IL22*, *IL2*, *IL1B*, *IL17A*, *IL12B*, *IFNG*, *CD40* were upregulated after stimulation with RA at weeks 6, 9 and 12; IL6 at weeks 9 and 12; and *PDCD1* expression at week 6 (Figure 3). Expression of *CD86* was downregulated at weeks 6, 9, and 12 and *ITGAM* expression was downregulated at weeks 12. Blood leukocytes stimulated with PPDA showed upregulation of *IL22* and *IFNG* genes at weeks 6, 9 and 12; *ITGAM* at weeks 6 and 9; *PDCD1* at week 6; and *CD40LG* at week 12 (Figure 3). Pathway analysis revealed that several of these genes participate in T-cell receptor and IL-17A signaling pathways (Figures S2, S3).

In the animals vaccinated with the MAP fusion protein particle vaccine, the expression of only a few genes were found to be modulated in antigen-stimulated leukocytes. The expression of *IL12B* and *PTX3* were increased at week 9 in RA and PPDA stimulated leukocytes, respectively, while *IL10* was upregulated at 12 weeks after PPDA stimulation compared to the PBS group.

In the Silirum®-vaccinated animals, expression of *PDL1*, *PDCD1*, *IFNG* and *TGFb*, *PTGS2*, *PDL1*, *IL22*, *IL2*, *IL12B*, *IFNG*, *CD40LG*, and *CD40* were upregulated in blood leukocytes stimulated with PPDA at weeks 6 and 9, respectively compared to the PBS group. Leukocytes from these animals stimulated with RA had increases in expression of *TLR4*, *TLR2*, *PDL1*, *PDCD1*, *CD40* and *IL22* genes at weeks 6 and 9, respectively. No samples were analyzed for gene expression at week 12 due to loss of mRNA during sample preparation.

Correlation between gene expression and cellular immune responses in recombinant MAP vaccinated animals

We performed network plot analysis to identify correlations between expression of 21 genes in RA-stimulated leukocytes and antigen-specific immune responses (antibody, IFN-γ and IL-17A cytokines) in cattle vaccinated with rMAP fusion protein at various

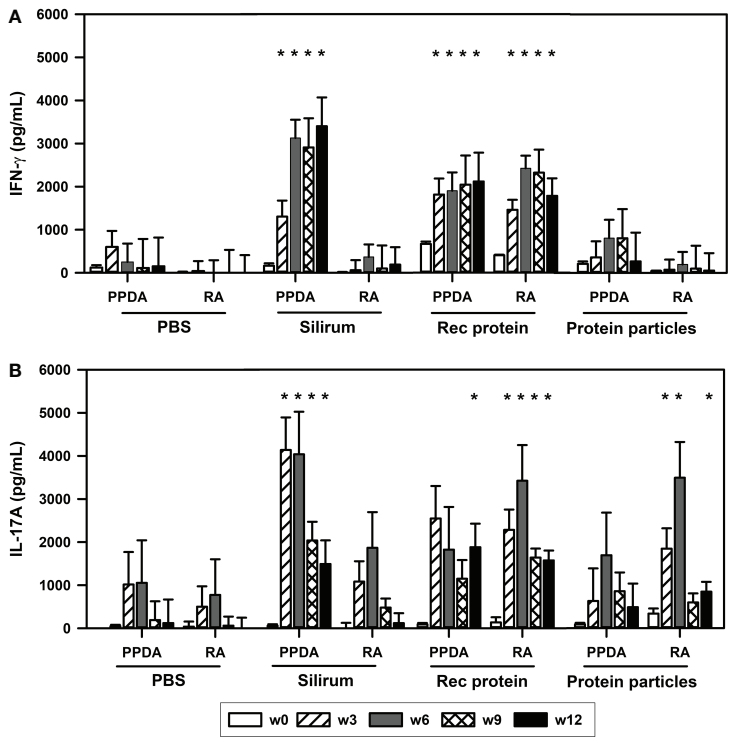

FIGURE 2
Antigen-specific cell-mediated immune responses in the vaccinated animals. Mean (+ SE) **(A)**, IFN-γ and **(B)**, IL-17A responses in the animals vaccinated with PBS; Silirum®; recombinant MAP fusion protein (Rec protein); and protein particles displaying MAP fusion protein (Protein particles). Whole blood from the vaccinated calves at weeks 0, 3, 6, 9 and 12 were stimulated *in vitro* with PBS, PPDA, or RA. IFN-γ and IL-17 levels were measured by ELISA. Results for IFN-γ and IL-17A cytokine levels are presented as difference obtained by subtracting values of PBS-from PPDA- or RA-induced IFN-γ and IL-17A cytokines. Significance indicated as *, $P < 0.05$ compared with the respective treatment in the PBS vaccinated animals.

time points (weeks 0, 6, 9 and 12). The analysis revealed expression of several genes involved in various immune pathways were highly correlated with humoral- and cell-mediated immune responses (Cor > 0.6) (Figure 4). For example, expression of pro-inflammatory cytokines and innate immune receptors genes including *IL1B*, *IL12B*, *PTGS2*, *TLR4*, and *PTX3* strongly correlated with antigen-specific cellular responses. In addition, T-cell activation and adaptive immunity cytokines genes including *PDL1*, *CD40*, *IL17A*, *IFNG*, and *IL22* highly correlated with antibody responses, IFN-γ and IL-17A cytokines. A few T-cell activation markers including *ITGAM*, *PDCD1*, and *CD86* were negatively correlated with RA-specific antibody, IFN-γ and IL-17A cytokines. Positive and negative correlations between the genes of various pathways were also observed as indicated by light red and light blue lines, respectively (Figure 4).

Recombinant MAP fusion protein does not compromise intradermal skin tests

A comparative cervical skin test was performed in the vaccinated animals to determine if vaccination of calves with the rMAP fusion protein or MAP fusion protein particle vaccines interfered with bovine tuberculosis diagnostic skin tests. Vaccination of calves with either the rMAP fusion protein or MAP fusion protein particle vaccine produced negative responses for both PPDB and PPDB-PPDA as indicated by no significant increase in skin thickness (Figure 5). In contrast, seven Silirum®-vaccinated calves were positive for PPDB with increase in skin thickness of ≥ 2 mm and six animals had increases of ≥ 4 mm (Figure 5). All these calves had a response to PPDA of 3 ≥mm. The differential skin test responses, PPDB-PPDA for the Silirum® group were all negative values (data not shown). Two animals given PBS showed weak reactivity (2- and 3-mm increase in skin thickness) to PPDA, likely reflecting exposure of calves to environment mycobacteria during the time course of the trial.

Discussion

Johne's disease (JD) is a severe intestinal disease of ruminants with considerable economic impacts. The currently available commercial vaccine Silirum® can offer some degree of

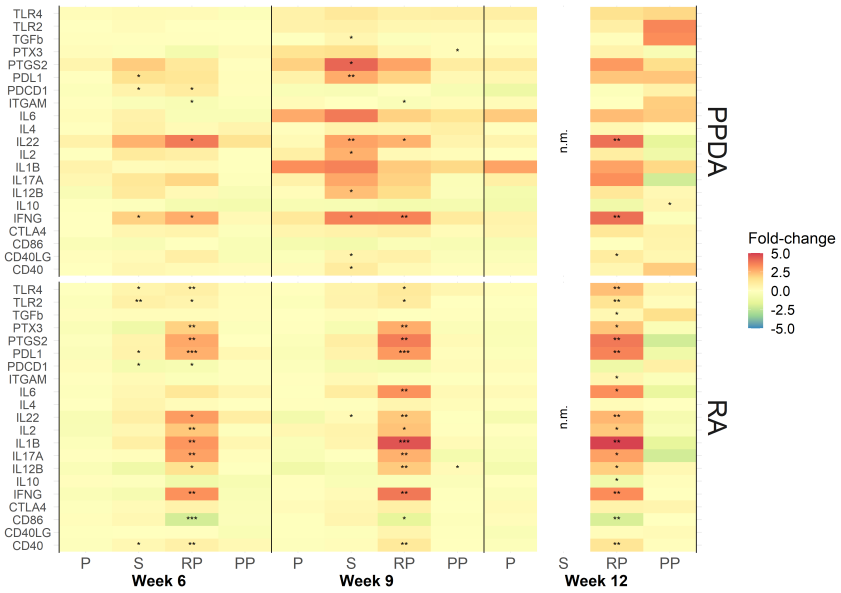

FIGURE 3
Expression of immune responsive genes in animal vaccinated with PBS (P), Silirum® (S), recombinant MAP protein (RP), and MAP fusion protein particles (PP). Leukocytes were stimulated *in vitro* with either media alone, PPDA or RA at a final concentration of 10 μg/mL for 24 h. Results are presented as ratios of fold-change (antigen stimulation/media alone) for each gene at weeks 6, 9 and 12 over expression at week 0. The data was log2 transformed for statistical analysis and statistical significance was calculated by comparing ratios of antigen stimulation/media alone of all the vaccine groups and week 0 expression of the PBS control group. Statistical significance was calculated compared with the PBS group (* = $P < 0.05$; ** = $P < 0.01$; *** = $P < 0.001$). Note: No responses were measured in Silirum®-vaccinated animals at week 12 due to RNA being lost during sample preparation.

protection to cattle against MAP infection by reducing MAP shedding. But the vaccine interferes with surveillance of bovine tuberculosis by causing reactivity to the tuberculin skin test. In the current study, the immunogenicity of a recombinant MAP (rMAP) fusion protein and a protein particle vaccine displaying the rMAP fusion protein was determined in cattle and compared with immune responses induced by Silirum®. Both the rMAP fusion protein and the protein particle vaccines induced antigen-specific T-cell immune responses in cattle, but responses to the particle vaccine were weaker than those generated by the rMAP fusion protein vaccine. These results in cattle did not confirm our previous results in mice, which demonstrated that the protein particle vaccine induced comparable Th1/Th17 cell-mediated immune responses to the rMAP fusion protein vaccine (27). In addition, only the rMAP fusion protein vaccine in the current study induced significant antibody responses to RA and PPDA. In contrast to vaccination with Silirum®, vaccination with rMAP fusion protein and protein particles did not compromise the bovine tuberculosis skin test.

The classical Th1 cell-mediated cytokine IFN-γ was significantly upregulated (both at the protein and mRNA levels) in blood cultures from the rMAP fusion protein group after stimulation with PPDA and RA. IFN-γ secreted by T cells (CD4+ and γδ) leads to the activation of antimycobacterial pathways and inhibiting intracellular bacterial growth (40–42). In addition, IL-12 is critical for induction of IFN-γ mediated Th1 protective immune responses (43, 44). In the current study, expression of genes of both these cytokines (*IL12* and *IFNG*) was also upregulated in the rMAP fusion protein vaccinated animals. While IFN-γ has long been considered as a hallmark cytokine in providing protection against mycobacterial intracellular pathogens (45), its role as a sole cytokine in providing protection against mycobacterial pathogens has been challenged (46, 47). Recent evidence indicates that Th17-mediated immune responses also contribute to the early inflammatory responses to mycobacterial infection, thus potentially play a crucial role in providing protective immunity against *M. tuberculosis* and MAP (46, 48–50). The current results demonstrated that antigen-specific IL-17A levels (both at the protein and mRNA levels) were significantly upregulated in animals vaccinated with the rMAP fusion protein. These responses were broadly comparable to responses induced by Silirum® vaccine. These data indicate the ability of rMAP fusion protein vaccine to stimulate both Th1- and Th17-mediated immune responses in cattle, which could provide protective immunity against MAP infection in ruminants.

A balance of Th1/Th17 responses is thought to be important in inducing protective immunity against mycobacteria (51–53). Transcription analysis using NanoString nCounter demonstrated that the expression of several Th1/Th17 immune response genes was upregulated in the vaccinated

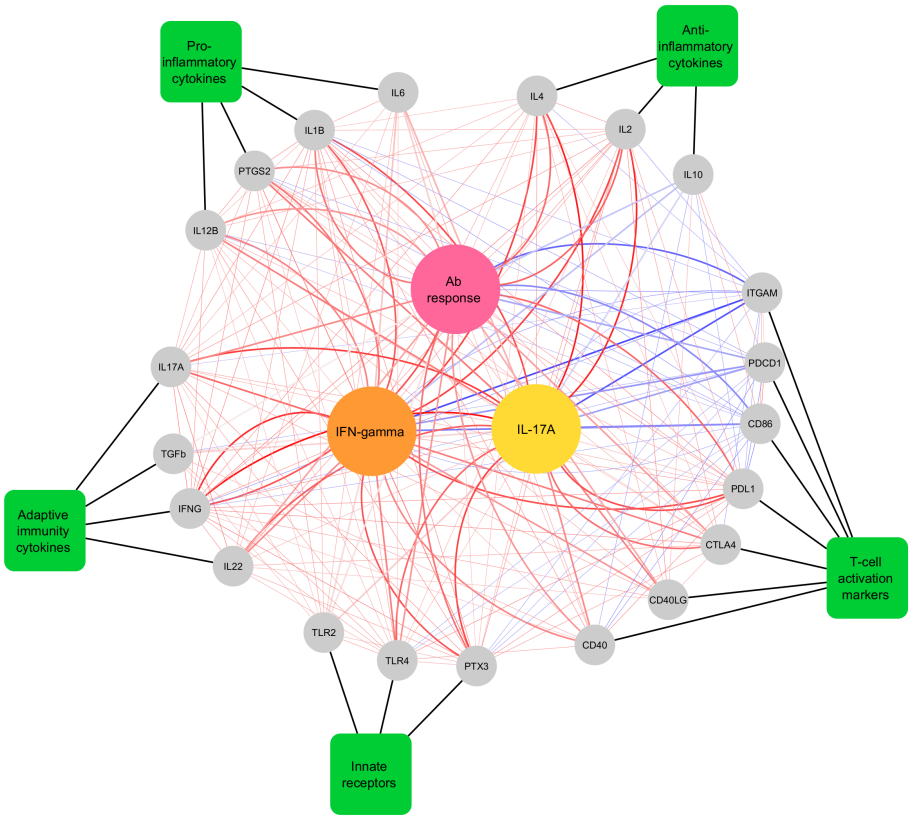

FIGURE 4
Network plot showing Pearson correlations and canonical correlations between differentially expressed genes, antibody levels and T cell-mediated cytokine responses in cattle vaccinated with rMAP fusion protein at weeks 0, 6, 9 and 12. Genes are displayed as grey circles, gene categories are displayed as green rectangles and the three central circles colored pink, yellow and orange are, antibody, IL-17A (pg/mL), and IFN-γ (pg/mL) responses to RA, respectively. Thick black lines indicate the functional group that the genes belong to. Thick red and blue lines indicate canonical correlations above |0.6| and thin red lines indicate significant ($P < 0.05$) Pearson correlations between genes. Red lines indicate positive associations and correlations, while blue lines indicate negative associations and correlations. Darker line colors indicate stronger associations and correlations.

animals. The results demonstrated that key regulators of Th17 immune responses, including *IL1B*, *IL6*, *IL12B*, *IL17A*, *IL22*, and *TGFB* were upregulated in the rMAP fusion protein vaccine group. Cytokines including IL-1β, IL-6 and TGF-β1 are secreted by the macrophages and/or APCs after antigen stimulation (54, 55), resulting in IL-17 and IL-22 production, which then leads to differentiation of naïve T cell to Th17-like cells (56, 57). In addition, IL-1β and IL-6 cytokines are thought to act in a positive feedback loop on the γδ T cells and on differentiating Th17 cells (57). In our study, increased mRNA levels of *IL1B*, *IL22* (week 6, 9 and 12) and *IL6* (week 9 and 12) along with increased expression of IL-17A (both protein and mRNA) were observed in the rMAP fusion protein vaccinated animals. Although specific cell types were not characterized in the current study, increased expression of these cytokines as well as *CD40*, a co-stimulatory protein expressed on dendritic cells (DCs) with an essential role in APC activation and Th17 cells differentiation (27, 58, 59), clearly suggest that the rMAP fusion protein vaccine induced Th17 cell-mediated responses in the vaccinated animals. In addition, the expression of IFN-γ (both protein and mRNA) was increased in the rMAP fusion protein vaccinated animals. IFN-γ along with other Th1 cytokines such as IL-1β, IL-2, IL-12 and TNF-α are thought to orchestrate complex immune responses during mycobacterial infection to mount Th1/Th17 balanced immune responses (52, 53). Significantly high levels of mRNA of these cytokines were produced in the rMAP fusion protein vaccinated animals upon stimulation with RA, indicating that balanced Th1/Th17 responses were induced in these animals.

The underlying molecular mechanisms of the host-pathogen interactions are complex in mycobacterial infection. Studies indicate that autophagy, a cell-autonomous host defense against intracellular pathogen, is one of the mechanisms in the host defense against intracellular mycobacterial infection (60, 61). Immune cells including monocytes, macrophages, and DCs recognize mycobacterial molecules *via* TLRs and NLRs to produce cytokines such as IL-1β, IL-12p70, and TNF-α (62–65) and are important regulators of autophagy-mediated host

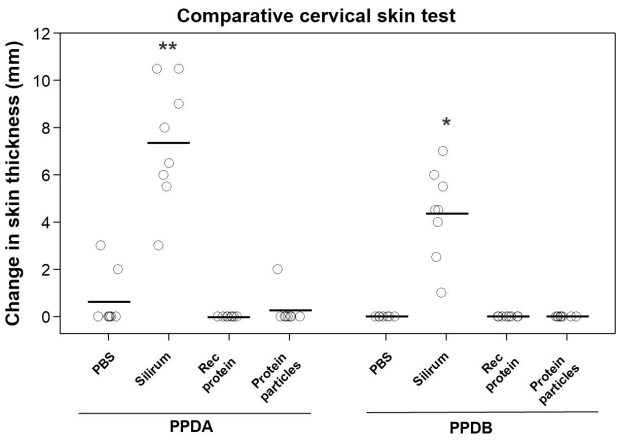

FIGURE 5
Comparative cervical tuberculin skin test in vaccinated animals. Skin thickness was measured before and at 72 h after injecting 0.1 mL of PPDA or PPDB intradermally at the side of the neck. Mean is represented by '—' for each group. Significance is represented by between different groups. Statistical significance was calculated compared with the PBS control group (* = $P < 0.05$; ** = $P < 0.01$).

defense against mycobacterial pathogens (66, 67). Therefore, it has been emphasized that vaccines activating autophagy in immune cells will elicit robust innate as well as adaptive immune responses to effectively clear intracellular mycobacterial infection (68–70). There was increased mRNA expression of some of the cytokine genes that participate in autophagy including *IL1B*, *IL6* and *IL12B* in both RA and PPDA re-stimulated leukocytes from both the rMAP fusion protein and Silirum® vaccinated animals. These findings provide some indirect evidence for activation of the autophagy pathway, which could be TLR-dependent as indicated by the increased expression of *TLR2* and *TLR4* in the vaccinated animals. TLR-mediated stimulation and maturation of APCs is essential for T-cell expansion (71) and their role in bridging innate and adaptive immune responses in mycobacterial infection is very well documented (72–74). Studies have demonstrated that mycobacterial antigens activate immune cells including APCs and DCs in TLR2- (63, 75–77) and TLR4-dependent manner (78) to elicit strong Th1 immune responses. Increased expression of *TLR2* and *TLR4* was observed in the animals vaccinated with the rMAP fusion protein and the MAP fusion protein particle vaccine, suggesting potential activation of TLR-signaling in these animals. Further studies will be needed to investigate if the rMAP fusion protein vaccine can provide protective immunity against MAP infection in ruminants.

Additionally, mycobacterial intracellular pathogens can manipulate cell death pathways in infected macrophages, which is another virulence mechanisms of mycobacterial defense against the host (79). Programmed death-1 (*PD-1*) receptor and its ligand, programmed death-ligand 1 (*PDL1*), which is expressed on DCs and APCs, play crucial roles in T cell receptor signaling (80, 81). However, the role of PD-1/PDL1 mechanism in mycobacterial immunity is controversial (82–84). Accumulating evidence suggests that *PDL1* expression on APCs increases during mycobacterial infection (85, 86), leading to the induction of regulatory T cell (Treg) responses (87). Studies on human DCs have demonstrated infection-induced *PDL1* was essential for the expansion of Treg (88, 89). Conversely, *PDL1* deficient mice were increasingly sensitive to tuberculosis infection (83, 90). In the current study, the expression of *PDL1* was induced in the animals vaccinated with rMAP fusion protein (weeks 6, 9 and 12) and Silirum® (weeks 6 and 9), suggesting that these vaccines may be contributing to T cell-mediated immune responses in the vaccinated animals. This observation is in line with a previous study which demonstrated that Bacillus Calmette-Guérin vaccine can induce *PDL1* expression on APCs (85). In addition, prostaglandin-endoperoxide synthase 2 (*PTGS2*), also known as cyclooxygenase-2 (*COX-2*) was upregulated in the animals vaccinated with rMAP fusion protein and Silirum®. Like *PDL1*, *PTGS2* has also been associated with Treg-mediated immune responses during mycobacterial infection (87, 91). Overall, the data indicate that the rMAP fusion protein and Silirum® vaccines can induce T cell-mediated immune responses, possibly by activating Treg responses in the vaccinated animals. Further studies are required to characterize functional immune cells in the vaccinated animals and confirm the ability of the vaccine to generate cell-mediated protective immunity.

The role of humoral responses against intracellular pathogens might be undervalued. Antibody-mediated immune responses induced by vaccination could be essential in controlling MAP infection (42, 92–94). In our study, strong antibody responses were observed in the calves administered with rMAP fusion protein vaccine. The increased expression of *CD40* in these animals, which has been implicated in the generation of high titers of class switched and high affinity

antibodies (95, 96), suggest that the rMAP fusion protein vaccine-induced antibody responses could provide protective immunity against MAP infection. Furthermore, the expression of pentraxin (*PTX3*) was also increased in the rMAP fusion protein vaccinated animals. *PTX3*, a soluble pattern recognition receptor, is a key component of the humoral arm of the innate immune system and has been suggested as the ancestor of antibodies and the complement cascade (97). These results concur with previous studies, which demonstrated increased expression of *PTX3* in human and bovine macrophages in response to *M. bovis* and MAP, respectively (63, 98). Moreover, studies have demonstrated increased expression of *PTX3* in TLR4-dependent manner and it exhibits opsonizing activity *via* TLR4 pathway during infection (99, 100). In the present study, increased expression of *TLR4* was also observed in the rMAP fusion protein group. While the role of *PTX3* in mycobacterial infection is unclear, it is possible that TLR-mediated opsonizing activity of *PTX3* could potentially promote phagocytosis of mycobacterial pathogens at early stages of infection by the tissue resident macrophages and thus contribute to the innate immune responses during mycobacterial infection.

Often mice are used as the initial model to measure vaccine efficacy, but the immunological responses observed in mice do not always correlate well with the responses observed in large animals (such as cattle, goats, and sheep) (26, 101). This was evident in our two independent studies conducted in mice and cattle. In the current study, the MAP fusion protein particle induced weaker cellular responses compared to the rMAP fusion protein vaccine in cattle, while the protein particle vaccine induced Th1/Th17 cell-mediated immune responses and reduced MAP burden in mice (27). Various studies have demonstrated that different immune responses can be generated for the same antigen when administered as a soluble antigen compared to delivery as a particulate vaccine (102, 103). Several reasons have been proposed for this, such as exposure of different immunostimulatory epitopes on antigens (104, 105), kinetics of soluble and particulate antigen trafficking into lymph nodes (106), processing and presentation of soluble proteins by different mechanisms compared to particulate antigens (14). Due to these possible differences in immune responses, a sequential approach to testing new vaccines is often adopted with large animals such as domestic livestock animals by firstly performing preliminary trials to evaluate their immune responses to the antigens. In the current study, the observed differences in cellular immune responses to protein particles in cattle compared to mice further supports the necessity of firstly performing immunological studies in the target species before proceeding to conduct large, long-duration and expensive MAP vaccine efficacy studies. Therefore, the current study focused on evaluating and reporting the immunogenicity of MAP antigens in two different forms (soluble and protein particles) by determining their ability to induce cellular immune responses in calves.

An important consideration in developing improved vaccines against MAP is the requirement to not interfere with the current on-farm bovine tuberculosis surveillance programme and allow differentiation of infected and vaccinated animals (DIVA). Animals vaccinated with Silirum® vaccine which contains an attenuated MAP strain generated immune responses against both cellular and secreted proteins of MAP, resulting in animals being susceptible to cross-reacting with mycobacterial antigens in PPDA and PPDB. This was evident as the Silirum® vaccinated animals produced positive responses to PPDB. Vaccination with the rMAP fusion protein or protein particles did not induce positive responses to PPDB or to the differential, PPDB-PPDA, in the intradermal skin test, indicating the advantage of using subunit vaccines containing defined mycobacterial antigens with the absence of cross-reactivity to tuberculin. The ability of rMAP fusion protein vaccine to induce strong humoral- and cell-mediated immune responses in the vaccinated animals, has the potential to provide protective immunity against MAP infection without interference with the current bovine tuberculosis skin test.

In summary the ability of two sub-unit vaccines, a soluble recombinant fusion protein of four different antigens of MAP and a protein particle vaccine displaying the same antigens was evaluated to induce antibody- and T-cell-mediated immune responses in cattle. The rMAP fusion protein vaccine induced antigen-specific antibodies as well as IFN-γ and IL-17A cytokines, indicating induction of Th2- and Th1/Th17-mediated immune responses in the vaccinated animals without cross-reactivity to the tuberculin skin test. Notably, transcription analysis of the vaccinated animals indicated upregulation of various genes including *TLR4*, *TLR2*, *PTX3*, *PTGS2*, *PDL1*, *IL1B*, *IL2*, *IL6*, *IL12B*, *IL17A*, *IL22*, *IFNG*, *CD40*, *CD86*, which are important regulators of several immune pathways during mycobacterial host-defense such as autophagy, antigen-presentation, manipulation of macrophage-mediated killing, Th17- and Treg-mediated responses. Taken together, these results indicate that the rMAP fusion protein vaccine induces strong humoral- and cell-mediated immune responses, which could protect cattle against MAP infection without compromising the diagnosis of bovine tuberculosis using the current skin test. These findings provide impetus to evaluate the efficacy of the vaccine in calves experimentally or naturally infected with MAP.

Data availability statement

The datasets presented in this study can be found in online repositories. The names of the repository/repositories and accession number(s) can be found below: GEO Accession viewer (nih.gov), GSE221544, samples GSM6883433 to GSM6883816.

Ethics statement

All animal experiments were approved by the Grasslands Animal Ethics Committee, AgResearch and conducted in compliance with the Animal Welfare Act 1999 (the Act) and the Animal Welfare (Records and Statistics) Regulations 1999.

Author contributions

SG, BB, and DW designed the study. BR selected the antigens for the study. SG performed all experimental work with input from TW, SG, and BB contributed to animal experimental design. AH helped in the Nanostring data analysis. PM performed statistical analysis. SG prepared the manuscript with input from BB, AH, BR, and DW. All authors contributed to the article and approved the submitted version.

Funding

This work was supported by the Agricultural and Marketing Research and Development Trust (AGMARDT) Post-Doctoral fellowship (Grant number: P15002) awarded to SG. Partial financial support was also contributed by Strategic Science Investment Fund provided by the Ministry of Business, Innovation and Employment (Wellington, New Zealand).

Acknowledgments

We thank the AgResearch farm staff for their support during the animal work.

Conflict of interest

Authors SG, TW, PM, AH, BB and DW were employed by company AgResearch.

The remaining author declare that the research was conducted in the absence of any commercial or financial relationships that could be construed as a potential conflict of interest.

Publisher's note

Supplementary material

The Supplementary Material for this article can be found online at: https://www.frontiersin.org/articles/10.3389/fimmu.2022.1087015/full#supplementary-material

References

1. Clarke CJ. The pathology and pathogenesis of paratuberculosis in ruminants and other species. *J Comp Pathol* (1997) 116(3):217–61. doi: 10.1016/S0021-9975(97)80001-1

2. Whitlock RH, Buergelt C. Preclinical and clinical manifestations of paratuberculosis (including pathology). *Vet Clin North Am Food Anim Pract* (1996) 12(2):345–56. doi: 10.1016/S0749-0720(15)30410-2

3. Garcia AB, Shalloo L. Invited review: The economic impact and control of paratuberculosis in cattle. *J Dairy Sci* (2015) 98(8):5019–39. doi: 10.3168/jds.2014-9241

4. Cho J, Tauer LW, Schukken YH, Gómez MI, Smith RL, Lu Z, et al. Economic analysis of *Mycobacterium avium* subspecies *paratuberculosis* vaccines in dairy herds. *J Dairy Sci* (2012) 95(4):1855–72. doi: 10.3168/jds.2011-4787

5. Whittington R, Donat K, Weber MF, Kelton D, Nielsen SS, Eisenberg S, et al. Control of paratuberculosis: who, why and how. *A Rev 48 countries. BMC Vet Res* (2019) 15(1):198. doi: 10.1186/s12917-019-1943-4

6. Garrido JM, Vazquez P, Molina E, Plazaola JM, Sevilla IA, Geijo MV, et al. Paratuberculosis vaccination causes only limited cross-reactivity in the skin test for diagnosis of bovine tuberculosis. *PloS One* (2013) 8(11):e80985. doi: 10.1371/journal.pone.0080985

7. Coad M, Clifford DJ, Vordermeier HM, Whelan AO. The consequences of vaccination with the johne's disease vaccine, gudair, on diagnosis of bovine tuberculosis. *Vet Rec* (2013) 172(10):266. doi: 10.1136/vr.101201

8. Juste RA, Geijo MV, Elguezabal N, Sevilla IA, Alonso-Hearn M, Garrido JM. Paratuberculosis vaccination specific and non-specific effects on cattle lifespan. *Vaccine* (2021) 39(11):1631–41. doi: 10.1016/j.vaccine.2021.01.058

9. Bannantine JP, Hines ME2nd, Bermudez LE, Talaat AM, Sreevatsan S, Stabel JR, et al. A rational framework for evaluating the next generation of vaccines against *Mycobacterium avium* subspecies *paratuberculosis*. *Front Cell Infect Microbiol* (2014) 4:126. doi: 10.3389/fcimb.2014.00126

10. Park HT, Yoo HS. Development of vaccines to *Mycobacterium avium* subsp. *paratuberculosis* infection. *Clin Exp Vaccine Res* (2016) 5(2):108–16. doi: 10.7774/cevr.2016.5.2.108

11. Bastida F, Juste RA. Paratuberculosis control: a review with a focus on vaccination. *J Immune Based Ther Vaccines* (2011) 9(1):8. doi: 10.1186/1476-8518-9-8

12. Macri C, Dumont C, Johnston AP, Mintern JD. Targeting dendritic cells: a promising strategy to improve vaccine effectiveness. *Clin Transl Immunol* (2016) 5(3):e66–e. doi: 10.1038/cti.2016.6

13. Grødeland G, Fossum E, Bogen B. Polarizing T and b cell responses by APC-targeted subunit vaccines. *Front Immunol* (2015) 6:367. doi: 10.3389/fimmu.2015.00367

14. Manolova V, Flace A, Bauer M, Schwarz K, Saudan P, Bachmann MF. Nanoparticles target distinct dendritic cell populations according to their size. *Eur J Immunol* (2008) 38(5):1404–13. doi: 10.1002/eji.200737984

15. Wallis J, Shenton DP, Carlisle RC. Novel approaches for the design, delivery and administration of vaccine technologies. *Clin Exp Immunol* (2019) 196(2):189–204. doi: 10.1111/cei.13287

16. Parlane NA, Gupta SK, Rubio-Reyes P, Chen S, Gonzalez-Miro M, Wedlock DN, et al. Self-assembled protein-coated polyhydroxyalkanoate beads: Properties and biomedical applications. *ACS Biomat Sci Eng* (2017) 3(12):3043–57. doi: 10.1021/acsbiomaterials.6b00355

17. Steinmann B, Christmann A, Heiseler T, Fritz J, Kolmar H. *In vivo* enzyme immobilization by inclusion body display. *Appl Environ Microbiol* (2010) 76 (16):5563. doi: 10.1128/AEM.00612-10

18. Singh M, Chakrapani A, O'Hagan D. Nanoparticles and microparticles as vaccine-delivery systems. *Expert Rev Vaccines* (2007) 6(5):797–808. doi: 10.1586/14760584.6.5.797

19. Nguyen B, Tolia NH. Protein-based antigen presentation platforms for nanoparticle vaccines. *NPJ Vaccines* (2021) 6(1):70. doi: 10.1038/s41541-021-00330-7

20. Abdellrazeq GS, Elnaggar MM, Bannantine JP, Schneider DA, Souza CD, Hwang J, et al. A peptide-based vaccine for *Mycobacterium avium* subspecies *paratuberculosis*. *Vaccine* (2019) 37(21):2783–90. doi: 10.1016/j.vaccine.2019.04.040

21. Legastelois I, Buffin S, Peubez I, Mignon C, Sodoyer R, Werle B. Non-conventional expression systems for the production of vaccine proteins and immunotherapeutic molecules. *Hum Vaccin Immunother* (2017) 13(4):947–61. doi: 10.1080/21645515.2016.1260795

22. Mahalik S, Sharma AK, Mukherjee KJ. Genome engineering for improved recombinant protein expression in *Escherichia coli*. *Microb Cell Fact* (2014) 13:177. doi: 10.1186/s12934-014-0177-1

23. Francis MJ. Recent advances in vaccine technologies. *Vet Clin North Am Small Anim Pract* (2018) 48(2):231–41. doi: 10.1016/j.cvsm.2017.10.002

24. Chen L-H, Kathaperumal K, Huang C-J, McDonough SP, Stehman S, Akey B, et al. Immune responses in mice to *Mycobacterium avium* subsp. *paratuberculosis* following vaccination with a novel 74F recombinant polyprotein. *Vaccine* (2008) 26(9):1253–62. doi: 10.1016/j.vaccine.2007.12.014

25. Kathaperumal K, Park SU, McDonough S, Stehman S, Akey B, Huntley J, et al. Vaccination with recombinant *Mycobacterium avium* subsp. *paratuberculosis* proteins induces differential immune responses and protects calves against infection by oral challenge. *Vaccine* (2008) 26(13):1652–63. doi: 10.1016/j.vaccine.2008.01.015

26. Chandra S, Faisal SM, Chen J-W, Chen T-T, McDonough SP, Liu S, et al. Immune response and protective efficacy of live attenuated *Salmonella* vaccine expressing antigens of *Mycobacterium avium* subsp. *paratuberculosis* against challenge in mice. *Vaccine* (2012) 31(1):242–51. doi: 10.1016/j.vaccine.2012.09.024

27. Gupta SK, Parlane NA, Luo D, Rehm BHA, Heiser A, Buddle BM, et al. Self-assembled particulate vaccine elicits strong immune responses and reduces *Mycobacterium avium* subsp. *paratuberculosis* infection in mice. *Sci Rep* (2020) 10(1):22289. doi: 10.1038/s41598-020-79407-7

28. Liu S, Tobias R, McClure S, Styba G, Shi Q, Jackowski G. Removal of endotoxin from recombinant protein preparations. *Clin Biochem* (1997) 30(6):455–63. doi: 10.1016/S0009-9120(97)00049-0

29. Gupta SK, Haigh BJ, Seyfert HM, Griffin FJ, Wheeler TT. Bovine milk RNases modulate pro-inflammatory responses induced by nucleic acids in cultured immune and epithelial cells. *Dev Comp Immunol* (2017) 68:87–97. doi: 10.1016/j.dci.2016.11.015

30. Rubio Reyes P, Parlane NA, Wedlock DN, Rehm BH. Immunogencity of antigens from *Mycobacterium tuberculosis*, self-assembled as particulate vaccines. *Int J Med Microbiol* (2016) 306(8):624–32. doi: 10.1016/j.ijmm.2016.10.002

31. Lange J, Ganesh S, Meier S, Kay JK, Crookenden MA, Walker CG, et al. Far-off and close-up feeding levels affect immunological performance in grazing dairy cows during the transition period. *J Anim Sci* (2019) 97(1):192–207. doi: 10.1093/jas/sky427

32. Heiser A, LeBlanc SJ, McDougall S. Pegbovigrastim treatment affects gene expression in neutrophils of pasture-fed, periparturient cows. *J Dairy Sci* (2018) 101 (9):8194–207. doi: 10.3168/jds.2017-14129

33. Malkov VA, Serikawa KA, Balantac N, Watters J, Geiss G, Mashadi-Hossein A, et al. Multiplexed measurements of gene signatures in different analytes using the nanostring nCounter assay system. *BMC Res Notes* (2009) 2(1):80. doi: 10.1186/1756-0500-2-80

34. Geiss GK, Bumgarner RE, Birditt B, Dahl T, Dowidar N, Dunaway DL, et al. Direct multiplexed measurement of gene expression with color-coded probe pairs. *Nat Biotechnol* (2008) 26(3):317–25. doi: 10.1038/nbt1385

35. Team, R. C.(2013). R: A language and environment for statistical computing

36. B. Wheeler M, Torchiano M. Permutation tests for linear models in r. *Compr R Arch Network* (2010) 1(2). (Available at https://CRAN.R-project.org/package=lmPerm)

37. Luo D, Ganesh S, Koolaard J. Calculate predicted means for linear models. Repository: CRAN (2014).

38. Rohart F, Gautier B, Singh A, KA LC. mixOmics: An r package for 'omics feature selection and multiple data integration. *PloS Comput Biol* (2017) 13(11): e1005752. doi: 10.1371/journal.pcbi.1005752

39. Kohl M, Wiese S, Warscheid B. Cytoscape: software for visualization and analysis of biological networks. *Methods Mol Biol* (2011) 696:291–303. doi: 10.1007/978-1-60761-987-1_18

40. Sweeney RW, Jones DE, Habecker P, Scott P. Interferon-gamma and interleukin 4 gene expression in cows infected with mycobacterium paratuberculosis. *Am J Vet Res* (1998) 59(7):842–7.

41. Vazquez P, Garrido JM, Juste RA. Specific antibody and interferon-gamma responses associated with immunopathological forms of bovine paratuberculosis in slaughtered friesian cattle. *PloS One* (2013) 8(5):e64568. doi: 10.1371/journal.pone.0064568

42. Waters WR, Miller JM, Palmer MV, Stabel JR, Jones DE, Koistinen KA, et al. Early induction of humoral and cellular immune responses during experimental *Mycobacterium avium* subsp. *paratuberculosis* infection calves. *Infect Immun* (2003) 71(9):5130–8. doi: 10.1128/IAI.71.9.5130-5138.2003

43. Cooper AM, Magram J, Ferrante J, Orme IM. Interleukin 12 (IL-12) is crucial to the development of protective immunity in mice intravenously infected with *Mycobacterium tuberculosis*. *J Exp Med* (1997) 186(1):39–45. doi: 10.1084/jem.186.1.39

44. Flynn JL, Goldstein MM, Triebold KJ, Sypek J, Wolf S, Bloom BR. IL-12 increases resistance of BALB/c mice to *Mycobacterium tuberculosis* infection. *J Immunol* (1995) 155(5):2515–24. doi: 10.4049/jimmunol.155.5.2515

45. Gurung RB, Purdie AC, Whittington RJ, Begg DJ. Cellular and humoral immune responses in sheep vaccinated with candidate antigens MAP2698c and MAP3567 from *Mycobacterium avium* subspecies *paratuberculosis*. *Front Cell Infect Microbiol* (2014) 4:93. doi: 10.3389/fcimb.2014.00093

46. Wozniak TM, Saunders BM, Ryan AA, Britton WJ. *Mycobacterium bovis* BCG-specific Th17 cells confer partial protection against *Mycobacterium tuberculosis* infection in the absence of gamma interferon. *Infect Immun* (2010) 78(10):4187–94. doi: 10.1128/IAI.01392-09

47. Sakai S, Kauffman KD, Sallin MA, Sharpe AH, Young HA, Ganusov VV, et al. CD4 T cell-derived IFN-γ plays a minimal role in control of pulmonary *Mycobacterium tuberculosis* infection and must be actively repressed by PD-1 to prevent lethal disease. *PloS Pathog* (2016) 12(5):e1005667. doi: 10.1371/journal.ppat.1005667

48. Cruz A, Khader SA, Torrado E, Fraga A, Pearl JE, Pedrosa J, et al. Cutting edge: IFN-gamma regulates the induction and expansion of IL-17-producing CD4 T cells during mycobacterial infection. *J Immunol* (2006) 177(3):1416–20. doi: 10.4049/jimmunol.177.3.1416

49. DeKuiper JL, Cooperider HE, Lubben N, Ancel CM, Coussens PM. *Mycobacterium avium* subspecies *paratuberculosis* drives an innate Th17-like T cell response regardless of the presence of antigen-presenting cells. *Front Vet Sci* (2020) 7:108. doi: 10.3389/fvets.2020.00108

50. DeKuiper JL, Coussens PM. Inflammatory Th17 responses to infection with *Mycobacterium avium* subspecies *paratuberculosis* (MAP) in cattle and their potential role in development of johne's disease. *Vet Immunol Immunopathol* (2019) 218:109954. doi: 10.1016/j.vetimm.2019.109954

51. Lyadova IV, Panteleev AV. Th1 and Th17 cells in tuberculosis: Protection, pathology, and biomarkers. *Mediators Inflamm* (2015) 2015:854507. doi: 10.1155/2015/854507

52. Matsuyama M, Ishii Y, Yageta Y, Ohtsuka S, Ano S, Matsuno Y, et al. Role of Th1/Th17 balance regulated by T-bet in a mouse model of mycobacterium avium complex disease. *J Immunol* (2014) 192(4):1707–17. doi: 10.4049/jimmunol.1302258

53. Wang X, Barnes PF, Huang F, Alvarez IB, Neuenschwander PF, Sherman DR, et al. Early secreted antigenic target of 6-kDa protein of mycobacterium tuberculosis primes dendritic cells to stimulate Th17 and inhibit Th1 immune responses. *J Immunol* (2012) 189(6):3092–103. doi: 10.4049/jimmunol.1200573

54. Sutton CE, Lalor SJ, Sweeney CM, Brereton CF, Lavelle EC, Mills KHG. Interleukin-1 and IL-23 induce innate IL-17 production from γδ T cells, amplifying Th17 responses and autoimmunity. *Immunity* (2009) 31(2):331–41. doi: 10.1016/j.immuni.2009.08.001

55. Veldhoen M, Hocking RJ, Atkins CJ, Locksley RM, Stockinger B. TGFβ in the context of an inflammatory cytokine milieu supports *De novo* differentiation of IL-17-Producing T cells. *Immunity* (2006) 24(2):179–89. doi: 10.1016/j.immuni.2006.01.001

56. Littman DR, Rudensky AY. Th17 and regulatory T cells in mediating and restraining inflammation. *Cell* (2010) 140(6):845–58. doi: 10.1016/j.cell.2010.02.021

57. Martin B, Hirota K, Cua DJ, Stockinger B, Veldhoen M. Interleukin-17-Producing γδ T cells selectively expand in response to pathogen products and environmental signals. *Immunity* (2009) 31(2):321–30. doi: 10.1016/j.immuni.2009.06.020

58. Enriquez AB, Sia JK, Dkhar HK, Goh SL, Quezada M, Stallings KL, et al. *Mycobacterium tuberculosis* impedes CD40-dependent notch signaling to restrict Th(17) polarization during infection. *iScience* (2022) 25(5):104305. doi: 10.1016/j.isci.2022.104305

59. Iezzi G, Sonderegger I, Ampenberger F, Schmitz N, Marsland BJ, Kopf M. CD40-CD40L cross-talk integrates strong antigenic signals and microbial stimuli to induce development of IL-17-producing CD4+ T cells. *Proc Natl Acad Sci USA* (2009) 106(3):876–81. doi: 10.1073/pnas.0810769106

60. Deretic V. *Autophagy in tuberculosis* Vol. 4. Cold Spring Harb Perspect Med (2014). p. a018481.

61. Castillo EF, Dekonenko A, Arko-Mensah J, Mandell MA, Dupont N, Jiang S, et al. Autophagy protects against active tuberculosis by suppressing bacterial burden and inflammation. *Proc Natl Acad Sci USA* (2012) 109(46):E3168–76. doi: 10.1073/pnas.1210500109

62. Mayer-Barber Katrin D, Andrade Bruno B, Barber Daniel L, Hieny S, Feng Carl G, Caspar P, et al. Innate and adaptive interferons suppress IL-1α and IL-1β production by distinct pulmonary myeloid subsets during *Mycobacterium tuberculosis* infection. *Immunity* (2011) 35(6):1023–34. doi: 10.1016/j.immuni.2011.12.002

63. Ariel O, Gendron D, Dudemaine PL, Gévry N, Ibeagha-Awemu EM, Bissonnette N. Transcriptome profiling of bovine macrophages infected by *Mycobacterium avium* spp. *paratuberculosis* depicts foam cell and innate immune tolerance phenotypes. *Front Immunol* (2019) 10:2874. doi: 10.3389/fimmu.2019.02874

64. Yamada H, Mizumo S, Horai R, Iwakura Y, Sugawara I. Protective role of interleukin-1 in mycobacterial infection in IL-1 alpha/beta double-knockout mice. *Lab Invest* (2000) 80(5):759–67. doi: 10.1038/labinvest.3780079

65. Yang R, Yang E, Shen L, Modlin RL, Shen H, Chen ZW. IL-12+IL-18 cosignaling in human macrophages and lung epithelial cells activates cathelicidin and autophagy, inhibiting intracellular mycobacterial growth. *J Immunol* (2018) 200(7):2405–17. doi: 10.4049/jimmunol.1701073

66. Jo EK. Autophagy as an innate defense against mycobacteria. *Pathog Dis* (2013) 67(2):108–18. doi: 10.1111/2049-632X.12023

67. Silwal P, Paik S, Kim JK, Yoshimori T, Jo EK. Regulatory mechanisms of autophagy-targeted antimicrobial therapeutics against mycobacterial infection. *Front Cell Infect Microbiol* (2021) 11:633360. doi: 10.3389/fcimb.2021.633360

68. Kim YS, Silwal P, Kim SY, Yoshimori T, Jo EK. Autophagy-activating strategies to promote innate defense against mycobacteria. *Exp Mol Med* (2019) 51 (12):1–10. doi: 10.1038/s12276-019-0290-7

69. Paik S, Kim JK, Chung C, Jo EK. Autophagy: A new strategy for host-directed therapy of tuberculosis. *Virulence* (2019) 10(1):448–59. doi: 10.1080/21505594.2018.1536598

70. Shariq M, Quadir N, Alam A, Zarin S, Sheikh JA, Sharma N, et al. The exploitation of host autophagy and ubiquitin machinery by *Mycobacterium tuberculosis* in shaping immune responses and host defense during infection. *Autophagy* (2022) 1-21. doi: 10.1080/15548627.2021.2021495

71. Wille-Reece U, Flynn BJ, Loré K, Koup RA, Miles AP, Saul A, et al. Toll-like receptor agonists influence the magnitude and quality of memory T cell responses after prime-boost immunization in nonhuman primates. *J Exp Med* (2006) 203 (5):1249–58. doi: 10.1084/jem.20052433

72. Philips JA, Ernst JD. Tuberculosis pathogenesis and immunity. *Annu Rev Pathol* (2012) 7(1):353–84. doi: 10.1146/annurev-pathol-011811-132458

73. Arsenault RJ, Maattanen P, Daigle J, Potter A, Griebel P, Napper S. From mouth to macrophage: mechanisms of innate immune subversion by *Mycobacterium avium* subsp. *paratuberculosis*. *Vet Res* (2014) 45(1):54. doi: 10.1186/1297-9716-45-54

74. Mortaz E, Adcock IM, Tabarsi P, Masjedi MR, Mansouri D, Velayati AA, et al. Interaction of pattern recognition receptors with mycobacterium tuberculosis. *J Clin Immunol* (2015) 35(1):1–10. doi: 10.1007/s10875-014-0103-7

75. Byun EH, Kim WS, Kim JS, Jung ID, Park YM, Kim HJ, et al. *Mycobacterium tuberculosis* Rv0577, a novel TLR2 agonist, induces maturation of dendritic cells and drives Th1 immune response. *FASEB J* (2012) 26(6):2695–711. doi: 10.1096/fj.11-199588

76. Khan A, Bakhru P, Saikolappan S, Das K, Soudani E, Singh CR, et al. An autophagy-inducing and TLR-2 activating BCG vaccine induces a robust protection against tuberculosis in mice. *NPJ Vaccines* (2019) 4:34. doi: 10.1038/s41541-019-0122-8

77. Weiss DJ, Souza CD, Evanson OA, Sanders M, Rutherford M. Bovine monocyte TLR2 receptors differentially regulate the intracellular fate of *Mycobacterium avium* subsp. *paratuberculosis* and *Mycobacterium avium* subsp. *avium*. *J Leukoc Biol* (2008) 83(1):48–55. doi: 10.1189/jlb.0707490

78. Byun EH, Kim WS, Kim JS, Won CJ, Choi HG, Kim HJ, et al. *Mycobacterium paratuberculosis* CobT activates dendritic cells *via* engagement of toll-like receptor 4 resulting in Th1 cell expansion. *J Biol Chem* (2012) 287 (46):38609–24. doi: 10.1074/jbc.M112.391060

79. Behar SM, Divangahi M, Remold HG. Evasion of innate immunity by *Mycobacterium tuberculosis*: is death an exit strategy? *Nat Rev Microbiol* (2010) 8 (9):668–74. doi: 10.1038/nrmicro2387

80. Duraiswamy J, Ibegbu CC, Masopust D, Miller JD, Araki K, Doho GH, et al. Phenotype, function, and gene expression profiles of programmed death-1(hi) CD8 T cells in healthy human adults. *J Immunol* (2011) 186(7):4200–12. doi: 10.4049/jimmunol.1001783

81. Fife BT, Pauken KE, Eagar TN, Obu T, Wu J, Tang Q, et al. Interactions between PD-1 and PD-L1 promote tolerance by blocking the TCR–induced stop signal. *Nat Immunol* (2009) 10(11):1185–92. doi: 10.1038/ni.1790

82. Day CL, Abrahams DA, Bunjun R, Stone L, de Kock M, Walzl G, et al. PD-1 expression on *Mycobacterium tuberculosis*-specific CD4 T cells is associated with bacterial load in human tuberculosis. *Front Immunol* (2018) 9:1995. doi: 10.3389/fimmu.2018.01995

83. Lázár-Molnár E, Chen B, Sweeney KA, Wang EJ, Liu W, Lin J, et al. Programmed death-1 (PD-1)-deficient mice are extraordinarily sensitive to tuberculosis. *Proc Natl Acad Sci USA* (2010) 107(30):13402–7. doi: 10.1073/pnas.1007394107

84. Kauffman KD, Sakai S, Lora NE, Namasivayam S, Baker PJ, Kamenyeva O, et al. PD-1 blockade exacerbates *Mycobacterium tuberculosis* infection in rhesus macaques. *Sci Immunol* (2021) 6(55). doi: 10.1126/sciimmunol.abf3861

85. Copland A, Sparrow A, Hart P, Diogo GR, Paul M, Azuma M, et al. Bacillus calmette-guérin induces PD-L1 expression on antigen-presenting cells *via* autocrine and paracrine interleukin-STAT3 circuits. *Sci Rep* (2019) 9(1):3655. doi: 10.1038/s41598-019-40145-0

86. Suarez GV, Melucci Ganzarain C, Vecchione MB, Trifone CA, Marín Franco JL, Genoula M, et al. PD-1/PD-L1 pathway modulates macrophage susceptibility to *Mycobacterium tuberculosis* specific CD8+ T cell induced death. *Sci Rep* (2019) 9(1):187. doi: 10.1038/s41598-018-36403-2

87. Holla S, Stephen-Victor E, Prakhar P, Sharma M, Saha C, Udupa V, et al. Mycobacteria-responsive sonic hedgehog signaling mediates programmed death-ligand 1- and prostaglandin E2-induced regulatory T cell expansion. *Sci Rep* (2016) 6(1):24193. doi: 10.1038/srep24193

88. Trinath J, Maddur MS, Kaveri SV, Balaji KN, Bayry J. *Mycobacterium tuberculosis* promotes regulatory T-cell expansion *via* induction of programmed death-1 ligand 1 (PD-L1, CD274) on dendritic cells. *J Infect Dis* (2012) 205(4):694–6. doi: 10.1093/infdis/jir820

89. Periasamy S, Dhiman R, Barnes PF, Paidipally P, Tvinnereim A, Bandaru A, et al. Programmed death 1 and cytokine inducible SH2-containing protein dependent expansion of regulatory T cells upon stimulation with *Mycobacterium tuberculosis*. *J Infect Dis* (2011) 203(9):1256–63. doi: 10.1093/infdis/jir011

90. Barber DL, Mayer-Barber KD, Feng CG, Sharpe AH, Sher A. CD4 T cells promote rather than control tuberculosis in the absence of PD-1-mediated inhibition. *J Immunol* (2011) 186(3):1598–607. doi: 10.4049/jimmunol.1003304

91. Garg A, Barnes PF, Roy S, Quiroga MF, Wu S, García VE, et al. Mannose-capped lipoarabinomannan- and prostaglandin E2-dependent expansion of regulatory T cells in human *Mycobacterium tuberculosis* infection. *Eur J Immunol* (2008) 38(2):459–69. doi: 10.1002/eji.200737268

92. Begg DJ, de Silva K, Carter N, Plain KM, Purdie A, Whittington RJ. Does a Th1 over Th2 dominancy really exist in the early stages of *Mycobacterium avium* subspecies *paratuberculosis* infections? *Immunobiology* (2011) 216(7):840–6. doi: 10.1016/j.imbio.2010.12.004

93. Pooley HB, Begg DJ, Plain KM, Whittington RJ, Purdie AC, de Silva K. The humoral immune response is essential for successful vaccine protection against paratuberculosis in sheep. *BMC Vet Res* (2019) 15(1):223. doi: 10.1186/s12917-019-1972-z

94. Arteche-Villasol N, Gutiérrez-Expósito D, Elguezabal N, Sevilla IA, Vallejo R, Espinosa J, et al. Influence of heterologous and homologous vaccines, and their components, on the host immune response and protection against experimental caprine paratuberculosis. *Front Vet Sci* (2022) 8. doi: 10.3389/fvets.2021.744568

95. Elgueta R, Benson MJ, de Vries VC, Wasiuk A, Guo Y, Noelle RJ. Molecular mechanism and function of CD40/CD40L engagement in the immune system. *Immunol Rev* (2009) 229(1):152–72. doi: 10.1111/j.1600-065X.2009.00782.x

96. Jing Z, McCarron MJ, Dustin ML, Fooksman DR. Germinal center expansion but not plasmablast differentiation is proportional to peptide-MHCII density *via* CD40-CD40L signaling strength. *Cell Rep* (2022) 39(5):110763. doi: 10.1016/j.celrep.2022.110763

97. Bottazzi B, Doni A, Garlanda C, Mantovani A. An integrated view of humoral innate immunity: pentraxins as a paradigm. *Annu Rev Immunol* (2010) 28:157–83. doi: 10.1146/annurev-immunol-030409-101305

98. Vouret-Craviari V, Matteucci C, Peri G, Poli G, Introna M, Mantovani A. Expression of a long pentraxin, PTX3, by monocytes exposed to the mycobacterial cell wall component lipoarabinomannan. *Infect Immun* (1997) 65(4):1345–50. doi: 10.1128/iai.65.4.1345-1350.1997

99. Jaillon S, Moalli F, Ragnarsdottir B, Bonavita E, Puthia M, Riva F, et al. The humoral pattern recognition molecule PTX3 is a key component of innate immunity against urinary tract infection. *Immunity* (2014) 40(4):621–32. doi: 10.1016/j.immuni.2014.02.015

100. Bozza S, Campo S, Arseni B, Inforzato A, Ragnar L, Bottazzi B, et al. PTX3 binds MD-2 and promotes TRIF-dependent immune protection in

aspergillosis. *J Immunol* (2014) 193(5):2340–8. doi: 10.4049/jimmunol.1400814

101. Faisal SM, Yan F, Chen T-T, Useh NM, Guo S, Yan W, et al. Evaluation of a *Salmonella* vectored vaccine expressing *Mycobacterium avium* subsp. *paratuberculosis* antigens against challenge in a goat model. *PloS One* (2013) 8 (8):e70171. doi: 10.1371/journal.pone.0070171

102. Lee JW, Parlane NA, Wedlock DN, Rehm BHA. Bioengineering a bacterial pathogen to assemble its own particulate vaccine capable of inducing cellular immunity. *Sci Rep* (2017) 7(1):41607. doi: 10.1038/srep41607

103. Chen S, Parlane NA, Lee J, Wedlock DN, Buddle BM, Rehm BHA. New skin test for detection of bovine tuberculosis on the basis of antigen-displaying polyester inclusions produced by recombinant vesch *Escherichia coli*. *Appl Environ Microbiol* (2014) 80(8):2526–35. doi: 10.1128/AEM.04168-13

104. Snapper CM. Distinct immunologic properties of soluble versus particulate antigens. *Front Immunol* (2018) 9. doi: 10.3389/fimmu.2018.00598

105. Bachmann MF, Jennings GT. Vaccine delivery: a matter of size, geometry, kinetics and molecular patterns. *Nat Rev Immunol* (2010) 10(11):787–96. doi: 10.1038/nri2868

106. de Veer M, Kemp J, Chatelier J, Elhay MJ, Meeusen ENT. The kinetics of soluble and particulate antigen trafficking in the afferent lymph, and its modulation by aluminum-based adjuvant. *Vaccine* (2010) 28(40):6597–602. doi: 10.1016/j.vaccine.2010.07.056

frontiers | Frontiers in Immunology

TYPE Review
PUBLISHED 10 March 2023
DOI 10.3389/fimmu.2023.1080238

OPEN ACCESS

EDITED BY
Suresh Kumar Tikoo,
University of Saskatchewan, Canada

REVIEWED BY
Xiuzhen Sheng,
Ocean University of China, China
Khawaja Ashfaque Ahmed,
University of Saskatchewan, Canada

*CORRESPONDENCE
Jesús Hernández
jhdez@ciad.mx

†These authors have contributed equally to this work

SPECIALTY SECTION
This article was submitted to Vaccines and Molecular Therapeutics, a section of the journal Frontiers in Immunology

RECEIVED 26 October 2022
ACCEPTED 27 February 2023
PUBLISHED 10 March 2023

CITATION
Melgoza-González EA, Bustamante-Córdova L and Hernández J (2023) Recent advances in antigen targeting to antigen-presenting cells in veterinary medicine.
Front. Immunol. 14:1080238.
doi: 10.3389/fimmu.2023.1080238

Recent advances in antigen targeting to antigen-presenting cells in veterinary medicine

Edgar Alonso Melgoza-González†, Lorena Bustamante-Córdova† and Jesús Hernández*

Laboratorio de Inmunología, Centro de Investigación en Alimentación y Desarrollo A. C., Hermosillo, Mexico

Advances in antigen targeting in veterinary medicine have gained traction over the years as an alternative approach for diseases that remain a challenge for traditional vaccines. In addition to the nature of the immunogen, antigen-targeting success relies heavily on the chosen receptor for its direct influence on the elicited response that will ensue after antigen uptake. Different approaches using antibodies, natural or synthetic ligands, fused proteins, and DNA vaccines have been explored in various veterinary species, with pigs, cattle, sheep, and poultry as the most frequent models. Antigen-presenting cells can be targeted using a generic approach, such as broadly expressed receptors such as MHC-II, CD80/86, CD40, CD83, etc., or focused on specific cell populations such as dendritic cells or macrophages (Langerin, DC-SIGN, XCR1, DC peptides, sialoadhesin, mannose receptors, etc.) with contrasting results. Interestingly, DC peptides show high specificity to DCs, boosting activation, stimulating cellular and humoral responses, and a higher rate of clinical protection. Likewise, MHC-II targeting shows consistent results in enhancing both immune responses; an example of this strategy of targeting is the approved vaccine against the bovine viral diarrhea virus in South America. This significant milestone opens the door to continuing efforts toward antigen-targeting vaccines to benefit animal health. This review discusses the recent advances in antigen targeting to antigen-presenting cells in veterinary medicine, with a special interest in pigs, sheep, cattle, poultry, and dogs.

KEYWORDS

antigen target, antigen presenting cell, receptors, veterinary, vaccines

1 Introduction

Antigen-presenting cells (APCs), such as macrophages, dendritic cells (DCs), and B lymphocytes, are a fundamental part of the innate immune system and play essential roles in initiating and regulating the adaptive response (1, 2). Its main function is recognizing, capturing, and processing antigens and presenting immunogenic peptides to naïve T lymphocytes to initiate the adaptive cellular immune response (3–6). Antigen recognition

and internalization are mediated by receptors on the surface of APCs. Through this mechanism of antigen capture, antigen-targeting strategies have been developed to enhance vaccine efficiency and have been widely explored for the last two decades as prophylactic and therapeutic tools for infectious diseases, autoimmunity and cancer (7–15).

The success of antigen-targeting strategies heavily relies on selecting the target receptor, the antigen being delivered, and the antigen carrier. Along with choosing a specific target receptor, the combination of the APC target and adjuvant utilized contributes to the polarization of the $CD4^+$ T lymphocyte response toward the Th1, Th2, Th17, or Treg profile (16–22). These characteristics play a key role in the immune response for future pathogen clearance. Several types of surface receptors are the focus of antigen-targeting research. Pattern-recognizing receptors, chemokine receptors, costimulatory molecules, and cell adhesion receptors are the most common. Interestingly, only a few receptors are known to be highly expressed or almost exclusive to a cell type, such as XCR1, Langerin, DEC205, and DC-SIGN for DCs or CD169, MMR, and CD163 for macrophages. Other molecules, such as MHC-II, CD80/86, CD40, CD83, and CD11c, are widely expressed by a variety of APCs. Among the most popular strategies to shape immune responses is using natural ligands such as glycans to target C-type lectin receptors or proteins (recombinant ligands or antibodies) that recognize surface receptors on APCs (Figure 1). DNA vaccines codifying recombinant proteins fused to the antigen of interest have also been evaluated (23–29). Likewise, the route of administration greatly impacts the development of systemic or mucosal responses, where intradermal, subcutaneous, intramuscular, and oral are the most common immunization routes (30–33).

The diversity of target receptors, antigens, carriers, adjuvants, and administration routes allows for the customization of targeting vaccine strategies to stimulate different aspects of the immune response and will directly impact the level of protection in the different animal species (Supplementary Table 1). However, to date, most evidence supporting antigen targeting has been produced using mice and guinea pigs as transitory models for humans. For this reason, the present review aimed to explore the different approaches and strategies reported encompassing the evaluation of antigen targeting as an immunoprophylactic tool in species of veterinary importance (Table 1) and not just animal models used as surrogates in human medical research.

2 Targeting using the C-type lectin receptor family

2.1 CLRs type I

2.1.1 DEC205

This endocytic receptor is predominantly expressed in dendritic cells, although it has also been reported in various cell types, such as macrophages, T lymphocytes, and B lymphocytes, with differential expression between species (101–104). In addition, it has been characterized in species such as mice, humans, sheep, cattle, and pigs (105–108). DEC205 can promote cross-presentation (the ability to capture, process, and present extracellular antigens with MHC-I to $CD8^+$ T cells) and is capable of being recycled, although the coupling of a ligand or antibody does not guarantee the activation or maturation of DCs (105, 109, 110).

Due to its impact on the poultry industry, avian influenza virus (AIV) antigens were targeted to DEC205 to promote an effective immune response in chickens. The targeting strategy consisted of subcutaneous immunization using an anti-DEC205 antibody to target AIV hemagglutinin protein (HA) to $DEC205^+$ cells. The results showed a significant improvement in the humoral response, evidenced by early production and higher levels of total and neutralizing antibodies (NAbs) in sera (49, 78). No effect on

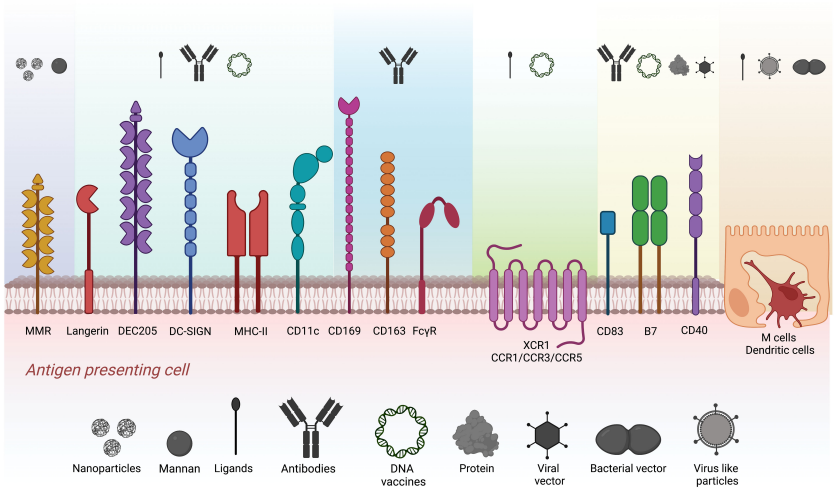

FIGURE 1
Strategies explored for antigen targeting to different APC populations. Target surface receptors on APCs and M cells evaluated in antigen targeting. Different colors represent the clusters of carriers such as nanoparticles, mannan, ligands, antibodies, DNA vaccines, proteins, virus-like particles, and viral and bacterial vectors used to target specific surface receptors.

TABLE 1 Reports of antigen targeting evaluations in common veterinary species.

Target	Target species						
	Sheep	*Swine*	*Cattle*	*Poultry*	*Dogs*	*Ferret*	*Rodents**
B7	(34–37)	(38–40)	(41)	–	–	–	(40, 42, 43)
CCR1/3/5	–	(44)	–	(45)	–	–	–
CD11c	(46)	(47, 48)	–	(49)	–	–	–
CD163	–	(50)	–	–	–	–	–
CD40	(51, 52)	–	(53)	(54–56)	(57)	–	–
CD83	–	–	–	(58, 59)	–	–	–
DCs	–	(60–65)	(66)	(67–71)	–	–	(60, 65, 66, 68, 72)
DC-SIGN	–	(73, 74)	–	–	–	–	–
DEC205	(46, 75)	(73, 76, 77)	(25)	(49, 78–80)	–	–	(75)
FcγR	–	(81)	–	–	–	–	–
Langerin	–	(73, 82, 83)	–	–	–	–	–
M cells	–	–	–	–	–	–	(84)
MMR	–	(85–87)	–	–	–	–	–
MHC-II	–	(24, 88, 89)	(90–94)	–	(95)	(24)	(24, 91–95)
Sialoadhesin	–	(50, 96, 97)	–	–	–	–	–
XCR1	–	(48, 98, 99)	(100)	–	–	–	–

*Included mice, rabbits, and guinea pigs. We included rodents and ferrets since they were used to evaluate antigen-targeting vaccines for veterinary medicine purposes. The extended information is listed in detail in Supplementary Table 1.
Symbol "-" represents the absence of antigen-targeting reports in those animal species.

proinflammatory cytokines such as IFN-γ, IL-6, and IL-1β was observed. Following a similar strategy, the HN antigen of the Newcastle disease virus (NDV) was targeted to DEC205$^+$ cells, resulting in enhanced production of total and NAbs compared with the nontargeted group (79). On the other hand, in a tumoral model induced by Rous sarcoma virus (RSV), subcutaneous targeting to DEC205 skewed the cytokine profile toward the Th1 response, as evidenced by an increase in IL-12, IL-2, and IFN-γ triggering the cellular immune response against the tumor (80).

In sheep, the intradermal injection of a DNA vaccine encoding an anti-DEC205 scFv fused with the Gn and Gc antigens of Rift Valley fever (RVFV) along with granulocyte-macrophage colony-stimulating factor (GM-CSF) promoted a higher frequency of IFN-γ$^+$ T lymphocytes and lower antibody titers compared to the nontargeted antigens (46). Contrary to the results in sheep, the murine counterpart for this study showed no improvement in the humoral response against RVFV, nor had any effect on the cellular response (75). Therefore, even though the strategy was the same, antigen targeting can differ between species, resulting in unpredictable immune responses. In cattle, the intradermal application of a DNA vaccine encoding an anti-DEC205, coupled with the CD40L activation domain and B and T-cell epitopes of *Anaplasma marginale* Merozoite Surface Protein-1 (MSP1), showed promising results. The proliferative response of CD4$^+$ T cells, IFN-γ production, and total IgG titers were significantly increased after a single application and increased after a second exposure (25).

In swine, there are limited and contrasting reports about the efficacy of DEC205$^+$ DC targeting. Evaluating the targeting of GP3, GP4, GP5, and M from PRRSV toward DCs through the intramuscular route promotes the response of CD4$^+$CD8$^+$ T lymphocytes positive for IFN-γ and IL-4, although it failed to stimulate the humoral response. These results were not significantly different from the nontargeting antigen group. As the authors mentioned, the immunization route could not be appropriate to target DCs because their presence in this tissue might be scarce (73). Afterward, Bustamante-Córdova et al. (76) evaluated the effect of targeting immunogenic peptides from PRRSV to intradermal DEC205$^+$ DCs. They found a higher antigen-specific IgG response compared to the control group but with no differences in T lymphocytes IFN-γ$^+$ (76). These results suggest that the route of administration can affect the induction of humoral or cellular immune responses. As a follow-up study, Melgoza-González et al. (77) evaluated antigen targeting using porcine circovirus 2 (PCV2) capsid protein (Cap). The cellular response of IFN-γ$^+$ CD4$^+$CD8$^+$ lymphocytes was enhanced compared to the control group, with a discrete effect on the humoral response (77). These results also suggest that antigen targeting using DEC-205 can stimulate a differential response according to the antigen used, highlighting the importance of the antigen in this kind of immunization system.

2.1.2 Macrophage mannose receptor

MMR is a surface endocytic and phagocytic receptor expressed on macrophages and some myeloid DC subsets (111). This receptor possesses multiple carbohydrate recognition domains that can bind

to mannan and fucose from exogenous antigens, playing a crucial role in the innate immune response (112).

To enhance antigen uptake by APCs, antigens targeting the mannose receptor have been explored in various studies. Mice immunized intradermally with mannosylated PCV2 nanoparticles presented higher levels of IgG, IL-4, and IL-2 than the nontargeted group, even in the absence of other adjuvants. Additionally, the study showed that the mannosylated protein presented a slow release when exposed to low pH in vitro, simulating lysosome conditions and furthering the potential of using mannosylation as a controlled-release tool for drugs (85).

In addition, the mannosylation of gelatin nanoparticles (MnGNPs) encapsulating inactivated PRRSV significantly improved antigen uptake compared with nonmannosylated gelatin particles by up to 15 times. Additionally, MnGNPs were capable of boosting the expression of SWC-3a, CD80, CD1, SLA-I, and SLA-II markers in monocyte-derived DCs (moDCs). The production levels of IL-1β, IL-6, IL-10, and IL-12 were significantly enhanced by MnGNPs, as was the specific cytotoxic T-cell activity. Further exploration of this strategy in vivo studies could position mannose receptor targeting as a prime candidate to aid vaccination efforts against otherwise difficult pathogens (86).

In addition to uptake enhancement, mannose receptor targeting through mannosylation of antigens has been proposed to be able to circumvent the detrimental effect of maternal-derived antibodies (MDA) in the vaccination of young animals (87). For this, mannosylated chitosan-based nanoparticles encapsulating swine influenza virus (SIV) antigens were administered intranasally in piglets following a prime-boost regimen. The strategy successfully enhanced heterologous and homologous IgA responses in the nasal mucosa and the respiratory system. Moreover, the mannosylated vaccine induced higher antigen-specific cell proliferation and IFN-γ expression than the commercial vaccine. In addition, significantly lower viral shedding, lower viral load in bronchoalveolar fluid and lung lysate along with fewer lung lesions were observed (87). In conclusion, the mannosylation of SIV antigens effectively elicited a robust and protective immune response in piglets despite the presence of MDA, highlighting its potential as a valuable vaccination strategy.

2.2 Type II CLRs

2.2.1 DC-SIGN (CD209)

This receptor can bind to mannose and fucose residues and is capable of not only recognizing but also internalizing several pathogens, such as *Mycobacterium tuberculosis, Candida albicans and Leishmania spp.*, among others (113–115). Although DC-SIGN expression is believed to be restricted to DCs, it is also expressed by macrophages (116, 117). Interestingly, as with other receptors from the CLR family, DC-SIGN enables cross-presentation (118, 119). The efficacy of antigen targeting to the porcine DC-SIGN receptor was first evaluated using a chimeric mouse x pig mAb anti-DC-SIGN fused to antigenic peptides from PRRSV using monophosphoryl-lipid A (MPLA) as an adjuvant and administered intradermally in a prime-boost approach. In this instance, a significant increase in IFN-γ-secreting $CD4^+$ and $CD4^+CD8^+$ T cells was observed in the targeted group in comparison with the nontargeted group. Unfortunately, there was no detectable effect on the humoral immune response in immunized pigs (74).

In a follow-up study, the PRRSV-antigenized chimeric mAb was injected intramuscularly and in the presence of Poly I:C as an adjuvant, an agonist of TLR3. This resulted in a modest stimulation of IFN-γ-secreting $CD4^+CD8^+$, IL-4^+ $CD4^+CD8^+$ T, and IL-4^+CD8^+ T cells at 42 days postvaccination compared to the negative control injected with PBS, but no difference was found when compared to the nontargeted group injected with antigens only. Again, no effect was found in the humoral immune response (73). Under the conditions evaluated, intramuscular targeting failed to induce an enhanced IL-4^+ and IFN-γ^+ T-cell response over the non-targeting group. The use of other routes of administration could improve the effects of targeting using DC-SIGN, such as the intradermal route due to the abundance of DCs present in the dermis (120), where several subpopulations of DC-SIGN$^+$ cells have been previously described in swine (121, 122). In this way, targeting DCs could be enhanced with the possibility of a higher effect of delivering antigens to skin DCs.

2.2.2 Langerin

CD207, also known as Langerin, is a receptor expressed in skin-resident APCs, such as epidermal Langerhans cells, and at lower levels in dermal Langerin$^+$ DCs and CD8α$^+$ DCs in lymph nodes (123–125). This endocytic receptor recognizes mannose, fucose, N-acetyl mannosamine, etc., via its carbohydrate recognition domain, mediating internalization, antigen processing, and cross-presentation (126–129). In mice, targeting Langerin$^+$ DCs triggers a Th1 immune response (101). Intradermal targeting of porcine epidemic diarrhea virus (PEDV) antigens to langerin receptors using cholera toxin as an adjuvant resulted in a significant increase in IFN-γ-secreting $CD4^+CD8^+$ T cells 7 days after vaccination. On the other hand, when administered intramuscularly, the humoral immune response was better stimulated, with higher production of IgG and IgA at 35 and 42 days postvaccination, respectively (82). In line with this, a similar strategy was applied to evaluate whether sow vaccination with targeted PEDV antigens could offer protection to piglets through maternal antibody transfer. In this case, a commercial nondisclosed adjuvant was utilized. While the humoral immune response was not greatly stimulated by antigen targeting, there was an increase in IFN-γ secreting T cells ($CD4^+$, $CD8^+$, and $CD4^+CD8^+$), IL-4^+CD4^+ and IL-$4^+CD4^+CD8^+$ cells at 7 days postvaccination compared to the commercial vaccine. Unfortunately, these results did not translate into protection for the piglets where clinical signs were similar in all challenged groups regardless of vaccine type (83).

Targeting PRRSV antigens to langerin receptors intramuscularly and in the presence of Poly I:C resulted in poor stimulation of the cellular and humoral immune responses with a slight increase in IL-4^+ $CD8^+$ T cells. Targeting the same antigenic peptides to other C-type receptors, such as DEC-205 and DC-SIGN, was able to better stimulate IFN-γ and IL-4 responses. Moreover, the langerin-targeted group

presented higher levels of viremia than the challenged control group in this study (73). Overall, langerin targeting failed to induce robust cellular and humoral responses, providing poor results regarding clinical signs and protection.

3 Targeting major histocompatibility class II

MHC-II is expressed on the surface of APCs, displaying exogenous antigens for antigen presentation to $CD4^+$ T lymphocytes (130, 131). MHC-II can be recycled from the cell surface and tagged for degradation into early endosomes with the possibility of promoting cross-presentation by $CD8a^+$ DCs (132–134).

Intradermal targeting of bovine MHC-II using an invariant chain motif coupled to MSP1 antigen along with the molecular adjuvants FLT3L and GM-CSF was evaluated in calves. The strategy resulted in enhanced proliferation of $CD4^+$ lymphocytes, a higher frequency of IFN-γ-secreting cells, and higher antibody IgG levels with a fast and robust recall response (90). This approach aimed to target intracellular MHC-II molecules in the endosome-lysosome stage during the antigen processing pathway.

Similarly, the APCH1 single chain fragment variable (scFv) antibody has been considered a molecular adjuvant that recognizes an invariant epitope of MHC class II-DR in several species. In swine, APCH1 joined to immunodominant antigens of the African swine fever virus (ASFV) were codified into a DNA vaccine and applied using an intramuscular-subcutaneous prime-boost strategy. Although targeting SLA-II elicited the proliferation of $CD4^+$ T cells, IFN-γ-secreting cells, and humoral responses, the latter lacked neutralizing activity and protective immunity against a lethal viral challenge with heterologous strains (88).

Intramuscular targeting of B and T-cell epitopes (BTTs) from foot and mouth disease virus (FMDV) to MHC-II-DR, without additional adjuvants, increased the frequency of IFN-γ secreting cells but did not stimulate the humoral immune response. Nonetheless, after a viral challenge, half of the pigs were partially protected, while the other half had complete protection against clinical signs of disease (89). Additionally, in swine, MHC-II targeting with HA of SIV was enough to stimulate significantly higher IgG and NAbs, while the nontargeting vaccine failed to elicit a humoral response (24).

MHC-II-targeting of enveloping E2 antigen from bovine viral diarrhea virus (BVDV) intramuscularly in guinea pigs and cattle promoted higher NAb titers. This humoral immune response was sufficient to promote total protection against a viral challenge, preventing the development of clinical signs (91). Moreover, the enhanced levels of NAbs in response to the targeted group were similar in titer and protection efficacy to the inactivated vaccine, even under field conditions. This strategy was approved as the first antigen-targeting vaccine commercially available in Peru and Argentina (92, 93). Later, VP2 of the Bluetongue virus (BTV) was coupled to APCH1 and used for intramuscular vaccination in guinea pigs, cattle, and mice. Four times lower amounts of antigens targeted through APCH1 elicited similar NAbs titers than the free VP2 antigen group in guinea pigs and cattle (94). In rabbits and mice, intramuscular targeting of VP60 from rabbit hemorrhagic disease virus (RHDV) mediated by APCH1 fusion protein provided protection after a viral challenge, allowing postchallenge survival (95). Clearly, targeting MHC-II in APCs, independent of the cell type and antigen delivered, seems to be an efficient strategy for the induction of humoral and cellular immune responses, promoting partial to complete protection after a challenge. It is worth mentioning that antigen targeting to MHC-II allows not only DCs to gain access to the antigen but also stimulates B lymphocytes, thus effectively activating cellular and humoral immune responses. These promising results and an approved vaccine in the market put this strategy at the forefront of antigen-targeting-based immunoprophylactic tools.

4 Targeting activation markers

4.1 CD40

CD40 is a surface costimulatory receptor from the tumor necrosis factor receptor family. It is expressed in monocytes, macrophages, B-lymphocytes, dendritic cells, and endothelial and epithelial cells (135). The interaction of CD40 and CD40L (expressed on $CD4^+$ helper T lymphocytes) regulates the expression of costimulatory molecules and the maturation of APCs (136) and triggers the process of DC-licensing. The latter empowers APCs for the activation and maintenance of cytotoxic T lymphocyte responses, increasing the levels of CD80/86 and interleukin-12 (137–139). The process also promotes B lymphocyte survival, class-switching, and antibody secretion, highlighting the role of DC-licensing in the regulation of B-cell responses in a T-cell independent way (140–142). Therefore, DC-licensing using CD40L or an anti-CD40 antibody for antigen delivery potentiates the APC to activate cytotoxic and humoral responses, independent of $CD4^+$ T lymphocyte cooperation. Additionally, using mAbs as agonists to CD40 enables efficient antigen cross-presentation (143, 144).

To evaluate CD40 targeting potential, a DNA vaccine based on bovine CD154 (CD40L) fused with bovine herpesvirus 1 (BHV-1) glycoprotein D (gD) was developed. CD154-gD was capable of binding bovine and ovine lymphocytes, and thus, sheep was used as the model for *in vivo* assays. Here, the targeted group showed antigen-specific IL-4-dependent lymphocyte proliferation, increased antibody levels, and high NAb titers after boosting (51). When tested in calves, similar antibody production was observed between calves and sheep. In calves, no effect was observed when targeting the gD antigen to the CD40 receptor regarding IFN-γ secreting cells, while the nontargeted group showed increased IFN-γ secreting cells at day 8 postchallenge. Moreover, no significant differences were found in clinical signs between targeted and nontargeted calves. These studies clearly show the different responses between species when a one-size-fits-all approach is applied (53).

A DNA vaccine encoding bovine CD154 protein fused to antigens of *Toxoplasma gondii*, specifically rhoptry protein 1 (ROP1), which participates in the initial stages of invasion. The vaccine was evaluated in sheep, where a strong IgG1 response was observed after 1 week of immunization, while IgG2 values were modest. Similarly, IFN-γ levels increased significantly after the first week postimmunization compared to the nontargeted group (52). Exploiting the benefits of viral vectors and antigen targeting, Thacker et al. (57) developed adenovirus 5 (Ad5) encoding CD40L fused to tumor-associated antigens using carcinoembryonic antigen as a model to elicit an antitumoral response in dogs. The strategy resulted in the activation of T lymphocytes in 3 out of the 5 immunized dogs, although a lower anti-CEA antibody response was observed in the targeted group than in the nontargeted group (57).

In a proof-of-concept report, Chen et al. (54) evaluated the ability of a previously developed mAb, anti-chicken CD40, to induce antigen-specific antibody responses using a peptide from the ectodomain of influenza virus matrix protein 2 (M2e) as a model antigen. Four days after a single immunization, a significant increase in antigen-specific IgG antibody levels was observed in the targeted group regardless of the dose (10, 30, and 90 μg). By day 14, doses of 30 and 90 μg still presented high levels of antigen-specific antibody response in the targeted group (54). Following this, the aforementioned Me2-antigenized antibody was used to stimulate mucosal antibody responses by exploring different administration routes: cloacal drinking, oculonasal administration, and oral immunization using an alginate sphere suspension. Similar to previous findings, antigen targeting to CD40 resulted in an early antigen-specific antibody response after a single dose at 7 days postimmunization. Interestingly, all routes, including subcutaneous routes, proved capable of inducing mucosal responses, as evidenced by high IgA levels in the trachea (55). Once its capacity to induce rapid antibody production was established, this antibody served as the basis for the development of a bispecific antibody that binds CD40 and the M2e peptide of the AIV (56). The bispecific antibody would then capture the $M2e^{+}$ viral particles in circulation and deliver them to $CD40^{+}$ APCs, potentiating antigen uptake and response, doubling as antigen carrier and adjuvant. High hemagglutination titers were observed when applied subcutaneously, in comparison with oral and ocular-nasal routes. A prime-boost strategy using a subcutaneous route of administration was capable of inducing complete protection against lethal H5N1 highly pathogenic AIV challenge. The proposed strategy is very promising for enhancing vaccine efficacy in chickens and could be adjusted into a more cost-effective tool in the future.

4.2 B7 (CD80/86)

CD80 and CD86, also known as B7, are both coreceptors expressed on all APCs, such as DCs, B lymphocytes, and macrophages, and play an essential role in T-cell activation (145, 146). Their ligands are CD28, which activates T lymphocytes, and CTLA-4 (CD152), which represses cell activation (147). Thus, antigen targeting to B7 through CTLA-4 has been explored as a strategy for reaching all subpopulations of APCs.

In sheep, phospholipase D (PLD) antigen from *Coryne bacterium pseudotuberculosis* was bound to bovine CTLA-4 and used to evaluate APC targeting by intramuscular DNA vaccination. When evaluating the humoral response, the total titers of PLD-specific antibodies were higher in the targeting group, allowing for enhanced clinical protection after *C. pseudotuberculosis* challenge (34). When the 45TR antigen from *Taenia ovis* was targeted using CTLA-4 in mice and sheep, an increased humoral response was observed in mice, specifically IgG1, but no positive effect on the humoral response was observed in sheep. Targeting the B7 coreceptor did not promote a protective effect against a *T. ovis* challenge in either species (35).

Fasciola hepatica has been described as a protozoan of importance in the livestock industry. In sheep, CatB from *F. hepatica* was targeted to APCs through CTLA-4 using a DNA prime/protein boost strategy. Immunized animals produced higher total IgG titers and lymphocyte proliferative responses than the nontargeted group (36, 42). However, when targeting the FhPGK antigen from *F. hepatica*, following a DNA prime/protein boost scheme, sheep were not protected against *F. hepatica* challenge, echoed by a failure to stimulate humoral and cellular immune responses (37).

In swine, a DNA vaccine encoding CTLA-4 and OVA as antigens augmented IgG1, IgG2, and IgA antibodies followed by 100% seroconversion after a complete immunization schedule (38). Likewise, an intradermal DNA vaccine consisting of the HANG34 peptide from SIV fused to CTLA-4 increased the total and NAbs reflected in a reduction in viral load and virus spread. However, there were no differences in pathological lesions compared with the nontargeted group (39).

Targeting GP5 protein from PRRSV via a DNA vaccine in mice favored an increase in total and NAbs along with higher IFN-γ expression in the targeted group (40). Additionally, using a tumor-induced swine model, targeting APCs using porcine CTLA-4 combined with a truncated diphtheria toxin fusion protein triggered the depletion of tumoral cells *in vivo* (43). On the other hand, targeting β-galactosidase (β-gal) from *Escherichia coli* (*E. coli*) to CTLA-4 on cattle through a DNA vaccine failed to stimulate the humoral and cellular immune response, even when trying different routes of immunization (41).

4.3 CD83

An early activation marker predominantly expressed in DCs and other APCs. Recent publications have just begun exploring CD83's potential for antigen targeting. Using scFv as a delivery system, an antigenic region of the hemagglutinin protein of H9N2 (HAH9) AIV was targeted toward the avian CD83 receptor. This approach significantly increased the expression of IFN-γ, IL-6, IL-1β, IL-4, and CXCL12 in stimulated splenocytes from immunized birds. Likewise, early antibody production, virus neutralization, and hemagglutination inhibition titers were significantly enhanced by CD83 targeting. In line with this, the targeted group showed lower

levels of viral shedding and high survival in challenged animals. Overall, this strategy seems to strongly induce a robust immune response capable of providing sufficient levels of protection in this model, comparable to traditional inactivated vaccines (58).

Shrestha et al. (2022) also evaluated the efficacy of the CD83 antigen-targeting strategy to circumvent the negative effects of MDA in traditional vaccines by immunizing progeny chickens after hatching (day 1 or 14). The antibody response to the targeted antigen was able to thrive with a steady and significant increase until the end of the evaluation at 84 days postvaccination; meanwhile, MDA levels started to decrease to marginal levels by days 28-35. The antibody levels and hemagglutination titers of the targeted group far surpassed those in the nontargeted group and traditional vaccine group, positioning the CD83 targeting strategy as an excellent candidate for next-generation vaccine development (59).

5 Targeting Dendritic cells (DC-peptides)

DC-peptides (DC-pep) are peptides obtained through phage display technologies with the ability to recognize DCs from other leucocyte populations, although their mechanism of action is unclear (148, 149). This approach has been widely studied to develop oral vaccines carried by lactic acid bacilli, thus eliciting mucosal immunity even without additional adjuvants (150). The most common bacteria used in DC-peptide targeting is *Lactobacillus plantarum*. In poultry, *L. plantarum* coated with 12-mer DC-pep and HN antigen from NDV enhanced the expression of mucosal secretory IgA (SIgA) as well as a higher frequency of splenic $CD4^+$ T cells. However, the hemagglutination inhibition titers and survival postchallenge were not improved (67). Targeting *L. plantarum* with HA from AIV H9N2 enhanced the expression of activation markers such as MHC-II and CD80/86. Additionally, obtaining a robust increase in mucosal SIgA, IgG, and the expression of IFN-γ, TNF-α, IL-6, IL-10, IL-12p70, and IL-4 reduced the tissue viral load, thus allowing for better clinical protection (68, 69). When *Enterococcus faecalis* expressing DC-pep carrying the 3-1E antigen from *Eimeria tenella*, causative of avian coccidiosis, was evaluated through oral vaccination, immunized chickens presented higher IgA and IgG titers as well as a higher frequency of $CD4^+$ T *cells* and expression of IFN-γ. However, the response was insufficient to provide protection after an experimental challenge (70).

Lactobacilli expressing DC-pep carrying different PEDV antigens, such as core neutralizing epitope (COE) or S, have been evaluated on swine DCs. The main results show enhanced activation markers such as CD80, CD86, and MHC-II on CD11c DCs and higher serum antibodies compared with the nontargeted group. In the same manner, the response of mucosal IgA was improved along with IL-4, IFN-γ, and the proliferative response (60). When evaluating the same strategy on swine, a biased reinforcement of the Th1 over Th2 profile was observed, as evidenced by a higher presence of $CD4^+IFN\text{-}\gamma^+$ cells than the presence of $CD4^+IL\text{-}4^+$ cells. Moreover, the probiotic/vaccine-targeted group presented a higher survival rate after a viral challenge with reduced viral load and symptom severity (61). Finally, targeting COE antigens in swine resulted in increased maturation of swine moDCs and DCs *in situ* by CD40, CD80, and CD86 expression, enhanced phagocytic activity, and TLR-2, TLR-6, and TLR-9 expression. The cellular immune response was also boosted by stimulating the expression of the Th1 cytokines IFN-γ, IL-12, and IL-17 (62). In mice, targeting *L. plantarum* DC-pep with the S antigen from PEDV enhanced the expression of CD80 in CD11c DCs and increased the titers of mucosal IgA and serum IgG along with IL-17 and IFN-γ expression. In addition, the targeting group presented higher virus neutralization up to 42 dpv (63).

Targeting E2 from BVDV in a murine model resulted in higher expression of CD40 on DCs without changes in CD86 expression. The humoral and cellular responses were significantly improved, as evidenced by a higher titer of IgG NAbs and mucosal IgA compared with the nontargeted group and lymphoproliferation in response to E2 stimuli (66). Similar results have been observed when targeting the S antigen from transmissible gastroenteritis virus (TGEV) in swine, with overexpression of the activation markers CD80/86, CD40 and MHC-II, TLR-2, and TLR-9 as well as IgG and mucosal antibodies. Additionally, the frequency of CD4 T lymphocytes $IFN\text{-}\gamma^+$, IL-4, IL-17, IFN-γ, and TGF-β levels were increased in mucosal-associated lymph tissue (64).

On the other hand, virus-like particles (VLPs) are commonly chosen platforms for vaccine design and development. Hence, VLPs were used and coated with DC-pep, carrying HN and M antigens from NDV but also HA from AIV as a bivalent vaccine candidate. The VLP-DC-pep targeting system enhanced the expression of the activation marker MHC-II on DCs, titers of mucosal IgA, and a higher frequency of splenic $CD4^+$ T cells, leading to a reduction in viral load (71).

VLPs from the PCV2 capsid carry DC-binding peptides to mouse DCs to improve both humoral and cellular immune responses. These resulted in higher activation marker expression of MHC-II, CD80, CD86, expression of IL-6, IL-10, IFN-γ lymphoproliferation, and anti-Cap IgG1 and IgG2a NAbs levels (65). In mice, targeting G antigen from rabies virus (RABV) showed a similar effect, increasing activation markers, total IgG antibodies, and both Th1 and Th2 mediated by $CD4^+$ $IFN\text{-}\gamma^+$ T and $CD4^+IL\text{-}4^+$ T cells with a skew to Th1 profile polarization. This humoral and cellular immune response provided approximately 60% of clinical protection after a viral challenge (72). It is interesting to highlight that although the targeting mechanism is not clearly defined, the approach using DC-pep targeting is undoubtedly highly efficient in promoting DC maturation, triggering the cellular response, especially Th1 cytokines, and enhancing the production of IgG and IgA antibodies. Therefore, the use of DC-pep is a promising strategy for developing new oral vaccines to control diseases affecting domestic animals by activating systemic and mucosal responses.

6 Targeting CD11c

The CD11c receptor belongs to the integrin family and is mostly expressed, but not restricted, by macrophages, DCs, and other myeloid cells (151, 152). CD11c is considered a DC marker in mice (153). The receptor participates in cell-to-cell adhesion but also mediates phagocytosis of extracellular material such as lipopolysaccharide, fibrinogen, collagen, etc. (154–156). In mice, CD11c is expressed at high levels on conventional DCs with the potential for cross-presentation when used in antigen targeting (157, 158). In chickens, an anti-CD11c scFv fused with the ectodomain of H9N2 influenza hemagglutinin induced prompt and effective antibody responses, with higher neutralization and hemagglutination inhibition titers than nontargeted vaccination. Additionally, CD11c targeting resulted in increased cellular responses with significantly higher cytokine production of IFN-γ, IL-6, IL-1β, and IL-4 compared to the DEC205 targeted group, which may be related to a greater expression of CD11c than DEC205 in chickens (49).

In sheep, the targeting of the Gn antigen peptide from RVFV to CD11c using a DNA vaccine resulted in poor production of antigen-specific antibodies in comparison with the nontargeted DNA vaccine group, which had higher mRNA expression levels than the targeted group. In any case, IFN-γ levels were not successfully stimulated by either DNA vaccine. Clinical scores were also lower in the nontargeted group, with CD11c targeting having almost double the score in immunized sheep (46).

SIV antigens have also been targeted to CD11c receptors using a mAb fused to target conserved antigens HA2, M2e, and NP. In this case, two routes were evaluated: intramuscular and intradermal. When applied intramuscularly, antigen targeting to porcine CD11c has been shown to significantly stimulate the IFN-γ T-cell response. Interestingly, the site of immunization appeared to have a greater effect on the elicited immune responses than the targeting itself. Intramuscular application was more effective overall, and intradermal immunization resulted in exacerbated clinical signs and viral shedding in challenged pigs, implying the significance of the delivery route along with the delivery vehicle (47). Finally, a combination of a DNA vaccine encoding a scFv anti-CD11c fused with various T-cell epitopes of PRRSV and a modified live virus (MLV) vaccine in a prime-boost strategy resulted in an increase in antigen-specific IFN-γ secreting cells (98).

7 Targeting sialoadhesins (Siglec and CD169)

Sialodhesin (Sn), CD169, or Siglec-1 is recognized as the sialic acid binding receptor and is well known as a highly expressed macrophage marker on tissue and secondary lymphoid organs (6, 159, 160). CD169 plays an important role in cell-to-cell adhesion and CD169$^+$ macrophage-mediated antigen delivery to lymphatic resident DCs, enabling cross-presentation (161–163). CD169 macrophages by themselves cannot cross-present antigens, but they are able to transfer antigens to DCs, enabling cross-presentation (162, 164).

As an endocytic receptor in APCs, the Sn receptor has been proposed as a tool to improve antigen uptake and enhance T-cell responses. Using a mouse mAb to target porcine Sn, Revilla et al. (96) were able to induce potent T proliferative responses in IFN-α-treated monocytes and moDCs, up to 100 times more than when an irrelevant isotype control mAb was administered (96). A follow-up study by this group evaluated the proficiency of this and other mouse mAb anti-Sn to induce antigen-specific proliferation in peripheral blood mononuclear cells (PBMCs) and antibody production following a prime and boost strategy. All three of the targeting mAbs tested were capable of significantly increasing antigen-specific IgG levels in sera, with IgG1 and IgG2 profiles very similar in proportion, and once more improving proliferative responses as previously observed (50).

Likewise, antigen-specific IgG and IgM production were also observed as a response to targeting human serum album chemically linked to mAb anti-Sn receptors in the absence of adjuvants when administered in pigs. Following this study, a recombinant mAb, anti-Sn, was used to deliver PRRSV GP4 to porcine macrophages by immunizing pigs intramuscularly and challenging them seven weeks postimmunization. The strategy resulted in an increase in antigen-specific IgG and NAbs titers in sera in a dose-dependent manner, as well as rapid virus clearance (97).

8 Targeting chemokine receptors

8.1 XCR1

XCR1 is a chemokine receptor whose unique ligand is the chemokine XCL1 and specifically chemoattracts the equivalent cDC1 population in mice and humans (165, 166). In many species, this chemokine receptor is considered a conserved marker on the subset of highly efficient cross-presenting cDC1 (167–169). Therefore, targeting XCR1 seems to be a highly specific strategy to deliver antigens to the cDC1 subset.

In swine, targeting intradermal XCR1$^+$ cDC1 with dimeric ligand XCL1 joined to M2e antigens from SIV resulted in higher total IgG anti-M2e antibodies. Additionally, targeting XCL1 enhances the IgG2 response in influenza-seronegative pigs and IgG1 in seropositive pigs, without a skewed effect by either CpG or MPLA adjuvants (99). Additionally, a DNA vaccine encoding the XCR1 ligand fused to B and T epitopes of the N antigen from PRRSV was used in a DNA-MLV prime-boost strategy in pigs. The DNA vaccine was combined with cationic polylactoglycolide acid (PLGA) nanoparticles. DNA vaccine alone failed to elicit humoral and cellular immune responses but, under a DNA-MLV prime-boost schedule, achieved enhancement of the anti-N IgG response (98). The authors discuss the possibility that nanoparticles affected the efficacy of the DNA vaccine and therefore, they restructured the strategy, employing naked DNA to deliver N, NSP1β, and pGP4GP5 M from PRSSV toward XCR1$^+$ DC, followed by a boost with an MLV. The XCR1 targeting-MVL boost allowed for a higher S/P ratio against the N antigen at 58 dpv; nonetheless, it was not possible to find significant levels of IFN-γ secreting cells after *in vitro* restimulation or clinical protection after heterologous

PRRSV challenge (48). It is important to highlight that in these last two PRRSV antigen-targeting studies, the authors used DNA vaccines without additional adjuvants or immunostimulants, which may be necessary for proper stimulation of the cellular response. In cattle, targeting XCR1 cDC1 with the XCL1 fusion protein carrying the multiepitope OB7 antigen of FMDV was applied intramuscularly alone or with oil adjuvant or poly I:C. XCR1 targeting allowed for higher total and NAbs compared to the nontargeted group, eliciting better clinical protection against viral challenges with FMDV. Interestingly, poly I:C weakened the humoral response (100).

Notably, since the cDC1 population is well known to skew toward the Th1 cytokine profile and XCR1 is highly conserved in this population, an increased cellular response would be expected as a result of XCR1 targeting (13, 170); nevertheless, this has not been evidenced by the reports mentioned above. In summary, these findings highlight the different outcomes for XCR1 targeting regarding the species, type of targeted vaccine, and type of adjuvant involved.

8.2 CCR1, CCR3, CCR5

Chemokine receptors, which are expressed in many cells, can effectively facilitate antigen uptake, processing, and presentation in APCs (171). In mice, targeting low immunogenic tumoral antigens to chemokine receptors successfully activated the adaptive immune response and protected against a lethal challenge without the need for adjuvants (172).

DNA vaccines containing either the gene for MIP1α chemokine, targeting CCR1/3/5 chemokine receptors or a scFv anti-MHC-II along with fused HA antigen of H7N1 AIV were developed to stimulate APC-specific responses. When tested in mice, CCR1/3/5 and MHC-II targeting resulted in slightly higher IFN-γ T-cell responses than CCR1/3/5 targeting (45).

A similar approach was evaluated in pigs using a DNA vaccine encoding the MIP1α chemokine fused to HA antigen from the H1N1 influenza virus. The antibody response favored the IgG2 isotype over IgG1, while virus neutralization titers appeared higher in the CCR1/3/5 targeted group than in the antigen-only group. In addition, T-cell responses were significantly enhanced in the targeted group in a cross-reactive manner, responding to H1, H5, and H13 influenza subtypes, 28 days postimmunization (44). These findings suggest a notably efficient cellular immune response elicited in pigs by this targeting strategy.

9 Others

9.1 CD163 (scavenger receptor)

The scavenger receptor, also known as the CD163 receptor, contains nine scavenger cysteine-rich domains and is restricted to cells of the monocytic lineage (173). It is expressed at high levels in mature macrophages and low levels in moDCs (174, 175). This endocytic receptor has been characterized in several species, although there is no evidence that targeting CD163 can allow for cross-presentation (176). Although CD163 has been widely studied concerning its participation in infectious diseases in pigs, its antigen-targeting potential has not been equally explored. A report from Poderoso et al. (50) showed that targeting mouse IgG as an immunogen to CD163 following a prime-boost strategy resulted in the stimulation of the proliferative response in PBMCs. Additionally, the humoral response was greatly enhanced compared to the isotype control as early as 2 weeks postimmunization and increased with a booster dose at 6 weeks post-priming. This humoral response was particularly skewed to the IgG2 subclass and remained significantly higher than the negative control until 17 weeks after immunization (50).

9.2 Fcγ-receptor

Fc-γ receptors (Fc-γR) are distributed ubiquitously in endothelial, myeloid, and lymphoid cells and perform an essential function in the immune system by recognizing antigen-antibody complexes, thus improving antigen capture and processing (177–179). It is well known that antigens fused to IgG-Fc domains significantly enhance the immunogenicity of the antigen due to increased uptake through Fc-g receptors (180–182).

In vitro studies have evaluated the potential of using Fc receptors for antigen targeting by using porcine moDCs. Immuno-complexes (ICs) composed of F4 fimbriae from enterotoxigenic *E. coli* and anti-F4 polyclonal antibodies were incubated with porcine monocytes and respective cytokines to stimulate the generation of moDCs. F4-IC was internalized and enhanced the upregulation of the DC activation markers MHC-II, CD40, and CD80/86. Subsequently, activated moDCs could induce robust lymphocyte proliferation compared with F4 antigen- or IgG-only treated moDCs. Moreover, stimulated moDCs enhanced their production of IL-1β, IL-6, IL-8, and TNF-α, similar to a flagellin control but higher than F4 antigen or IgG-only treated moDCs. These findings demonstrate the maturation of moDCs induced by targeting Fc receptors and their potential use in antigen-targeting-based vaccines (81).

9.3 M-cells

In hopes of enhancing mucosal immune responses against pathogens, M-cell targeting was evaluated using a targeted unit named ligand Co-1 coupled with TB1 protein of FMDV and displayed in *Lactococcus lactis* (*L. lactis*-TB1-Co1) for increased stimulation. Mice and guinea pigs were orally immunized with *L. lactis*-TB1-Co1 and subsequently challenged 30 days postvaccination. In mice, the results showed increased antigen-specific IgA levels in sera, intestinal, and lung lavage fluids in the targeted group in comparison to the nontargeted and inactivated vaccine groups. Regarding cellular

immune stimulation, mice in the targeted group presented higher T-cell proliferation and appeared to have enhanced IFN-γ and IL-2 production than the nontargeted group. The effect on humoral and cellular immune responses in guinea pigs was not as evident as in mice, although 60% protection was observed when animals were challenged. Once more, these findings highlight the different responses between species to a single targeting strategy (84).

10 Conclusions and future directions

The use of antigen-targeting strategies in the field of veterinary medicine has been evaluated in several species; swine is the most scrutinized specie, followed by chickens, cattle, and sheep. The available information shows highly heterogeneous responses according to the type of APC receptors targeted pertaining to humoral, cellular, and clinical protection. Most studies that determined clinical protection were evaluated under controlled experimental conditions; however, their efficacy under field conditions remains unknown. Remarkably, among all the vaccination routes evaluated in antigen targeting, oral vaccination with DC-pep-expressing lactobacillus seems to be a very promising strategy, showing high consistency in the induction of both mucosal and systemic responses. On the other hand, parenteral targeting with MHC-II-DR has also been widely successful, culminating in the approval of a commercial vaccine in South America.

It is important to continue with the development and evaluation of APC-targeting vaccines and generate knowledge that undoubtedly could help to modify conditions to redefine current vaccine trends and improve animal health. It is important to explore several routes of administration, antigens, and adjuvants since a one-size-fits-all strategy is very unlikely to work for all species and diseases. When the target receptor is mainly expressed on DCs, the intradermal or dermal route must be elected over the intramuscular route. Additionally, it is important to explore the nasal or intrauterine route due to the abundance of DCs in these sites. In this line, when the target receptor is mainly expressed on macrophages, the intramuscular route or oral route could be priorities. It is also important to keep in mind the use of new technologies, such as mRNA. This technology could be an interesting option to improve the benefits of antigen targeting for the control of diseases affecting veterinary medicine.

Author contributions

Conceptualization, JH, EM-G and LB-C. Data curation, EM-G and LB-C. Writing—original draft preparation, EM-G and LB-C. Writing—review and editing, JH, EM-G and LB-C. Supervision, JH. funding acquisition, JH. All authors contributed to the article and approved the submitted version.

Acknowledgments

EM-G received a scholarship from the Consejo Nacional de Ciencia y Tecnología (CONACyT) and is currently enrolled in the program Doctorado en Ciencias of the Centro de Investigación en Alimentación y Desarrollo. A. C. (CIAD). Figure 1 was created with BioRender.com.

Conflict of interest

The authors declare that the research was conducted in the absence of any commercial or financial relationships that could be construed as a potential conflict of interest.

Publisher's note

Supplementary material

The Supplementary Material for this article can be found online at: https://www.frontiersin.org/articles/10.3389/fimmu.2023.1080238/full#supplementary-material

References

1. Banchereau J, Steinman RM. Dendritic cells and the control of immunity. *Nature* (1998) 392(6673):245–52. doi: 10.1038/32588

2. den Haan JM, Arens R, van Zelm MC. The activation of the adaptive immune system: cross-talk between antigen-presenting cells, T cells and b cells. *Immunol letters.* (2014) 162(2):103–12. doi: 10.1016/j.imlet.2014.10.011

3. Fadilah S, Cheong S. Dendritic cell immunobiology and potential roles in immunotherapy. *Malaysian J Pathol* (2007) 29(1):1.

4. Rodríguez-Pinto D. B cells as antigen presenting cells. *Cell Immunol* (2005) 238 (2):67–75. doi: 10.1016/j.cellimm.2006.02.005

5. Unanue ER. Antigen-presenting function of the macrophage. *Annu Rev Immunol* (1984) 2(1):395–428. doi: 10.1146/annurev.iy.02.040184.002143

6. Martinez-Pomares L, Gordon S. CD169+ macrophages at the crossroads of antigen presentation. *Trends Immunol* (2012) 33(2):66–70. doi: 10.1016/j.it.2011.11.001

7. He L-Z, Crocker A, Lee J, Mendoza-Ramirez J, Wang X-T, Vitale LA, et al. Antigenic targeting of the human mannose receptor induces tumor immunity. *J Immunol* (2007) 178(10):6259–67. doi: 10.4049/jimmunol.178.10.6259

8. Sancho D, Mourão-Sá D, Joffre OP, Schulz O, Rogers NC, Pennington DJ, et al. Tumor therapy in mice *via* antigen targeting to a novel, DC-restricted c-type lectin. *J Clin Invest* (2008) 118(6):2098–110. doi: 10.1172/JCI34584

9. Chen Y, Wu J, Wang J, Zhang W, Xu B, Xu X, et al. Targeted delivery of antigen to intestinal dendritic cells induces oral tolerance and prevents autoimmune diabetes in NOD mice. *Diabetologia* (2018) 61(6):1384–96. doi: 10.1007/s00125-018-4593-3

10. Ring S, Maas M, Nettelbeck DM, Enk AH, Mahnke K. Targeting of autoantigens to DEC205+ dendritic cells in vivo suppresses experimental allergic encephalomyelitis in mice. *J Immunol* (2013) 191(6):2938–47. doi: 10.4049/jimmunol.1202592

11. Spiering R, Margry B, Keijzer C, Petzold C, Hoek A, Wagenaar-Hilbers J, et al. DEC205+ dendritic cell–targeted tolerogenic vaccination promotes immune tolerance in experimental autoimmune arthritis. *J Immunol* (2015) 194(10):4804–13. doi: 10.4049/jimmunol.1400986

12. van Dinther D, Lopez Venegas M, Veninga H, Olesek K, Hoogterp L, Revet M, et al. Activation of CD8+ T cell responses after melanoma antigen targeting to CD169+ antigen presenting cells in mice and humans. *Cancers* (2019) 11(2):183. doi: 10.3390/cancers11020183

13. Fossum E, Grødeland G, Terhorst D, Tveita AA, Vikse E, Mjaaland S, et al. Vaccine molecules targeting Xcr1 on cross-presenting DCs induce protective CD8+ T-cell responses against influenza virus. *Eur J Immunol* (2015) 45(2):624–35. doi: 10.1002/eji.201445080

14. Bonifaz L, Bonnyay D, Mahnke K, Rivera M, Nussenzweig MC, Steinman RM. Efficient targeting of protein antigen to the dendritic cell receptor DEC-205 in the steady state leads to antigen presentation on major histocompatibility complex class I products and peripheral CD8+ T cell tolerance. *J Exp Med* (2002) 196(12):1627–38. doi: 10.1084/jem.20021598

15. Bonifaz LC, Bonnyay DP, Charalambous A, Darguste DI, Fujii S-I, Soares H, et al. in vivo targeting of antigens to maturing dendritic cells *via* the DEC-205 receptor improves T cell vaccination. *J Exp Med* (2004) 199(6):815–24. doi: 10.1084/jem.20032220

16. Grødeland G, Fossum E, Bogen B. Polarizing T and b cell responses by APC-targeted subunit vaccines. *Front Immunol* (2015) 6:367. doi: 10.3390/vaccines7020043

17. Schlecht G, Loucka J, Najar H, Sebo P, Leclerc C. Antigen targeting to CD11b allows efficient presentation of CD4+ and CD8+ T cell epitopes and in vivo Th1-polarized T cell priming. *J Immunol* (2004) 173(10):6089–97. doi: 10.4049/jimmunol.173.10.6089

18. Pantel A, Cheong C, Dandamudi D, Shrestha E, Mehandru S, Brane L, et al. A new synthetic TLR4 agonist, GLA, allows dendritic cells targeted with antigen to elicit Th1 T-cell immunity *in vivo*. *Eur J Immunol* (2012) 42(1):101–9. doi: 10.1002/eji.201141855

19. Sulczewski FB, Martino LA, Almeida B, Zaneti AB, Ferreira NS, Amorim K, et al. Conventional type 1 dendritic cells induce TH1, TH1-like follicular helper T cells and regulatory T cells after antigen boost *via* DEC205 receptor. *Eur J Immunol* (2020) 50 (12):1895–911. doi: 10.1002/eji.202048694

20. Loschko J, Heink S, Hackl D, Dudziak D, Reindl W, Korn T, et al. Antigen targeting to plasmacytoid dendritic cells *via* siglec-h inhibits Th cell-dependent autoimmunity. *J Immunol* (2011) 187(12):6346–56. doi: 10.4049/jimmunol.1102307

21. Hulse KE, Reefer AJ, Engelhard VH, Satinover SM, Patrie JT, Chapman MD, et al. Targeting fel d 1 to FcγRI induces a novel variation of the Th2 response in subjects with cat allergy. *J Allergy Clin Immunol* (2008) 121(3):756–62. e4. doi: 10.1016/j.jaci.2007.10.016

22. Joffre OP, Sancho D, Zelenay S, Keller AM, Reis e Sousa C. Efficient and versatile manipulation of the peripheral CD4+ T-cell compartment by antigen targeting to DNGR-1/CLEC9A. *Eur J Immunol* (2010) 40(5):1255–65. doi: 10.1002/eji.201040419

23. Johannssen T, Lepenies B. Glycan-based cell targeting to modulate immune responses. *Trends Biotechnol* (2017) 35(4):334–46. doi: 10.1016/j.tibtech.2016.10.002

24. Grodeland G, Fredriksen AB, Løset GÅ, Vikse E, Fugger L, Bogen B. Antigen targeting to human HLA class II molecules increases efficacy of DNA vaccination. *J Immunol* (2016) 197(9):3575–85. doi: 10.4049/jimmunol.1600893

25. Njongmeta LM, Bray J, Davies CJ, Davis WC, Howard CJ, Hope JC, et al. CD205 antigen targeting combined with dendritic cell recruitment factors and antigen-linked CD40L activation primes and expands significant antigen-specific antibody and CD4+ T cell responses following DNA vaccination of outbred animals. *Vaccine* (2012) 30 (9):1624–35. doi: 10.1016/j.vaccine.2011.12.110

26. Nchinda G, Kuroiwa J, Oks M, Trumpfheller C, Park CG, Huang Y, et al. The efficacy of DNA vaccination is enhanced in mice by targeting the encoded protein to dendritic cells. *J Clin Invest* (2008) 118(4):1427–36. doi: 10.1172/JCI34224

27. Lam JS, Huang H, Levitz SM. Effect of differential n-linked and O-linked mannosylation on recognition of fungal antigens by dendritic cells. *PloS One* (2007) 2 (10):e1009. doi: 10.1371/journal.pone.0001009

28. Tan MAA, Mommaas AM, Drijfhout JW, Jordens R, Onderwater JJ, Verwoerd D, et al. Mannose receptor-mediated uptake of antigens strongly enhances HLA class II-restricted antigen presentation by cultured dendritic cells. *Eur J Immunol* (1997) 27 (9):2426–35. doi: 10.1002/eji.1830270942

29. Shi Y, Halperin SA, Lee SF. Expression, purification, and functional analysis of an antigen-targeting fusion protein composed of CD40 ligand and the c-terminal fragment of ovalbumin. *Protein Expression Purification.* (2018) 142:37–44. doi: 10.1016/j.pep.2017.09.015

30. Romani N, Thurnher M, Idoyaga J, Steinman RM, Flacher V. Targeting of antigens to skin dendritic cells: Possibilities to enhance vaccine efficacy. *Immunol Cell Biol* (2010) 88(4):424–30. doi: 10.1038/icb.2010.39

31. Volckmar J, Knop L, Stegemann-Koniszewski S, Schulze K, Ebensen T, Guzmán CA, et al. The STING activator c-di-AMP exerts superior adjuvant properties than the formulation poly (I: C)/CpG after subcutaneous vaccination with soluble protein antigen or DEC-205-mediated antigen targeting to dendritic cells. *Vaccine* (2019) 37 (35):4963–74. doi: 10.1016/j.vaccine.2019.07.019

32. Tenbusch M, Ignatius R, Nchinda G, Trumpfheller C, Salazar AM, Töpfer K, et al. Immunogenicity of DNA vaccines encoding simian immunodeficiency virus antigen targeted to dendritic cells in rhesus macaques. *PloS One* (2012) 7(6):e39038. doi: 10.1371/journal.pone.0039038

33. Kim S-H, Jang Y-S. Antigen targeting to m cells for enhancing the efficacy of mucosal vaccines. *Exp Mol Med* (2014) 46(3):e85–e. doi: 10.1038/emm.2013.165

34. Chaplin PJ, De Rose R, Boyle JS, McWaters P, Kelly J, Tennent JM, et al. Targeting improves the efficacy of a DNA vaccine against *Corynebacterium pseudotuberculosis* in sheep. *Infection immunity.* (1999) 67(12):6434–8. doi: 10.1128/IAI.67.12.6434-6438.1999

35. Drew DR, Boyle J, Lew A, Lightowlers M, Chaplin P, Strugnell R. The comparative efficacy of CTLA-4 and l-selectin targeted DNA vaccines in mice and sheep. *Vaccine* (2001) 19(31):4417–28. doi: 10.1016/S0264-410X(01)00196-7

36. Kennedy NJ, Spithill TW, Tennent J, Wood PR, Piedrafita D. DNA Vaccines in sheep: CTLA-4 mediated targeting and CpG motifs enhance immunogenicity in a DNA prime/protein boost strategy. *Vaccine* (2006) 24(7):970–9. doi: 10.1016/j.vaccine.2005.08.076

37. Wesołowska A, Basałaj K, Zawistowska-Deniziak A, Januszkiewicz K, Ljunggren MK, Jedlina L, et al. The failure of a DNA prime/protein boost regime and CTLA-4 mediated targeting to improve the potency of a DNA vaccine encoding *Fasciola hepatica* phosphoglycerate kinase in sheep. *Veterinary Immunol immunopathology.* (2019) 217:109941. doi: 10.1016/j.vetimm.2019.109941

38. Tachedjian M, Boyle JS, Lew AM, Horvatic B, Scheerlinck J-PY, Tennent JM, et al. Gene gun immunization in a preclinical model is enhanced by B7 targeting. *Vaccine* (2003) 21(21-22):2900–5. doi: 10.1016/S0264-410X(03)00162-2

39. Sisteré-Oró M, Vergara-Alert J, Stratmann T, López-Serrano S, Pina-Pedrero S, Córdoba L, et al. Conserved HA-peptide NG34 formulated in pCMV-CTLA4-Ig reduces viral shedding in pigs after a heterosubtypic influenza virus SwH3N2 challenge. *PloS One* (2019) 14(3):e0212431. doi: 10.1371/journal.pone.0212431

40. Wang Y, Zhao H, Ma Z, Wang Y, Feng W-h. CTLA4 mediated targeting enhances immunogenicity against PRRSV in a DNA prime/killed virus boost strategy. *Veterinary Immunol immunopathology* (2013) 154(3-4):121–8. doi: 10.1016/j.vetimm.2013.05.008

41. Shkreta L, Talbot BG, Lacasse P. Optimization of DNA vaccination immune responses in dairy cows: Effect of injection site and the targeting efficacy of antigen-bCTLA-4 complex. *Vaccine* (2003) 21(19-20):2372–82. doi: 10.1016/S0264-410X(03)00097-5

42. Jayaraj R, Piedrafita D, Spithill T, Smooker P. Evaluation of the immune responses induced by four targeted DNA vaccines encoding the juvenile liver fluke antigen, cathepsin b in a mouse model. *Genet Vaccines Ther* (2012) 10(1):1–9. doi: 10.1186/1479-0556-10-7

43. Peraino JS, Schenk M, Zhang H, Li G, Hermanrud CE, Neville DMJr., et al. A truncated diphtheria toxin based recombinant porcine CTLA-4 fusion toxin. *J Immunol Methods* (2013) 391(1-2):103–11. doi: 10.1016/j.jim.2013.02.015

44. Grodeland G, Fossum E, Bogen B. Targeting of HA to chemokine receptors induces strong and cross-reactive T cell responses after DNA vaccination in pigs. *Vaccine* (2020) 38(6):1280–5. doi: 10.1016/j.vaccine.2019.11.084

45. Andersen TK, Zhou F, Cox R, Bogen B, Grødeland G. A DNA vaccine that targets hemagglutinin to antigen-presenting cells protects mice against H7 influenza. *J virology.* (2017) 91(23):e01340–17. doi: 10.1128/JVI.01340-17

46. Chrun T, Lacôte S, Urien C, Jouneau L, Barc C, Bouguyon E, et al. A rift valley fever virus gn ectodomain-based DNA vaccine induces a partial protection not improved by APC targeting. *NPJ Vaccines* (2018) 3(1):1–13. doi: 10.1038/s41541-018-0052-x

47. Bernelin-Cottet C, Deloizy C, Stanek O, Barc C, Bouguyon E, Urien C, et al. A universal influenza vaccine can lead to disease exacerbation or viral control depending on delivery strategies. *Front Immunol* (2016) 7:641. doi: 10.3389/fimmu.2016.00641

48. Bernelin-Cottet C, Urien C, Fretaud M, Langevin C, Trus I, Jouneau L, et al. A DNA prime immuno-potentiates a modified live vaccine against the porcine reproductive and respiratory syndrome virus but does not improve heterologous protection. *Viruses* (2019) 11(6):576. doi: 10.3390/v11060576

49. Shrestha A, Sadeyen J-R, Lukosaityte D, Chang P, Van Hulten M, Iqbal M. Targeting haemagglutinin antigen of avian influenza virus to chicken immune cell receptors Dec205 and CD11c induces differential immune-potentiating responses. *Vaccines* (2021) 9(7):784. doi: 10.3390/vaccines9070784

50. Poderoso T, Martínez P, Álvarez B, Handler A, Moreno S, Alonso F, et al. Delivery of antigen to sialoadhesin or CD163 improves the specific immune response in pigs. *Vaccine* (2011) 29(29-30):4813–20. doi: 10.1016/j.vaccine.2011.04.076

51. Manoj S, Griebel PJ, Babiuk LA. Targeting with bovine CD154 enhances humoral immune responses induced by a DNA vaccine in sheep. *J Immunol* (2003) 170(2):989–96. doi: 10.4049/jimmunol.170.2.989

52. Hiszczyńska-Sawicka E, Li H, Xu JB, Holec-Gąsior L, Kur J, Sedcole R, et al. Modulation of immune response to *Toxoplasma gondii* in sheep by immunization with a DNA vaccine encoding ROP1 antigen as a fusion protein with ovine CD154. *Veterinary Parasitol* (2011) 183(1-2):72–8. doi: 10.1016/j.vetpar.2011.06.010

53. Manoj S, Griebel PJ, Babiuk LA, Van Drunen Littel-Van Den Hurk S. Modulation of immune responses to bovine herpesvirus-1 in cattle by immunization

with a DNA vaccine encoding glycoprotein d as a fusion protein with bovine CD154. *Immunology* (2004) 112(2):328–38. doi: 10.1111/j.1365-2567.2004.01877.x

54. Chen C-H, Abi-Ghanem D, Waghela SD, Chou W-K, Farnell MB, Mwangi W, et al. Immunization of chickens with an agonistic monoclonal anti-chicken CD40 antibody–hapten complex: Rapid and robust IgG response induced by a single subcutaneous injection. *J Immunol Methods* (2012) 378(1-2):116–20. doi: 10.1016/j.jim.2012.02.006

55. Chou W-K, Chen C-H, Vuong CN, Abi-Ghanem D, Waghela SD, Mwangi W, et al. Significant mucosal sIgA production after a single oral or parenteral administration using in vivo CD40 targeting in the chicken. *Res Veterinary Science.* (2016) 108:112–5. doi: 10.1016/j.rvsc.2016.08.013

56. Vuong CN, Chou W-K, Briggs W, Faulkner O, Wolfenden A, Jonas M, et al. Crude inactivated influenza a virus adjuvated with a bispecific antibody complex targeting chicken CD40 and AIV M2e confers protection against lethal HPA I challenge in chickens. *Monoclonal Antibodies Immunodiagnosis Immunother* (2018) 37(6):245–51. doi: 10.1089/mab.2018.0040

57. Thacker EE, Nakayama M, Smith BF, Bird RC, Muminova Z, Strong TV, et al. A genetically engineered adenovirus vector targeted to CD40 mediates transduction of canine dendritic cells and promotes antigen-specific immune responses *in vivo*. *Vaccine* (2009) 27(50):7116–24. doi: 10.1016/j.vaccine.2009.09.055

58. Shrestha A, Sadeyen J-R, Lukosaityte D, Chang P, Smith A, Van Hulten M, et al. Selectively targeting haemagglutinin antigen to chicken CD83 receptor induces faster and stronger immunity against avian influenza. *NPJ Vaccines* (2021) 6(1):1–12. doi: 10.1038/s41541-021-00350-3

59. Shrestha A, Meeuws R, Sadeyen J-R, Chang P, Van Hulten M, Iqbal M. Haemagglutinin antigen selectively targeted to chicken CD83 overcomes interference from maternally derived antibodies in chickens. *NPJ Vaccines* (2022) 7(1):1–8. doi: 10.1038/s41541-022-00448-2

60. Wang X, Wang L, Huang X, Ma S, Yu M, Shi W, et al. Oral delivery of probiotics expressing dendritic cell-targeting peptide fused with porcine epidemic diarrhea virus COE antigen: A promising vaccine strategy against PEDV. *Viruses* (2017) 9(11):312. doi: 10.3390/v9110312

61. Hou X, Jiang X, Jiang Y, Tang L, Xu Y, Qiao X, et al. Oral immunization against PEDV with recombinant lactobacillus casei expressing dendritic cell-targeting peptide fusing COE protein of PEDV in piglets. *Viruses* (2018) 10(3):106. doi: 10.3390/v10030106

62. Xia T, Yang H, Guo Y, Guo T, Xin L, Jiang Y, et al. Human dendritic cell targeting peptide can be targeted to porcine dendritic cells to improve antigen capture efficiency to stimulate stronger immune response. *Front Immunol* (2022) 13. doi: 10.3389/fimmu.2022.950597

63. Huang K-Y, Yang G-L, Jin Y-B, Liu J, Chen H-L, Wang P-B, et al. Construction and immunogenicity analysis of lactobacillus plantarum expressing a porcine epidemic diarrhea virus s gene fused to a DC-targeting peptide. *Virus Res* (2018) 247:84–93. doi: 10.1016/j.virusres.2017.12.011

64. Jin Y-B, Yang W-T, Shi C-W, Feng B, Huang K-Y, Zhao G-X, et al. Immune responses induced by recombinant lactobacillus plantarum expressing the spike protein derived from transmissible gastroenteritis virus in piglets. *Appl Microbiol Biotechnol* (2018) 102(19):8403–17. doi: 10.1007/s00253-018-9205-0

65. Lu Y, Liu Z-H, Li Y-X, Xu H-L, Fang W-H, He F. Targeted delivery of nanovaccine to dendritic cells *via* DC-binding peptides induces potent antiviral immunity *in vivo*. *Int J Nanomedicine* (2022) 17:1593. doi: 10.2147/IJN.S357462

66. Wang Y, Feng B, Niu C, Jia S, Sun C, Wang Z, et al. Dendritic cell targeting of bovine viral diarrhea virus E2 protein expressed by lactobacillus casei effectively induces antigen-specific immune responses *via* oral vaccination. *Viruses* (2019) 11 (6):575. doi: 10.3390/v11060575

67. Jiang Y, Hu J, Guo Y, Yang W, Ye L, Shi C, et al. Construction and immunological evaluation of recombinant lactobacillus plantarum expressing HN of Newcastle disease virus and DC-targeting peptide fusion protein. *J Biotechnol* (2015) 216:82–9. doi: 10.1016/j.jbiotec.2015.09.033

68. Sun Y, Qian J, Xu X, Tang Y, Xu W, Yang W, et al. Dendritic cell-targeted recombinantLactobacilli induce DC activation and elicit specific immune responses against G57 genotype of avian H9N2 influenza virus infection. *Veterinary Microbiol* (2018) 223:9–20. doi: 10.1016/j.vetmic.2018.07.009

69. Shi S-H, Yang W-T, Yang G-L, Zhang X-K, Liu Y-Y, Zhang L-J, et al. Lactobacillus plantarum vaccine vector expressing hemagglutinin provides protection against H9N2 challenge infection. *Virus Res* (2016) 211:46–57. doi: 10.1016/j.virusres.2015.09.005

70. Chen W, Ma C, Wang D, Li G, Ma D. Immune response and protective efficacy of recombinant enterococcus faecalis displaying dendritic cell–targeting peptide fused with eimeria tenella 3-1E protein. *Poultry science.* (2020) 99(6):2967–75. doi: 10.1016/j.psj.2020.03.014

71. Xu X, Qian J, Qin L, Li J, Xue C, Ding J, et al. Chimeric Newcastle disease virus-like particles containing DC-binding peptide-fused haemagglutinin protect chickens from virulent Newcastle disease virus and H9N2 avian influenza virus challenge. *Virologica Sinica.* (2020) 35(4):455–67. doi: 10.1007/s12250-020-00199-1

72. Wang J, Jiang H, Yang R, Zhang S, Zhao W, Hu J, et al. Construction and evaluation of recombinant lactobacillus plantarum NC8 delivering one single or two copies of G protein fused with a DC-targeting peptide (DCpep) as novel oral rabies vaccine. *Veterinary Microbiol* (2020) 251:108906. doi: 10.1016/j.vetmic.2020.108906

73. Subramaniam S, Piñeyro P, Derscheid RJ, Madson DM, Magstadt DR, Meng X-J. Dendritic cell-targeted porcine reproductive and respiratory syndrome virus (PRRSV) antigens adjuvanted with polyinosinic-polycytidylic acid (poly (I: C)) induced non-protective immune responses against heterologous type 2 PRRSV challenge in pigs. *Veterinary Immunol immunopathology.* (2017) 190:18–25. doi: 10.1016/j.vetimm.2017.07.003

74. Subramaniam S, Piñeyro P, Tian D, Overend C, Yugo DM, Matzinger SR, et al. in vivo targeting of porcine reproductive and respiratory syndrome virus antigen through porcine DC-SIGN to dendritic cells elicits antigen-specific CD4T cell immunity in pigs. *Vaccine* (2014) 32(50):6768–75. doi: 10.1016/j.vaccine.2014.10.005

75. Chrun T, Lacôte S, Urien C, Richard C-A, Tenbusch M, Aubrey N, et al. A DNA vaccine encoding the gn ectodomain of rift valley fever virus protects mice *via* a humoral response decreased by dec205 targeting. *Front Immunol* (2019) 10:860. doi: 10.3389/fimmu.2019.00860

76. Bustamante-Córdova L, Reséndiz-Sandoval M, Hernández J. Evaluation of a recombinant mouse X pig chimeric anti-porcine DEC205 antibody fused with structural and nonstructural peptides of PRRS virus. *Vaccines* (2019) 7(2):43. doi: 10.3390/vaccines7020043

77. Melgoza-González EA, Reséndiz-Sandoval M, Hinojosa-Trujillo D, Hernández-Valenzuela S, García-Vega M, Mata-Haro V, et al. Antigen targeting of porcine skin DEC205+ dendritic cells. *Vaccines* (2022) 10(5):684. doi: 10.3390/vaccines10050684

78. Jáuregui-Zúñiga D, Pedraza-Escalona M, Espino-Solís GP, Quintero-Hernández V, Olvera-Rodríguez A, Díaz-Salinas MA, et al. Targeting antigens to Dec-205 on dendritic cells induces a higher immune response in chickens: Hemagglutinin of avian influenza virus example. *Res veterinary science.* (2017) 111:55–62. doi: 10.1016/j.rvsc.2016.12.002

79. Jáuregui-Zúñiga D, Pedraza-Escalona M, Merino-Guzman R, Possani LD. Construction and expression of a single-chain variable fragment antibody against chicken DEC 205 for targeting the bacterial expressed hemagglutinin-neuraminidase of Newcastle disease virus. *Veterinary Immunol immunopathology.* (2019) 212:9–14. doi: 10.1016/j.vetimm.2019.05.001

80. Mucksová J, Plachý J, Staněk O, Hejnar J, Kalina J, Benešová B, et al. Cytokine response to the RSV antigen delivered by dendritic cell-directed vaccination in congenic chicken lines. *Veterinary Res* (2017) 48(1):1–14. doi: 10.1186/s13567-017-0423-8

81. Devriendt B, Verdonck F, Summerfield A, Goddeeris BM, Cox E. Targeting of *Escherichia coli* F4 fimbriae to fcγ receptors enhances the maturation of porcine dendritic cells. *Veterinary Immunol immunopathology* (2010) 135(3-4):188–98. doi: 10.1016/j.vetimm.2009.11.013

82. Subramaniam S, Cao D, Tian D, Cao QM, Overend C, Yugo DM, et al. Efficient priming of CD4 T cells by langerin-expressing dendritic cells targeted with porcine epidemic diarrhea virus spike protein domains in pigs. *Virus Res* (2017) 227:212–9. doi: 10.1016/j.virusres.2016.10.007

83. Subramaniam S, Yugo DM, Heffron CL, Rogers AJ, Sooryanarain H, LeRoith T, et al. Vaccination of sows with a dendritic cell-targeted porcine epidemic diarrhea virus S1 protein-based candidate vaccine reduced viral shedding but exacerbated gross pathological lesions in suckling neonatal piglets. *J Gen Virology.* (2018) 99(2):230–9. doi: 10.1099/jgv.0.001001

84. Zhang F, Zhang Z, Li X, Li J, Lv J, Ma Z, et al. Immune responses to orally administered recombinant *Lactococcus lactis* expressing multi-epitope proteins targeting m cells of foot-and-Mouth disease virus. *Viruses* (2021) 13(10):2036. doi: 10.3390/v13102036

85. Wu Y, Yan C, Ja He, Xiong W, Wu S, Liu S, et al. Reversible mannosylation as a covalent binding adjuvant enhances immune responses for porcine circovirus type 2 vaccine. *ACS Omega.* (2018) 3(12):17341–7. doi: 10.1021/acsomega.8b02264

86. Huang J, Liu H, Wang M, Bai X, Cao J, Zhang Z, et al. Mannosylated gelatin nanoparticles enhanced inactivated PRRSV targeting dendritic cells and increased T cell immunity. *Veterinary Immunol Immunopathology.* (2021) 235:110237. doi: 10.1016/j.vetimm.2021.110237

87. Renu S, Feliciano-Ruiz N, Patil V, Schrock J, Han Y, Ramesh A, et al. Immunity and protective efficacy of mannose conjugated chitosan-based influenza nanovaccine in maternal antibody positive pigs. *Front Immunol* (2021) 12:584299. doi: 10.3389/fimmu.2021.584299

88. Argilaguet J, Pérez-Martín E, Gallardo C, Salguero F, Borrego B, Lacasta A, et al. Enhancing DNA immunization by targeting ASFV antigens to SLA-II bearing cells. *Vaccine* (2011) 29(33):5379–85. doi: 10.1016/j.vaccine.2011.05.084

89. Borrego B, Argilaguet JM, Pérez-Martín E, Dominguez J, Pérez-Filgueira M, Escribano JM, et al. A DNA vaccine encoding foot-and-mouth disease virus b and T-cell epitopes targeted to class II swine leukocyte antigens protects pigs against viral challenge. *Antiviral Res* (2011) 92(2):359–63. doi: 10.1016/j.antiviral.2011.07.017

90. Mwangi W, Brown WC, Splitter GA, Davies CJ, Howard CJ, Hope JC, et al. DNA Vaccine construct incorporating intercellular trafficking and intracellular targeting motifs effectively primes and induces memory b-and T-cell responses in outbred animals. *Clin Vaccine Immunol* (2007) 14(3):304–11. doi: 10.1128/CVI.00363-06

91. Aguirreburualde MSP, Gómez MC, Ostachuk A, Wolman F, Albanesi G, Pecora A, et al. Efficacy of a BVDV subunit vaccine produced in alfalfa transgenic plants. *Veterinary Immunol immunopathology* (2013) 151(3-4):315–24. doi: 10.1016/j.vetimm.2012.12.004

92. Bellido D, Baztarrica J, Rocha L, Pecora A, Acosta M, Escribano JM, et al. A novel MHC-II targeted BVDV subunit vaccine induces a neutralizing immunological response in guinea pigs and cattle. *Transboundary Emerging Diseases*. (2021) 68 (6):3474–81. doi: 10.1111/tbed.13952

93. Pecora A, Malacari DA, Aguirreburualde MSP, Bellido D, Escribano JM, Santos MJD, et al. Development of an enhanced bovine viral diarrhea virus subunit vaccine based on E2 glycoprotein fused to a single chain antibody which targets to antigen-presenting cells. *Rev Argent Microbiologia*. (2015) 47(1):4–8. doi: 10.1016/j.ram.2014.12.004

94. Legisa DM, Aguirreburualde MP, Gonzalez F, Marin-Lopez A, Ruiz V, Wigdorovitz A, et al. An experimental subunit vaccine based on bluetongue virus 4 VP2 protein fused to an antigen-presenting cells single chain antibody elicits cellular and humoral immune responses in cattle, guinea pigs and IFNAR (–/–) mice. *Vaccine* (2015) 33(22):2614–9. doi: 10.1016/j.vaccine.2015.03.067

95. Gil F, Pérez-Filgueira M, Barderas µg, Pastor-Vargas C, Alonso C, Vivanco F, et al. Targeting antigens to an invariant epitope of the MHC class II DR molecule potentiates the immune response to subunit vaccines. *Virus Res* (2011) 155(1):55–60. doi: 10.1016/j.virusres.2010.08.022

96. Revilla C, Poderoso T, Martínez P, Álvarez B, López-Fuertes L, Alonso F, et al. Targeting to porcine sialoadhesin receptor receptor improves antigen presentation to T cells. *Veterinary Res* (2009) 40(3):1–15. doi: 10.1051/vetres:2008052

97. Ooms K, Van Gorp H, Botti S, Van Gaever T, Delputte PL, Nauwynck HJ. Evaluation of viral peptide targeting to porcine sialoadhesin using a porcine reproductive and respiratory syndrome virus vaccination-challenge model. *Virus Res* (2013) 177(2):147–55. doi: 10.1016/j.virusres.2013.07.019

98. Bernelin-Cottet C, Urien C, Stubsrud E, Jakob V, Bouguyon E, Bordet E, et al. A DNA-modified live vaccine prime–boost strategy broadens the t-cell response and enhances the antibody response against the porcine reproductive and respiratory syndrome virus. *Viruses* (2019) 11(6):551. doi: 10.3390/v11060551

99. Deloizy C, Fossum E, Barnier-Quer C, Urien C, Chrun T, Duval A, et al. The anti-influenza M2e antibody response is promoted by XCR1 targeting in pig skin. *Sci Rep* (2017) 7(1):1–12. doi: 10.1038/s41598-017-07372-9

100. Li K, Bao H, Wei G, Li D, Chen Y, Fu Y, et al. Molecular vaccine prepared by fusion of XCL1 to the multi-epitope protein of foot-and-mouth disease virus enhances the specific humoural immune response in cattle. *Appl Microbiol Biotechnol* (2017) 101 (21):7889–900. doi: 10.1007/s00253-017-8523-y

101. Idoyaga J, Lubkin A, Fiorese C, Lahoud MH, Caminschi I, Huang Y, et al. Comparable T helper 1 (Th1) and CD8 T-cell immunity by targeting HIV gag p24 to CD8 dendritic cells within antibodies to langerin, DEC205, and Clec9A. *Proc Natl Acad Sci* (2011) 108(6):2384–9. doi: 10.1073/pnas.1019547108

102. Kato M, McDonald KJ, Khan S, Ross IL, Vuckovic S, Chen K, et al. Expression of human DEC-205 (CD205) multilectin receptor on leukocytes. *Int Immunol* (2006) 18(6):857–69. doi: 10.1093/intimm/dxl022

103. Auray G, Keller I, Python S, Gerber M, Bruggmann R, Ruggli N, et al. Characterization and transcriptomic analysis of porcine blood conventional and plasmacytoid dendritic cells reveals striking species-specific differences. *J Immunol* (2016) 197(12):4791–806. doi: 10.4049/jimmunol.1600672

104. Talker SC, Baumann A, Barut GT, Keller I, Bruggmann R, Summerfield A. Precise delineation and transcriptional characterization of bovine blood dendritic-cell and monocyte subsets. *Front Immunol* (2018) 9:2505. doi: 10.3389/fimmu.2018.02505

105. Flores-Mendoza L, Sotelo-Mundo RR, Dawson H, Mwangi W, Hernández J. Characterization of porcine CD205. *Dev Comp Immunol* (2010) 34(7):715–21. doi: 10.1016/j.dci.2010.02.010

106. Kato M, Neil TK, Clark GJ, Morris CM, Sorg R, Hart DN. cDNA cloning of human DEC-205, a putative antigen-uptake receptor on dendritic cells. *Immunogenetics* (1998) 47(6):442–50. doi: 10.1007/s002510050381

107. Swiggard WJ, Mirza A, Nussenzweig MC, Steinman RM. DEC-205, a 205-kDa protein abundant on mouse dendritic cells and thymic epithelium that is detected by the monoclonal antibody NLDC-145: Purification, characterization, and n-terminal amino acid sequence. *Cell Immunol* (1995) 165(2):302–11. doi: 10.1006/cimm.1995.1218

108. Gliddon DR, Hope JC, Brooke GP, Howard CJ. DEC-205 expression on migrating dendritic cells in afferent lymph. *Immunology* (2004) 111(3):262–72. doi: 10.1111/j.0019-2805.2004.01820.x

109. Jiang W, Swiggard WJ, Heufler C, Peng M, Mirza A, Steinman RM, et al. The receptor DEC-205 expressed by dendritic cells and thymic epithelial cells is involved in antigen processing. *Nature* (1995) 375(6527):151. doi: 10.1038/375151a0

110. Joffre OP, Segura E, Savina A, Amigorena S. Cross-presentation by dendritic cells. *Nat Rev Immunol* (2012) 12(8):557–69. doi: 10.1038/nri3254

111. Stahl PD, Ezekowitz RAB. The mannose receptor is a pattern recognition receptor involved in host defense. *Curr Opin Immunol* (1998) 10(1):50–5. doi: 10.1016/S0952-7915(98)80031-9

112. Allavena P, Chieppa M, Monti P, Piemonti L. From pattern recognition receptor to regulator of homeostasis: the double-faced macrophage mannose receptor. *Crit Reviews™ Immunol* (2004) 24(3):179–92. doi: 10.1615/CritRevImmunol.v24.i3.20

113. Tailleux L, Schwartz O, Herrmann J-L, Pivert E, Jackson M, Amara A, et al. DC-SIGN is the major *Mycobacterium tuberculosis* receptor on human dendritic cells. *J Exp Med* (2003) 197(1):121–7. doi: 10.1084/jem.20021468

114. Cambi A, Gijzen K, de Vries IJM, Torensma R, Joosten B, Adema GJ, et al. The c-type lectin DC-SIGN (CD209) is an antigen-uptake receptor for *Candida albicans* on dendritic cells. *Eur J Immunol* (2003) 33(2):532–8. doi: 10.1002/immu.200310029

115. Colmenares M, Puig-Kroüger A, Pello O, Corbı AL, Rivas L. Dendritic cell (DC)-specific intercellular adhesion molecule 3 (ICAM-3)-grabbing nonintegrin (DC-SIGN, CD209), a c-type surface lectin in human DCs, is a receptor for LeishmaniaAmastigotes. *J Biol Chem* (2002) 277(39):36766–9. doi: 10.1074/jbc.M205270200

116. Soilleux EJ, Morris LS, Leslie G, Chehimi J, Luo Q, Levroney E, et al. Constitutive and induced expression of DC-SIGN on dendritic cell and macrophage subpopulations *in situ* and *in vitro*. *J leukocyte Biol* (2002) 71(3):445–57. doi: 10.1189/jlb.71.3.445

117. Geijtenbeek TB, Torensma R, van Vliet SJ, van Duijnhoven GC, Adema GJ, van Kooyk Y, et al. Identification of DC-SIGN, a novel dendritic cell–specific ICAM-3 receptor that supports primary immune responses. *Cell* (2000) 100(5):575–85. doi: 10.1016/S0092-8674(00)80693-5

118. Tacken PJ, Ginter W, Berod L, Cruz LJ, Joosten B, Sparwasser T, et al. Targeting DC-SIGN *via* its neck region leads to prolonged antigen residence in early endosomes, delayed lysosomal degradation, and cross-presentation. *Blood J Am Soc Hematology*. (2011) 118(15):4111–9. doi: 10.1182/blood-2011-04-346957

119. van Kooyk Y, Unger WW, Fehres CM, Kalay H, García-Vallejo JJ. Glycan-based DC-SIGN targeting vaccines to enhance antigen cross-presentation. *Mol Immunol* (2013) 55(2):143–5. doi: 10.1016/j.molimm.2012.10.031

120. Summerfield A, Meurens F, Ricklin ME. The immunology of the porcine skin and its value as a model for human skin. *Mol Immunol* (2015) 66(1):14–21. doi: 10.1016/j.molimm.2014.10.023

121. Marquet F, Bonneau M, Pascale F, Urien C, Kang C, Schwartz-Cornil I, et al. Characterization of dendritic cells subpopulations in skin and afferent lymph in the swine model. *PloS One* (2011) 6(1):e16320. doi: 10.1371/journal.pone.0016320

122. Marquet F, Manh T-PV, Maisonnasse P, Elhmouzi-Younes J, Urien C, Bouguyon E, et al. Pig skin includes dendritic cell subsets transcriptomically related to human CD1a and CD14 dendritic cells presenting different migrating behaviors and T cell activation capacities. *J Immunol* (2014) 193(12):5883–93. doi: 10.4049/jimmunol.1303150

123. Tripp CH, Chang-Rodriguez S, Stoitzner P, Holzmann S, Stössel H, Douillard P, et al. Ontogeny of Langerin/CD207 expression in the epidermis of mice. *J Invest Dermatol* (2004) 122(3):670–2. doi: 10.1111/j.0022-202X.2004.22337.x

124. Idoyaga J, Suda N, Suda K, Park CG, Steinman RM. Antibody to Langerin/CD207 localizes large numbers of CD8α+ dendritic cells to the marginal zone of mouse spleen. *Proc Natl Acad Sci* (2009) 106(5):1524–9. doi: 10.1073/pnas.0812247106

125. Bursch LS, Wang L, Igyarto B, Kissenpfennig A, Malissen B, Kaplan DH, et al. Identification of a novel population of langerin+ dendritic cells. *J Exp Med* (2007) 204 (13):3147–56. doi: 10.1084/jem.20071966

126. Valladeau J, Ravel O, Dezutter-Dambuyant C, Moore K, Kleijmeer M, Liu Y, et al. Langerin, a novel c-type lectin specific to langerhans cells, is an endocytic receptor that induces the formation of birbeck granules. *Immunity* (2000) 12(1):71–81. doi: 10.1016/S1074-7613(00)80160-0

127. Idoyaga J, Cheong C, Suda K, Suda N, Kim JY, Lee H, et al. Cutting edge: Langerin/CD207 receptor on dendritic cells mediates efficient antigen presentation on MHC I and II products *in vivo*. *J Immunol* (2008) 180(6):3647–50. doi: 10.4049/jimmunol.180.6.3647

128. Fehres CM, Duinkerken S, Bruijns S, Kalay H, Van Vliet SJ, Ambrosini M, et al. Langerin-mediated internalization of a modified peptide routes antigens to early endosomes and enhances cross-presentation by human langerhans cells. *Cell Mol Immunol* (2017) 14(4):360–70. doi: 10.1038/cmi.2015.87

129. Stambach NS, Taylor ME. Characterization of carbohydrate recognition by langerin, a c-type lectin of langerhans cells. *Glycobiology* (2003) 13(5):401–10. doi: 10.1093/glycob/cwg045

130. Watts C. Capture and processing of exogenous antigens for presentation on MHC molecules. *Annu Rev Immunol* (1997) 15:821. doi: 10.1146/annurev.immunol.15.1.821

131. Shin J-S, Ebersold M, Pypaert M, Delamarre L, Hartley A, Mellman I. Surface expression of MHC class II in dendritic cells is controlled by regulated ubiquitination. *Nature* (2006) 444(7115):115–8. doi: 10.1038/nature05261

132. Furuta K, Walseng E, Roche PA. Internalizing MHC class II–peptide complexes are ubiquitinated in early endosomes and targeted for lysosomal degradation. *Proc Natl Acad Sci* (2013) 110(50):20188–93. doi: 10.1073/pnas.1312994110

133. van Niel G, Wubbolts R, Stoorvogel W. Endosomal sorting of MHC class II determines antigen presentation by dendritic cells. *Curr Opin Cell Biol* (2008) 20 (4):437–44. doi: 10.1016/j.ceb.2008.05.011

134. Dickgreber N, Stoitzner P, Bai Y, Price KM, Farrand KJ, Manning K, et al. Targeting antigen to MHC class II molecules promotes efficient cross-presentation and enhances immunotherapy. *J Immunol* (2009) 182(3):1260–9. doi: 10.4049/jimmunol.182.3.1260

135. van Kooten C, Banchereau J. CD40-CD40 ligand. *J leukocyte Biol* (2000) 67 (1):2–17. doi: 10.1002/jlb.67.1.2

136. Quezada SA, Jarvinen LZ, Lind EF, Noelle RJ. CD40/CD154 interactions at the interface of tolerance and immunity. *Annu Rev Immunol* (2004) 22:307. doi: 10.1146/annurev.immunol.22.012703.104533

137. Cella M, Scheidegger D, Palmer-Lehmann K, Lane P, Lanzavecchia A, Alber G. Ligation of CD40 on dendritic cells triggers production of high levels of interleukin-12 and enhances T cell stimulatory capacity: TT help *via* APC activation. *J Exp Med* (1996) 184(2):747–52. doi: 10.1084/jem.184.2.747

138. Kelleher M, Beverley PC. Lipopolysaccharide modulation of dendritic cells is insufficient to mature dendritic cells to generate CTLs from naive polyclonal CD8+ T cells in vitro, whereas CD40 ligation is essential. *J Immunol* (2001) 167(11):6247–55. doi: 10.4049/jimmunol.167.11.6247

139. Borrow P, Tishon A, Lee S, Xu J, Grewal IS, Oldstone M, et al. CD40L-deficient mice show deficits in antiviral immunity and have an impaired memory CD8+ CTL response. *J Exp Med* (1996) 183(5):2129–42. doi: 10.1084/jem.183.5.2129

140. Mackay F, Schneider P, Rennert P, Browning J. BAFF AND APRIL: a tutorial on b cell survival. *Annu Rev Immunol* (2003) 21:231. doi: 10.1146/annurev.immunol.21.120601.141152

141. Konrad A, Cong Y, Duck W, Borlaza R, Elson CO. Tight mucosal compartmentation of the murine immune response to antigens of the enteric microbiota. *Gastroenterology* (2006) 130(7):2050–9. doi: 10.1053/j.gastro.2006.02.055

142. Craxton A, Magaletti D, Ryan EJ, Clark EA. Macrophage-and dendritic cell–dependent regulation of human b-cell proliferation requires the TNF family ligand BAFF. *Blood* (2003) 101(11):4464–71. doi: 10.1182/blood-2002-10-3123

143. Cohn L, Chatterjee B, Esselborn F, Smed-Sörensen A, Nakamura N, Chalouni C, et al. Antigen delivery to early endosomes eliminates the superiority of human blood BDCA3+ dendritic cells at cross presentation. *J Exp Med* (2013) 210(5):1049–63. doi: 10.1084/jem.20121251

144. Yin W, Gorvel L, Zurawski S, Li D, Ni L, Duluc D, et al. Functional specialty of CD40 and dendritic cell surface lectins for exogenous antigen presentation to CD8+ and CD4+ T cells. *EBioMedicine* (2016) 5:46–58. doi: 10.1016/j.ebiom.2016.01.029

145. Lim TS, Goh JKH, Mortellaro A, Lim CT, Hämmerling GJ, Ricciardi-Castagnoli P. CD80 and CD86 differentially regulate mechanical interactions of T-cells with antigen-presenting dendritic cells and b-cells. *PloS one* (2012) 7(9):e45185. doi: 10.1371/journal.pone.0045185

146. Balbo P, Silvestri M, Rossi G, Crimi E, Burastero S. Differential role of CD80 and CD86 on alveolar macrophages in the presentation of allergen to T lymphocytes in asthma. *Clin Exp Allergy* (2001) 31(4):625–36. doi: 10.1046/j.1365-2222.2001.01068.x

147. Rudd CE, Taylor A, Schneider H. CD28 and CTLA-4 coreceptor expression and signal transduction. *Immunol Rev* (2009) 229(1):12–26. doi: 10.1111/j.1600-065X.2009.00770.x

148. Curiel TJ, Morris C, Brumlik M, Landry SJ, Finstad K, Nelson A, et al. Peptides identified through phage display direct immunogenic antigen to dendritic cells. *J Immunol* (2004) 172(12):7425–31. doi: 10.4049/jimmunol.172.12.7425

149. Ma S, Qiao X, Xu Y, Wang L, Zhou H, Jiang Y, et al. Screening and identification of a chicken dendritic cell binding peptide by using a phage display library. *Front Immunol* (2019) 10:1853. doi: 10.3389/fimmu.2019.01853

150. Vilander AC, Dean GA. Adjuvant strategies for lactic acid bacterial mucosal vaccines. *Vaccines* (2019) 7(4):150. doi: 10.3390/vaccines7040150

151. Geissmann F, Jung S, Littman DR. Blood monocytes consist of two principal subsets with distinct migratory properties. *Immunity* (2003) 19(1):71–82. doi: 10.1016/S1074-7613(03)00174-2

152. Probst H, Tschannen K, Odermatt B, Schwendener R, Zinkernagel R, Van Den Broek M. Histological analysis of CD11c-DTR/GFP mice after in vivo depletion of dendritic cells. *Clin Exp Immunol* (2005) 141(3):398–404. doi: 10.1111/j.1365-2249.2005.02868.x

153. Van Brussel I, Van Vré EA, De Meyer GR, Vrints CJ, Bosmans JM, Bult H. Expression of dendritic cell markers CD11c/BDCA-1 and CD123/BDCA-2 in coronary artery disease upon activation in whole blood. *J Immunol Methods* (2010) 362(1-2):168–75. doi: 10.1016/j.jim.2010.09.031

154. Sándor N, Lukacsi S, Ungai-Salanki R, Orgovan N, Szabó B, Horváth R, et al. CD11c/CD18 dominates adhesion of human monocytes, macrophages and dendritic cells over CD11b/CD18. *PloS One* (2016) 11(9):e0163120. doi: 10.1371/journal.pone.0163120

155. Ihanus E, Uotila LM, Toivanen A, Varis M, Gahmberg CG. Red-cell ICAM-4 is a ligand for the monocyte/macrophage integrin CD11c/CD18: characterization of the binding sites on ICAM-4. *Blood* (2007) 109(2):802–10. doi: 10.1182/blood-2006-04-014878

156. Ingalls RR, Golenbock DT. CD11c/CD18, a transmembrane signaling receptor for lipopolysaccharide. *J Exp Med* (1995) 181(4):1473–9. doi: 10.1084/jem.181.4.1473

157. Castro FV, Tutt AL, White AL, Teeling JL, James S, French RR, et al. CD11c provides an effective immunotarget for the generation of both CD4 and CD8 T cell responses. *Eur J Immunol* (2008) 38(8):2263–73. doi: 10.1002/eji.200838302

158. Cruz LJ, Rosalia RA, Kleinovink JW, Rueda F, Löwik CW, Ossendorp F. Targeting nanoparticles to CD40, DEC-205 or CD11c molecules on dendritic cells for efficient CD8+ T cell response: A comparative study. *J Controlled Release.* (2014) 192:209–18. doi: 10.1016/j.jconrel.2014.07.040

159. Hartnell A, Steel J, Turley H, Jones M, Jackson DG, Crocker PR. Characterization of human sialoadhesin, a sialic acid binding receptor expressed by resident and inflammatory macrophage populations. *Blood J Am Soc Hematology.* (2001) 97(1):288–96. doi: 10.1182/blood.V97.1.288

160. O'Neill AS, van den Berg TK, Mullen GE. Sialoadhesin–a macrophage-restricted marker of immunoregulation and inflammation. *Immunology* (2013) 138 (3):198–207. doi: 10.1111/imm.12042

161. van Dinther D, Veninga H, Iborra S, Borg EG, Hoogterp L, Olesek K, et al. Functional CD169 on macrophages mediates interaction with dendritic cells for CD8+ T cell cross-priming. *Cell Rep* (2018) 22(6):1484–95. doi: 10.1016/j.celrep.2018.01.021

162. Van den Berg T, Breve J, Damoiseaux J, Döpp E, Kelm S, Crocker P, et al. Sialoadhesin on macrophages: its identification as a lymphocyte adhesion molecule. *J Exp Med* (1992) 176(3):647–55. doi: 10.1084/jem.176.3.647

163. Crocker PR, Freeman S, Gordon S, Kelm S. Sialoadhesin binds preferentially to cells of the granulocytic lineage. *J Clin Invest* (1995) 95(2):635–43. doi: 10.1172/JCI117708

164. Grabowska J, Lopez-Venegas MA, Affandi AJ, Den Haan JM. CD169+ macrophages capture and dendritic cells instruct: The interplay of the gatekeeper and the general of the immune system. *Front Immunol* (2018) 9:2472. doi: 10.3389/fimmu.2018.02472

165. Dorner BG, Dorner MB, Zhou X, Opitz C, Mora A, Güttler S, et al. Selective expression of the chemokine receptor XCR1 on cross-presenting dendritic cells determines cooperation with CD8+ T cells. *Immunity* (2009) 31(5):823–33. doi: 10.1016/j.immuni.2009.08.027

166. Bachem A, Güttler S, Hartung E, Ebstein F, Schaefer M, Tannert A, et al. Superior antigen cross-presentation and XCR1 expression define human CD11c+ CD141+ cells as homologues of mouse CD8+ dendritic cells. *J Exp Med* (2010) 207 (6):1273–81. doi: 10.1084/jem.20100348

167. Crozat K, Guiton R, Contreras V, Feuillet V, Dutertre C-A, Ventre E, et al. The XC chemokine receptor 1 is a conserved selective marker of mammalian cells homologous to mouse CD8α+ dendritic cells. *J Exp Med* (2010) 207(6):1283–92. doi: 10.1084/jem.20100223

168. Li K, Wei G, Cao Y, Li D, Li P, Zhang J, et al. The identification and distribution of cattle XCR1 and XCL1 among peripheral blood cells: new insights into the design of dendritic cells targeted veterinary vaccine. *PloS One* (2017) 12(1):e0170575. doi: 10.1371/journal.pone.0170575

169. Deloizy C, Bouguyon E, Fossum E, Sebo P, Osicka R, Bole A, et al. Expanding the tools for identifying mononuclear phagocyte subsets in swine: Reagents to porcine CD11c and XCR1. *Dev Comp Immunol* (2016) 65:31–40. doi: 10.1016/j.dci.2016.06.015

170. Gudjonsson A, Lysén A, Balan S, Sundvold-Gjerstad V, Arnold-Schrauf C, Richter L, et al. Targeting influenza virus hemagglutinin to Xcr1+ dendritic cells in the absence of receptor-mediated endocytosis enhances protective antibody responses. *J Immunol* (2017) 198(7):2785–95. doi: 10.4049/jimmunol.1601881

171. Biragyn A, Ruffini PA, Coscia M, Harvey LK, Neelapu SS, Baskar S, et al. Chemokine receptor-mediated delivery directs self-tumor antigen efficiently into the class II processing pathway in vitro and induces protective immunity *in vivo*. *Blood* (2004) 104(7):1961–9. doi: 10.1182/blood-2004-02-0637

172. Biragyn A, Tani K, Grimm MC, Weeks S, Kwak LW. Genetic fusion of chemokines to a self tumor antigen induces protective, T-cell dependent antitumor immunity. *Nat Biotechnol* (1999) 17(3):253–8. doi: 10.1038/6995

173. Sarrias MR, Gronlund J, Padilla O, Madsen J, Holmskov U, Lozano F. The scavenger receptor cysteine-rich (SRCR) domain: An ancient and highly conserved protein module of the innate immune system. *Crit Reviews™ Immunol* (2004) 24(1):1–37. doi: 10.1615/CritRevImmunol.v24.i1.10

174. Sulahian TH, Högger P, Wahner AE, Wardwell K, Goulding NJ, Sorg C, et al. Human monocytes express CD163, which is upregulated by IL-10 and identical to p155. *Cytokine* (2000) 12(9):1312–21. doi: 10.1006/cyto.2000.0720

175. Chamorro S, Revilla C, Alvarez B, Alonso F, Ezquerra A, Domínguez J. Phenotypic and functional heterogeneity of porcine blood monocytes and its relation with maturation. *Immunology* (2005) 114(1):63–71. doi: 10.1111/j.1365-2567.2004.01994.x

176. Van Gorp H, Delputte PL, Nauwynck HJ. Scavenger receptor CD163, a jack-of-all-trades and potential target for cell-directed therapy. *Mol Immunol* (2010) 47(7-8):1650–60. doi: 10.1016/j.molimm.2010.02.008

177. Anderson CL, Shen L, Eicher DM, Wewers MD, Gill JK. Phagocytosis mediated by three distinct fc gamma receptor classes on human leukocytes. *J Exp Med* (1990) 171 (4):1333–45. doi: 10.1084/jem.171.4.1333

178. Kerntke C, Nimmerjahn F, Biburger M. There is (scientific) strength in numbers: A comprehensive quantitation of fc gamma receptor numbers on human and murine peripheral blood leukocytes. *Front Immunol* (2020) 11:118. doi: 10.3389/fimmu.2020.00118

179. Amigorena S, Bonnerot C. Fc receptor signaling and trafficking: A connection for antigen processing. *Immunol Rev* (1999) 172(1):279–84. doi: 10.1111/j.1600-065X.1999.tb01372.x

180. Soleimanpour S, Farsiani H, Mosavat A, Ghazvini K, Eydgahi MRA, Sankian M, et al. APC targeting enhances immunogenicity of a novel multistage fc-fusion tuberculosis vaccine in mice. *Appl Microbiol Biotechnol* (2015) 99(24):10467–80. doi: 10.1007/s00253-015-6952-z

181. Alleva DG, Delpero AR, Scully MM, Murikipudi S, Ragupathy R, Greaves EK, et al. Development of an IgG-fc fusion COVID-19 subunit vaccine, AKS-452. *Vaccine* (2021) 39(45):6601–13. doi: 10.1016/j.vaccine.2021.09.077

182. Kim MY, Copland A, Nayak K, Chandele A, Ahmed MS, Zhang Q, et al. Plant-expressed fc-fusion protein tetravalent dengue vaccine with inherent adjuvant properties. *Plant Biotechnol J* (2018) 16(7):1283–94. doi: 10.1111/pbi.12869

frontiers | Frontiers in Immunology

TYPE Correction
PUBLISHED 07 June 2023
DOI 10.3389/fimmu.2023.1188815

OPEN ACCESS

EDITED AND REVIEWED BY
Botond Z. Igyártó,
Thomas Jefferson University, United States

*CORRESPONDENCE
Jesús Hernández
jhdez@ciad.mx

†These authors have contributed equally to this work

RECEIVED 17 March 2023
ACCEPTED 30 May 2023
PUBLISHED 07 June 2023

CITATION
Melgoza-González EA, Bustamante-Córdova L and Hernández J (2023) Corrigendum: Recent advances in antigen targeting to antigen-presenting cells in veterinary medicine. *Front. Immunol.* 14:1188815. doi: 10.3389/fimmu.2023.1188815

Corrigendum: Recent advances in antigen targeting to antigen-presenting cells in veterinary medicine

Edgar Alonso Melgoza-González†, Lorena Bustamante-Córdova† and Jesús Hernández*

Laboratorio de Inmunología, Centro de Investigación en Alimentación y Desarrollo A. C., Hermosillo, Mexico

KEYWORDS

antigen target, antigen presenting cell, receptors, veterinary, vaccines

A corrigendum on

Recent advances in antigen targeting to antigen-presenting cells in veterinary medicine

by Melgoza-González EA, Bustamante-Córdova L and Hernández J (2023). *Front. Immunol.* 14:1080238. doi: 10.3389/fimmu.2023.1080238

In the published article, there was an error in Figure 1 as published. We noticed an error in Figure 1 related to the structure of one of the receptors (Langerin). The corrected Figure 1 and its caption appear below.

Strategies explored for antigen targeting to different APC populations. Target surface receptors on APCs and M cells evaluated in antigen targeting. Different colors represent the clusters of carriers such as nanoparticles, mannan, ligands, antibodies, DNA vaccines, proteins, virus-like particles, and viral and bacterial vectors used to target specific surface receptors.

The authors apologize for this error and state that this does not change the scientific conclusions of the article in any way. The original article has been updated.

Publisher's note

All claims expressed in this article are solely those of the authors and do not necessarily represent those of their affiliated organizations, or those of the publisher, the editors and the reviewers. Any product that may be evaluated in this article, or claim that may be made by its manufacturer, is not guaranteed or endorsed by the publisher.

10.3389/fimmu.2023.1188815

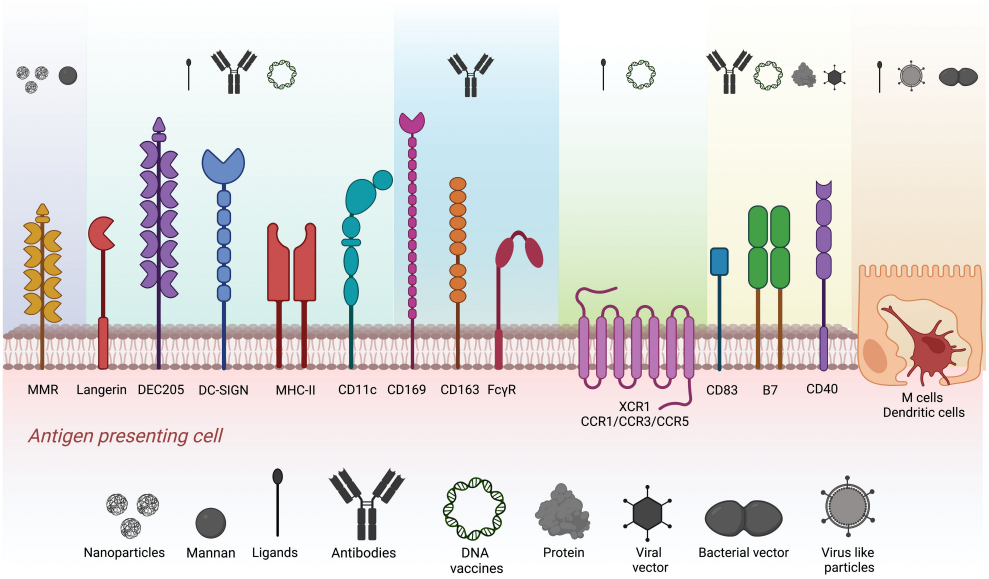

FIGURE 1
Strategies explored for antigen targeting to different APC populations. Target surface receptors on APCs and M cells evaluated in antigen targeting. Different colors represent the clusters of carriers such as nanoparticles, mannan, ligands, antibodies, DNA vaccines, proteins, virus-like particles, and viral and bacterial vectors used to target specific surface receptors.

frontiers | Frontiers in Immunology

TYPE Original Research
PUBLISHED 14 March 2023
DOI 10.3389/fimmu.2023.1138961

OPEN ACCESS

EDITED BY
Denis Archambault,
Université du Québec à Montréal, Canada

REVIEWED BY
Nan Wu,
Institute of Hydrobiology (CAS), China
Oystein Evensen,
Norwegian University of Life Sciences, Norway

*CORRESPONDENCE
Stéphane Biacchesi
stephane.biacchesi@inrae.fr
Sandra Souto
sandra.souto@usc.es

†Deceased

SPECIALTY SECTION
This article was submitted to Vaccines and Molecular Therapeutics, a section of the journal Frontiers in Immunology

RECEIVED 06 January 2023
ACCEPTED 23 February 2023
PUBLISHED 14 March 2023

CITATION
Souto S, Mérour E, Le Coupanec A, Lamoureux A, Bernard J, Brémont M, Millet JK and Biacchesi S (2023) Recombinant viral hemorrhagic septicemia virus with rearranged genomes as vaccine vectors to protect against lethal betanodavirus infection.
Front. Immunol. 14:1138961.
doi: 10.3389/fimmu.2023.1138961

Recombinant viral hemorrhagic septicemia virus with rearranged genomes as vaccine vectors to protect against lethal betanodavirus infection

Sandra Souto[1*], Emilie Mérour[2], Alain Le Coupanec[2], Annie Lamoureux[2], Julie Bernard[2], Michel Brémont[2†], Jean K. Millet[2] and Stéphane Biacchesi[2*]

[1]Microbiology and Parasitology, Universidade de Santiago de Compostela, Santiago de Compostela, Spain, [2]Université Paris-Saclay, INRAE, UVSQ, Virologie et Immunologie Moléculaires, Jouy-en-Josas, France

The outbreaks of viral hemorrhagic septicemia (VHS) and viral encephalopathy and retinopathy (VER) caused by the enveloped novirhabdovirus VHSV, and the non-enveloped betanodavirus nervous necrosis virus (NNV), respectively, represent two of the main viral infectious threats for aquaculture worldwide. Non-segmented negative-strand RNA viruses such as VHSV are subject to a transcription gradient dictated by the order of the genes in their genomes. With the goal of developing a bivalent vaccine against VHSV and NNV infection, the genome of VHSV has been engineered to modify the gene order and to introduce an expression cassette encoding the major protective antigen domain of NNV capsid protein. The NNV Linker-P specific domain was duplicated and fused to the signal peptide (SP) and the transmembrane domain (TM) derived from novirhabdovirus glycoprotein to obtain expression of antigen at the surface of infected cells and its incorporation into viral particles. By reverse genetics, eight recombinant VHSVs (rVHSV), termed NxGyCz according to the respective positions of the genes encoding the nucleoprotein (N) and glycoprotein (G) as well as the expression cassette (C) along the genome, have been successfully recovered. All rVHSVs have been fully characterized *in vitro* for NNV epitope expression in fish cells and incorporation into VHSV virions. Safety, immunogenicity and protective efficacy of rVHSVs has been tested *in vivo* in trout (*Oncorhynchus mykiss)* and sole (*Solea senegalensis*). Following bath immersion administration of the various rVHSVs to juvenile trout, some of the rVHSVs were attenuated and protective against a lethal VHSV challenge. Results indicate that rVHSV N2G1C4 is safe and protective against VHSV challenge in trout. In parallel, juvenile sole were injected with rVHSVs and challenged with NNV. The rVHSV N2G1C4 is also safe, immunogenic and efficiently protects sole against a lethal NNV challenge, thus presenting a promising starting point for the development of a bivalent live attenuated vaccine candidate for the protection of these two commercially valuable fish species against two major diseases in aquaculture.

KEYWORDS

Novirhabdovirus, betanodavirus, VHSV, NNV, live attenuated vaccine, trout, sole

Introduction

Nervous necrosis virus (NNV) is the causative agent of viral nervous necrosis (VNN), a devastating neurological disease, also known as viral encephalopathy and retinopathy (VER). The most common clinical signs of NNV infection are abnormal swimming behavior, loss of appetite and changes in fish coloration. Lesions observed in NNV-infected fish clearly demonstrate its marked neurotropism, the virus preferentially infects nerve cells, especially those of the central nervous system and retina (1). NNV has been isolated from a wide range of both marine and freshwater fish species and is responsible for significant losses in aquaculture industry as mortality rates of up to 100% are observed in larvae and juveniles infected by the virus (2). This small (~30 nm diameter), spherical, non-enveloped virus belongs to the *Betanodavirus* genus in the *Nodaviridae* family (3). Its genome contains two single-stranded positive-sense RNA molecules of approximately 3.1 kb (RNA1) and 1.4 kb (RNA2). An additional nonencapsidated subgenomic RNA coterminal with the 3' end of RNA1 (RNA3, ~0.4 kb) is transcribed during virus replication. The three RNAs are capped at their 5' ends but lack poly(A) tails at their 3' ends (4). RNA1 encodes the viral RNA-dependent RNA polymerase (RdRp, 110 kDa), whereas RNA2 encodes the capsid protein (40-42 kDa) and RNA3 encodes two small non-structural proteins B1 and B2, which have antagonistic effects on cell survival (5).

The NNV isolates have been classified into four genotypes: striped jack nervous necrosis virus (SJNNV), tiger puffer nervous necrosis virus (TPNNV), redspotted grouper nervous necrosis virus (RGNNV) and barfin flounder nervous necrosis virus (BFNNV), based on a small highly variable sequence of RNA2, the so-called T4 region (6). Furthermore, these four genotypes group into three distinct serotypes A, B, and C with RGNNV belonging to serotype C (7). RGNNV has been the predominant genotype in Europe, although the emergence of reassortant strains, between the RGNNV and SJNNV genotypes, has undergone a dramatic expansion in the past few decades in the South of Europe (8–10) posing a significant risk to the cultivation of species of great economic importance such as gilthead sea bream (*Sparus aurata*), turbot (*Scophthalmus maximus*), European sea bass (*Dicentrarchus labrax*) and Senegalese sole (*Solea senegalensis*) (11–13). Vaccination is considered crucial for VER prevention and control since no effective treatments are available for this disease in aquaculture. A significant number of new experimental vaccines for this virus have been described in recent years, yet only two are commercialized in Europe, based on an inactivated RGNNV strain delivered by injection. Thus, both vaccines are restricted to the RGNNV genotype and one fish species (European sea bass). Therefore, the search for a more effective immunization system that covers a wider number of species and genotypes is still pending.

Vaccines based on inactivated viruses are usually very safe, but immune responses elicited are generally different from that produced by the live pathogen. In contrast, the use of attenuated live viruses has led to better responses but has raised safety concerns about the possibility of reversion to a virulent phenotype. Viruses from different families have been genetically engineered to develop vector-based vaccines aimed at protecting against viral diseases. The viral vectors frequently used include vaccinia virus (*Poxviridae*), Venezuelan equine encephalitis virus (*Togaviridae*), human adenovirus (*Adenoviridae*), Sendai virus (*Paramyxoviridae*), and vesicular stomatitis virus (*Rhabdoviridae*). Rhabdoviruses (14) represent promising platforms for developing novel vaccines (15–19) because they have been shown to be an effective means for heterologous antigen expression *in vivo* due to their high carrying capacity and genomic stability (20). A member of this family, the viral hemorrhagic septicemia virus (VHSV), is the causative agent of a very contagious and acute systemic disease leading to high mortality in a large panel of wild and commercial fish species worldwide (21). VHSV is listed as notifiable by the World Organization for Animal Health (WOAH/OIE). VHSV is considered as a serious economic and social threat for fish farms with significant environmental impact on natural resources. VHSV has been isolated from more than 82 different freshwater and marine species throughout the Northern Hemisphere, including North America, Asia, and Europe, including rainbow trout (*Oncorhynchus mykiss*), turbot, sea bass and sole (22). This virus is enveloped and its genome consists of a non-segmented negative-sense single-stranded RNA molecule of about 11 kilobases which encode six proteins in the order 3'-N-P-M-G-NV-L-5' (23, 24). The viral RNA encodes five structural proteins. A nucleoprotein (N) which tightly encapsidates viral genome and antigenome RNAs together with a polymerase-associated phosphoprotein (P) and the large RNA-dependent RNA polymerase (L), hence forming a helical ribonucleoprotein complex (RNP). The matrix protein (M) interacts with the RNP and the viral envelope where the unique viral surface glycoprotein (G) is inserted by its transmembrane (TM) domain. In contrast to other rhabdoviruses, the VHSV genome possesses an additional gene, located between the G and L genes, that encodes a small non-structural NV protein essential for host innate immunity evasion (25–28). Due to the presence of the NV gene, VHSV is classified together with infectious hematopoietic necrosis virus (IHNV) in the genus *Novirhabdovirus*.

For Rhabdoviruses, the gene order is crucial for virus replication due to a decreasing gradient of transcription from the 3' to the 5' end. The viral polymerase binds to the 3' end of the genome and starts transcription in a sequential gene-start-gene-end mechanism resulting in one mRNA species for each viral gene (29–32). Between each gene, the polymerase can dissociate from the genome, resulting in a gradient of expression in which the 3' proximal genes are more transcribed than those located at the 5' end. The modification of the gene order has an important impact on virus replication and pathogenicity as demonstrated by Wertz and colleagues on vesicular stomatitis virus (VSV) (33, 34) and our group on IHNV (19). In both cases, the N gene position seems to be one of the most critical factors for viral pathogenicity. Indeed, decreasing the amount of N protein by moving N gene downstream along the genome delayed the kinetics of replication and increased interferon expression leading to an attenuated phenotype (19, 35). These recombinant viruses were less pathogenic but maintained their immunogenicity *in vivo* due in part to the concomitant upstream

displacement of the G gene within the genome allowing for increased expression of the G protein, the main target for neutralizing antibodies (19, 33–37). These data demonstrate that moving the N and G genes along the rhabdovirus genome is a promising approach for vaccine development in fish and mammals.

In this study, we develop a strategy to produce a live-attenuated vaccine against both VHS and VER by engineering the genome of VHSV to modify the gene order and to introduce an expression cassette encoding the major protective antigenic domain of NNV capsid protein allowing its incorporation into VHSV virions. Eight recombinant VHSVs (rVHSV), termed NxGyCz according to the respective positions of the genes encoding the nucleoprotein (N) and glycoprotein (G) as well as the expression cassette (C) along the genome, have been produced and tested for their safety, immunogenicity and protective efficacy in two fish species.

Results

Characterization of recombinant VHSVs expressing NNV epitopes

Recombinant rVHSVs expressing NNV capsid or capsid domains were generated as described previously (18, 38), using the expression cassette inserted in the non-coding region between N and P genes. The encoding nucleotide sequences of the full-length NNV capsid or derived domains, which are known to be highly immunogenic (7) were cloned in this expression cassette in fusion with the signal peptide (SP) sequence derived from the IHNV glycoprotein G gene, and the transmembrane sequence (TM) from VHSV G gene. The expression cassettes were flanked with the gene start and gene end signals of VHSV in order to be recognized by the viral polymerase and to direct the efficient expression of heterologous genes (Figure 1A). Four recombinant viruses were produced expressing a membrane-targeted capsid protein (CP), a secreted form of the capsid protein (CAP), the linker region and the protruding domain (LP), which contained the major protective epitopes against NNV (39, 40) or a duplication of this LP domain (LP2) (Figures 1A, B). All recombinant viruses were readily recovered using the established reverse genetics system for VHSV (27). Recombinant viruses were amplified through 2 passages in fish EPC cells. Titers reached 2×10^8 PFU/mL for rVHSV-CP, 2.5×10^8 PFU/mL for rVHSV-CAP and 1×10^8 PFU/mL for both rVHSV-LP and rVHSV-LP2 (Figure 1A).

To assess the expression of NNV antigens by rVHSVs, EPC cells were infected with each recombinant virus at a multiplicity of infection (MOI) of 0.01. At 24 h post-infection, the expression of the NNV capsid protein or capsid domains was evaluated by indirect immunofluorescence on fixed or live infected cells (Figure 2). All recombinant viruses enabled the expression of the capsid protein or capsid domains in the cytoplasm of infected EPC cells, as shown by the co-labelling with anti-VHSV G mAb and anti-NNV pAb (Figure 2A). Next, we analyzed the expression of NNV capsid in live infected EPC cells to ensure the correct routing of the antigen along the secretory pathway towards the plasma membrane (Figure 2B). All recombinant viruses expressed and correctly addressed NNV capsid or capsid domains at the surface of infected EPC cells, a pattern of expression similar to that observed for VHSV G. The secreted form of the NNV capsid

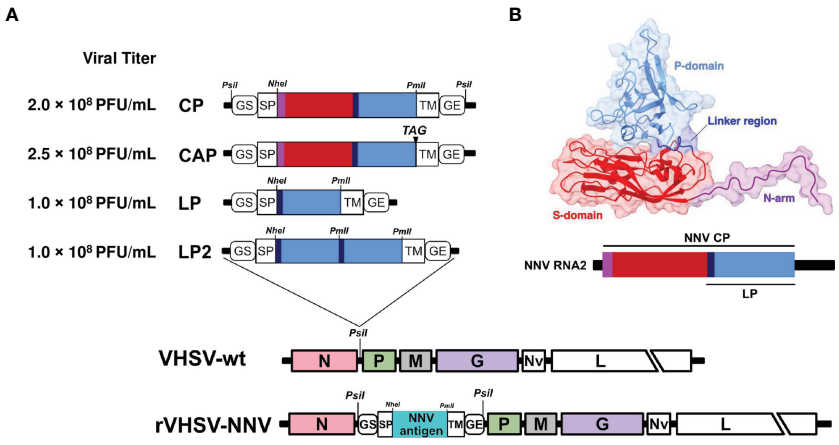

FIGURE 1
Construction of recombinant VHSV vectors expressing NNV capsid or capsid domains. **(A)** Schematic representation of NNV epitopes inserted in VHSV expression cassette driving antigen expression at the cell surface and incorporation in recombinant virus particles. The cassette is located between N and P genes in the VHSV genome. GS; gene start, GE; gene end, SP; signal peptide and TM; transmembrane domain (both SP and TM are derived from VHSV G). Full-length NNV capsid (CP or CAP including the stop codon TAG) or domains of CP (LP and LP2; P-domain plus linker region in single copy or in duplicate, respectively) were cloned in VHSV expression cassette. Unique enzyme restriction sites used in those constructs are indicated. **(B)** Structure of nervous necrosis virus (NNV) capsid protein. Ribbon diagram with surfaces displayed of a capsid subunit based on the PDB structure 4WIZ. Molecular visualizations were performed using Chimera X. Each capsid subunit is composed of three main domains: the N-terminal arm (N-arm), shown in purple (residues at the N-terminal extremity of the N-arm are not shown since they were found to be disordered), the shell domain (S-domain), shown in red, and the protrusion domain (P-domain), shown in light blue. The linker region, shown in blue, connects the S-domain with the P-domain. Below is a representation of the NNV genomic RNA2 with the regions encoding the different domains of the capsid.

10.3389/fimmu.2023.1138961

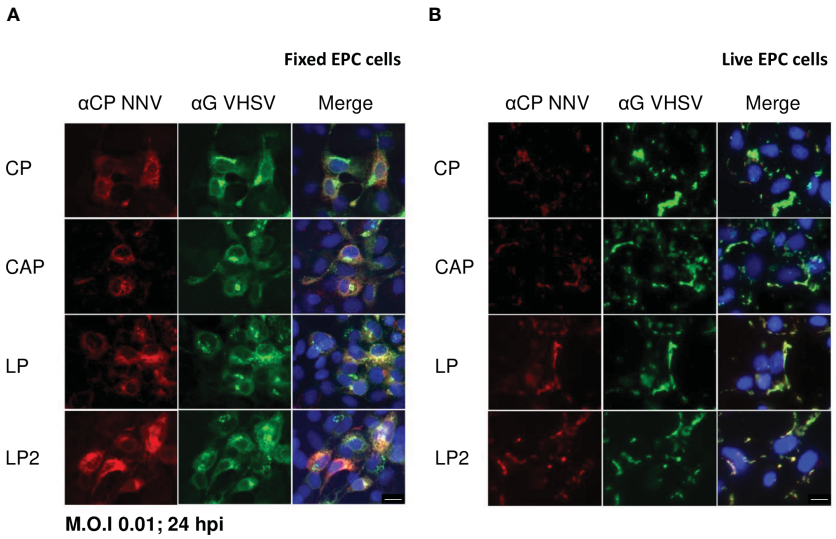

FIGURE 2
Expression of NNV antigens in rVHSVs infected cells. The expression of NNV antigens was assessed by indirect immunofluorescence assays on EPC cells. The cells were infected with rVHSV-CP, rVHSV-CAP, rVHSV-LP or rVHSV-LP2 at an MOI of 0.01 and incubated at 14 °C. **(A)** At 24 h post-infection, cells were fixed and permeabilized with alcohol/acetone and NNV and VHSV G expression were detected using a pAb against NNV (red) and a mAb against VHSV G (green), respectively. **(B)** At 24 h post-infection, membrane expression of NNV antigens was visualized on live cells in PBS using the same antibodies. Nuclei were stained with Hoechst (blue). Bars, 10 µm.

protein was also detected at the surface of the infected cells probably due to its propensity to interact with lipid bilayers (41).

The incorporation efficiency of heterologous antigens at the surface of recombinant Novirhabdoviruses with an expression cassette inserted between N and P genes has been previously demonstrated in the laboratory (18, 38). The NNV antigen could not be clearly visualized on SDS-PAGE after Coomassie blue staining as it co-migrated with the N of VHSV (Figure 3A). We therefore validated the expression of the NNV antigen at the surface of the VHSV platforms by Western-blot assay on sucrose-purified viruses. Figure 3B shows that rVHSV-CP and rVHSV-LP2 both express the NNV antigen at the expected size (43 kDa and 35 kDa, respectively). Other forms of LP2 antigens (around 40 and 30 kDa) were also detected and are likely due to as yet uncharacterized post-

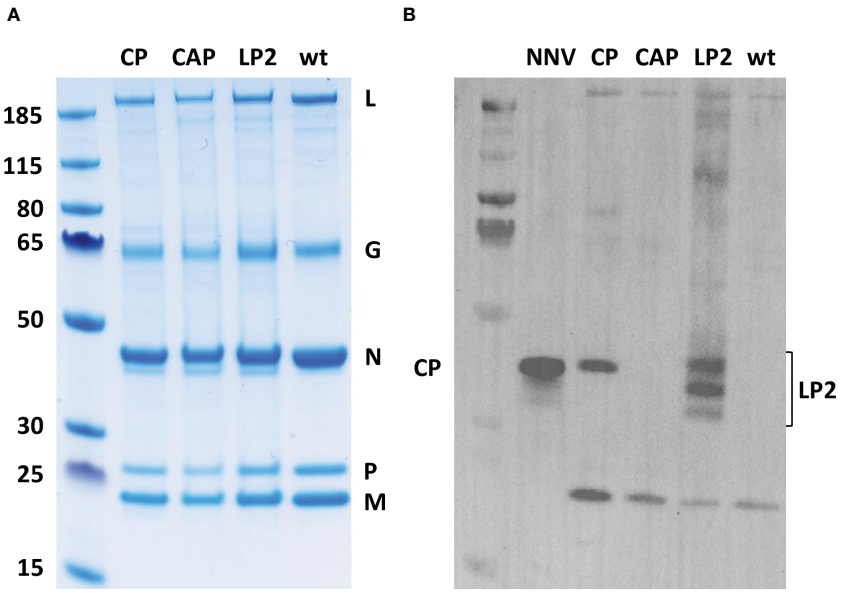

FIGURE 3
Analysis of NNV antigens incorporation in recombinant virus particles. **(A)** Six micrograms of sucrose-purified viral proteins were separated on a 4-12% polyacrylamide gel and stained by Coomassie blue. **(B)** Two micrograms of sucrose-purified viral proteins were denatured, loaded and migrated on an SDS page gel. The gel was electrotransferred onto a PVDF membrane and NNV antigens were detected with a rabbit pAb directed against NNV.

10.3389/fimmu.2023.1138961

translational modifications of this domain. In contrast, no NNV antigen was detected in rVHSV-CAP virions which express a secreted form of NNV capsid without VHSV G-derived TM domain, thus demonstrating the specificity of the NNV antigen incorporation into rVHSV particles.

Recovery of rVHSVs with rearranged gene order

Unique restriction enzyme sites were introduced by site-directed mutagenesis immediately upstream and downstream of the start and the stop codons of each ORF in the VHSV genome. Restriction enzyme sites were *HpaI* for N gene, *PmlI* for P gene, *SnaBI* for M gene, *BstZ17I* for G gene and *PmeI* for the NV gene, respectively (Figure 4A). The recombinant viruses were readily recovered as previously described (19, 27). Recombinant viruses with rearranged gene order were named according to their respective N and G gene position: N1G4 (3'-N-P-M-G-NV-L-5') which corresponds to the recombinant virus that contains additional restriction enzyme sites introduced to each ORF (designated RES) or the wild-type virus (wt), N2G3 (3'-P-N-G-M-NV-L-5') and N2G4 (3'-P-N-M-G-NV-L-5'), (Figure 4A). Based on the data obtained for IHNV (19), two gene orders were directly tested for VHSV, N2G3 and N2G4, for which the balance between attenuation and immunogenicity was optimal for IHNV, in order to evaluate the effect of such approach for VHSV attenuation.

The pathogenicity of the rVHSV was assessed by infecting juvenile rainbow trout (mean weight of 1.8 g) with the selected viruses and mortality rates were recorded daily for up to 21 days. As shown in Figure 4B, a similar fish mortality rate was observed between N1G4(wt) and N1G4-RES. For both viruses, the mortality started at day 5-6 post infection and reached 82% to 92% of cumulative mortality, respectively, at day 21. These data indicated that the addition of 10 restriction enzyme sites in the VHSV genome has a limited effect on virus pathogenicity. In contrast, N2G4 and N2G3 were attenuated *in vivo* inducing only 57% and 45% of cumulative mortality, respectively, at day 21. This confirms that changing the gene order impacts pathogenicity.

Characterization of rVHSVs expressing a duplication of NNV LP domain in a gene order attenuated backbone

Based on above results, the position of N and G genes along the VHSV genome has a great effect on VHSV virulence in trout. Therefore, N gene was kept at position 2 in order to maintain a basal level of attenuation. In parallel, the G gene and the NNV epitope expressing cassette were inserted at different positions along the VHSV genome to balance their levels of expression and thus their potential immunogenicity *in vivo*. Seven cDNA constructs were designed and termed NxGyCz according to the respective positions of N and G genes as well as the expression cassette C along the genome: N2G5C3, N2G4C3, N2G3C4, N2G3C5, N2G5C1,

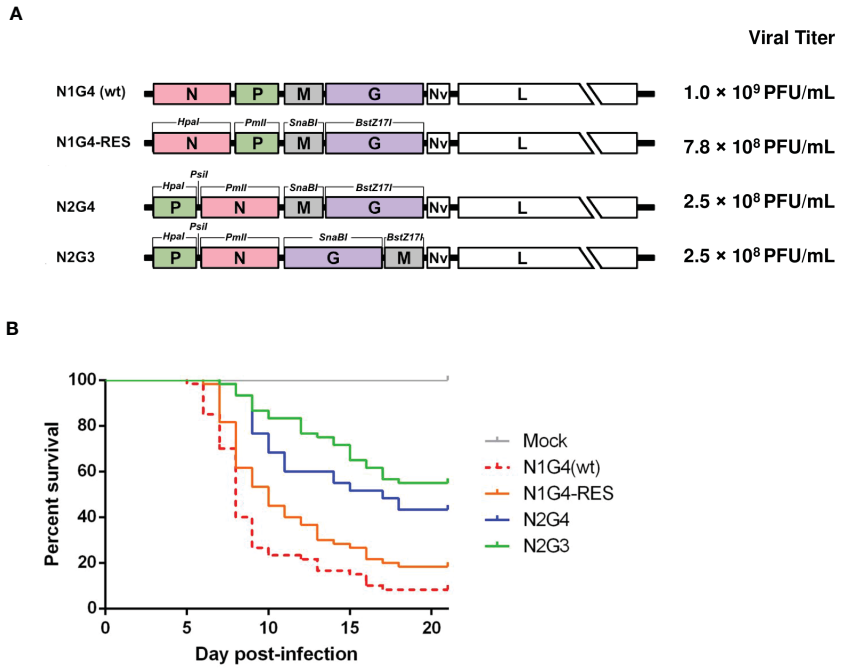

FIGURE 4
VHSV genome rearrangement. **(A)** Schematic representation of the engineered rVHSV genomes with rearranged gene order. Restriction enzyme sites inserted by site-directed mutagenesis at the beginning and the end of the N, P, M, G and NV ORF are indicated on the N1G4-RES genome. **(B)** INRA synthetic strain virus-free juvenile rainbow trout (n = 50 per group, mean weight 1.8 g) were infected by bath immersion with rVHSVs as indicated (final titer, 5 × 10^4 PFU/mL) for 2 h at 10°C. Mortality rates were recorded daily and is presented as percent of survival.

N2G1C4 and N2G1C5 (Figure 5). Based on three criteria: level of expression, level of incorporation in VHSV virion and high immunogenicity as duplication of NNV major epitope domain, the LP2 antigen was selected and inserted in these constructs. The recombinant viruses, rVHSV$_{GO}$-NNV (with GO for modified gene order), were successfully recovered by reverse genetics and amplified in fish cells, except for N2G3C5 for which a total cytopathic effect (CPE) was never achieved. They reached titers ranging between 1.5×10^6 PFU/mL to 2×10^7 PFU/mL, but somewhat attenuated compared to the rVHSV N1G5C2 with the N gene in first position (2.5×10^8 PFU/mL).

The expression of NNV LP2 antigen by rVHSV$_{GO}$-NNV was assessed in EPC cells. At 24 h post-infection, the expression of the LP2 antigen was evaluated by indirect immunofluorescence on fixed cells (Figure 6A). All recombinant viruses expressed the LP2 antigen in infected EPC cells, as shown by the co-labelling with anti-VHSV G mAb and anti-NNV pAb. The incorporation efficiency of the LP2 antigens at the surface of rVHSV$_{GO}$-NNV virions was verified by Western-blot assay on sucrose-purified viruses. Figure 6B shows that all rVHSV$_{GO}$-NNV expressed the LP2 antigen at the expected size.

Safety and protective efficacy of rVHSV$_{GO}$-NNV in rainbow trout

The safety and protective efficacy of the rVHSV$_{GO}$-NNV was assessed by infecting highly sensitive juvenile rainbow trout (mean weight of 0.8 g) and recording mortality rates daily for up to 35 days (Figure 7). As shown in Figure 8, rVHSV$_{GO}$-NNV were almost completely attenuated. The mortality started at day 11, day 16 and day 18 post infection for N2G5C1, N2G1C5 and N2G4C3, respectively. The residual virulence for these three viruses at day 35 was ranging around 2 to 8% of cumulative mortality. N2G5C3 and N2G1C4 were completely attenuated in juvenile trout. No mortality was recorded for both viruses during the 35-day period, similarly to what is observed with the mock-infected fish control condition.

At 35 days post-immunization, the potential of rVHSV$_{GO}$-NNV as live vaccine was tested by challenging the surviving trout by bath immersion with a lethal dose of wild-type VHSV (Figure 7). As shown in Figure 8, the mortality in the mock-vaccinated group reached 98% whereas it reached 82% for both N2G5C3 and N2G3C4 groups, 54% for N2G4C3 group, 48% for N2G1C5 group, 22% for N2G1C4 group and 12% for N2G5C1 group. The highest calculated Relative Percent of Survival (RPS) were 78% and 80% for N2G1C4 and N2G5C1, respectively (Table 1). In contrast to N2G5C1 inducing 8% of mortality during the immunization step, no mortality was recorded during the immunization for N2G1C4 immunized group. Thus, the overall protection of 78% induced upon vaccination with N2G1C4 by bath immersion makes this virus a promising vaccine candidate.

Safety, immunogenicity and protective efficacy of rVHSV$_{GO}$-NNV in Senegalese sole

The safety and immunogenicity of the rVHSV$_{GO}$-NNV was assessed by infecting juvenile sole. Fifty sole (mean weight of 4 g) per group were acclimated at 13°C, the optimal temperature for VHSV replication, and then injected by intra-peritoneal route with 1×10^5 PFU of rVHSV$_{GO}$-NNV per fish (Figure 7). 7 days later, the temperature of water in tanks was progressively increased to 22°C,

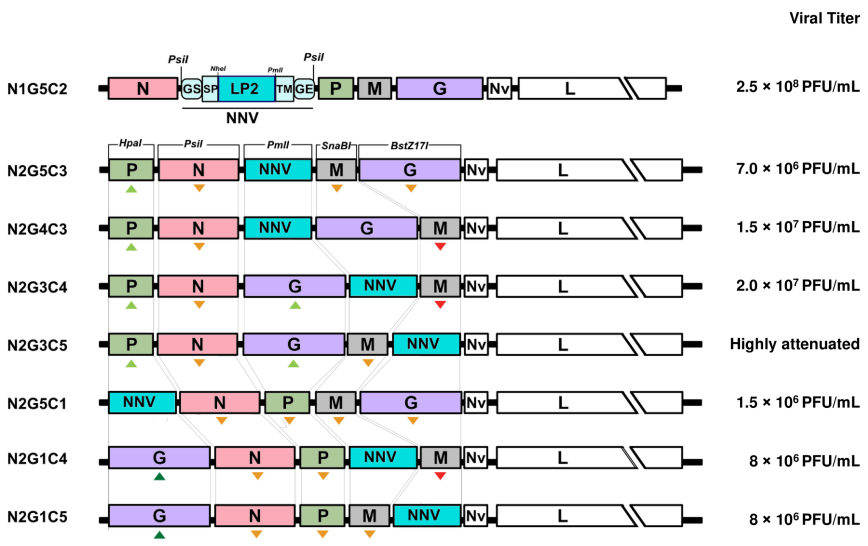

FIGURE 5
Recombinant VHSV expressing NNV epitopes with rearranged genome. Schematic representation of the engineered rVHSV genomes expressing NNV epitopes with rearranged gene order. Nine rVHSV, termed NxGyCz according to the respective positions of the genes encoding the nucleoprotein (N) and glycoprotein (G) as well as the expression cassette (C) along the genome. Viral titers (PFU/mL) obtained after two passages in EPC cells are indicated on the right.

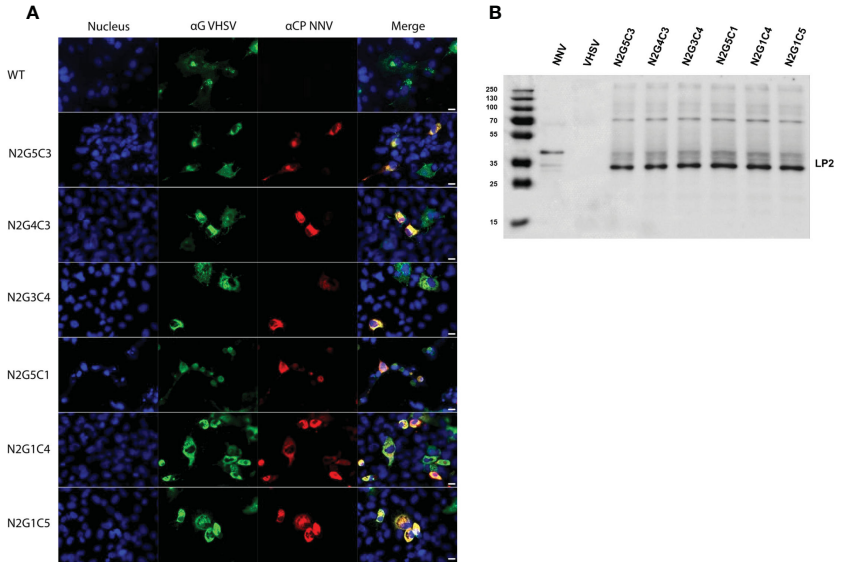

FIGURE 6
Characterization of rVHSV$_{GO}$-NNV *in vitro* in fish cells and validation of NNV epitope incorporation in recombinant virus particles. **(A)** The expression of NNV antigens was assessed by indirect immunofluorescence assays on EPC cells. The cells were infected with rVHSV$_{GO}$-NNV at an MOI of 0.1 and incubated at 14 °C. At 72 h post-infection, cells were fixed and permeabilized with alcohol/acetone and NNV and VHSV G expression were detected using a pAb against NNV (red) and a mAb against VHSV G (green), respectively. Nuclei were stained with Hoechst (blue). Bars, 10 µm. **(B)** Two micrograms of sucrose-purified viruses were denatured, loaded and migrated on an SDS page gel. NNV LP2 antigen was detected with a rabbit pAb directed against NNV.

the optimal temperature for NNV replication. After 21 days, six fish per group were sacrificed and blood samples were taken. The levels of anti-NNV antibodies in sera from immunized sole was evaluated by ELISA. As shown in Figure 9A, specific and significant antibody responses were detected for two immunized groups: N2G5C1 and N2G1C4. In parallel, the mortality rates were recorded daily for up to 25 days. As shown in Figure 9B, rVHSV$_{GO}$-NNV were completely attenuated and safe in sole. No mortality was recorded

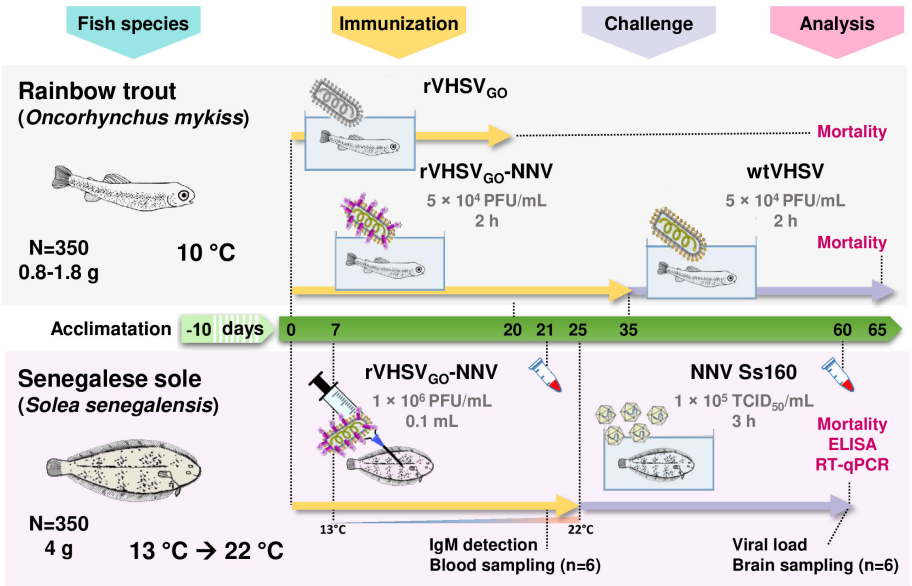

FIGURE 7
Experimental setup. Three different fish experiments were performed. The first on trout was designed to test the attenuation provided by the gene order rearrangement of the VHSV genome. The second on trout was conducted to test the safety and the protective efficacy of rVHSV$_{GO}$-NNV against a lethal VHSV challenge. All trout infections were performed by bath immersion with a viral load of 5 x 10^4 PFU/mL in 3 L of water. The third was conducted on sole to test the safety, the immunogenicity and the protective efficacy of rVHSV$_{GO}$-NNV against a lethal NNV challenge. The immunizations and the lethal NNV challenge were performed by injecting 1 x 10^5 PFU of rVHSV$_{GO}$-NNV per fish and bath immersion with 1 x 10^5 TCID$_{50}$/mL of NNV, respectively.

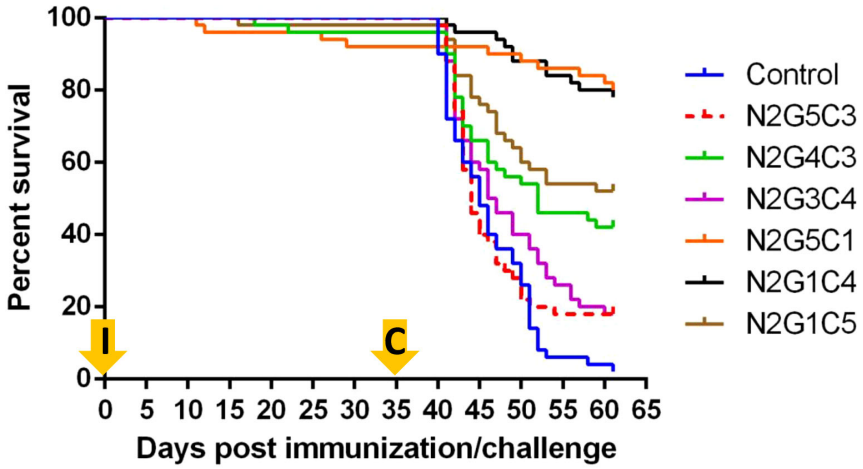

FIGURE 8
Fish survival curves following infection of trout by bath immersion with rVHSV$_{GO}$-NNV. Fifty virus-free juvenile rainbow trout (mean weight of 0.8 g) were infected with 6 rVHSV$_{GO}$-NNV as described in materials and methods. Fish mortality rates were recorded every day for 35 days. Then, rVHSV$_{GO}$-NNV-immunized fish were challenged with wtVHSV. Fish mortality rates were recorded every day for 30 additional days.

for all viruses during the 25-day period as for the mock-infected fish.

At 25 days post-immunization when the water temperature in the tanks reached 22°C, the protective efficacy of rVHSV$_{GO}$-NNV was tested by challenging the sole with the wild-type NNV by bath immersion (1×10^5 TCID$_{50}$/mL) (Figure 7). As shown in Figure 9B, the mortality in the mock-vaccinated group reached 88% whereas it reached 68% for both N2G5C3 and N2G3C4 groups, 52% for N2G1C5 group, 48% for N2G4C3 group, 32% for N2G5C1 group and 26% for N2G1C4 group. The highest calculated RPS were 64% and 70% for N2G5C1 and N2G1C4, respectively (Table 2). Both recombinant viruses are associated with considerably reduced NNV load in the brain tissues of surviving fish by almost 10,000-fold compared to non-immunized fish as measured by RT-qPCR (Figure 9C) and some of the fish in both groups have no detectable amount of NNV. A significant reduction of NNV load in brain (100-fold compared to control fish) was also observed in dead fish immunized by N2G1C4. The efficient protection induced by these two rVHSV$_{GO}$-NNV was in accordance with the significant antibody titers measured in both immunized groups (Figure 9A). Thus, the overall protections of 78% in trout and 70% in sole induced upon vaccination with N2G1C4 make this recombinant and attenuated virus a promising vaccine candidate.

To gain structural insights into the LP2 construct used in our study, we generated a structural model using AlphaFold 2 based on the protein sequence of the SpSsIAusc16003 isolate, which is a RGNNV/SJNNV reassortant with a capsid protein related to SJNNV (serotype A) (Figure 10). The LP2 construct consists of a tandem repeat of the linker (L) and protrusion (P) domains located at the external tip of the viral capsid protein (Figures 10A, B). AlphaFold 2 is a powerful deep learning algorithm providing a breakthrough in structural prediction for proteins (43). AlphaFold 2 readily predicts protein structures with atomic accuracy without the need for structural templates, as long as enough orthologs are

TABLE 1 Summary of percent cumulative mortality observed in trout infected by rVHSVGO-LinkerP2NNV and challenged by VHSV.

Virus[a]	% cumulative mortality		RPS[d]
	Immunization[b]	Challenge[c]	
N2G5C3	0	82	16
N2G4C3	4	54	45
N2G3C4	0	82	16
N2G5C1	8	12	80
N2G1C4	0	22	78
N2G1C5	0	48	51
Control[e]	0	98	_

[a]Groups of 50 trout (mean weight of 0.81 g) were immunized by bath immersion with the indicated viruses (5×10^4 PFU/mL).
[b]Cumulative percent of mortality at day 35 postimmunization.
[c]VHSV challenge by bath immersion (5×10^4 PFU/mL) was performed at day 35 postimmunization and ended at day 61.
[d]Relative percent survival (RPS) = 1 - (percent mortality in group/percent mortality in control) × 100 (42).
[e]Group of fish immunized with virus-free culture medium and challenged with VHSV at day 35 postimmunization.

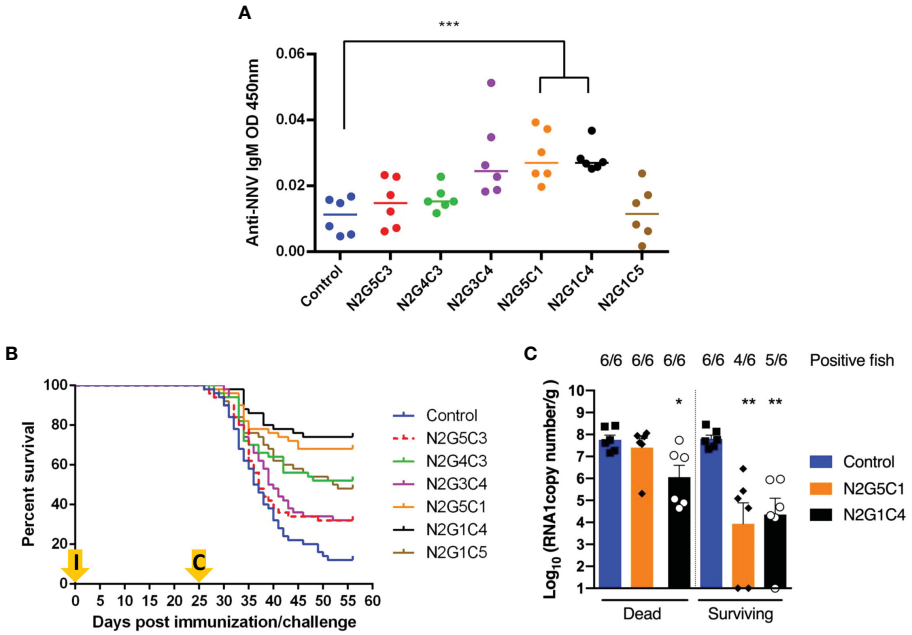

FIGURE 9
Fish survival curves following immunization by injection of sole with rVHSV$_{GO}$-NNV and challenge with NNV by bath immersion. Fifty virus-free juvenile sole (mean weight of 4 g) were injected with 6 rVHSV$_{GO}$-NNV as described in materials and methods. **(A)** Twenty-one days post infection, six fish per group were sacrificed and blood samples were taken. The levels of anti-NNV antibodies in sera from immunized sole was evaluated by ELISA. **(B)** Fish mortality rates were recorded every day for 25 days. Then, rVHSV$_{GO}$-NNV-immunized fish were challenged with NNV by bath immersion. Fish mortality rates were recorded every day for 31 additional days. **(C)** NNV replication in brain tissues of immunized fish. Six dead fish and six surviving fish randomly harvested at day 30 post-challenge in the indicated groups were analyzed by RT-qPCR. Virus loads are expressed as RNA1 copy per gram of brain. Number of positive fish are indicated above each histogram. For statistical analysis, a comparison between groups was performed with a one-way ANOVA and Tukey's multiple comparison tests using GraphPad Prism (GraphPad, San Diego, CA). Groups that are significantly different are denoted *($p < 0.05$), **($p < 0.01$), ***($p < 0.001$).

available for generating multiple sequence alignments enabling covariance evaluation. AlphaFold 2 was able to generate an accurate model of LP2 with an overall confidence score (pLDDT) of 88.2 out of 100, close to the score of 90 corresponding to models with highly confident predictions of both backbone and residue side chain orientations. Viewed from the side, the LP2 model presents a bi-lobed "butterfly" structure of the LP dimer with each lobe consisting of a monomer of the pyramidal protrusion domain connected *via* the linker domain (Figure 10B). In the side view, the C-terminus of LP2 is shown to indicate where the VHSV TM domain connects (not modeled). Previous serological analyses of chimeric capsid proteins have shown that the region determining antigenic diversity spans residues 257-341 for the capsid of SJNNV (serotype A) (7). These residues are color-coded onto the modeled structure in magenta (Figure 10B). Both side and top views show that the repeated 257-341 region of the protrusion domains are

TABLE 2 Summary of percent cumulative mortality observed in sole injected with rVHSVGO-LinkerP2NNV and challenged by NNV.

Virus[a]	% cumulative mortality		RPS[d]
	Immunization[b]	Challenge[c]	
N2G5C3	0	68	23
N2G4C3	0	48	45
N2G3C4	0	68	23
N2G5C1	0	32	64
N2G1C4	0	26	70
N2G1C5	0	52	41
Control[e]	0	88	_

[a]Group of 50 sole (mean weight of 4 g) were immunized by injection with the indicated viruses (1×10^5 PFU/fish).
[b]Cumulative percent of mortality at day 25 postimmunization.
[c]NNV challenge was performed by bath immersion (1×10^5 $TCID_{50}$/mL) at day 25 postimmunization and ended at day 56.
[d]Relative percent survival (RPS) = 1 - (percent mortality in group/percent mortality in control) × 100 (42).
[e]Group of 50 fish immunized with virus-free culture medium and challenged with NNV at day 25 postimmunization.

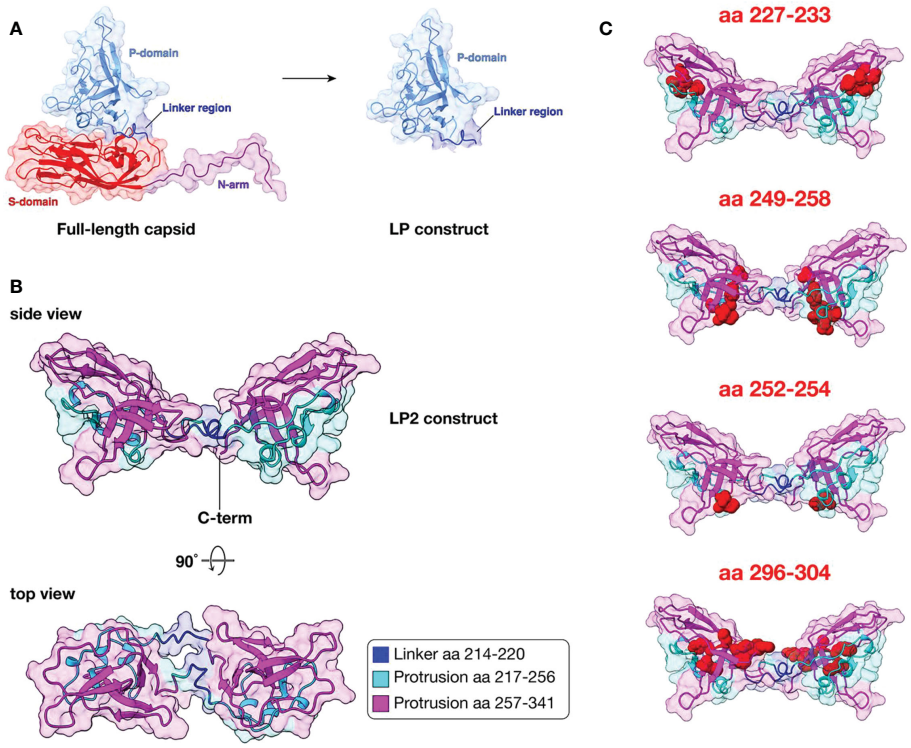

FIGURE 10
Structural model of the LP2 antigen using AlphaFold 2. **(A)** Structure of nervous necrosis virus (NNV) full-length capsid and Linker-Protrusion (LP) construct. Ribbon diagram with surfaces displayed of NNV capsid subunit and LP construct based on the PDB structure 4WIZ. Molecular visualizations were performed using Chimera X. **(B)** AlphaFold 2 structural model of LP2 construct. The capsid protein sequence (accession no. NC_024493.1) of the betanodavirus isolate SpSslAusc16003 (related to serotype A SJNNV) was used to generate an AlphaFold 2 structural model using ColabFold. Molecular visualization was performed using UCSF ChimeraX. The structural prediction with highest confidence score (pLDDT of 88.2/100) is shown. The C-terminus of the LP2 construct is shown in the side view to indicate where the TM domain of VHSV is connected (not modeled). The sub-regions of the Linker (L) and Protrusion (P domains) are color-coded according to the color legend on the figure. **(C)** Mapping of known neutralizing epitopes onto LP2 structural model. Confirmed or predicted protrusion domain neutralizing epitopes corresponding to amino acids 227-233, 249-258, 252-254, and 296-304 are highlighted as red spheres. See text for the references describing each epitope.

clearly surface-exposed, suggesting that they are readily accessible to neutralizing antibodies (Figure 10B). We further mapped onto the LP2 structural model confirmed or predicted protrusion domain neutralizing epitopes (Figure 10C). The amino acids (aa) corresponding to the following epitopes were highlighted as red spheres in the LP2 model: aa 227-233 (44); aa 249-258 (45); aa 252-254 (40); and aa 296-304 (46). The mapping suggests that the LP2 construct correctly presents these epitopes at the surface of each LP monomer and would thus allow for antibody binding at these sites.

Discussion

In the current study, we aimed to generate live-attenuated VHSV vectors expressing NNV major protective antigen in order to characterize their safety, immunogenicity and protective efficacy against these two major diseases for trout and sole aquaculture. Therefore, the VHSV infectious cDNA (27) was modified by rearranging the gene order as a stable attenuation strategy (19, 35, 47) and the addition of an expression cassette driving the insertion of the antigen of interest at the plasma membrane of the infected cells and its incorporation in the newly formed virion (18, 38). Both modifications of the viral genome intrinsically lead to virus attenuation by changing the gradient of viral gene expression, thus several positions of N and G genes together with the expression cassette were tested to find the best combination. Among all $rVHSV_{GO}$-NNV tested here, N2G1C4 presents the best balance between attenuation and protective efficacy. N2G1C4 is safe for both fish species and protects trout and sole against a lethal challenge with VHSV or NNV, respectively. This protection is in accordance with the induction of specific NNV antibodies in sole and should be further tested for its duration. Thus, N2G1C4 represents a promising candidate for the development of a bivalent live attenuated vaccine in order to protect two commercially valuable fish species against infections by these two major pathogens.

One of the challenges in developing live vaccines is to attenuate the virus without substantially reducing its immunogenicity. The genome architecture of *Rhabdoviridae* is highly conserved and viral mRNAs are expressed in a gradient, such that viral proteins at the 3' proximal end of the viral genome are produced at higher levels than those at the distal end (29, 31). Thus, the rearrangement of gene order has been proposed as an approach to make terrestrial and aquatic rhabdoviruses more suitable as platforms for vaccine

development (19, 34) or as candidates for oncolytic virus therapy (48). Homologous recombination appears to be very rare in mononegaviruses (49), making the rearrangement of gene order a safe method to attenuate mononegaviral-derived vectors minimizing the risk of reversion to a virulent phenotype. As previously demonstrated for IHNV, another *Novirhabdovirus*, recombinant viruses with rearranged genomes were highly stable following up to 10 successive passages in fish cells (19).

As previously shown (19), rIHNV N2G3 and N2G4 exhibited slower replication kinetics, reduced viral production (10- to 50-fold reduction compared to the wild-type virus, respectively) and were strong inducer of interferon and interferon stimulated genes (ISGs) in trout cells. More interestingly, they were almost completely attenuated with a residual virulence in juvenile trout (mean weight of 0.7 g) around 15% of cumulative mortality for both viruses versus 90% for the wild-type virus at 35 days post-infection. Trout immunized with rIHNV N2G3 were highly protected against a subsequent infection by a virulent IHNV strain, with RPS from 68% to 86% depending on the mean weight of the fish at the beginning of the experiment (0.7 g and 1 g, respectively). Therefore, we focused first on these two specific gene orders in order to evaluate their respective effect on VHSV virulence in trout. As observed with IHNV, the decrease in N protein expression by moving the N gene in second position in the genome significantly reduced VHSV virulence in trout. Both rVHSV N2G3 and N2G4 were attenuated but a higher residual virulence was observed compared to their IHNV counterparts with a cumulative mortality rate in juvenile trout (mean weight of 1.8 g) of 45% and 57%, respectively, versus 92% for the wild-type virus at 21 days post-infection. These first results represented a solid starting point in order to introduce the expression cassette which was expected have an additional attenuation effect on VHSV. Indeed, the insertion of the expression cassette in position 4 in the N2G3 backbone led to a 10-fold reduction in the final titer of the N2G3C4 (2.5×10^8 PFU/mL versus 2×10^7 PFU/mL), which resulted in total loss of virulence in trout. Unfortunately, the N2G3C4 recombinant virus was found to be over-attenuated as it did not protect immunized fish against a lethal VHSV challenge.

In total six different gene rearrangements were tested in order to find the best balance between attenuation and immunogenicity, since attenuation can result in reduced immunogenicity. With regard to resistance to infection, the protective role of VHSV-neutralizing antibodies has been clearly demonstrated in trout (50). The VHSV glycoprotein G is the neutralization antigen and the major protective antigen. Experimental vaccines designed to induce specific antibodies against VHSV glycoprotein G provide resistance to infection (51–53). One strategy was to move the G gene in the first position and thus increase the expression of this major protective antigen while maintaining the N gene in second position to keep the attenuation effect by reducing the expression of the N protein, leading to N2G1C4 that displays the best balance between attenuation and immunogenicity. This is in accordance with previous studies showing that the expression of the VSV glycoprotein G or the Human respiratory syncytial virus (RSV) fusion F and glycoprotein G could be improved by moving it to a promoter-proximal position (33, 47), while the N gene position was found to be one of the most critical factors regulating rhabdovirus pathogenicity (19, 35). For rIHNV N2G3 and N2G4, lower levels of N transcription were clearly correlated with stronger induction of type I IFN (19). It is possible that a decrease in replication efficiency gives the cell an advantage to mount a strong IFN response, but, this might also be a consequence of the N protein inhibition of the IFN induction pathway, as recently suggested for novirhabdoviruses (54, 55). Therefore, we suggest that higher induction of IFN together with higher expression of the protective antigen contribute to rVHSV N1G1C4 attenuation, immunogenicity and protective immunity in trout and sole.

The NNV antigens that were designed and analyzed in this study are based on the capsid (coat) protein, which is the sole structural protein found in betanodavirus particles. During virion formation multiple capsid proteins self-assemble into a T=3 icosahedral structure, with a total of 180 capsid proteins arranged in 60 trimers (39). As its name implies, the pyramid-like protrusion (P) domain is exposed at the surface of viral particles and harbors both host cell receptor binding and virus neutralization epitope sites. Three serotypes of NNV have been characterized, with SJNNV grouped as serotype A betanodavirus, the cold-water betanodaviruses TPNNV and BFNNV grouping in serotype B, and RGNNV belonging to serotype C (7). Based on antigenic and infectivity assays of the serotype C RGNNV under various physicochemical conditions, Gye and Nishizawa have suggested that the sites responsible for antigenicity and infectivity are distinct (56). In our study, different capsid-derived antigen constructs of the SpSsIAusc16003 isolate, a RGNNV/SJNNV reassortant with a capsid protein related to SJNNV (serotype A) were initially tested, including the linker-protrusion domain (LP) construct (8). The LP2 construct consisting of a tandem repeat of the linker-protrusion domain was then selected and used in subsequent immunization/challenge and ELISA assays. Structural modeling using AlphaFold 2, a highly accurate computational method, revealed that the LP2 construct forms a bi-lobed "butterfly" structure with each lobe consisting of one LP monomer. Each LP monomer exposes a region spanning residues 257-341 which was previously shown to be a determinant of antigenic diversity for the capsid of SJNNV (serotype A) (7). In addition, previously characterized (aa 227-233, aa 249-258, aa 252-254) or predicted (aa 296-304) neutralizing epitopes map to surface-exposed areas of each LP monomer (40, 44–46). Of note, with the exception of the epitope spanning residues 252-254, the so-called "PAN" epitope which corresponds to the three amino acids found in SJNNV (serotype A) capsid, the other previously described epitopes were based on RGNNV (serotype C). Alignment between SJNNV and RGNNV capsid sequences revealed differences in amino acid composition for the 4 epitopes (44). In particular, in their recently published work based on RGNNV (serotype C), Zhang and colleagues mapped the linear epitope $_{227}$SLYNDSL$_{233}$ as the binding site of a monoclonal antibody (Mab 2B7) they produced in mouse and which was shown to be neutralizing. For comparison, the sequence found at residues 227-233 for the SJNNV (serotype A) capsid is $_{227}$PLHNDSI$_{233}$. Interestingly, the authors showed that of the three substitutions found when comparing the 227-233 segment of RGNNV and SJNNV capsids, only the Y229H substitution interfered with MAb

2B7 antibody binding (44). In their discussion, the authors state that pre-immunization of juvenile groupers with the RGNNV 227-233 peptide failed to elicit protective immunity against RGNNV challenge. This result suggests that the native structural context in which the 227-233 segment is presented, such as in our LP2 construct, may be an important contributing factor to obtain immune protection. It is also noteworthy to highlight that another major benefit of our approach using the LP2 construct, where LP is found in duplicate is the possibility to generate an antigen with two protrusion domains derived from two serotypes, for example with serotype A (SJNNV) and serotype C (RGNNV) which are antigenically distinct (7), thus paving the way to the development of a "divalent"-NNV candidate vaccine.

Moreover, Senegalese sole are also susceptible to marine VHSV isolates but are not affected by freshwater isolates, such as the VHSV 23-75 strain used as vaccine vector in the present study (57). Therefore, it should be of great interest to evaluate the level of protection conferred by rVHSV N1G1C4 against infection by marine VHSV strains in immunized sole. Another option would be to pseudotype the rVHSV 23-75 strain with the glycoprotein of a marine strain, novirhabdoviruses being extremely flexible in their capacity to accommodate heterologous glycoproteins (58). This could be the starting point for the development of a bivalent live attenuated vaccine candidate for the protection of senegalese sole against two major diseases. In conclusion, these results validate the gene rearrangement approach as a potent and stable attenuation strategy for fish Novirhabdoviruses and open new perspectives to design a live attenuated vaccine platform for fish vaccinology.

Methods

Cells and virus

Epithelioma Papulosum Cyprini (EPC) cells were maintained at 24°C in GMEM/HEPES 25 mM medium supplemented with 2 mM L-glutamine (PAA) and with 10% fetal bovine serum (FBS) (Eurobio) (59). rVHSV were propagated in monolayer cultures of EPC cells at 15°C as previously described (27). Virus titers were determined by plaque assays on EPC cells under an agarose overlay (0.35% agarose in Glasgow's modified Eagle's medium with 25 mM HEPES supplemented with 2% fetal bovine serum and 2 mM L-glutamine). At 3 to 4 days postinfection, cell monolayers were fixed with 10% formalin and stained with crystal violet. Recombinant vaccinia virus expressing the T7 RNA polymerase, vTF7-3, was kindly provided by B. Moss (National Institutes of Health, Bethesda, Md.) (60).

NNV strain SpSsIAusc16003 (herein Ss160) was grown in E-11 cells, a clone of SSN-1 (61), derived from striped snakehead (*Channa striatus*) at 25°C in L-15 Leibovitz (Lonza) medium supplemented with 2% FBS.

Virus purification

For virus purification, wild-type and recombinant VHSVs were mass produced in EPC cells, clarified by low-speed centrifugation (4,000 rpm for 15 min), concentrated 10-fold by ultracentrifugation at 24,000 rpm in a SW28 Beckman rotor for 90 minutes and finally purified by ultracentrifugation at 34,000 rpm in a SW41 Beckman rotor for 4 hours through a 25% (w/v) sucrose cushion in TEN buffer (10 mM Tris-HCl [pH = 7.5], 150 mM NaCl, 1 mM EDTA [pH = 8]). The viral pellet was then resuspended in TEN buffer and viral protein yields of each preparation were quantified by using the Micro BCA assay protein quantification Kit (Pierce) in accordance with the manufacturer's instructions.

Similarly, NNV was grown in a confluent monolayer of E-11 cells maintained in a 150 cm^2 flask, when the cytopathic effect was extensive, the cell medium was collected and centrifuged at 3,000 × *g* for 10 min at 4°C. The supernatant was centrifuged at 25,000 rpm for 1 h in an SW32Ti rotor (Beckman Coulter). The virus was then pelleted in an ultracentrifuge at 35,000 rpm at 4°C in a SW55Ti rotor (Beckman Coulter) through a 30% (w/v) sucrose cushion in TEN buffer. Pelleted virus was resuspended in TEN buffer for SDS–PAGE.

Plasmid constructs and recombinant virus recovery

The recombinant cassette integrated into VHSV cDNA between the N and P genes was constructed as previously described (18, 38). The full-length or domains of the NNV capsid gene (GenBank # NC_024493) was amplified by polymerase chain reaction (PCR) from the infectious cDNA encoding RNA2 pBS160 R2 (62) and specifics primers (Table 3). Amplified capsid PCR products were cloned into pJET 1.2 plasmid and sequenced to check the integrity of the nucleotide sequence prior to the insertion into pVHSV cassette using *NheI* and *PmlI* enzyme restriction sites (Figure 1A).

The different cDNA constructs with rearranged gene order were obtained by gene swap using restriction enzymes (RE), that generate blunt ends, inserted at the beginning and the end of the N, P, M, G, and NV open reading frames (ORF): N (*HpaI*), P (*PmlI*), M (*SnaBI*), G (*BstZ17I*) and NV (*PmeI*) genes (Figure 4A). For the insertion of these restriction sites, fragments of the pVHSV (27) were amplified and cloned into pJET 1.2 cloning vectors (Thermo Fischer Scientific) for further site-directed mutagenesis (QuikChange Site-directed mutagenesis Kit, Stratagene) using the primers in Table 3: Fragment *SacII/PsiI* (N gene, primers 5NHPA/3NHPA); fragment *PsiI/NsiI* (P gene, primers 5PPML/3PPML); fragment *NsiI/MfeI* (M gene, primers 5MSNA/3MSNA); and fragment *MfeI/NdeI* (G gene, primers 5GBST/3GBST; NV gene, primers 5NVPME/3NVPME). After mutagenesis, all fragments were incorporated back into pVHSV, leading to the pVHSV-RES.

cDNA copies of the N, P, M, and G genes flanked by the proper RE sites were obtained by PCR using the Phusion High-Fidelity DNA polymerase (see primers VHSN, VHSP, VHSM and VHSG with proper RE in Table 3) and cloned into pJET 1.2 cloning vector. All cloned genes were sequenced to check the integrity of the nucleotide sequence. Each gene was successively exchanged in the pVHSV-RES, leading to pVHSV N2G4 and pVHSV N2G3 (numbers referring to the positions of the N and G genes in the final cDNA genome) (Figure 4A).

10.3389/fimmu.2023.1138961

TABLE 3 Primers used in the study.

Primer	Sequence (5′ to 3′)[a]	Restriction site
5NNV CP	CCCGCTAGCATGGTACGCAAAGGTGATAAGAAATTGG	*NheI*
3NNV CP	GGGCACGTGTTAGTTTTCCGAGTCAACACGGGTG	*PmlI*
5NNV CAP	CCCGCTAGCGTACGCAAAGGTGATAAGAAATTGGC	*NheI*
3NNV CAP	GGGCACGTGGTTTTCCGAGTCAACACGGGTGAAGAGC	*PmlI*
5NNV LP	CCCGCTAGCACACCTGAGGACACCACCGCTCCAATTACTACC	*NheI*
5NNV LP2bis	CCCCACGTGACACCTGAGGACACCACCGCTCCAATTACTACC	*PmlI*
5NHPA	CAAAAGAACTCAGT**GTTAAC**ATGGAAGGAGGAATCGTGC	*HpaI*
3NHPA	GACTACCCCGAGGACTCTGACTAA**GTTAAC**CTCCCGTCTCATAACC	*HpaI*
5PPML	GCAAGACAAACACTGAGATCAC**GTG**ATGGCTGATATTGAGATGAGC	*PmlI*
3PPML	GGACAAGCTAGAGTAG**CACGTG**CACAACGCATCACACAG	*PmlI*
5MSNA	GGCAACCAACAACT**TACGTA**ATGGCTCTGTTCAAAAGAAAGCG	*SnaBI*
3MSNA	CCTCTGTCCGACCTTGGTAG**TA**CG**T**AAGGACCGACTCAGGC	*SnaBI*
5GBST	GTACACAACAAGCTAGA**GTATAC**ATGGAATGGAACACTTTTTTCTTG	*BstZ17I*
3GBST	CTAGAAGTCAGACGGTCTGAG**TATAC**CTGTCCGAATGACC	*BstZ17I*
5NVPME	GGCACCTTTATGAT**GTTT**AAAC**A**TGGCGACCCAACCCGCGC	*PmeI*
3NVPME	GGCTCTGGGCTCACCTCCTGAG**TTTAAAC**GCCGTCTCTCAG	*PmeI*
5VHSN_Spe	ACTAGTATGGAAGGAGGAATTCGTGCAGCG	*SpeI*
3VHSN_Spe	ACTAGTTTAGTCAGAGTCCTCGGGGTAGTCG	*SpeI*
5VHSN_Pml	AGTCACGTGATGGAAGGAGGAATTCGTGCAGCG	*PmlI*
3VHSN_Pml	GAGCACGTGTTAGTCAGAGTCCTCGGGGTAGTCG	*PmlI*
5VHSP_Hpa	GATGTTAACATGGCTGATATTGAGATGAGCGAGTCCTTGG	*HpaI*
3VHSP_Hpa	GTGGTTAACCTACTCTAGCTTGTCCAGCTCCGCC	*HpaI*
5VHSG_Snab	AGATACGTAATGGAATGGAACACTTTTTTCTTGGTGATC	*SnaBI*
3VHSG_Snab	CAGTACGTATCAGACCGTCTGACTTCTAGAGAACTGCTGC	*SnaBI*
5VHSM_BstZ	ACTGTATACATGGCTCTGTTCAAAAGAAAGCGCACC	*BstZ17I*
3VHSM_BstZ	CCTGTATACCTACCAAGGTCGGACAGAGGAGGTTCCAG	*BstZ17I*
5VHSM_Snab	TACGTAATGGCTCTGTTCAAAAGAAAGCGCACC	*SnaBI*
3VHSM_Snab	TACGTACTACCAAGGTCGGACAGAGGAGGTTCCAG	*SnaBI*
5VHSG_BstZ	GTATACATGGAATGGAACACTTTTTTCTTGGTGATC	*BstZ17I*
3VHSG_BstZ	GTATACTCAGACCGTCTGACTTCTAGAGAACTGCTGC	*BstZ17I*
5VHSG_Pml	CACGTGATGGAATGGAACACTTTTTTCTTGGTGATC	*PmlI*
3VHSG_Pml	CACGTGTCAGACCGTCTGACTTCTAGAGAACTGCTGC	*PmlI*
5SP_LP2	ACATACGTAATGGACACCACGATCACCACTCCG	*SnaBI*
3LP2_TM	ATGTACGTATCAGACCGTCTGACTTCTAGAGAACTGCTG	*SnaBI*
5VHSgfpPsi	CGATTATAACAAGACAAACAACTAGTATGGTGAGCAAGGG	*PsiI*
3VHSgfp Psi/Spe	ATTCTTATAATCGTGCCGTTTTTTTCTATCTATGACTAGTTTACTTGTACAGCTCGTCCATGCCG	*PsiI/SpeI*

a. Restriction enzyme sites are underlined; mutated nucleotides are boldfaced.

In order to construct rearranged VHSV genomes expressing an additional gene (Figure 5), the EGFP cassette, previously described (27), was amplified by PCR from the pVHSV-EGFP and modified to contain two *SpeI* RE sites upstream and downstream the EGFP ORF using the primers 5VHSgfp Psi/3VHSgfp Psi/Spe (Table 3). This fragment was cloned into a pJET 1.2 cloning vector and then the EGFP ORF was exchanged with the N gene using the *SpeI* RE sites. Finally, the N cassette was inserted into pVHSV-RES using the *PsiI* RE site. Each gene was successively exchanged in the pVHSV-RES containing the expression cassette. Eight pVHSV constructs, termed NxGyCz according to the respective positions of the genes encoding the N and the G as well as the expression cassette C along the genome: pVHSV-N2G5C3, -N2G4C3, -N2G3C4, -N2G3C5, -N2G4C1, -N2G5C1, -N2G1C4 and -N2G1C5.

The rVHSVs were readily recovered by transfection of pVHSV constructs together with the helper plasmids pT7-N, pT7-P and pT7-L in EPC cells infected with vTF7-3 vaccinia virus, as previously described (for a review see (63)). Viral titers were determined after 2 passages on EPC cells.

Indirect immunofluorescence analysis on fixed and living cells

EPC cells grown in 24-well plates were infected with the rVHSV expressing NNV epitopes (passage 2, MOI of 0.1). At 24 h or 72 h post-infection, cells were fixed with a mixture of ethanol and acetone (1:1, v/v) at -20°C for 20 min and washed with PBS. Primary mouse monoclonal antibody (mAb) 192A17 (dilution 1:1,000) against VHSV G and rabbit polyclonal antibody (pAb) 484.2.2009 against NNV (dilution 1:5,000; kindly provided by Dr. Anna Toffan (7)) were incubated in PBS-Tween 0.05% for 45 min at room temperature (RT) and washed 3 times with PBS-Tween 0.05%. Cells were then incubated with Alexa Fluor 488-conjugated goat anti-mouse and Alexa Fluor 594-conjugated goat anti-rabbit immunoglobulins diluted to 1:1,000 (Invitrogen) in PBS-Tween 0.05% for 45 min at RT. Cell monolayers were then visualized with a UV-light microscope (Carl Zeiss). For live cells, infected cell monolayers were directly incubated with primary antibodies in GMEM 10% FBS cell culture medium for 45 min at RT. After 3 washes with the same medium, cells were incubated with both 488 and 594 Alexa Fluor-conjugated immunoglobulins (dilution 1:1,000) for 45 min at RT. Three washes were performed and nuclei were stained with Hoechst (dilution 1:1,000; Thermo scientific). Cell monolayers were then visualized with a UV-light microscope (Carl Zeiss).

Protein electrophoresis and Western blot assays

Aliquots of sucrose-purified recombinant viruses were separated on a sodium dodecyl sulfate 4-12% polyacrylamide gel (SDS-PAGE; Life technologies) and electrotransferred onto a polyvinylidene difluoride membrane (ImmobilonP; Millipore). The membrane was saturated in Tris-Buffer Saline containing 0.05% of Tween 20 (TBST) supplemented with 5% skim-milk for 1 h at RT, then incubated with a rabbit pAb 484.2.2009 in TBST 5% milk (dilution 1:7,000) for 1 h at RT. After three washes with TBST, the membrane was incubated for 1 h at RT with horseradish peroxidase (HRP) conjugated anti-rabbit antibody (1:10,000; Sera Care) in TBST 3% milk. After extensive washing with TBST, peroxidase activity was revealed by incubation with ECL Western Blotting Detection Reagents (ECL; Pierce) according to the manufacturer's instructions.

Ethics statement

All animal studies were carried out in strict accordance with the European guidelines and recommendations on animal experimentation and welfare (European Union directive 2010/63). All animal experiment procedures were approved by the local ethics committee on animal experimentation (COMETHEA INRAE no. 45) and were authorized by the Ministère de l'Éducation nationale, de l'Enseignement supérieur et de la Recherche under the numbers: APAFIS#2545-2015121515466368 v1 and APAFIS#29801-2021021110262075 v2. Experimental protocols with sole were approved by the Bioethics and Experimental Animal Welfare Committees of the University of Santiago de Compostela and Xunta de Galicia (Permit Id. 15010/2020/004).

To minimize animal suffering and distress, all manipulations were carried out under light anesthesia. Anesthesia was performed by bath immersion with tricaine 0.005%. A lethal challenge with VHSV typically results in acute disease characterized by exophthalmia, anemia and punctiform hemorrhages, whilst NNV infection lead to anemia, and abnormal swimming due to neurological disorders. Therefore, fish were monitored twice a day for clinical signs and survival. Upon display of typical infection symptoms, animals were humanely euthanized by bath immersion using a lethal dose of tricaine 0.015%.

Experimental fish infection

As summarized in Figure 7, 50 INRA synthetic strain virus-free juvenile rainbow trout (mean weight, 0.8 to 1.8 g) were infected by immersion in tanks filled with 3 L of freshwater with rVHSV viruses (final titer, 5×10^4 PFU/mL) for 2 h at 10°C. Tanks were then filled up to 30 L with freshwater. Controls were mock infected fish kept under the same conditions. Mortalities were recorded daily. Challenges with wild-type VHSV were performed under similar conditions 35 days after immunization. Senegalese sole (~4 g, on average) were acclimatized to 13°C (immunization temperature) for 10 days in our facilities prior to immunization (see Figure 7). After the acclimation period, fish were gently sedated with MS-222 and injected intraperitoneally with 0.1 mL of mutant rVHSV viruses (1×10^6 PFU/mL) and kept in 5 L opaque tanks containing seawater (n = 50/tank). After 7 days the water temperature was increased 1°C/day to reach 22°C (challenge temperature) on day 25. Blood samples (n = 6 per group) were taken 21 days post-immunization and the surviving fish were challenged by immersion in a bath containing the lethal Ss160.03 NNV strain at a concentration of 10^5 $TCID_{50}$/mL for 3 h with strong aeration. Mortalities and clinical signs were recorded

daily. Control fish were mock immunized/infected with L-15 medium under the same conditions. Brains from six dead (at different time post-challenge) or surviving fish were aseptically collected in each group. The organs were individually homogenized and diluted 1:10 (w/v) in Earle's balanced salt solution (Hyclone) supplemented with penicillin (1000 UI ml−1), streptomycin (1000 µg ml−1), gentamicin (500 µg ml−1) and fungizone (20 µg ml−1). The homogenates were clarified by centrifugation at 2000 g for 20 min at 4°C. An aliquot of 0.1 ml of each sample was used for RNA extraction, and subjected to RT-qPCR as described previously (64). Viral load data were calculated as RNA1 copies per gram of brain tissue.

Indirect ELISA for anti-betanodavirus antibody analyses

The level of anti-betanodavirus antibodies in sera from immunized sole have been evaluated following the indirect ELISA procedure previously reported (65). Briefly, sera from sole immunized with the different recombinant viruses (20 µg of total proteins) were diluted in coating buffer [100 mM Bicarbonate/Carbonate, pH 9.6] and immobilized in 96 High Binding flat-bottomed plates (Sarsted, Newton, NC, USA) overnight at 4°C. The samples were blocked with 5% skimmed milk in PBST for 1 h. Afterwards, incubation with a rabbit anti-NNV (484.2.2009, 1:10,000) was performed for 1 h at room temperature. Following washing steps, the samples were incubated with the anti-rabbit IgG-HRP (Sigma Aldrich; 1:25,000) for 1 h at RT. The reaction was revealed with 100 µL per well of 3,3',5,5'-tetramethylbenzidine single solution (ThermoFisher, Waltham, MA, USA) for 20 min and stopped by adding 50 µL of 2 M sulfuric acid. Optical density (OD) was measured at 450 nm. Resulting OD values were normalized by subtracting the OD values of the negative control (omitting fish sera) wells. All assays were performed in duplicate and previously assayed positive serum was used as a positive control.

Structural prediction of LP2 antigen construct using AlphaFold 2

The protein sequence (accession no. NC_024493.1) encoding the capsid of the betanodavirus isolate SpSsIAusc16003 was used to generate structural predictions of the LP2 antigen construct using AlphaFold 2 (43). The open-source software, ColabFold (https://github.com/sokrypton/ColabFold) was used to implement AlphaFold 2 (66). The predicted structure with the highest confidence score (pLDDT) was subsequently used for molecular visualization using UCSF ChimeraX (67).

Data availability statement

The original contributions presented in the study are included in the article/supplementary material. Further inquiries can be directed to the corresponding authors.

Ethics statement

The animal study was reviewed and approved by COMETHEA INRAE no. 45 and the Ministère de l'Éducation nationale, de l'Enseignement supérieur et de la Recherche under the numbers: APAFIS#2545-2015121515466368 v1 and APAFIS#29801-2021021110262075 v2 and by Bioethics and Experimental Animal Welfare Committees of the University of Santiago de Compostela and Xunta de Galicia (Permit Id. 15010/2020/004).

Author contributions

SS, EM, MB, JM and SB conceived and designed the experiments. SS, EM, AC, AL and JB performed the experiments. SS, JM and SB analyzed the data. SS, JM and SB wrote the paper. All authors contributed to the article and approved the submitted version.

Funding

SS was funded with a postdoctoral grant from Consellería de Cultura, Educación y Universidad, Xunta de Galicia (postdoctoral grant ED481B-2018/002). SS would like to thank the group of viral pathology at Institute of Aquaculture (USC) for their contribution to this work. AC has been financially supported by the Research Council of Norway.

Acknowledgments

We are grateful to members of the fish facilities for taking care of experimental fish (IERP, Experimental Unit of Rodents and Fish, INRAE). We thank Dr. Anna Toffan for the gift of NNV pAb.

Conflict of interest

The authors declare that the research was conducted in the absence of any commercial or financial relationships that could be construed as a potential conflict of interest.

Publisher's note

References

1. Mladineo I. The immunohistochemical study of nodavirus changes in larval, juvenile and adult sea bass tissue. *J Appl Ichthyology* (2003) 19:366–70. doi: 10.1111/j.1439-0426.2003.00489.x

2. Bandin I, Souto S. Betanodavirus and VER disease: A 30-year research review. *Pathogens* (2020) 9(2):106. doi: 10.3390/pathogens9020106

3. Sahul Hameed AS, Ninawe AS, Nakai T, Chi SC, Johnson KL, Ictv Report C. ICTV virus taxonomy profile: Nodaviridae. *J Gen Virol* (2019) 100:3–4. doi: 10.1099/jgv.0.001170

4. Comps M, Pépin JF, Bonami JR. Purification and characterization of two fish encephalitis viruses (FEV) infecting lates calcarifer and dicentrarchus labrax. *Aquaculture* (1994) 123:1–10. doi: 10.1016/0044-8486(94)90114-7

5. Munday BL, Kwang J, Moody N. Betanodavirus infections of teleost fish: A review. *J Fish Dis* (2002) 25:127–42. doi: 10.1046/j.1365-2761.2002.00350.x

6. Nishizawa T, Furuhashi M, Nagai T, Nakai T, Muroga K. Genomic classification of fish nodaviruses by molecular phylogenetic analysis of the coat protein gene. *Appl Environ Microbiol* (1997) 63:1633–6. doi: 10.1128/aem.63.4.1633-1636.1997

7. Panzarin V, Toffan A, Abbadi M, Buratin A, Mancin M, Braaen S, et al. Molecular basis for antigenic diversity of genus betanodavirus. *PloS One* (2016) 11:e0158814. doi: 10.1371/journal.pone.0158814

8. Olveira JG, Souto S, Dopazo CP, Thiery R, Barja JL, Bandin I. Comparative analysis of both genomic segments of betanodaviruses isolated from epizootic outbreaks in farmed fish species provides evidence for genetic reassortment. *J Gen Virol* (2009) 90:2940–51. doi: 10.1099/vir.0.013912-0

9. Toffan A, Pascoli F, Pretto T, Panzarin V, Abbadi M, Buratin A, et al. Viral nervous necrosis in gilthead sea bream (Sparus aurata) caused by reassortant betanodavirus RGNNV/SJNNV: An emerging threat for Mediterranean aquaculture. *Sci Rep* (2017) 7:46755. doi: 10.1038/srep46755

10. Volpe E, Gustinellia A, Caffaraa M, Errania F, Quagliob F, Fioravantia ML, et al. Viral nervous necrosis outbreaks caused by the RGNNV/SJNNV reassortant betanodavirus in gilthead sea bream (*Sparus aurata*) and European sea bass (*Dicentrarchus labrax*). *Aquaculture* (2020) 523:735155. doi: 10.1016/j.aquaculture.2020.735155

11. Biasini L, Berto P, Abbadi M, Buratin A, Toson M, Marsella A, et al. Pathogenicity of different betanodavirus RGNNV/SJNNV reassortant strains in European Sea bass. *Pathog 11* (2022) 11:458. doi: 10.3390/pathogens11040458

12. Kaplan M, Pekmez K, Cagirgan AA, Arslan F, Ozkan B, Kalayci G. The first detection of betanodavirus reassortant genotype (RGNNV/SJNNV) isolated from gilthead sea bream (Sparus aurata) in the Turkish coastlines: The importance of screening and monitoring studies for identifying the source of the infection. *J Fish Dis* (2022) 45:783–93. doi: 10.1111/jfd.13603

13. Souto S, Lopez-Jimena B, Alonso MC, Garcia-Rosado E, Bandin I. Experimental susceptibility of European sea bass and Senegalese sole to different betanodavirus isolates. *Vet Microbiol* (2015) 177:53–61. doi: 10.1016/j.vetmic.2015.02.030

14. Walker PJ, Freitas-Astua J, Bejerman N, Blasdell KR, Breyta R, Dietzgen RG, et al. ICTV virus taxonomy profile: Rhabdoviridae 2022. *J Gen Virol 103* (2022) 99:447–8. doi: 10.1099/jgv.0.001020

15. Case JB, Rothlauf PW, Chen RE, Kafai NM, Fox JM, Smith BK, et al. Replication-competent vesicular stomatitis virus vaccine vector protects against SARS-CoV-2-Mediated pathogenesis in mice. *Cell Host Microbe* (2020) 28:465–474.e4. doi: 10.1016/j.chom.2020.07.018

16. Henao-Restrepo AM, Longini IM, Egger M, Dean NE, Edmunds WJ, Camacho A, et al. Efficacy and effectiveness of an rVSV-vectored vaccine expressing Ebola surface glycoprotein: interim results from the Guinea ring vaccination cluster-randomised trial. *Lancet* (2015) 386:857–66. doi: 10.1016/S0140-6736(15)61117-5

17. Lundstrom K. Self-replicating vehicles based on negative strand RNA viruses. *Cancer Gene Ther* (2022). doi: 10.1038/s41417-022-00436-7

18. Rouxel RN, Merour E, Biacchesi S, Bremont M. Complete protection against influenza virus H1N1 strain A/PR/8/34 challenge in mice immunized with non-adjuvanted novirhabdovirus vaccines. *PloS One* (2016) 11:e0164245. doi: 10.1371/journal.pone.0164245

19. Rouxel RN, Tafalla C, Merour E, Leal E, Biacchesi S, Bremont M. Attenuated infectious hematopoietic necrosis virus with rearranged gene order as potential vaccine. *J Virol* (2016) 90:10857–66. doi: 10.1128/JVI.01024-16

20. Willemsen A, Zwart MP. On the stability of sequences inserted into viral genomes. *Virus Evol* (2019) 5:vez045. doi: 10.1093/ve/vez045

21. Biacchesi S, Brémont M. Vaccination against viral hemorrhagic septicemia and infectious hematopoietic necrosis. In: Gudding R, Lillehaug A, Evensen Ø., editors. *Fish vaccination*. Chichester, UK.: John Wiley & Sons, Ltd (2014). p. 334–40.

22. OIE Aquatic Animal Health. Manual of diagnostic tests for aquatic animals. In: *Chapter 2.3.10. infection with viral haemorrhagic septicaemia virus*. Paris, France: World Organisation for Animal Health (2021) 377–401.

23. Schutze H, Enzmann PJ, Mundt E, Mettenleiter TC. Identification of the non-virion (NV) protein of fish rhabdoviruses viral haemorrhagic septicaemia virus and infectious haematopoietic necrosis virus. *J Gen Virol* (1996) 77(Pt 6):1259–63. doi: 10.1099/0022-1317-77-6-1259

24. Schutze H, Mundt E, Mettenleiter TC. Complete genomic sequence of viral hemorrhagic septicemia virus, a fish rhabdovirus. *Virus Genes* (1999) 19:59–65. doi: 10.1023/A:1008140707132

25. Baillon L, Merour E, Cabon J, Louboutin L, Quenault H, Touzain F, et al. A single amino acid change in the non-structural NV protein impacts the virulence phenotype of viral hemorrhagic septicemia virus in trout. *J Gen Virol* (2017) 98:1181–4. doi: 10.1099/jgv.0.000830

26. Baillon L, Merour E, Cabon J, Louboutin L, Vigouroux E, Alencar ALF, et al. The viral hemorrhagic septicemia virus (VHSV) markers of virulence in rainbow trout (Oncorhynchus mykiss). *Front Microbiol* (2020) 11:574231. doi: 10.3389/fmicb.2020.574231

27. Biacchesi S, Lamoureux A, Merour E, Bernard J, Bremont M. Limited interference at the early stage of infection between two recombinant novirhabdoviruses: Viral hemorrhagic septicemia virus and infectious hematopoietic necrosis virus. *J Virol* (2010) 84:10038–50. doi: 10.1128/JVI.00343-10

28. Biacchesi S, Merour E, Chevret D, Lamoureux A, Bernard J, Bremont M. NV proteins of fish novirhabdovirus recruit cellular PPM1Bb protein phosphatase and antagonize RIG-I-Mediated IFN induction. *Sci Rep* (2017) 7:44025. doi: 10.1038/srep44025

29. Abraham G, Banerjee AK. Sequential transcription of the genes of vesicular stomatitis virus. *Proc Natl Acad Sci USA* (1976) 73:1504–8. doi: 10.1073/pnas.73.5.1504

30. Albertini AA, Ruigrok RW, Blondel D. Rabies virus transcription and replication. *Adv Virus Res* (2011) 79:1–22. doi: 10.1016/B978-0-12-387040-7.00001-9

31. Iverson LE, Rose JK. Localized attenuation and discontinuous synthesis during vesicular stomatitis virus transcription. *Cell* (1981) 23:477–84. doi: 10.1016/0092-8674(81)90143-4

32. Liang B. Structures of the mononegavirales polymerases. *J Virol* (2020) 94:e00175-20. doi: 10.1128/JVI.00175-20

33. Flanagan EB, Ball LA, Wertz GW. Moving the glycoprotein gene of vesicular stomatitis virus to promoter-proximal positions accelerates and enhances the protective immune response. *J Virol* (2000) 74:7895–902. doi: 10.1128/JVI.74.17.7895-7902.2000

34. Flanagan EB, Zamparo JM, Ball LA, Rodriguez LL, Wertz GW. Rearrangement of the genes of vesicular stomatitis virus eliminates clinical disease in the natural host: new strategy for vaccine development. *J Virol* (2001) 75:6107–14. doi: 10.1128/JVI.75.13.6107-6114.2001

35. Wertz GW, Perepelitsa VP, Ball LA. Gene rearrangement attenuates expression and lethality of a nonsegmented negative strand RNA virus. *Proc Natl Acad Sci USA* (1998) 95:3501–6. doi: 10.1073/pnas.95.7.3501

36. Ball LA, Pringle CR, Flanagan B, Perepelitsa VP, Wertz GW. Phenotypic consequences of rearranging the P, M, and G genes of vesicular stomatitis virus. *J Virol* (1999) 73:4705–12. doi: 10.1128/JVI.73.6.4705-4712.1999

37. Flanagan EB, Schoeb TR, Wertz GW. Vesicular stomatitis viruses with rearranged genomes have altered invasiveness and neuropathogenesis in mice. *J Virol* (2003) 77:5740–8. doi: 10.1128/JVI.77.10.5740-5748.2003

38. Nzonza A, Lecollinet S, Chat S, Lowenski S, Merour E, Biacchesi S, et al. A recombinant novirhabdovirus presenting at the surface the e glycoprotein from West Nile virus (WNV) is immunogenic and provides partial protection against lethal WNV challenge in BALB/c mice. *PloS One* (2014) 9:e91766. doi: 10.1371/journal.pone.0091766

39. Chen NC, Yoshimura M, Guan HH, Wang TY, Misumi Y, Lin CC, et al. Crystal structures of a piscine betanodavirus: Mechanisms of capsid assembly and viral infection. *PloS Pathog* (2015) 11:e1005203. doi: 10.1371/journal.ppat.1005203

40. Nishizawa T, Takano R, Muroga K. Mapping a neutralizing epitope on the coat protein of striped jack nervous necrosis virus. *J Gen Virol 80 (Pt* (1999) 11):3023–7. doi: 10.1099/0022-1317-80-11-3023

41. Ito Y, Okinaka Y, Mori K, Sugaya T, Nishioka T, Oka M, et al. Variable region of betanodavirus RNA2 is sufficient to determine host specificity. *Dis Aquat Organ* (2008) 79:199–205. doi: 10.3354/dao01906

42. Amend DF. Potentcy testing of fish vaccines. *Developments Biol Standardization* (1981) 49:447–54.

43. Jumper J, Evans R, Pritzel A, Green T, Figurnov M, Ronneberger O, et al. Highly accurate protein structure prediction with AlphaFold. *Nature* (2021) 596:583–9. doi: 10.1038/s41586-021-03819-2

44. Zhang Z, Xing J, Tang X, Sheng X, Chi H, Zhan W. Identification of b-cell epitopes on capsid protein reveals two potential neutralization mechanisms in red-spotted grouper nervous necrosis virus. *J Virol* (2023) 97:e0174822. doi: 10.1128/jvi.01748-22

45. Lin CF, Jiang HK, Chen NC, Wang TY, Chen TY. Novel subunit vaccine with linear array epitope protect giant grouper against nervous necrosis virus infection. *Fish Shellfish Immunol* (2018) 74:551–8. doi: 10.1016/j.fsi.2018.01.029

46. Joshi A, Pathak DC, Mannan MA, Kaushik V. In-silico designing of epitope-based vaccine against the seven banded grouper nervous necrosis virus affecting fish species. *Netw Model Anal Health Inform Bioinform* (2021) 10:37. doi: 10.1007/s13721-021-00315-5

47. Krempl C, Murphy BR, Collins PL. Recombinant respiratory syncytial virus with the G and f genes shifted to the promoter-proximal positions. *J Virol* (2002) 76:11931–42. doi: 10.1128/JVI.76.23.11931-11942.2002

48. Pesko K, Voigt EA, Swick A, Morley VJ, Timm C, Yin J, et al. Genome rearrangement affects RNA virus adaptability on prostate cancer cells. *Front Genet* (2015) 6:121. doi: 10.3389/fgene.2015.00121

49. Chare ER, Gould EA, Holmes EC. Phylogenetic analysis reveals a low rate of homologous recombination in negative-sense RNA viruses. *J Gen Virol* (2003) 84:2691–703. doi: 10.1099/vir.0.19277-0

50. Lorenzen N, Cupit PM, Einer-Jensen K, Lorenzen E, Ahrens P, Secombes CJ, et al. Immunoprophylaxis in fish by injection of mouse antibody genes. *Nat Biotechnol* (2000) 18:1177–80. doi: 10.1038/81169

51. Boudinot P, Blanco M, de Kinkelin P, Benmansour A. Combined DNA immunization with the glycoprotein gene of viral hemorrhagic septicemia virus and infectious hematopoietic necrosis virus induces double-specific protective immunity and nonspecific response in rainbow trout. *Virology* (1998) 249:297–306. doi: 10.1006/viro.1998.9322

52. Lecocq-Xhonneux F, Thiry M, Dheur I, Rossius M, Vanderheijden N, Martial J, et al. A recombinant viral haemorrhagic septicaemia virus glycoprotein expressed in insect cells induces protective immunity in rainbow trout. *J Gen Virol* (1994) 75(Pt 7):1579–87. doi: 10.1099/0022-1317-75-7-1579

53. Lorenzen N, Olesen NJ, Jorgensen PE, Etzerodt M, Holtet TL, Thogersen HC. Molecular cloning and expression in escherichia coli of the glycoprotein gene of VHS virus, and immunization of rainbow trout with the recombinant protein. *J Gen Virol* (1993) 74(Pt 4):623–30. doi: 10.1099/0022-1317-74-4-623

54. Lu X, Li W, Guo J, Jia P, Zhang W, Yi M, et al. N protein of viral hemorrhagic septicemia virus suppresses STAT1-mediated MHC class II transcription to impair antigen presentation in Sea perch, lateolabrax japonicus. *J Immunol* (2022) 208:1076–84. doi: 10.4049/jimmunol.2100939

55. Wang ZX, Zhou Y, Lu LF, Lu XB, Ni B, Liu MX, et al. Infectious hematopoietic necrosis virus n protein suppresses fish IFN1 production by targeting the MITA. *Fish Shellfish Immunol* (2020) 97:523–30. doi: 10.1016/j.fsi.2019.12.075

56. Gye HJ, Nishizawa T. Sites responsible for infectivity and antigenicity on nervous necrosis virus (NNV) appear to be distinct. *Sci Rep* (2021) 11:3608. doi: 10.1038/s41598-021-83078-3

57. Lopez-Vazquez C, Conde M, Dopazo CP, Barja JL, Bandin I. Susceptibility of juvenile sole solea senegalensis to marine isolates of viral haemorrhagic septicaemia virus from wild and farmed fish. *Dis Aquat Organ* (2011) 93:111–6. doi: 10.3354/dao02299

58. Biacchesi S, Bearzotti M, Bouguyon E, Bremont M. Heterologous exchanges of the glycoprotein and the matrix protein in a novirhabdovirus. *J Virol* (2002) 76:2881–9. doi: 10.1128/JVI.76.6.2881-2889.2002

59. Fijan N, Sulimanovic M, Bearzotti M, Muzinic D, Zwillenberg LO, Chilmonczyk S, et al. Some properties of the *Epithelioma papulosum cyprini* EPC cell line from carp cyprinus carpio. *Annales l'Institut Pasteur Virol* (1983) 134E:207–20. doi: 10.1016/S0769-2617(83)80060-4

60. Fuerst TR, Niles EG, Studier FW, Moss B. Eukaryotic transient-expression system based on recombinant vaccinia virus that synthesizes bacteriophage T7 RNA polymerase. *Proc Natl Acad Sci USA* (1986) 83:8122–6. doi: 10.1073/pnas.83.21.8122

61. Iwamoto T, Nakai T, Mori K, Arimoto M, Furusawa I. Cloning of the fish cell line SSN-1 for piscine nodaviruses. *Dis Aquat Organ* (2000) 43:81–9. doi: 10.3354/dao043081

62. Souto S, Merour E, Biacchesi S, Bremont M, Olveira JG, Bandin I. *In vitro* and *in vivo* characterization of molecular determinants of virulence in reassortant betanodavirus. *J Gen Virol* (2015) 96:1287–96. doi: 10.1099/vir.0.000064

63. Biacchesi S. The reverse genetics applied to fish RNA viruses. *Vet Res* (2011) 42:12. doi: 10.1186/1297-9716-42-12

64. Olveira JG, Souto S, Bandin I, Dopazo CP. Development and validation of a SYBR green real time PCR protocol for detection and quantification of nervous necrosis virus (NNV) using different standards. *Anim (Basel)* (2021) 11:1100. doi: 10.3390/ani11041100

65. Valero Y, Olveira JG, Lopez-Vazquez C, Dopazo CP, Bandin I, Inactivated Vaccine Induces Innate BEI. And adaptive responses and elicits partial protection upon reassortant betanodavirus infection in Senegalese sole. *Vaccines (Basel)* (2021) 9:458. doi: 10.3390/vaccines9050458

66. Mirdita M, Schutze K, Moriwaki Y, Heo L, Ovchinnikov S, Steinegger M. ColabFold: making protein folding accessible to all. *Nat Methods* (2022) 19:679–82. doi: 10.1038/s41592-022-01488-1

67. Pettersen EF, Goddard TD, Huang CC, Meng EC, Couch GS, Croll TI, et al. UCSF ChimeraX: Structure visualization for researchers, educators, and developers. *Protein Sci* (2021) 30:70–82. doi: 10.1002/pro.3943

frontiers | Frontiers in Immunology

TYPE Original Research
PUBLISHED 30 March 2023
DOI 10.3389/fimmu.2023.1143034

OPEN ACCESS

EDITED BY
Brad Pickering,
National Centre for Foreign Animal Disease (NCFAD), Canada

REVIEWED BY
Guy Palmer,
Washington State University, United States
Shawn Babiuk,
National Centre for Foreign Animal Disease (NCFAD), Canada

*CORRESPONDENCE
Ros Chapman
ros.chapman@uct.ac.za

SPECIALTY SECTION
This article was submitted to Vaccines and Molecular Therapeutics, a section of the journal Frontiers in Immunology

RECEIVED 12 January 2023
ACCEPTED 21 March 2023
PUBLISHED 30 March 2023

CITATION
Whittle L, Chapman R, Douglass N, Jaffer M, Margolin E, Rybicki E and Williamson A-L (2023) Development of a dual vaccine against East Coast fever and lumpy skin disease.
Front. Immunol. 14:1143034.
doi: 10.3389/fimmu.2023.1143034

Development of a dual vaccine against East Coast fever and lumpy skin disease

Leah Whittle[1,2], Ros Chapman[1,2]*, Nicola Douglass[1,2], Mohamed Jaffer[3], Emmanuel Margolin[1,2,4], Edward Rybicki[1,4] and Anna-Lise Williamson[1,2]

[1]Institute of Infectious Disease and Molecular Medicine, Faculty of Health Sciences, University of Cape Town, Cape Town, South Africa, [2]Division of Medical Virology, Department of Pathology, Faculty of Health Sciences, University of Cape Town, Cape Town, South Africa, [3]Electron Microscope Unit, University of Cape Town, Cape Town, South Africa, [4]Biopharming Research Unit, Department of Molecular and Cell Biology, Faculty of Science, University of Cape Town, Cape Town, South Africa

East Coast fever is an acute bovine disease caused by the apicomplexan parasite *Theileria parva* and is regarded as one of the most important tick-vectored diseases in Africa. The current vaccination procedure has many drawbacks, as it involves the use of live *T. parva* sporozoites. As a novel vaccination strategy, we have constructed the recombinant lumpy skin disease virus (LSDV) named LSDV-SODis-p67HA-BLV-Gag, encoding a modified form of the *T. parva* p67 surface antigen (p67HA), as well as the bovine leukemia virus (BLV) gag gene for the formation of virus-like particles (VLPs) to potentially enhance p67 immunogenicity. In place of the native sequence, the chimeric p67HA antigen has the human tissue plasminogen activator signal sequence and the influenza hemagglutinin A2 transmembrane domain and cytoplasmic tail. p67HA was detected on the surface of infected cells, and VLPs comprising BLV Gag and p67HA were produced. We also show that higher multiple bands observed in western blot analysis are due to glycosylation of p67. The two vaccines, pMExT-p67HA (DNA) and LSDV-SODis-p67HA-BLV-Gag, were tested for immunogenicity in mice. p67-binding antibodies were produced by vaccinated animals, with higher titers detected in mice vaccinated with the recombinant LSDV. This candidate dual vaccine warrants further testing in cattle.

KEYWORDS

***Theileria parva*, East Coast fever, p67, VLPs, Gag, LSDV, poxvirus, vaccine**

1 Introduction

Tick-borne diseases are a major challenge to cattle farmers in Africa. Of these, East Coast fever (ECF) is considered one of the most burdensome in the affected east and sub-Saharan regions (1–5). The disease is acute and characterized by a fever, respiratory distress, mucosal petechiae and recumbency. Severe cases often result in death after three weeks due to fluid build-up in the lungs and consequent respiratory failure (6, 7). The

causative agent, the apicomplexan parasite *Theileria parva*, is transmitted to cattle or buffalo *via* the brown ear tick *Rhipicephalus appendiculatus* (8). Currently, cattle are immunized against ECF by the infection and treatment method (ITM) which involves the use of live *T. parva* sporozoites and the immediate administration of long-acting oxytetracycline (9). While this does provide effective protection against ECF, there are many drawbacks to this method which include 1) the production of live *T. parva* sporozoites is a lengthy process that requires cattle, rabbits and ticks, 2) liquid nitrogen is required for storage and transport of live parasites and 3) cattle immunized by this method become *T. parva* carriers and can spread the disease 4) the potential development of oxytetracycline resistance (10–13).

Other vaccine platforms have the potential to overcome the logistics of using a live unattenuated parasite as a vaccine. Lumpy skin disease virus (LSDV) would be an ideal candidate to vector *T. parva* antigens. Poxviruses are relatively stable and can be freeze-dried, they do not require animals for vaccine production and pose no risk to establishing a *T. parva* carrier state (14). In addition, their large genomes can tolerate the insertion of multiple foreign genes, and poxviruses are known to induce strong humoral and cellular immune responses (15, 16). LSDV has the added advantage of providing protection against lumpy skin disease (LSD) (17). LSD is a serious threat to the cattle industry and many African countries affected by it are also affected by ECF (8, 18). LSD is characterized by fever, ocular and nasal discharge, and painful nodular lesions (19, 20). Infertility, loss of body weight and decreased milk production also have negative economic impacts in affected regions (21). A number of live attenuated LSDV strains have been developed to protect cattle against LSD, such as the Neethling vaccine strain produced by Onderstepoort Biological Products (OBP) currently used in South Africa (22). Attenuated LSDV has been used in experimental vaccines to vector the antigens of other pathogens, not only limited to cattle, which include those of human immunodeficiency virus (HIV), rabies virus and Rift Valley fever virus (23–25). Our group has constructed an improved LSDV recombinant backbone named nLSDVSODis-UCT which is based on the Neethling vaccine strain (26). When used to vector bovine ephemeral fever virus (BEFV) antigens, vaccinated cattle produced BEFV neutralizing antibodies at titers considered protective and survived virulent LSDV challenge (17). Therefore, nLSDVSODis-UCT would be an ideal choice for a poxvirus-vectored ECF vaccine.

Many efforts have been made to develop a novel ECF vaccine using the *T. parva* major sporozoite surface protein p67 (27). The antigen induces sporozoite neutralizing antibodies in cattle, however only partial protection against *T. parva* challenge has been attained (28). Others have shown that the immunogenicity of p67 truncated to its C-terminal region (p67C) was improved when placed on the surface of baculovirus virions, hepatitis B VLPs or associated with silica vesicles, in comparison to free soluble p67C (28, 29). Therefore, we hypothesized that a less-truncated p67 displayed on a particle may provide an even further improved p67-based vaccine. We have previously attempted to improve the immunogenicity by displaying p67 with an influenza hemagglutinin A2 (HA_2) anchor on the surface of retrovirus Gag virus-like particles (VLPs) (30). The antigen named p67HA retains all the known immunogenic regions of p67 and would potentially benefit from the immunogenic enhancement of VLP display. p67HA was characterized using DNA mammalian expression vectors and was shown to be immunogenic in mice.

DNA vaccines have previously yielded unsuccessful results in cattle (31, 32) and LSDV has been shown to be a good vaccine vector (17). We therefore constructed a recombinant LSDV, LSDV-SODis-p67HA-BLV-Gag, to express the described p67HA together with bovine leukemia virus (BLV) Gag so as to generate VLPs. Expression of the antigens were characterized by immunostaining and electron microscopy, and the immunogenicity of the recombinant LSDV was compared to the p67HA DNA vaccine in mice. We also investigated glycosylation of recombinant p67 expressed in mammalian cells using soluble purified p67.

2 Materials and methods

2.1 Cells, fertilized hens' eggs, viruses and antibodies

Madin Darby bovine epithelial kidney cells (MDBK) (CCL-22™ ATCC®, USA), baby hamster kidney fibroblast 21 cells (BHK-21) (CCL-10™ ATCC, USA), HeLa cells (CCL-2™ ATCC®, USA) and primary fetal lamb testes (LT) cells were cultured in Dulbecco's modified Eagle's medium with GlutaMAX™ (DMEM) (Thermo Fisher Scientific, USA) containing 10% fetal bovine serum (FBS) (Thermo Fisher Scientific, USA, or HyClone™ Cytiva, USA for LT cells) and 1X penicillin/streptomycin (1000 U/ml each, Lonza, Belgium), at 37°C with 5% CO_2.

Specific pathogen-free (SPF) Leghorn chicken eggs (AviFarms, RSA) were maintained in accordance with the University of Cape Town (UCT) Animal Ethics Committee (AEC) protocol AEC 018-022.

nLSDVSODis-UCT was used as the LSDV backbone and for experimental controls. The virus is based on the Neethling vaccine strain originally obtained from Onderstepoort Biological Products (OBP, RSA), which was modified to encode a synthetic, improved and stabilized superoxide dismutase gene (SODis) (26). The parent virus, LSDV (SODis)BEFV-Gb, has nLSDVSODis-UCT encoding the BEFV glycoprotein Gb antigen and eGFP, under the control of the respective vaccinia virus (VACV) mH5 and synthetic pSS poxvirus promoters, all inserted between open reading frame (ORF) 49 and 50 (17).

Rabbit polyclonal anti-p67 raised against the peptide LKKTLQPGKTSTGETC (GenScript, China) which contained the *T. parva* sporozoite neutralizing epitope recognized by the monoclonal AR22.7 (33), mouse monoclonal anti-BLV p24 (Gag) (BLV-3, VMRD, USA) and mouse monoclonal anti-X6 His (MCA1396, Bio-Rad, USA) were used as primary antibodies.

2.2 Design, construction and passage of the recombinant LSDV

The *T. parva* modified p67 major sporozoite surface antigens named p67HA and p67ΔTM have been described previously (30)

(Figure 1A). The p67 amino acid regions are identical to wild-type p67 (Muguga, GenBank: AAA98601.1). p67HA is the primary immunogen in this study whereas p67ΔTM purified from HEK293T cell media was used for assays.

The transfer vector pUC57-p67HA-BLV-Gag-mCherry (Figure 1B) was constructed to have the genes for p67HA, BLV gag (GenBank: AP018021.1) (30) and fluorescent marker mCherry, with the respective TTTTTCT, TTTTTAT and TTTTTGT poxvirus terminators, under the control of the respective VACV mH5, synthetic pLEO and modified fowlpox mFP promoters (35). This expression cassette was flanked by the 3' ends of LSDV ORFs 49 and 50, and all genetic elements were amplified in the plasmid backbone pUC57-Simple (GenScript, China).

LSDV-SODis-p67HA-BLV-Gag was made by homologous recombination between the transfer vector pUC57-p67HA-BLV-Gag-mCherry and parent virus LSDV(SODis)BEFV-Gb (Figure 1B). LT cells were infected with LSDV(SODis)BEFV-Gb in DMEM at a range of multiplicities of infection (MOI) from 0.05 to 0.5, for two hours in 12-well plates. The media was removed and cells were subsequently transfected with 5 µg of pUC57-p67HA-BLV-Gag-mCherry linearized with KpnI and PacI (FastDigest, Thermo Fisher Scientific, USA), using 3 µl XtremeGENE™ HP (Roche, Switzerland) in DMEM. At two day's post infection, cells were lysed by two freeze/thaw cycles (-80°C/37°C). The resulting lysates were passaged in MDBK cells and foci of MDBK cells that fluoresced red due to potential infection with LSDV-SODis-p67HA-BLV-Gag were physically scraped with a 10 µl pipette tip, placed into 100 µl DMEM in 1.5 ml microcentrifuge tubes, and lysed by two freeze/thaw cycles. Lysates were repeatedly passaged in MDBK cells until no green fluorescence (due to parent LSDV) was observed.

LSDV-SODis-p67HA-BLV-Gag was passaged twice in chick chorioallantoic membranes (CAMs) to remove any bovine viral diarrhea virus (BVDV) which may have been present in the MDBK cells. This was carried out as previously described (36). Further passages were performed in LT cells or BHK-21 cells to maintain BVDV-free stocks. Micrographs were obtained with AxioVert A.1 inverted fluorescence microscopes and Zen Blue 3.1 software (Zeiss, Germany).

2.3 Preparation of LSDV stocks

High titer stocks of LSDV-SODis-p67HA-BLV-Gag and nLSDVSODis-UCT were prepared by infecting MDBK, LT or BHK-21 cells in 175 cm^3 flasks or HYPERFlasks® (Corning®, USA) at MOIs 0.0025 to 0.005. Once all cells were infected and about 50% of cells had lifted, the flasks were frozen and thawed twice and lysates were clarified by low speed centrifugation at 320 x g for 10 min. Supernatants were placed into SS34 tubes and underlaid with 1-1.5 ml of 36% (w/v) sucrose diluted in 1X PBS. Viruses were pelleted by centrifugation at 27 000-39 000 x g for 1-2 hrs at 4°C. The pellets were resuspended in 1X PBS and stored at -80°C until needed. Prepared stocks were titrated by infecting MDBK cells in 96-well plates with serial dilutions of the stock (10^{-1} to 10^{-12} in DMEM) and tissue culture infectious dose at 50% infection ($TCID_{50}$) was determined using the method described by Reed and Muench (37).

2.4 PCR confirmation of the insert

Amplification of the insert between ORFs 49 and 50 by polymerase chain reaction (PCR) was performed to confirm the presence of the expression cassette. DNA extracted from cells was used as template with forward (5' GAGTGAAGCCTGGAACAT 3') and reverse (5' ACTCTATCGCATCTGGAAACT 3') primers (17), Phusion® High Fidelity DNA Polymerase (New England Biolabs, USA) and Phusion HF Buffer. The reaction parameters were as follows: initial denaturation at 98°C for 1 min, cycling conditions (25 cycles) of denaturation at 98°C for 30 s, annealing at 60°C for 30 s and extension at 72°C for 3 min, followed by a final single extension step at 72°C for 10 min. The products were resolved by electrophoresis in 0.8% agarose gels with 0.25 µg/ml ethidium bromide and 1X Tris borate EDTA (TBE) buffer.

2.5 Confirmation of p67HA and BLV Gag expression

The expression of p67HA and BLV Gag was confirmed by SDS PAGE and western blot analysis. MDBK cells or BHK-21 cells were infected with virus at MOIs 0.25-0.5. After 2-3 days, media was removed and cells were lysed with 200 µl Glo Lysis Buffer (Promega, USA) according to the manufacturer's protocol. Media and lysates were clarified by centrifugation at 13 500 x g for 10 min, and the resulting supernatants were incubated at 95°C for 5 min in Laemmli buffer. Samples were separated in resolving gels containing 10% bis-acrylamide and detected as previously described (30). Goat anti-rabbit-IgG (A3687, Sigma, USA) and goat anti-mouse-IgG (ab97020, Abcam, UK), both conjugated to alkaline phosphatase, were used as secondary antibodies at 1:10 000.

2.6 Immunofluorescent staining of fixed and live cells

Immunostaining of fixed MDBK cells in 24-well plates infected with LSDV-SODis-p67HA-BLV-Gag at MOI 0.05 was performed as previously described at two days post-infection (30, 38). Live staining of HeLa cells infected with virus at MOI 0.05 in 4-well Permanox® chamber slides (Thermo Fisher Scientific, USA) coated with poly-L-lysine (P8920, Sigma, USA) was performed at two days post infection as previously described (30, 38) using 1:100 anti-p67 antibody. Donkey anti-rabbit-IgG conjugated to Alexa Fluor 488 (Life Technologies, USA) was used as the secondary antibody at 1:1000.

2.7 Glycosylation status of p67ΔTM

N-linked and O-linked glycosylation sites in wild-type p67 (GenBank: AAA98601.1) - excluding the SS and anchor - were predicted with NetNGlyc-1.0 (39) and NetOGlyc-4.0 (40). Purified p67ΔTM was subjected to deglycosylation by treatment of 5 µg protein with PNGase F (New England Biolabs, USA) and 10 µg protein with Protein Deglycosylation Mix II (New England Biolabs, USA) according to the manufacturer's protocol. SDS PAGE and western blots of the samples were carried out as described further above using 1:1000 anti-His antibody.

2.8 Electron microscopy

To isolate BLV Gag VLPs and poxvirions, MDBK cells in 75 cm^3 flasks were infected with virus at MOIs 0.5 and 1. At three days post-infection, media from the flasks were harvested and fresh DMEM was added to each flask. Cells attached to the flasks were lysed in the fresh DMEM by two freeze/thaw cycles. The lysate and harvested media were clarified by centrifugation at 1260 x g for 10 min, placed into SS34 tubes, underlaid with 5 ml 12% OptiPrep™ (Sigma-Aldrich, USA) diluted in 1X Tris-buffered saline (TBS) and centrifuged at 48 000 x g for 1 hr at 4°C. Immunogold-labelling of VLPs and negative staining of pelleted poxvirus diluted 1:10 in TBS, with goat anti-rabbit-IgG conjugated to 10 nm colloidal gold (G7402, Sigma, USA) was performed as previously described (30). SDS PAGE and western blots were performed on isolated VLP samples as described earlier.

For ultra-thin sections, MDBK cells in 6-well plates were infected with virus at MOI 1. Two days post-infection, cells were fixed in the plate with 1 ml 2.5% glutaraldehyde diluted in PBS for 5 min at room temperature. Cells were scraped off the wells, placed into microcentrifuge tubes and centrifuged for 3 min at 15 900 x g. The pellets were resuspended in 1 ml PBS and centrifuged at 2350 x g for 2 min. The cell pellets were fixed a second time with 50 µl 2.5% glutaraldehyde for 1 hr at room temperature and washed twice with 100 µl PBS by pelleting at 2350 x g and resuspending. Low melting point agarose, 2% in H_2O at 37°C, was added to cells and allowed to set. Samples were cut into 1 cm^3 blocks, incubated in 0.5% tannic acid at room temperature for 1 hr, washed twice with PBS, fixed with 1% osmium tetroxide in PBS at room temperature for 1 hr, washed twice in PBS for 5 min and washed once in H_2O for 5 min. Samples were dehydrated by an ethanol gradient: 30%, 50%, 70%, 80%, 90%, 95%, 100%, 10 min per percentage and incubated again in 100% ethanol for 10 min. The dehydrated samples were incubated twice in acetone for 10 min, overnight in 400 µl 1:1 acetone:resin (agar low viscosity resin, Agar Scientific, UK) and for 8 hrs in a 1:3 acetone: resin mixture. Samples were incubated overnight in 100% resin, replaced with fresh 100% resin, orientated into molds and set at 60°C for 24 hrs. Sections were placed on copper grids and stained with 2% uranyl acetate and lead citrate.

Grids were viewed by conventional transmission electron microscopy (TEM) with a Tecnai F20 microscope (Thermo Fisher (formerly FEI), Eindhoven, Netherlands) at the UCT Electron Microscope Unit.

2.9 Mouse immunizations

Mouse experiments were conducted at the UCT Research Animal Facility after approval by the UCT AEC for protocol AEC 020-020. Four groups of female BALB/c mice, five mice per group, were inoculated intramuscularly twice, 28 days apart, with 100 µl PBS (Thermo Fisher Scientific, USA), 100 µg pMExT-p67HA plasmid (30), 10^6 ffu nLSDVSODis-UCT or 10^6 ffu LSDV-SODis-p67HA-BLV-Gag. Plasmid and viruses were diluted in 100 µl PBS, and mice were injected with 50 µl inoculum per hind leg. End-bleeds were obtained by cardiac puncture on day 42 (PBS and pMExT-p67HA) and day 44 (nLSDVSODis-UCT and LSDV-SODis-p67HA-BLV-Gag).

2.10 Enzyme-linked immunosorbent assays

ELISAs to detect the presence of p67-binding and BLV Gag-binding antibodies in mouse sera were carried out as previously described using plates coated with purified p67ΔTM or purified BLV Gag (30). End-point titers were determined as the highest dilution that had an ELISA signal at least two-fold greater than that of the average PBS group 10^{-1} dilution reading. Data were analyzed in GraphPad Prism 5.0 (GraphPad, USA) whereby a one-way ANOVA and *post-hoc* Bonferroni test were conducted.

3 Results

3.1 Passage of LSDV-SODis-p67HA-BLV-Gag

LSDV-SODis-p67HA-BLV-Gag was designed to express p67HA on the surface of BLV Gag VLPs to potentially enhance the immunogenicity of the p67 antigen (Figure 1). The fluorescent marker mCherry was included in the expression cassette to enable the recombinant virus to be distinguishable (red) from the parent virus (green) (Figure 1B). To construct the virus, at passage 0 (P0), LT cells were infected with the parent virus LSDV(SODis)BEFV-Gb and transfected with the transfer vector to enable homologous recombination to occur (Figure 2). The recombinant was isolated by physically picking red-fluorescing foci and passaging the resultant lysate in MDBK cells until no green fluorescence was seen - at P3. MDBK cells were used for this purpose as LSDV forms distinct foci, easy to pick, in this cell line. Unfortunately, MDBK cells harbour BVDV, a contaminating virus that cannot be present in LSDV stocks intended for cattle vaccination (36). Therefore, LSDV-SODis-p67HA-BLV-Gag was passaged twice in the CAMs of fertilized hens' eggs at P10 and P11 to remove BVDV. Infected CAMs showed typical white pocks characteristic of LSDV infection. Further passages were performed in LT cells or BHK-21 cells to have stocks free from BVDV. BHK-21 cells were used for later

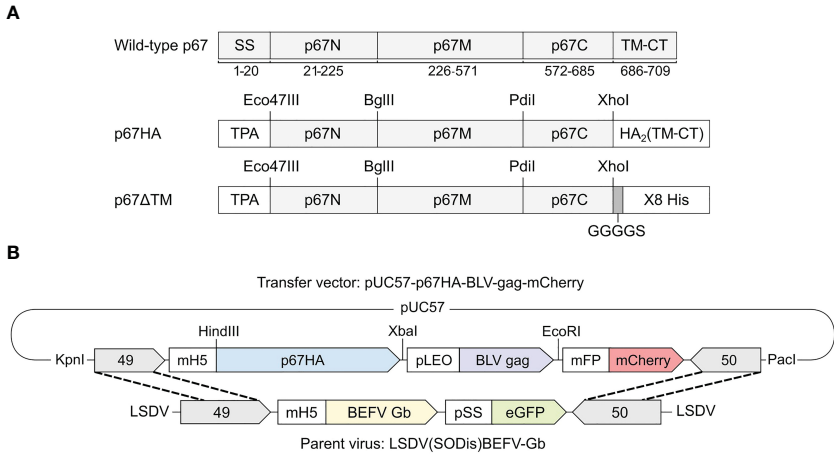

FIGURE 1
(A) Schematic diagrams of the recombinant antigens p67HA and p67ΔTM in comparison to wild-type p67 (Muguga, GenBank: AP018021.1) with labelled amino acid residue positions underneath. The p67N, p67M and p67C regions based on B-cell epitope distribution are annotated as previously described (34). Both p67HA and p67ΔTM had the native signal sequence (SS) replaced with that of the human tissue plasminogen activator (TPA). The native predicted transmembrane domain and cytoplasmic tail (TM-CT) were replaced with those of influenza virus A H5N1 hemagglutinin 2 (HA_2) for p67HA or were replaced with a GGGGS linker and 8X His tag for p67ΔTM. **(B)** Schematic diagram of the transfer vector pUC57-p67HA-BLV-Gag-mCherry for homologous recombination with the parent virus LSDV(SODis)BEFV-Gb genome between ORFs 49 and 50 to generate LSDV-SODis-p67HA-BLV-Gag. Restriction enzyme sites that were used for cloning or removal of the expression cassette from pUC57-Simple are labelled.

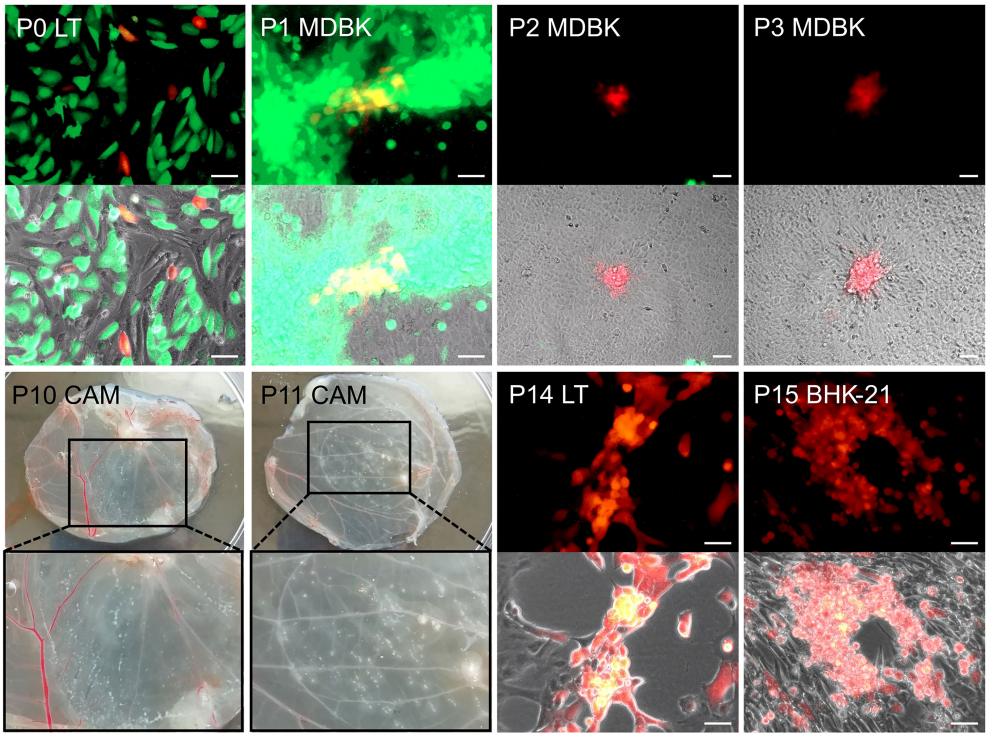

FIGURE 2
Generation and passage of LSDV-SODis-p67HA-BLV-Gag. The recombinant virus (mCherry; red) was constructed in LT cells at passage 0 (P0) by infection with LSDV(SODis)BEFV-Gb (eGFP; green) and transfection with the transfer vector. P1 MDBK = first passage of the lysate in MDBK cells, P2 MDBK = second passage in MDBK cells, P3 MDBK = third passage in MDBK cells. P10 CAM and P11 CAM show passage of the recombinant in CAMs of fertilized hens' eggs. Magnified inserts show regions of LSDV white pocks. Later passages were performed in LT (P14 LT) and BHK-21 (P15 BHK-21) cells. Micrographs were taken using fluorescence only (upper panels) and fluorescence with phase (lower panels). All scale bars: 50 µm.

10.3389/fimmu.2023.1143034

passages, once this cell line was shown to be permissive for LSDV growth (35).

3.2 Verification and characterization of LSDV-SODis-p67HA-BLV-Gag

The insert between LSDV ORFs 49 and 50 was amplified by PCR to confirm the presence of the expression cassette (Figures 3A, B). LSDV-SODis-p67HA-BLV-Gag gave a product slightly larger than the expected 5801 bp size (Figure 3B), however sequencing showed that this product was correct. The expected product was seen for the nLSDVSODis-UCT positive control, and no LSDV (SODis)BEFV-Gb parent virus was detected.

SDS PAGE and western blotting confirmed the expression of the p67HA and BLV Gag proteins from cells infected with LSDV-SODis-p67HA-BLV-Gag (Figure 3C). BLV Gag was detected in lysate and media near the expected 43 kDa size, whereas p67HA which translates to 77 kDa was observed as multiple proteins with a predominant form slightly below 130 kDa in the lysate. Immunofluorescent staining of fixed infected MDBK cells further confirmed the expression of p67HA as seen by the overlap of green

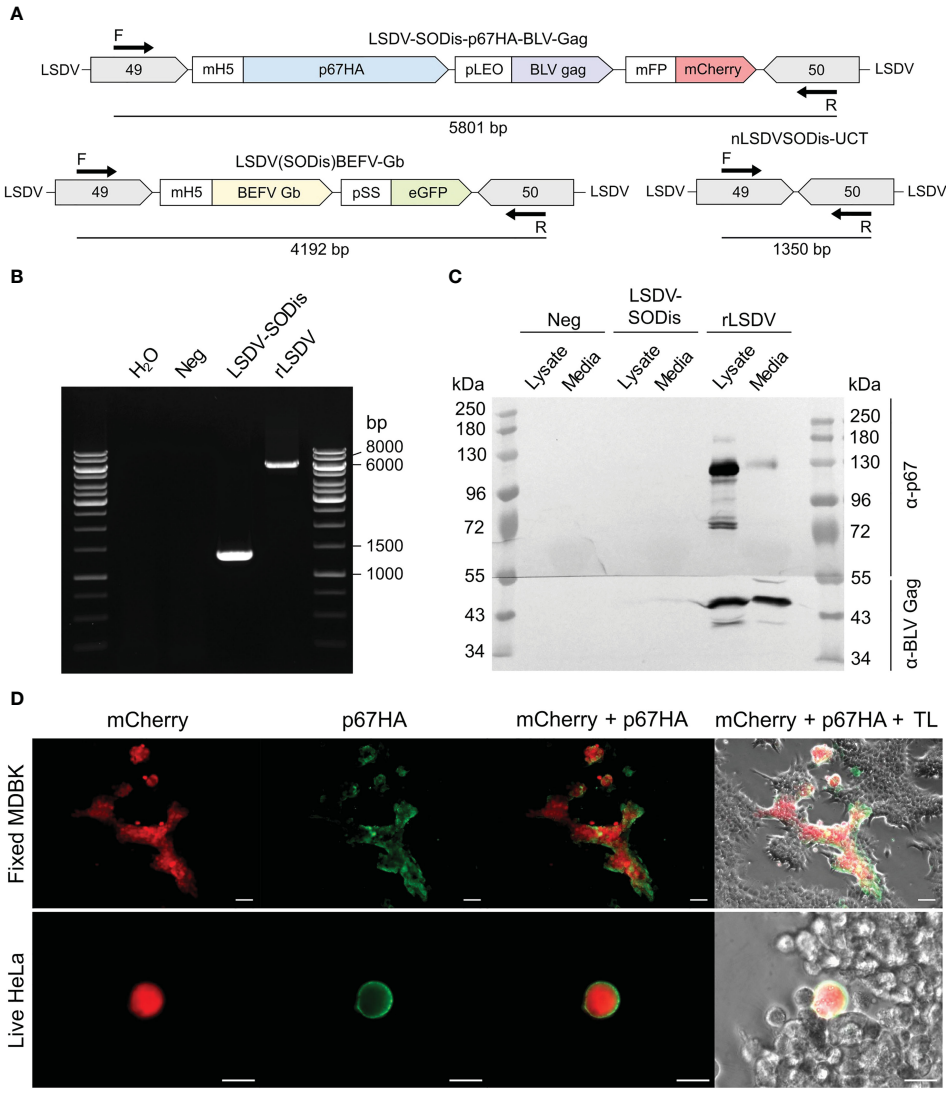

FIGURE 3
(A) Schematic diagrams of PCR product sizes expected to be amplified by the forward (F) and reverse (R) primers from LSDV-SODis-p67HA-BLV-Gag, the parent virus LSDV(SODis)BEFV-Gb, and the control virus nLSDVSODis-UCT which contained no insert. **(B)** Gel electrophoresis of PCR products from samples that had no template (H_2O) or from DNA extracted from MDBK cells infected with no virus (Neg), nLSDVSODis-UCT (LSDV-SODis) or LSDV-SODis-p67HA-BLV-Gag (rLSDV). **(C)** SDS PAGE and western blot of samples from MDBK cells. The membrane was cut in half and probed with either anti-p67 antibody (α-p67) or anti-BLV-p24 (Gag) antibody (α-BLV Gag). **(D)** Immunofluorescent staining of fixed MDBK cells (scale bar: 50 μm) and live HeLa cells (scale bar: 20 μm), both infected with LSDV-SODis-p67HA-BLV-Gag at MOI 0.05, seen with mCherry, probed with anti-p67 antibody and a secondary antibody conjugated to Alexa Fluor 488 (green). TL: Transmitted light.

and red fluorescence (Figure 3D). Live cell immunofluorescent staining was performed, as incorporation into BLV Gag VLPs requires the antigen to be present at the plasma membrane. Surface localization of p67HA was confirmed on infected HeLa cells (Figure 3D).

3.3 Electron microscopy of LSDV-SODis-p67HA-BLV-Gag virions and BLV Gag VLPs

Conventional TEM was performed to confirm BLV Gag VLP formation when expressed from cells infected with LSDV-SODis-p67HA-BLV-Gag and to investigate pox virion morphology. Isolated pox virions had characteristics typical of intracellular LSDV (Figure 4A). BLV Gag VLPs purified from the corresponding cell media samples appeared as expected (Figure 4B), however low numbers of VLPs were isolated. Low numbers of gold particles to detect p67HA on VLPs were also observed. SDS PAGE and western blotting of the cell lysate and isolated VLP samples showed that p67HA was detected in both samples (Figure 4C). In the VLP sample, the majority of p67HA appeared as a higher molecular weight protein (>135 kDa), whereas the predominant form in the lysate was closer to 100 kDa. Ultra-thin sectioning was performed on infected MDBK cells to further confirm BLV Gag VLP formation (Figure 4D). Areas near the plasma membrane and between adjacent cells contained circular structures which resembled VLPs. These were not seen in sectioned MDBKs infected with nLSDVSODis-UCT or uninfected MDBK cells (not shown). LSDV-SODis-p67HA-BLV-Gag observed in sections showed typical poxvirus morphologies.

3.4 Glycosylation status of p67ΔTM

The presence of glycans on a protein can affect its mobility during SDS PAGE and give rise to additional bands on a western blot. As this may explain the different sizes of p67 protein seen on blots, such as in Figure 4C, we investigated the presence of N-linked and O-linked glycans on the protein. The soluble p67ΔTM protein (Figure 1A) was used for this purpose as it was purified from cell media and provided a relatively clean sample (30). The p67 regions that are identical amongst wild-type p67, p67HA and p67ΔTM were analyzed with NetNGlyc-1.0 and NetOGlyc-4.0 to predict the glycosylation sites (Figure 5A). Seven N-linked sites were predicted, as was previously described by others (41, 42), and 95 O-linked sites were predicted, shown as a range (exact sites shown in Table S1).

p67ΔTM was deglycosylated with PNGase F to remove N-linked glycans and treated with a deglycosylation mix to remove both N-linked and O-linked glycans (Figure 5B). The doublet >100 kDa resolved into one band after treatment with PNGase F, indicating that p67ΔTM has N-linked glycans. The band and smear up to ~160 kDa all resolved into a single band following treatment with the deglycosylation mix, indicating that the higher molecular weight protein is heavily O-linked glycosylated. The lower molecular weight form above 58 kDa had no mobility shift.

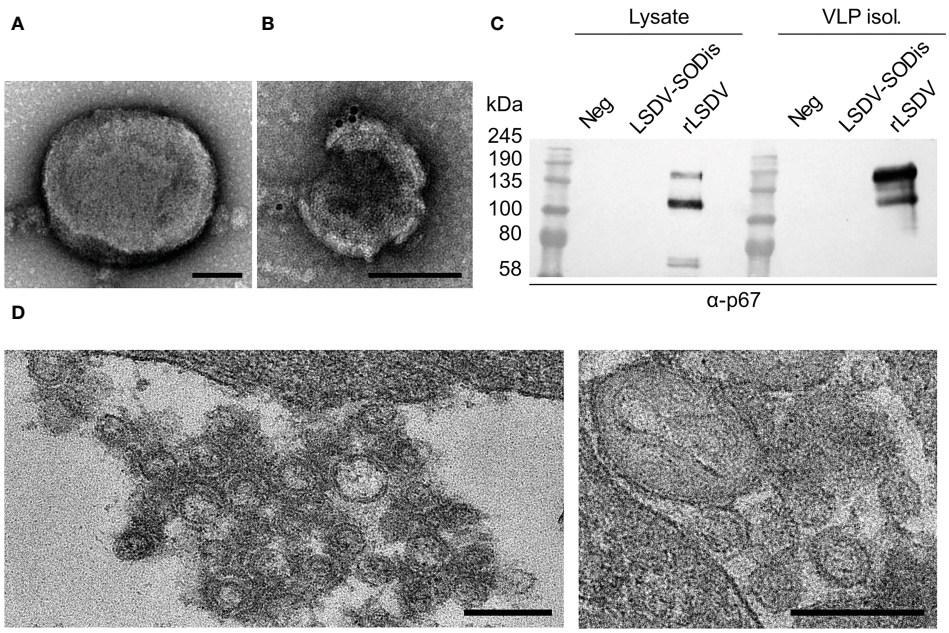

FIGURE 4
TEM of **(A)** LSDV-SODis-p67HA-BLV-Gag pox virion isolated from MDBK cells; **(B)** BLV Gag VLP isolated from infected MDBK cell media with immunogold labelling of p67HA (10 nm colloidal gold); both scale bars: 100 nm. **(C)** SDS PAGE and western blot of samples corresponding to **(A, B)** either uninfected MDBK cells (Neg), or infected with nLSDVSODis-UCT (LSDV-SODis) or LSDV-SODis-p67HA-BLV-Gag (rLSDV). VLP isol.: VLP isolation samples from cell media. **(D)** Potential BLV Gag VLPs in thin sections of MDBK cells infected with LSDV-SODis-p67HA-BLV-Gag. Scale bars: 250 nm.

10.3389/fimmu.2023.1143034

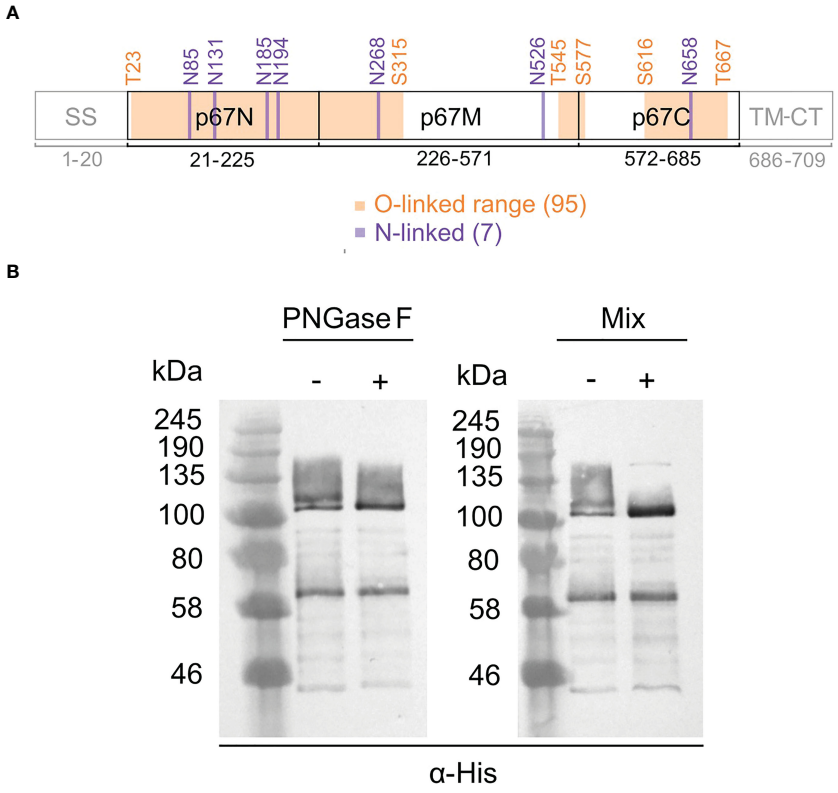

FIGURE 5
Glycosylation of p67ΔTM. **(A)** Predicted N-linked and O-linked glycosylation sites on p67 regions identical to wild-type p67 (GenBank: AAA98601.1), p67HA and p67ΔTM. O-linked sites are depicted as ranges. Labelled amino acid residue positions correspond to those in wild-type p67. **(B)** SDS PAGE and western blot of purified p67ΔTM protein treated (+) with PNGase F to remove N-linked glycans or a protein deglycosylation mix (Mix) to remove both N-linked and O-linked glycans or left untreated (-). Lanes were loaded with 40 ng of protein and blots were probed with anti-His antibody (α-His).

3.5 Immunogenicity of LSDV-SODis-p67HA-BLV-Gag in mice

The ability of LSDV-SODis-p67HA-BLV-Gag to elicit humoral responses against p67HA and BLV Gag was investigated in mice. Four groups of female BALB/c mice were inoculated as shown in Figure 6. The DNA plasmid pMExT-p67HA was used as a control, as we had previously shown this plasmid to induce p67-binding antibodies in mice after four inoculations (30). The plasmid consists of the pTHpCapR/pMExT mammalian expression vector backbone (38, 43) encoding the p67HA antigen present in LSDV-SODis-p67HA-BLV-Gag (Figure 1A).

An ELISA using plates coated with p67ΔTM showed that both pMExT-p67HA and LSDV-SODis-p67HA-BLV-Gag elicited p67-binding antibodies in mice (Figure 7A). Mouse #3 in the pMExT-p67HA group had no response, and why this occurred is unknown. Mice inoculated with LSDV-SODis-p67HA-BLV-Gag had endpoint titers almost 10-fold higher compared to those inoculated with pMExT-p67HA, however the differences were not statistically significant (Figure 7B).

Responses to BLV Gag were investigated using plates coated with BLV Gag protein purified from *E. coli* (30). LSDV-SODis-p67HA-BLV-Gag elicited low titers of BLV Gag-binding antibodies, which were significantly different from the nLSDVSODis-UCT control group but not to those that received pMExT-p67HA (Figure 8). A summary of the endpoint titers can be found in Table S2.

4 Discussion

The vaccine currently in use against ECF is effective at protecting cattle, however, has many limitations that can be improved upon. Our goal was to produce a novel vaccine that may address these issues by combining our p67HA-VLP system with our recombinant nLSDVSODis-UCT backbone to develop a dual vaccine that potentially protects against both ECF and LSD (26, 30).

Most efforts to produce a novel vaccine that avoids the use of live *T. parva* have investigated the use of the p67 antigen, as it is conserved across many *T. parva* strains and can induce neutralizing antibodies to prevent sporozoite invasion (33). These have included chimeric p67 recombinants, truncation of the protein to known immunogenic regions, and expression in bacteria, insect cells *via* recombinant baculovirus, and mammalian cell expression systems (28, 42, 44). A peculiar characteristic of the antigen is its mobility after SDS PAGE and western blotting. The predominant protein extracted from sporozoite lysate appears to be 67 kDa, however

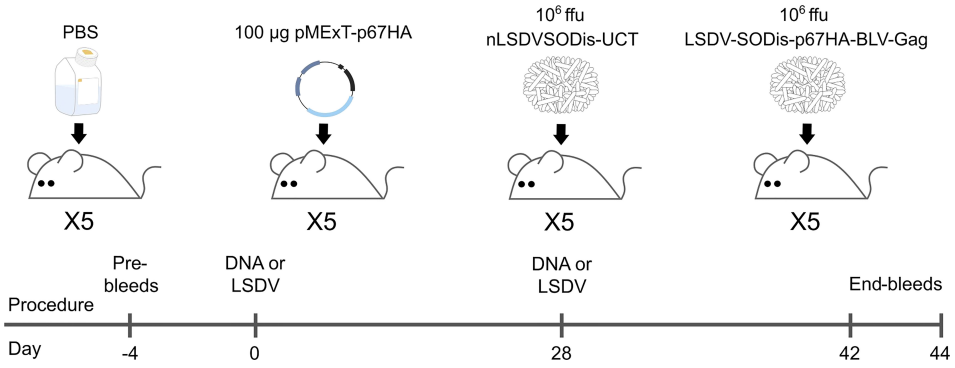

FIGURE 6
Inoculation and bleed schedule for BALB/c mice injected intramuscularly. End-bleeds were performed for the PBS and DNA groups on Day 42, and for the LSDV groups on Day 44.

recombinant forms as described earlier all tend to produce p67 at a range of sizes, often showing much larger proteins predominating in cell media (33, 42, 45, 46). This characteristic was observed for p67HA when expressed from LSDV (Figures 3C; 4C). We have previously seen this pattern of expression for p67HA, p67ΔTM and p67 with the native TM-CT when expressed in HEK293T cells using the pMExT DNA plasmid (30). Tebaldi et al. (42) have demonstrated that larger soluble ~140 kDa forms are possibly p67 aggregates that only dissociate under severe denaturation conditions. p67 has one cysteine residue (C416) in p67M, therefore the formation of dimers *via* disulphide bonds is not impossible. p67HA also showed similar large proteins in blots; one slightly above 100 kDa and another at ~140 kDa (Figure 4C). As p67ΔTM showed a very similar pattern of expression, the protein purified from HEK293T cell media was used to investigate p67 glycosylation. Deglycosylation experiments showed that the antigen has both N-linked and O-linked glycans (Figure 5B). Treatment with PNGase F gave a result that was almost identical to that of Nene et al. (45); Kaba et al. (46), where they treated insect cells expressing p67 through baculovirus, with or without the TM respectively, with tunicamycin to prevent N-linked glycosylation of the protein. Interestingly, Tebaldi et al. (42) had a conflicting result where treatment of their p67ΔTM from HEK293T cell media with PNGase F showed no mobility shift. They, however, used the native SS whereas we used the TPA SS, and different SS can result in differences in glycosylation (47, 48). If one compares p67HA in the lysate versus the medium (VLPs), the opposite band predominates for the different samples (Figure 4C). If the glycosylation status of p67ΔTM is taken into account, it is likely that p67HA present on the cell surface and VLPs is the most processed, glycosylated form, whereas p67HA in the lysate represents the protein before undergoing processing. Processing and the addition of glycans progresses as proteins are trafficked through the endoplasmic reticulum and Golgi body, therefore one would expect the most processed form to be on the cell surface (49). Besides explaining the appearance of p67 on western blots, glycosylation may have conformational and immunological implications. For some viruses, such as HIV, neutralizing antibodies have epitopes that

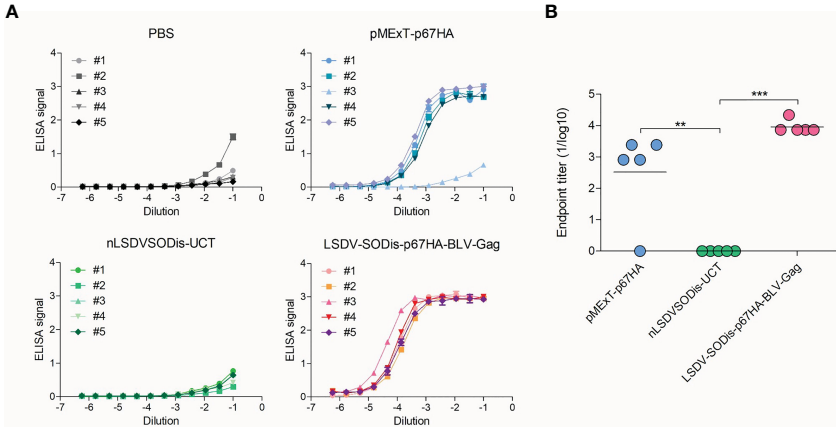

FIGURE 7
ELISAs to detect p67-binding IgG antibodies in vaccinated mouse sera. **(A)** ELISA signal (absorbance at 450-540 nm) vs Dilution for each mouse in each group, where a number refers to individual mice. Readings are shown with ± SEM. **(B)** End-point titers (1/log10) for each group. Values were set to zero if no response was observed. Values for each mouse are shown with the mean, with **p<0.01 and ***p<0.001 after a one-way ANOVA and Bonferroni *post-hoc* test.

10.3389/fimmu.2023.1143034

are dependent on the presence of glycans. Conversely, glycan shielding of epitopes can also occur whereby the presence of glycans sterically blocks the binding of antibodies, as seen for the heavily glycosylated Ebola virus glycoprotein (50). Whether these factors are relevant for p67 is currently unknown. As yet, no glycans have been found experimentally on sporozoite-derived p67 (41). Thus, one can hypothesize that non-glycosylated p67 maybe the most suitable form for eliciting neutralizing antibodies to *T. parva* sporozoites.

The expression of p67HA on the surface of HeLa cells was shown by immunofluorescence, and electron microscopy confirmed the presence of BLV Gag VLPs (Figures 3D; 4). However, the amount of p67HA on the surface of VLPs was considerably lower compared to when expressed from DNA plasmids, which employed the constitutive cytomegalovirus (CMV) promoter (30). The mH5 and pLEO promoters, which were used for the control of p67HA and BLV Gag respectively, both induce gene expression at the early and late stages of the poxvirus life cycle (51, 52). However, different promoters can have different strengths at different times, and therefore the timing of p67HA and BLV Gag expression may be slightly different (53). Furthermore, the production of p67HA-BLV Gag VLPs would require both proteins to be present at the same assembly point, which may be affected by differential trafficking of the two proteins through the cytoplasm of recombinant LSDV-infected cells. Isolation of VLPs was also met with difficulties as low numbers of VLPs were observed. VLP isolation was also met with technical challenges with a different recombinant nLSDVSODis-UCT encoding HIV-1 Gag under the pLEO promoter (unpublished data). HIV-1 Gag only associates with the plasma membrane after a threshold cytoplasmic concentration of the protein is reached (54). This may explain the lower numbers of isolated VLPs from cell media if relatively lower expression of Gag from LSDV occurred.

Nevertheless, LSDV-SODis-p67HA-BLV-Gag elicited p67-binding antibodies in mice with an average titer that was almost 10-fold higher than that of the pMExT-p67HA DNA plasmid, although the difference was not statistically significant (Figure 7). Live-virus vaccines often induce stronger responses than DNA vaccines used alone, therefore this result was expected. Others have demonstrated recombinant p67 immunogenicity in mice, which then proved immunogenic in cattle. Kaba et al. (29) showed that when inoculated into mice, p67ΔSS fused to GFP (GFP: p67ΔSS, produced in insect cells), and p67C fused to baculovirus GP64 and displayed on baculovirus particles (GP64: p67C) resulted in antibody titers over 5-fold higher than that of other truncated p67 proteins (GFP:p67C/p67N, p67C produced in *E. coli*, and GP64:p67N). These two antigens also induced *T. parva* sporozoite neutralizing antibodies in mice, and GFP:p67ΔSS was the superior antigen in their cattle immunogenicity study.

Surprisingly, mice inoculated with LSDV-SODis-p67HA-BLV-Gag had relatively low responses to BLV Gag (Figure 8). This was unexpected as the DNA plasmid pMEx-BLV-gag, which encoded the same gag gene, previously gave good responses in mice (30). The implication is that the immune response to p67 was not linked to that of BLV Gag and that the increased p67HA antibody response may have been due to the p67 being presented on poxvirus particles and not predominantly on BLV VLPs. The lower level of detection of p67HA on LSDV-produced Gag particles would support this theory. As described earlier, the pLEO promoter is a synthetic early-late optimized promoter (52) which should be expressed before and after LSDV DNA replication. The expression was reported to be high in the first hour resulting in good CD8+ T-cell responses, so another possibility is that a cellular immune response is being activated.

In conclusion we have constructed a novel LSDV candidate ECF vaccine expressing a chimeric protein p67HA expressed on the surface of infected cells and BLV Gag. We further show that our p67 is glycosylated when expressed in mammalian cells, which may explain the multiple large proteins observed in western blot

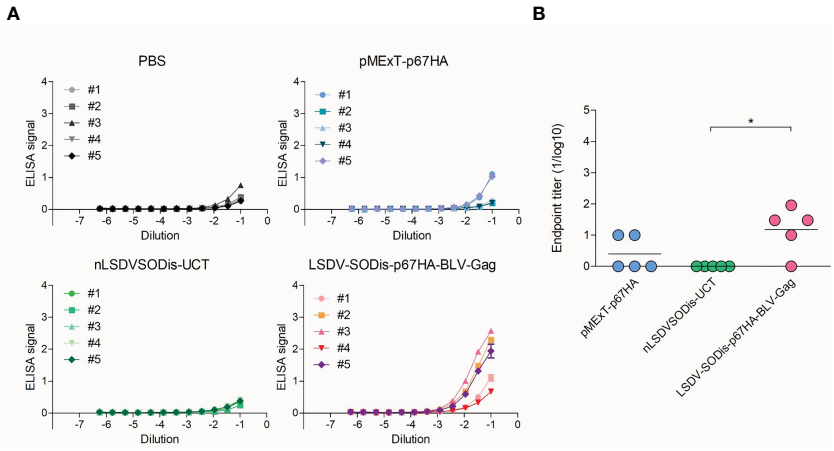

FIGURE 8
ELISAs to detect BLV Gag-binding IgG antibodies in vaccinated mouse sera. **(A)** ELISA signal (absorbance at 450-540 nm) vs Dilution for each mouse in each group, where a number refers to individual mice. Readings are shown with ± SEM. **(B)** End-point titers (1/log10) for each group. Values were set to zero if no response was observed. Values for each mouse are shown with the mean, with *p<0.05 after a one-way ANOVA and Bonferroni *post-hoc* test.

analysis. LSDV-SODis-p67HA-BLV-Gag elicited p67 and BLV-Gag binding antibodies in mice. This vaccine is currently being investigated in cattle to assess its efficacy against ECF.

Data availability statement

The original contributions presented in the study are included in the article/Supplementary Material. Further inquiries can be directed to the corresponding author.

Ethics statement

The animal study was reviewed and approved by the Animal Ethics Committee of the University of Cape Town.

Author contributions

LW: methodology, investigation, data curation, formal analysis and writing (original draft, review and editing). RC: methodology, supervision and writing (review and editing). ND: methodology, investigation and writing (review and editing). MJ: methodology and investigation. EM: methodology and investigation. ER: conceptualization, supervision and writing (review and editing). A-LW: conceptualization, supervision, methodology, funding acquisition and writing (review and editing). All authors contributed to the article and approved the submitted version.

Funding

This work is based on the research supported in part by the National Research Foundation of South Africa (Grant Numbers 64815 and 138792) and the Poliomyelitis Research Foundation (Grant Number 19/85).

Acknowledgments

We would like to thank Rodney Lucas and the UCT RAF for carrying out the mouse experiments, as well as Gerald Chege and Alana Keyser for assisting with downstream immunogenicity assays.

Conflict of interest

Patent applications have been filed on LSDV-SODis-p67HA-BLV-Gag and pMExT-p67HA PCT/IB2022/056970, PA175637/PCT, as well as for the nLSDVSODis-UCT backbone CT/IB2019/054090, PA166012PCT.

Publisher's note

Supplementary material

The Supplementary Material for this article can be found online at: https://www.frontiersin.org/articles/10.3389/fimmu.2023.1143034/full#supplementary-material

References

1. Malak AK, Mpoke L, Banak J, Muriuki S, Skilton RA, Odongo D, et al. Prevalence of livestock diseases and their impact on livelihoods in central equatoria state, southern Sudan. *Prev Vet Med* (2012) 104:216–23. doi: 10.1016/j.prevetmed.2011.12.001

2. Mumba C, Hasler B, Muma JB, Munyeme M, Sitali DC, Skjerve E, et al. Practices of traditional beef farmers in their production and marketing of cattle in Zambia. *Trop Anim Health Prod* (2018) 50:49–62. doi: 10.1007/s11250-017-1399-0

3. Boucher F, Moutroifi Y, Ali M, Moindjie Y, Soule M, Charafouddine O, et al. Impact of East coast fever on grande comore: Assessment taking a participatory epidemiology approach. *Trop Anim Health Prod* (2019) 51:99–107. doi: 10.1007/s11250-018-1664-x

4. Nthiwa D, Alonso S, Odongo D, Kenya E, Bett B. A participatory epidemiological study of major cattle diseases amongst maasai pastoralists living in wildlife-livestock interfaces in maasai Mara, Kenya. *Trop Anim Health Prod* (2019) 51:1097–103. doi: 10.1007/s11250-018-01790-1

5. Bantuzeko Kwankanaba K, Mushagalusa AC, Barume CA, Mugumaarhahama Y, Sefu AG. Farmers' perceptions on technical controls and risk factors of East coast fever caused by *Theileria parva* in mountainous kivu, democratic republic of Congo. *J Ani. Plant Sci* (2022) 51:9213–26. doi: 10.35759/JAnmPlSci.v51-2.1

6. Rowlands GJ, Musoke AJ, Morzaria SP, Nagda SM, Ballingall KT, Mckeever DJ. A statistically derived index for classifying East coast fever reactions in cattle challenged with *Theileria parva* under experimental conditions. *Parasitology* (2000) 120:371–81. doi: 10.1017/S0031182099005600

7. Fry LM, Schneider DA, Frevert CW, Nelson DD, Morrison WI, Knowles DP. East Coast fever caused by *Theileria parva* is characterized by macrophage activation associated with vasculitis and respiratory failure. *PloS One* (2016) 11:e0156004. doi: 10.1371/journal.pone.0156004

8. Nene V, Kiara H, Lacasta A, Pelle R, Svitek N, Steinaa L. The biology of *Theileria parva* and control of East coast fever - current status and future trends. *Ticks Tick-borne Dis* (2016) 7:549–64. doi: 10.1016/j.ttbdis.2016.02.001

9. Radley DE, Brown CGD, Cunningham MP, Kimber CD, Musisi FL, Payne RC, et al. East Coast fever 3: Chemoprophylactic immunization of cattle using oxytetracycline and a combination of *Theilerial* strains. *Veterinary Parasitol* (1975) 1:51–60. doi: 10.1016/0304-4017(75)90007-2

10. De Deken R, Martin V, Saido A, Madder M, Brandt J, Geysen D. An outbreak of East coast fever on the Comoros: a consequence of the import of immunised cattle from Tanzania? *Vet Parasitol* (2007) 143:245–53. doi: 10.1016/j.vetpar.2006.08.018

11. Di Giulio G, Lynen G, Morzaria S, Oura C, Bishop R. Live immunization against East coast fever - current status. *Trends Parasitol* (2009) 25:85–92. doi: 10.1016/j.pt.2008.11.007

12. Singer AC, Shaw H, Rhodes V, Hart A. Review of antimicrobial resistance in the environment and its relevance to environmental regulators. *Front Microbiol* (2016) 7:1728. doi: 10.3389/fmicb.2016.01728

13. Bishop R, Odongo DO, Spooner PR, Morzaria SP, Oura CAL, Skilton RA. Multilocus genotyping of *Theileria parva* isolates associated with a live vaccination trial

in Kenya provides evidence for transmission of immunizing parasites into local tick and cattle populations. *Transboundary Emerging Dis* (2020) 67:88–98. doi: 10.1111/tbed.13417

14. Alcock R, Cottingham MG, Rollier CS, Furze J, De Costa SD, Hanlon M, et al. Long-term thermostabilization of live poxviral and adenoviral vaccine vectors at supraphysiological temperatures in carbohydrate glass. *Sci Transl Med* (2010) 2:19ra12. doi: 10.1126/scitranslmed.3000490

15. Thiel V, Herold J, Schelle B, Siddell SG. Infectious RNA transcribed *in vitro* from a cDNA copy of the human coronavirus genome cloned in vaccinia virus. *J Gen Virol* (2001) 82:1273–81. doi: 10.1099/0022-1317-82-6-1273

16. Sanchez-Sampedro L, Perdiguero B, Mejias-Perez E, Garcia-Arriaza J, Di Pilato M, Esteban M. The evolution of poxvirus vaccines. *Viruses* (2015) 7:1726–803. doi: 10.3390/v7041726

17. Douglass N, Omar R, Munyanduki H, Suzuki A, Mutowembwa P, Kara P, et al. The development of dual vaccines against lumpy skin disease (LSD) and bovine ephemeral fever (BEF). *Vaccines* (2021) 9. doi: 10.3390/vaccines9111215

18. OIE-WAHIS. *Events management [Online]* (2022). Available at: https://wahis.woah.org/#/event-management (Accessed December 2022).

19. Coetzer JAW, Tuppurainen E. Lumpy skin disease. *Infect Dis livestock* (2004) 2:1268–76.

20. Moller J, Moritz T, Schlottau K, Krstevski K, Hoffmann D, Beer M, et al. Experimental lumpy skin disease virus infection of cattle: comparison of a field strain and a vaccine strain. *Arch Virol* (2019) 164:2931–41. doi: 10.1007/s00705-019-04411-w

21. Abutarbush SM, Ababneh MM, Al Zoubi IG, Al Sheyab OM, Al Zoubi MG, Alekish MO, et al. Lumpy skin disease in Jordan: Disease emergence, clinical signs, complications and preliminary-associated economic losses. *Transbound Emerg Dis* (2015) 62:549–54. doi: 10.1111/tbed.12177

22. OBP. *Lumpy skin disease vaccine for cattle* (2022). Available at: https://www.obpvaccines.co.za/resources/productInserts/LUMPY%20SKIN%20DISEASE%20VACCINES%20FOR%20CATTLE.pdf.

23. Aspden K, Van Dijk AA, Bingham J, Cox D, Passmore JA, Williamson A-L. Immunogenicity of a recombinant lumpy skin disease virus (neethling vaccine strain) expressing the rabies virus glycoprotein in cattle. *Vaccine* (2002) 20:2693–701. doi: 10.1016/S0264-410X(02)00203-7

24. Wallace DB, Mather A, Kara PD, Naicker L, Mokoena NB, Pretorius A, et al. Protection of cattle elicited using a bivalent lumpy skin disease virus-vectored recombinant rift valley fever vaccine. *Front Vet Sci* (2020) 7:256. doi: 10.3389/fvets.2020.00256

25. Chapman R, Van Diepen M, Douglass N, Galant S, Jaffer M, Margolin E, et al. Assessment of an LSDV-vectored vaccine for heterologous prime-boost immunizations against HIV. *Vaccines* (2021) 9. doi: 10.3390/vaccines9111281

26. Douglass N, Munyanduki H, Omar R, Gers S, Mutowembwa P, Heath L, et al. Influence of the viral superoxide dismutase (SOD) homologue on lumpy skin disease virus (LSDV) growth, histopathology and pathogenicity. *Vaccines* (2020) 8. doi: 10.3390/vaccines8040664

27. Nene V, Morrison WI. Approaches to vaccination against *Theileria parva* and *Theileria annulata*. *Parasite Immunol* (2016) 38:724–34. doi: 10.1111/pim.12388

28. Lacasta A, Mody KT, De Goeyse I, Yu C, Zhang J, Nyagwange J, et al. Synergistic effect of two nanotechnologies enhances the protective capacity of the *Theileria parva* sporozoite p67C antigen in cattle. *J Immunol* (2021) 206:686–99. doi: 10.4049/jimmunol.2000442

29. Kaba SA, Schaap D, Roode EC, Nene V, Musoke AJ, Vlak JM, et al. Improved immunogenicity of novel baculovirus-derived *Theileria parva* p67 subunit antigens. *Veterinary Parasitol* (2004) 121:53–64. doi: 10.1016/j.vetpar.2004.02.013

30. Whittle L, Chapman R, Van Diepen M, Rybicki EP, Williamson A-L. Characterization of a novel chimeric theileria parva p67 antigen which incorporates into virus-like particles and is highly immunogenic in mice. *Vaccines* (2022) 10. doi: 10.3390/vaccines10020210

31. Babiuk LA, Pontarollo R, Babiuk S, Loehr B, Van Drunen Littel-Van Den Hurk S. Induction of immune responses by DNA vaccines in large animals. *Vaccine* (2003) 21:649–58. doi: 10.1016/S0264-410X(02)00574-1

32. Fry LM, Bastos RG, Stone BC, Williams LB, Knowles DP, Murphy SC. Gene gun DNA immunization of cattle induces humoral and CD4 T-cell-mediated immune responses against the *Theileria parva* polymorphic immunodominant molecule. *Vaccine* (2019) 37:1546–53. doi: 10.1016/j.vaccine.2019.02.009

33. Nene V, Gobright E, Bishop R, Morzaria S, Musoke A. Linear peptide specificity of bovine antibody responses to p67 of *Theileria parva* and sequence diversity of sporozoite neutralizing epitopes: implications for a vaccine. *Infection Immun* (1999) 67:1261–6. doi: 10.1128/IAI.67.3.1261-1266.1999

34. Kaba SA, Nene V, Musoke AJ, Vlak JM, Van Oers MM. Fusion to green fluorescent protein improves expression levels of *Theileria parva* sporozoite surface antigen p67 in insect cells. *Parasitology* (2002) 125:497–505. doi: 10.1017/S003118200200241X

35. van Diepen M, Chapman R, Douglass N, Whittle L, Chineka N, Galant S, et al. Advancements in the growth and construction of recombinant lumpy skin disease virus (LSDV) for use as a vaccine vector. *Vaccines* (2021) 9. doi: 10.3390/vaccines9101131

36. Munyanduki H, Omar R, Douglass N, Williamson AL. Removal of bovine viral diarrhea virus (BVDV) from lumpy skin disease virus (LSDV) vaccine stocks by passage on chorioallantoic membranes of fertilized hens' eggs. *J Virol Methods* (2020) 275:113752. doi: 10.1016/j.jviromet.2019.113752

37. Reed LJ, Muench H. A simple method of estimating fifty percent endpoints. *Am J Hygiene* (1938) 27:493–7. doi: 10.1093/oxfordjournals.aje.a118408

38. van Diepen M, Margolin E, Chapman R, Douglass N, Galant S, Ximba P, et al. Prime-boost iunizations with DNA, modified vaccinia virus Ankara, and protein-based vaccines elicit robust HIV-1 tier 2 neutralizing antibodies against the CAP256 superinfecting virus. *J Virol* (2019) 93:e02155-18. doi: 10.1128/JVI.02155-18

39. Gupta R, Brunak S. Prediction of glycosylation across the human proteome and the correlation to protein function. *Pac Symp Biocomput* (2002) 7:310-322.

40. Steentoft C, Vakhrushev SY, Joshi HJ, Kong Y, Vester-Christensen MB, Schjoldager KT, et al. Precision mapping of the human O-GalNAc glycoproteome through SimpleCell technology. *EMBO J* (2013) 32:1478–88. doi: 10.1038/emboj.2013.79

41. Nene V, Iams KP, Gobright E, Musoke A. Characterisation of the gene encoding a candidate vaccine antigen of *Theileria parva* sporozoites. *Mol Biochem Parasitol* (1992) 51:17–28. doi: 10.1016/0166-6851(92)90196-Q

42. Tebaldi G, Williams LB, Verna AE, Macchi F, Franceschi V, Fry LM, et al. Assessment and optimization of *Theileria parva* sporozoite full-length p67 antigen expression in mammalian cells. *PloS Negl Trop Dis* (2017) 11:e0005803. doi: 10.1371/journal.pntd.0005803

43. Tanzer FL, Shephard EG, Palmer KE, Burger M, Williamson A-L, Rybicki EP. The porcine circovirus type 1 capsid gene promoter improves antigen expression and immunogenicity in a HIV-1 plasmid vaccine. *Virol J* (2011) 8. doi: 10.1186/1743-422X-8-51

44. Kaba SA, Musoke AJ, Schaap D, Schetters T, Rowlands J, Vermeulen AN, et al. Novel baculovirus-derived p67 subunit vaccines efficacious against East coast fever in cattle. *Vaccine* (2005) 23:2791–800. doi: 10.1016/j.vaccine.2004.10.043

45. Nene V, Inumaru S, Mckeever D, Morzaria S, Shaw M, Musoke A. Characterization of an insect cell-derived *Theileria parva* sporozoite vaccine antigen and immunogenicity in cattle. *Infection Immun* (1995) 63:503–8. doi: 10.1128/iai.63.2.503-508.1995

46. Kaba SA, Salcedo AM, Wafula PO, Vlak JM, Van Oers MM. Development of a chitinase and v-cathepsin negative bacmid for improved integrity of secreted recombinant proteins. *J Virol Methods* (2004) 122:113–8. doi: 10.1016/j.jviromet.2004.07.006

47. Rutkowski DT, Ott CM, Polansky JR, Lingappa VR. Signal sequences initiate the pathway of maturation in the endoplasmic reticulum lumen. *J Biol Chem* (2003) 278:30365–72. doi: 10.1074/jbc.M302117200

48. Yolitz J, Schwing C, Chang J, Van Ryk D, Nawaz F, Wei D, et al. Signal peptide of HIV envelope protein impacts glycosylation and antigenicity of gp120. *Proc Natl Acad Sci U.S.A.* (2018) 115:2443–8. doi: 0.1073/pnas.1722627115

49. Schjoldager KT, Narimatsu Y, Joshi HJ, Clausen H. Global view of human protein glycosylation pathways and functions. *Nat Rev Mol Cell Biol* (2020) 21:729–49. doi: 10.1038/s41580-020-00294-x

50. Francica JR, Varela-Rohena A, Medvec A, Plesa G, Riley JL, Bates P. Steric shielding of surface epitopes and impaired immune recognition induced by the Ebola virus glycoprotein. *PloS Pathog* (2010) 6:e1001098. doi: 10.1371/journal.ppat.1001098

51. Wyatt LS, Shors ST, Murphy BR, Moss B. Development of a replication-deficient recombinant vaccinia virus vaccine effective against parainfluenza virus 3 infection in an animal model. *Vaccine* (1996) 14:1451–8. doi: 10.1016/S0264-410X(96)00072-2

52. Di Pilato M, Mejias-Perez E, Gomez CE, Perdiguero B, Sorzano CO, Esteban M. New vaccinia virus promoter as a potential candidate for future vaccines. *J Gen Virol* (2013) 94:2771–6. doi: 10.1099/vir.0.057299-0

53. Alharbi NK. Poxviral promoters for improving the immunogenicity of MVA delivered vaccines. *Hum Vaccin Immunother* (2019) 15:203–9. doi: 10.1080/21645515.2018.1513439

54. Fogarty KH, Berk S, Grigsby IF, Chen Y, Mansky LM, Mueller JD. Interrelationship between cytoplasmic retroviral gag concentration and gag-membrane association. *J Mol Biol* (2014) 426:1611–24. doi: 10.1016/j.jmb.2013.11.025

frontiers | Frontiers in Immunology

TYPE Review
PUBLISHED 14 April 2023
DOI 10.3389/fimmu.2023.1156451

OPEN ACCESS

EDITED BY
Brad Pickering,
National Centre for Foreign Animal Disease (NCFAD), Canada

REVIEWED BY
Julie Moreno,
Colorado State University, United States
Kurt Zuelke,
Texas A&M University, United States

*CORRESPONDENCE
Scott Napper
scott.napper@usask.ca

SPECIALTY SECTION
This article was submitted to Vaccines and Molecular Therapeutics, a section of the journal Frontiers in Immunology

RECEIVED 01 February 2023
ACCEPTED 31 March 2023
PUBLISHED 14 April 2023

CITATION
Napper S and Schatzl HM (2023) Oral vaccination as a potential strategy to manage chronic wasting disease in wild cervid populations.
Front. Immunol. 14:1156451.
doi: 10.3389/fimmu.2023.1156451

Oral vaccination as a potential strategy to manage chronic wasting disease in wild cervid populations

Scott Napper[1,2]* and Hermann M. Schatzl[3]

[1]Vaccine and Infectious Disease Organization, University of Saskatchewan, Saskatoon, SK, Canada, [2]Department of Biochemistry, Microbiology and Immunology, University of Saskatchewan, Saskatoon, SK, Canada, [3]Calgary Prion Research Unit, Faculty of Veterinary Medicine, University of Calgary, Calgary, AB, Canada

Prion diseases are a novel class of infectious disease based in the misfolding of the cellular prion protein (PrP^{C}) into a pathological, self-propagating isoform (PrP^{Sc}). These fatal, untreatable neurodegenerative disorders affect a variety of species causing scrapie in sheep and goats, bovine spongiform encephalopathy (BSE) in cattle, chronic wasting disease (CWD) in cervids, and Creutzfeldt-Jacob disease (CJD) in humans. Of the animal prion diseases, CWD is currently regarded as the most significant threat due its ongoing geographical spread, environmental persistence, uptake into plants, unpredictable evolution, and emerging evidence of zoonotic potential. The extensive efforts to manage CWD have been largely ineffective, highlighting the need for new disease management tools, including vaccines. Development of an effective CWD vaccine is challenged by the unique biology of these diseases, including the necessity, and associated dangers, of overcoming immune tolerance, as well the logistical challenges of vaccinating wild animals. Despite these obstacles, there has been encouraging progress towards the identification of safe, protective antigens as well as effective strategies of formulation and delivery that would enable oral delivery to wild cervids. In this review we highlight recent strategies for antigen selection and optimization, as well as considerations of various platforms for oral delivery, that will enable researchers to accelerate the rate at which candidate CWD vaccines are developed and evaluated.

KEYWORDS

chronic wasting disease, oral vaccine, wildlife, prion, cervid

Prion diseases

Prion diseases are a unique category of infectious disease in which the molecular basis of infectivity resides in the misfolding of a normal cellular protein (PrP^{C}) into a pathological, self-propagating conformation (PrP^{Sc}) (1). Prion diseases can arise from genetic polymorphisms that predispose PrP to misfold, uptake/ingestion of PrP^{Sc} from the

environment or dietary sources, iatrogenic transmission, or sporadic forms that lack a defined cause (2).

Chronic wasting disease

Chronic wasting disease (CWD) is a prion disease of cervids, including deer, moose, and elk (3). Since its first characterization within captive mule deer of Colorado and Wyoming in 1967, CWD has made steady progression through wild cervid populations of North America (3). As of late 2022, CWD has been detected in free ranging cervids in 30 US states and 4 Canadian provinces (www.usgs.gov). Prevalence of CWD has reached over 40% for free-ranging populations in endemic areas and can be as high as 80–90% in captive populations (4–6). This pattern of emergence and spread suggests CWD is a relatively new disease, likely originating within the last hundred years. Prior to that, there may have been isolated, sporadic cases, but, for undefined reasons, the disease did not become endemically established until more recent times.

While often regarded as a North American problem, CWD has been detected in South Korea as well as three Scandinavian countries (7, 8). While the South Korea cases of CWD appear to be imported from North America, comparative transmission studies indicate sufficient differences to indicate that the European cases likely represent sporadic disease (9–11). This highlights the potential for spontaneous emergence of CWD, as well as new forms of the disease, in previously uncontaminated ecosystems. The extent to which CWD will gain a foothold within these regions has yet to be determined.

Over recent decades CWD has had substantial impact on the health and viability of North American cervid populations (6, 12). Should CWD continue its current trajectory, the anticipated outcomes range from a dramatic reduction in cervid numbers to a complete loss of these species (5, 13). Even the most optimistic of these outlooks is cause for considerable concern. Outside of their intrinsic importance, cervids are critical components of delicate ecosystems; threats to cervid health are certain to have negative consequences on other species as well threatening food security for Indigenous and Arctic populations. There is also tremendous economic activity associated with both wild and farmed cervids. Elk and deer farms, once thriving industries within North America, have suffered greatly since the emergence of CWD (14). The big game hunting industry, valued at over 26 billion dollars in the US in 2016, has also suffered considerable setbacks (6, 12). As damaging as these impacts have been, it is not difficult to envision scenarios, such as the disease spilling over into additional species, that would result in far more dire consequences.

Host range of chronic wasting disease

Outside the immediate threat to cervids, the extent to which CWD may threaten other species, including humans, remains a critical question. Fortunately, the transmission of prion diseases across species is restricted, to varying extents, by species barriers. For example, during the BSE crisis of the 1980s, species barriers served to protect millions of people who consumed prion-infected beef, limiting disease transmission to approximately two hundred unfortunate individuals who contracted variant Creutzfeldt-Jacob disease (vCJD), a fatal, untreatable neurodegenerative disorder (15). Species barriers reflect the ability of infecting prions to initiate misfolding of host PrP (16–18). This, in turn, depends on sequence differences between the invading and host PrPs, as well as structural characteristics of the infecting prion amyloid. There is not an established method for predicting the ease of transmission across various species, although different species are known to have unique susceptibilities to prion infection (19).

It is encouraging that infection studies of transgenic mice expressing ovine, bovine, and human PrP indicate minimal transmissibility of CWD (20–23). CWD has, however, been experimentally transmitted to several species, including cattle, pigs, cats, hamsters, and bank voles (24–27). While these infection models often utilize doses and routes of infection that differ from "real world" infection, this nevertheless highlights the theoretical potential for CWD to infect these species. Of which, the spectre of transmission of CWD to cattle is particularly concerning as this could result in a "second-generation" BSE outbreak of similar economic and human health consequences as the first, but with the additional challenge associated with managing an environmental source of infection. There is also considerable concern that the northern migration of CWD could result in transmission to caribou which are an important food source for Northern communities and whose numbers and extensive patterns of migration could provide a mechanism to further accelerate the geographical spread of the disease (28).

There is conflicting evidence on the extent to which CWD represents a threat to human health. Opportunities certainly exist for zoonotic transmission; it is estimated that approximately 10,000 CWD-infected cervids are consumed by humans each year (29). While there isn't an obvious increase in the rate of human prion disease amongst consumers of cervid meat, this must be balanced with the appreciation that transmission is likely quite inefficient, that the number of people consuming cervid food products is low (at least relative to those consuming beef products during the BSE outbreak), and that rates of occurrence of human prion disease must be evaluated against a baseline of sporadic cases, which occur at a rate of one to two cases per million people annually (30). With that, establishing the zoonotic potential of CWD from epidemiological data may be problematic, particularly if human CWD should manifest with similar symptoms as CJD. Several experimental studies support the zoonotic potential of CWD, including a recent study in which infection of transgenic mice expressing human PrP resulted in atypical disease and fecal prion shedding (31). The efficient *in vitro* conversion of human PrP by CWD prions (32, 33) also supports the zoonotic potential. With respect to the transmissibility of CWD to non-human primates, squirrel monkeys are susceptible to intracerebral and oral infection (34). However, studies in *Cynomolgus* macaques, generally regarded as the most relevant non-human primate model for zoonotic transmission studies, present conflicting results; some efforts

indicate an absence of transmission (34–36) while other studies show susceptibility to both oral challenge and intracerebral infection (37).

It is also important not to adopt too reductionist of a perspective on the zoonotic potential of CWD, nor to consider the disease as a static threat. Transmission of CWD to humans through intermediate species, including cattle or pigs, could have the same functional consequences as direct transmission from cervids. Further, the existence of various CWD prion strains, as well as the potential for new strains of novel traits, including species tropisms, also needs to be acknowledged. Such strains could emerge during passage within cervids or through any number of intermediate species. The number and diversity of PrP sequence polymorphisms within species sharing the environment with cervids offers troubling opportunity for the emergence of new strains. Collectively, given the fatal and untreatable nature of prion diseases, coupled with the dynamic nature of the threat, a conservative approach to zoonotic potential of CWD seems justified.

Efforts to control chronic wasting disease

Outbreaks of other prion diseases have been successfully managed in the absence of a vaccine. For Kuru, this was achieved through alterations to human behavior with the cessation of cannibalistic funeral rituals (38). For BSE, changes to animal management practises, in particular removal of high-risk materials from animal feed, was sufficient to control the disease (39). Unfortunately, aspects of CWD make its control far more problematic. Firstly, the existence of CWD within wild animals complicates disease surveillance as well as implementation of control measures. Animals infected with CWD shed substantial amounts of prions into the environment *via* their urine, feces, and saliva (40, 41). Once in the environment, these prions display remarkable durability, resulting in long-term contamination of soil and water, which provides additional mechanisms for geographical spread and undermines efforts to protect farmed cervids through tightened biosecurity (42, 43). Finally, that CWD is among the most contagious of the prion diseases further challenges its management (3).

Thus far the efforts by U.S. and Canadian government agencies to manage CWD have fallen short of desired goals. Even within the controlled environment of farmed animals, the efforts to manage CWD through double-fencing, increased restrictions on the transport of animals, decommissioning and depopulation of infected farms, have been insufficient to control the disease at an industry level. Not surprisingly, it has proven even more difficult to manage CWD in wild animal populations. Efforts such as depopulation and selective harvesting of animals have been ineffective in stopping the expansion of CWD throughout North America. There is clear and urgent need for new tools to control CWD. Historically, vaccines have been the most effective method for management of human and animal infectious diseases and there is optimism borne of evidence that the development of an effective prion vaccine, including orally administered vaccines, is achievable.

Opportunities and challenges for CWD vaccines

Relative to many of the other proteinopathies, the prion diseases are advantaged for vaccine development in that PrP represents a clearly defined, cell-surface accessible, immunotherapeutic target. Further, numerous investigations confirm the ability for antibodies to PrP to inhibit prion propagation *in vitro* as well as for passive and active immunization to inhibit disease progression in animal models. While encouraging, the development of prion vaccines is challenged by unique aspects of prion biology including defining safe and protective antigens, overcoming immunological tolerance, and obtaining a better understanding of the extent, and mechanisms, by which immunotherapy impacts disease initiation and progression. This information is critical to provide rationale criteria for optimizing desired vaccine traits as well as allowing the establishment of realistic benchmarks of vaccine efficacy.

Components of a CWD vaccine

Antigen selection

For traditional infectious diseases, the vaccine antigen is represented either by the entirety (killed or attenuated vaccines) or a specific molecular component (subunit vaccines) of the disease-associated microbe. Prion diseases are unique in that the entirety of the infectious threat is represented by a single protein. While this seemingly simplifies antigen selection, there are opportunities to utilize limited segments of the protein to achieve conformation specific (PrP^C vs PrP^{Sc}) immune responses or to prioritize specific regions of PrP based on anticipated outcomes of safety and/or efficiency.

PrP^C as the immunotherapeutic target

Given the opportunity to target PrP^C or PrP^{Sc}, it may seem counterintuitive to prioritize the healthy conformation. There are, however, strong rationalizations for this approach. It is well established that PrP^C is essential for prion propagation; prion disease progression cannot proceed in the absence of the PrP^C substrate. This is most conclusively demonstrated by the fact that PrP-/- animals completely resist prion infection (44). Efforts to develop vaccines that induce PrP^C reactive antibodies look to achieve the same functional outcome through either immunological depletion of PrP^C and/or blocking its ability to serve as a substrate for conversion into PrP^{Sc} (45, 46) (Figure 1). Antibodies to PrP^C block the generation of PrP^{Sc} *in vitro* and extensive investigations have demonstrated that vaccines which induce PrP^C reactive antibodies can delay, to varying degrees, the onset of prion disease symptoms (46–49).

Safety is a pivotal consideration during development of any vaccine; this takes on even greater importance for diseases caused by self-proteins. The strategy of deliberately targeting of PrP^C, which is

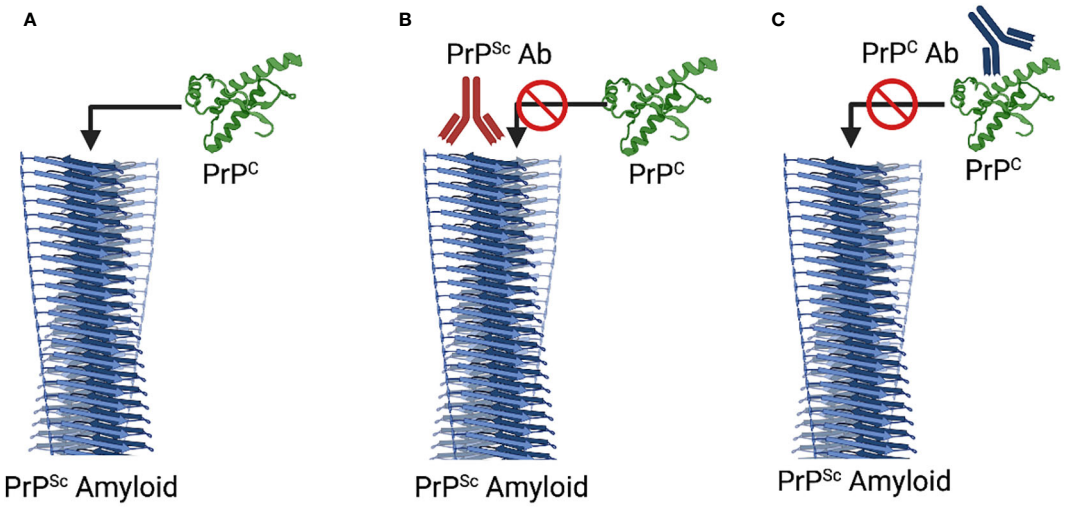

FIGURE 1
Mechanisms of Immunotherapeutic Intervention. **(A)** Natural Progression. The PrP^{Sc} serves as a template to promote the misfolding and incorporation of PrP^{C}. **(B)** PrP^{Sc}-Specific Immunotherapy. Antibodies to PrP^{Sc}, through disruption of the interaction between PrP^{Sc} and PrP^{C} block induced misfolding of PrP^{C}. **(C)** PrP^{C}-Specific Immunotherapy. Antibodies to PrP^{C} can block the interaction with PrP^{Sc} as well as depleting PrP^{C}. Notably the two mechanisms are not in exclusion of each other such that additive or synergist benefit could occur through dual targeting of each isoform. Diagram created with Biorender.

available for antibody binding in otherwise healthy animals, has raised apprehensions of the safety of this immunological approach. Those concerns are supported by early evidence which seemed to indicate the potential for PrP^{C}-reactive antibodies to have pathological consequences. PrP^{C} reactive antibodies, as well as their Fab fragments, were found to induce neuronal apoptosis in the brain (50, 51), although more recent investigations challenge this result (52). Within experimental systems, PrP^{C} reactive antibodies can activate inappropriate cell signal events (53, 54), superoxide mediated cytotoxicity (55), and stimulation of suppressor T-cell lymphocytes (56), although the significance of these responses is unclear.

Reassuringly, there is an absence of reported pathologies from numerous vaccine trials, employing a variety antigens and strategies of formulation and delivery to achieve PrP^{C} reactive immune responses. While this helps to alleviate some of the concerns of targeting PrP^{C}, it is important to note that the priority of those investigations was to quantify vaccine efficacy, not safety, and it is possible that subtle vaccine-associated pathologies may have escaped the attention of the researchers. It would also be premature to assume the safety of all PrP^{C}-associated vaccines as antibodies with reactivities to different regions of PrP have unique potentials for pathology; antibodies to the octarepeat are well tolerated while those against the folded globular domain are implicated in neurotoxicity (55). Another important consideration is whether the binding of antibodies to various regions are associated with a gain, or loss, of function. Loss of PrP^{C} function seems well tolerated, as evidenced by the absence of any profound phenotypic consequences with genetic ablation of PrP (44). Gain-of-function changes would be more difficult to anticipate in terms of their occurrence and consequences. Thus, while the current evidence suggests the safety and effectiveness of targeting PrP^{C}, it is important to evaluate any candidate CWD vaccines on a case-by-case basis. Collectively, however, is generally accepted that PrP^{C} is a viable antigen for prion vaccines, with demonstrated potentially for efficacy in inhibiting disease progression in the absence of adverse side effects.

PrP^{Sc} as the immunotherapeutic target

Strategies to develop vaccines that restrict the induced immune responses to PrP^{Sc} are motivated by considerations of safety and efficacy. From the perspective of safety, restricting immune responses to the misfolded conformation may mitigate concerns over the safety of induction of immune responses to a widely expressed self-protein; concerns which, whether experimentally demonstrated or merely perceived, could impact vaccine approval, licensure, and utilization. For efficacy, prioritizing the misfolded species could focus the immune response to the most pressing threat while sparing the function of the healthy form of the protein (Figure 1). While conceptually appealing, conformation-specific immunotherapy depends on identification of epitopes, termed disease specific epitopes (DSEs), that are specifically exposed for antibody binding in the misfolded state.

Disease specific epitopes

Efforts to identify regions of PrP exposed for antibody binding in the misfolded protein are complicated by the tendency of PrP^{Sc} to form insoluble aggregates which are unsuitable for most biophysical techniques. Instead, the initial PrP DSEs were identified through lower resolution biophysical techniques, rationale deduction, and

bioinformatic approaches. The first DSE emerged from a biophysical investigation which indicated that misfolding of PrP^{C} to PrP^{Sc} resulted in the surface exposure of tyrosine residues which was further determined to correspond a YYR motif of beta-strand 2 (57, 58). Soon after, a second DSE, corresponding to a YML sequence of the opposing beta-strand was hypothesized, and confirmed, to undergo similar repositioning to surface exposure with misfolding (59). A third DSE, corresponding to the loop region between beta-strand 2 and alpha-helix 2, was identified through a bioinformatic approaches that anticipate protein regions with the greatest propensity to unfold (60). This third DSE was designed Rigid Loop (RL) to reflect the unusual rigidity of this region in cervid PrP (61). Notably, high resolution structures of prion amyloids have recently been determined through cryo-electron microscopy, which should enable the identification of additional DSEs (62, 63).

Vaccines to each of the three PrP DSEs have been shown to induce antibodies that can discriminate PrP^{C} and PrP^{Sc} with specific reactivity to the pathological conformation (58, 64). This specificity is maintained in univalent and multivalent vaccine formats (64). Antibodies to each DSEs have also been confirmed in *in vitro* assays to neutralize PrP^{Sc} (65). Of the DSEs, protective efficacy has only been evaluated for a parenterally administered, univalent vaccine based on the YYR DSE. The results of those trials, performed in two different large animal models, revealed conflicting results; the vaccine delayed disease onset in a sheep challenge model (66) but accelerated disease in elk exposed to environmental prions (67). While each model utilized oral routes of infection, the sheep were infected once with a large challenge dose while the elk, housed in a prion-infected environment, were subjected to prolonged, low-level exposure prions. It is not clear whether these different outcomes reflect differences in the species or the challenge models.

Others have developed PrP^{Sc} specific vaccines through the design of recombinant antigens in which discontinuous, surface-exposed residues in PrP^{Sc} are presented in a molecular scaffold designed to mimic a proposed 4-rung beta solenoid fold of PrP^{Sc} (68). While recent determinations of the structure of the prion amyloid through cryo-electron microscopy challenge the beta solenoid model of PrP^{Sc} (62, 63), a vaccine based on this antigen, termed $VPrP^{Sc}$, induced PrP^{Sc}-reactive antibodies and resulted in a dramatic delay in the onset of symptoms in a transgenic mouse model of a genetic human prion disease (69).

Potential dangers of PrP^{Sc} reactivity

Targeting PrP^{Sc}, whose presence is unique to prion infection, seems a rational approach to mitigate safety concerns associated with induction of auto-reactive antibodies. This strategy, however, merely shifts, rather than alleviates, the safety concerns. Immunotherapy based on targeting of PrP^{Sc} gives rise to new apprehensions that these antibodies could function as templates, or chaperones, to promote formation of PrP^{Sc}. Antibody induced misfolding of PrP^{C} has the theoretical potential to initiate prion disease in otherwise healthy subjects. Thus far, these hypothetical concerns are not supported by experimental evidence. Antibodies to the YYR DSE did enhance the presentation of these regions but failed to generate PrP^{Sc} (57). Similarly, prolonged incubation of brain homogenates with polyclonal antibodies to the three DSEs failed to generate PrP^{Sc} (64, 66). Finally, induction of high titre PrP^{Sc}-specific antibodies in prion-disease sensitized transgenic mice did not result in clinical nor biochemical indications of prion disease after eight months (70).

While the inability of PrP^{Sc} reactive antibodies to promote misfolding of wildtype PrP is reassuring, there may be elevated opportunities for antibody-induced misfolding with naturally occurring PrP polymorphisms associated with genetic prion disease. In nanopore and immunoprecipitation experiments, PrP^{Sc}-specific antibodies bound to a PrP variant associated with early onset familial dementia, indicating the occurrence, and recognition, of conformational differences and/or partially unfolded species resulting from this mutation (71). Although prolonged *in vitro* incubation of the PrP^{Sc}-specific antibodies with the misfolding prone PrP^{C} did not generate PrP^{Sc}, this nevertheless raises concern of this strategy of vaccination in outbred populations with a range of PrP polymorphisms. Thus, like the situation with the PrP^{C}-specific vaccines, the safety of PrP^{Sc}-specific vaccines will need to be evaluated on a case-by-case basis with appropriate consideration of naturally occurring PrP polymorphisms.

Collectively, it is generally accepted that PrP^{Sc} is also a viable target for prion vaccines, with demonstrated efficacy in inhibiting disease progression in the absence of adverse side effects. Importantly, antigen selection for a prion vaccine may not need to represent an either/or situation of PrP^{C} versus PrP^{Sc}. As each target offers distinct, and potentially complimentary benefits to inhibit disease progression there could be value in the development of vaccines which induce antibodies against both conformations. This outcome which could be investigated through either a single antigen or a multivalent approach that combines top candidate PrP^{C} and PrP^{Sc} reactive antigens.

Antigen optimization (overcoming self tolerance)

Independent of the desired specificity, overcoming immunological tolerance is a shared challenge to the development of any prion vaccine. Immune tolerance refers to the unresponsiveness of the immune system to self-molecules due to developmental depletion of T and B lymphocytes with reactivities to self-antigens. Immune tolerance serves to prevent autoimmune disorders but also opposes efforts to develop vaccines against self-proteins. PrP^{C} falls within the jurisdiction of immune tolerance, and, as the conversion to PrP^{Sc} does not involve alteration to the polypeptide sequence, immune privilege also extends to the pathological isoform. Consequently, most prion infections progress to their fatal outcomes in the absence of an induced immune response (72–76). Thus, the unique biology of prion infection offers sanctuary from immune activation, enabling unfettered disease progression, and challenging the development of vaccines; overcoming immune tolerance is a central obstacle to the development of prion vaccines (77).

As immune tolerance is based on host PrP, one strategy to overcome self-tolerance is to utilize PrP from heterologous species

as vaccine antigens; that species-specific variations of PrP sequence can provide versions of the protein that are recognized as foreign by the immune system. For example, while mouse PrP fails to induce immune responses in BALB/c mice (78), bovine and sheep PrP were highly immunogenic (79). A stipulation to this approach is ensuring that the antibodies induced to the heterologous PrP have sufficient cross-reactivity to enable binding of the infecting and/or host PrP. There are examples in which antibodies to heterologous PrP antigens are unable to bind PrP^{C} or PrP^{Sc} (80). Alternatively, presentation of PrP as aggregation-prone recombinant dimers can also overcome immune tolerance, even to homologous sequences (45, 46). Finally, alternative strategies of antigen formulation and delivery can overcome self-tolerance; presentation of PrP in the context of Dynabeads (81) or polylactide-coglycolide nanospheres (48) have enabled creation of immunogenic vaccines.

The obstacle of self-tolerance is further complicated for peptide-based vaccines, as these minimal antigens are often weakly immunogenicity. Early efforts to translate the DSE sequences into vaccines faced considerable challenges; a vaccine based on the YYR DSE induced only weak IgM responses, even when conjugated to an immunogenic carrier and formulated with harsh adjuvants (57). One effective strategy to improve the immunogenicity of these peptides is to expand their lengths through the inclusion of naturally occurring residues flanking the region of interest. In performing these expansions, it is critical to ensure that PrP^{Sc} specificity is maintained; that increased immunogenicity is not at the expense of PrP^{Sc} specificity. The direction and extent of expansion of these core sequences can be performed through *in silico* analysis to anticipate immunogenicity based on the inclusion of endogenous B-cell epitopes (82). Through optimization of core sequences, as well as presentation of these optimized sequences on suitable carrier proteins, the three DSEs were translated into vaccines that exhibit strong immunogenicity while maintaining PrP^{Sc} specificity (64).

Rationale selection and optimization of peptide antigens is critical, but often insufficient, to overcome immune tolerance. To elicit the T-cell help required for strong immune humoral responses peptide antigens must usually be presented in the context of immunogenic carrier proteins. A variety of carrier proteins have been investigated including Leuktoxin of *Mannheimia haemolytica* (58), rabies glycoprotein G (83), blue carrier protein (84), cholera toxin (85), heat-labile enterotoxin B subunit (86) and heat shock proteins (87). Certain carriers, such as cholera toxin and *Escherichia coli* heat-labile enterotoxin, are better suited for mucosal vaccines (88) while others, like rabies glycoprotein, are of particular interest for their ability to induce strong, sustained immune responses including within the context of oral vaccines (89, 90).

Biological vectors for an oral CWD vaccine

Many of the initial efforts to develop CWD vaccines involved parenteral administration, this allowed researchers to prioritize the identification of protective antigens without the additional challenges associated with oral vaccines. While injected vaccines could find application for farmed cervids, there is recognition of the eventual necessity for orally administered vaccines. Outside of the obvious practical perspectives of vaccinating wild animals, there is also emerging recognition that protection against CWD infection, which occurs through oral routes, may depend on the induction of strong mucosal responses.

Several successful examples of oral vaccines for wildlife offer assurance of the viability of this approach and may provide framework for design of oral CWD vaccines. Most notably, oral rabies vaccines have been incredibly successful in management of that disease (91). As the protective antigen of those vaccines, glycoprotein G, is also an effective carrier for PrP antigens, it may be possible to transform established oral vaccines for rabies into CWD vaccines through the simple inclusion of the additional PrP epitopes. That effective oral rabies vaccines, utilizing different biological vectors to deliver the glycoprotein G gene, support the versatility of this approach for adaptation to cervids.

Adenovirus vectors

One of the commercialized oral rabies vaccines, OnRab, utilizes a human adenovirus platform to deliver genetic material corresponding to the rabies glycoprotein G protein (89). This system demonstrates considerable potential as an oral vaccine platform for CWD as it possesses a broad species and tissue tropism, induces systemic and humoral immunity, and can be orally dosed (92, 93). A candidate oral CWD vaccine was constructed using a replication incompetent human adenovirus encoding the truncated rabies glycoprotein G with an expanded C-terminal region to represent a series of tandem repeats of the RL DSE. Following oral administration to white-tailed deer this vaccine induced PrP^{Sc}-specific systemic and mucosal immune responses after two immunizations, confirming the ability of the vector to infect cells of the cervid gastro-intestinal tract (83). There were no indications of adverse health effects and shedding of the vector was limited to a brief period following administration (83). There is opportunity to build on these highly promising results by using replication-competent virus, which is anticipated to achieve in greater levels of antigen expression with superior immune responses (94).

Vaccinia virus

A second licenced oral rabies vaccine, RABORAL V-RG, utilizes an attenuated recombinant vaccinia virus vector engineered to express the rabies virus glycoprotein G. This vaccine has proven highly effective in controlling rabies without any reports of adverse reactions in wildlife or domestic animals (90). Vaccinia virus (VV), most famous for serving as the foundation as the smallpox vaccine, has shown considerable potential for the development of vaccines for other infectious diseases due to its large genome which can accommodate large inserts (10-15kb) of foreign genes, established safety profile, stable antigen expression, and ease of storage (95).

Lambda phage

Bacteriophage are structurally stable, amenable to genetic manipulation, strongly immunogenic, and, as they are omnipresent within the mammalian digestive tract and replicate exclusively within bacteria, generally regarded as safe to eukaryotes (96). These traits are all consistent with an oral delivery platform. This was investigated through presentation of the three PrP DSEs as recombinant fusions of the capsid head protein D of lambda phage. These modified phage particles were taken up by the Peyer's patches of the small intestine of calves resulting in the induction of strong mucosal (IgA) responses to the peptide epitopes (97).

Bacterial delivery

Some of the earliest efforts to develop oral prion vaccines utilized attenuated strains of *Salmonella enterica* expressing tandem copies of PrP (98). These attenuated strains reached the gut lymphoid follicles of deer, enabling antigen delivery and induction of immune responses in the absence of any pathologies (99). These oral vaccines resulted in a significant delay in the onset of CWD in white-tailed deer with one of the animals, who demonstrated particularly high anti-PrP titres in both saliva (IgA) and blood (IgG), remaining symptom free after 3 years (100). While the extensive vaccination protocol, involving eight immunizations, would limit the real-world potential of these results, these efforts nevertheless highlight the potential for oral vaccines to serve as a valuable tool for control of CWD.

Systemic vs mucosal responses

The route of vaccine delivery impacts the nature of the induced immune response. Parenterally administered vaccines tend to favor peripheral humoral responses (IgG) with muted responses of mucosal antibodies (IgA) while mucosal administration favors a more balanced IgG/IgA response (101). This holds true for prion vaccines; parenteral administration of a DSE-based prion vaccine resulted in IgG responses which were an order of magnitude higher than the IgA antibodies while the same epitope, delivered through oral administration with a viral vector, induced a balanced serum IgG to fecal IgA responses (58, 83). A similarly balanced epitope-specific IgG and IgA responses were achieved with mucosal delivery of prion vaccines through bacterial vectors (98–100) as well as carrier proteins specialized for mucosal delivery (86, 88).

Control of CWD within wild animal populations necessitates the use of oral vaccines. With that, it is important to consider how this route of delivery could impact disease control at the level of individual animals as well as the overall population. Orally transmitted prion diseases, including CWD, occur in three stages; uptake at mucosal surfaces, peripheral amplification, and transmission to the CNS (102, 103). It is necessary to contemplate how each of these stages offers unique potentials and challenges for immunotherapeutic intervention as relating to different routes of vaccine administration.

In general, the most effective way to deal with an infectious disease is to prevent it from occurring. This seems particularly true for prion diseases as once infection had initiated, immunotherapy, at least to date, has been limited to slowing, rather than stopping, disease progression. Blocking the uptake, or neutralizing the infectivity, of gut-associated prions could represent an ideal strategy to protect animals from CWD (Figure 2). In a best-case scenario, antibodies at the mucosal surface could prevent the uptake of prions from the digestive tract to prevent infection. This is likely dependent on oral vaccinations for induction of mucosal IgA antibodies; the strong peripheral immune responses from parental administration offer greater extent of protection in peripheral rather than oral challenge models (104).

During the second stage of CWD infection, peripheral amplification, the priority shift to slowing disease progression by blocking the ability of PrP^{Sc} to recruit new PrP^{C} into the growing amyloid. This can be achieved by neutralizing the infectivity of PrP^{Sc}, depleting PrP^{C}, or both. Those mechanisms utilize IgG

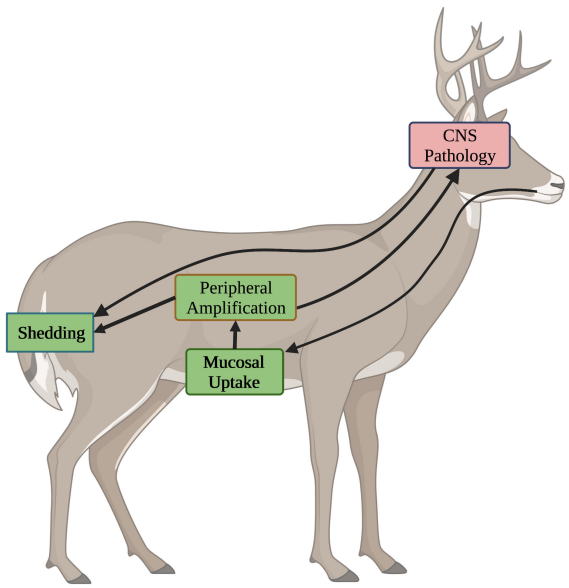

FIGURE 2
Stages of CWD and Opportunities for Immunotherapeutic Intervention. CWD progresses through four different stages, each of which presents distinct opportunities and challenges for immunotherapeutic intervention. Stages where oral vaccines are anticipated to have positive impact are highlighted in green. Stages which are unlikely to impacted by oral vaccines are shown in red. 1) Mucosal Uptake. Following oral ingestion, environmental prions are taken up through mucosal surfaces. Induction of IgA antibodies through oral vaccines offer the best chance to block uptake. 2) Peripheral Amplification. Following uptake, prions undergo a stage of peripheral amplification. Induction of IgG antibodies, through either oral or injected vaccines can inhibit this process. 3) Shedding. Prions generated in periphery and CNS of the infected host are shed in saliva, urine, and feces. IgG antibodies, induced through injected or oral vaccines, may restrict prion amplification to reduce shedding. 4) CNS Pathology. After peripheral amplification, prions migrate to the CNS where they exert pathological consequences. While the BBB limits access of antibodies to the CNS, IgG antibodies, induced through either oral or injected vaccination, may minimize pathology.

antibodies as effectors of the response. The consequences of slowing the production of PrP^{Sc} are two-fold. First, this may delay the time frame of which peripheral loads of PrP^{Sc} reach thresholds that promote spillover of the disease to the CNS. As the symptoms of prion disease are associated with CNS pathology, this would serve to prolong the asymptomatic period between infection and onset of symptoms. While this would certainly be valuable for vaccines against human prion diseases, it is less important for controlling CWD within wild populations. Indeed, prolonging the lifespan of an infected animal, enabling greater opportunities for shedding prions into the environment, could be counterproductive. Strong peripheral responses, which inhibit the progression of PrP^{Sc}, may serve to reduce the infectious load generated within an animal. This, in turn, would reduce the amount of infectious material released to the environment which, in time, could serve to slow disease progression at the population level (Figure 2). While strong peripheral responses are likely best achieved through parenteral administration, oral vaccines may also induce high enough levels of IgG antibodies to reduce the amount of PrP^{Sc} generated, and shed, by infected animals.

The final stage of CWD occurs when the infectious agent reaches the CNS. Here the options for immunotherapy are limited by the impermeability of the blood brain barrier (BBB) to antibodies (105, 106). Concentrations of IgG antibodies in the CNS are typically two to three orders of magnitude lower than in serum (107). This trend has also been observed for prion vaccines (58). With this, neither orally nor parenterally administered vaccines are likely to have much impact on disease progression once the prions have reached the CNS (Figure 2). Although reducing peripheral amplification may delay the time required to reach thresholds that favor spillover into the CNS. Prions generated in the CNS will contribute to environmental contamination through retrograde transport to the periphery with subsequent shedding and/or through environmental contamination *via* the animal carcass, including the brain. The minimal ability to slow disease progression in the brain and prolong the lifespan of the infected animal may benefit disease control at a population level by minimizing the duration of time for which infected animals generate and shed prions. As the priority of the CWD vaccines is to protect populations, rather than individuals, the relative inability of orally or parenterally administered vaccines to impact prion disease progression in the CNS may be an acceptable, and even desirable, trait.

Collectively, induction of systemic and mucosal immune responses may be beneficial for an effective vaccine for CWD. When dealing with oral models of prion infection, the greatest extents of protection correlated with high titres of both IgG and IgA antibodies, as compared to either high titres of either IgG or IgA alone (99).

Prospective impacts of vaccines for control of CWD

Considering the challenges associated with development of effective prion vaccines, it is probably overly optimistic to hope for vaccine that achieves absolute, sterilizing protection. Fortunately, while this extent of protection would obviously be highly desirable, it is not prerequisite for the vaccines to be an asset in control of the disease. Immunization of wildlife could contribute to disease management on two fronts.

Firstly, by diminishing the quantities of prions generated within an infected animal, and subsequently released into the environment, it may be possible to slow, and even reverse, the trend towards an increasing environmental burden of prions which should, in time, be reflected in fewer new cases. That would further serve to further reduce the extent of environmental contamination. Given the durability of prions within the environment and the slow progression of disease within individual animals, this will be a prolonged process. Parallel efforts to decontaminate environments and minimize new infections would serve to complement and enhance this contribution of vaccines to control of CWD.

A second mechanism by which oral CWD vaccines could contribute to control of CWD is through containment of the disease to endemic areas. Given the gradual, predictable, patterns of migration of the disease, coupled with knowledge of the location of populations of vulnerable populations, like the Northern caribou, it may be possible to use a ring vaccination approach to stop, or at least limit, further spread.

The feasibility for strategic placement of oral vaccines, with respect to the timing and geography of vaccine dispersal, to control infectious diseases within wildlife is well supported by the examples of various oral vaccines that have been successfully employed for the control of rabies. Notably, many of the oral vaccines under development for CWD utilize similar biological vectors as the oral rabies vaccines and would have similar traits in terms of cost and environmental durability.

Conclusions

After decades of research, effective vaccines for the prion diseases, as well as the conceptually related prion-like diseases, such as Alzheimer's and Parkinson's disease, remain elusive. While this highlights the magnitude of this challenge, this is an active branch of vaccinology that continues to advance and evolve, offering hope for critical breakthroughs. As these proteinopathies share a common mechanism by which a misfolded self-protein serves as a self-propagating catalyst for additional misfolding events, the lessons learned within vaccine development efforts of each disease, in terms of identification of protect antigens and strategies of vaccine formulation and delivery, may serve common benefit. An important distinction, however, is that the criteria of an "effective" vaccines for human proteinopathies would likely be quite distinct traits than that of a vaccine for control of CWD in wildlife. Within human disease, vaccines that prolong lifespan and minimize disease symptoms would be celebrated achievements. For CWD, however, a vaccine that prolonged the duration of which an infected animal could generate and release prions into the environment would be inconsistent with the goals of disease management, that the priority of CWD vaccines is to save populations, rather than individual animals.

Recent progress in the identification of protective antigens, strategies to overcome immune tolerance, and efforts to translate these approaches into oral vaccines gives hope for the development of oral CWD vaccines. It is critical, however, not to underestimate the challenges presented by CWD, including occurrence in wildlife species, widespread geographic occurrence, environmental persistence, unique molecular mechanisms, and the dynamic nature of the threat (3, 108, 109). Any expectations of the extent and time frames in which the trajectory of the disease can be impacted with a vaccine must be balanced against the magnitude of these obstacles. Indeed, the challenges of CWD are likely too numerous and diverse to hope that any single disease control measure can function as a complete solution. More realistically, an oral CWD vaccine could contribute as a valuable component of a multi-pronged approach that could include strategic culling, utilizing genetic resistance, and decontamination of environmental prions.

Author contributions

SN and HS co-developed and co-wrote this manuscript. Both authors contributed to the article and approved the submitted version.

Funding

This work was supported by funding of the Alberta Conservation Association, Saskatchewan Fish and Wildlife Development Fund, and Alberta Environment and Parks. VIDO receives operational funding from the Government of Saskatchewan through Innovation Saskatchewan and the Ministry of Agriculture and from the Canada Foundation for Innovation through the Major Science Initiatives for its CL3 facility.

Conflict of interest

The authors declare that the research was conducted in the absence of any commercial or financial relationships that could be construed as a potential conflict of interest.

Publisher's note

References

1. Prusiner SB. Proteinaceous infectious particles cause scrapie. *Science* (1982) 216:136–44. doi: 10.1126/science.6801762

2. Prusiner SB. Prions. *Proc Natl Acad Sci USA* (1998) 95(23):13363–83. doi: 10.1073/pnas.95.23.13363

3. Williams ES. Chronic wasting disease. *Vet Pathol* (2005) 42(5):530–49. doi: 10.1354/vp.42-5-530

4. Haley NJ, Hoover EA. Chronic wasting disease of cervids: current knowledge and future perspectives. *Annu Rev Anim BioSci* (2015) 3(1):305–25. doi: 10.1146/annurev-animal-022114-111001

5. Edmunds DR, Kauffman MJ, Schumaker BA, Lindzey FG, Cook WE, Kreeger TJ, et al. Chronic wasting disease drives population decline of white-tailed deer. *PLoS One* (2016) 11(8):e0161127. doi: 10.1371/journal.pone.0161127

6. DeVivo MT, Edmunds DR, Kauffman MJ, Schumaker BA, Binfet J, Kreeger TJ, et al. Endemic chronic wasting disease causes mule deer population decline in Wyoming. *PLoS One* (2017) 12(10):e0186512. doi: 10.1371/journal.pone.0186512

7. Benestad SL, Mitchell G, Simmons M, Ytrehus B, Vikøren T. First case of chronic wasting disease in Europe in a Norwegian free-ranging reindeer. *Vet Res* (2016) 47 (1):88. doi: 10.1186/s13567-016-0375-4

8. Benestad SL, Telling GC. Chronic wasting disease: an evolving prion disease of cervids. *Handb Clin Neurol* (2018) 153:135–51. doi: 10.1016/B978-0-444-63945-5.00008-8

9. Kim TY, Shon HJ, Joo YS, Mun UK, Kang KS, Lee YS. Additional cases of chronic wasting disease in imported deer in Korea. *J Vet Med Sci* (2005) 67(8):753–9. doi: 10.1292/jvms.67.753

10. Bian J, Kim S, Kane SJ, Crowell J, Sun JL, Christiansen J, et al. Adaptive selection of a prion strain conformer corresponding to established north American CWD during propagation of novel emergent Norwegian strains in mice expressing elk or deer prion protein. *PLoS Pathog* (2021) 17(7):e1009748. doi: 10.1371/journal.ppat.1009748

11. Tranulis MA, Gavier-Widén D, Våge J, Nöremark M, Korpenfelt SL, Hautaniemi M, et al. Chronic wasting disease in Europe: new strains on the horizon. *Acta Vet Scand* (2021) 63(1):48. doi: 10.1186/s13028-021-00606-x

12. Hannaoui S, Schatzl HM, Gilch S. Chronic wasting disease: Emerging prions and their potential risk. *PLoS Pathog* (2017) 13(11):e1006619. doi: 10.1371/journal.ppat.1006619

13. Rivera NA, Brandt AL, Novakofski JE, Mateus-Pinilla NE. Chronic wasting disease in cervids: Prevalence, impact and management strategies. *Vet Med (Auckl)* (2019) 10:123–39. doi: 10.2147/VMRR.S197404

14. Chiavacci SJ. The economic costs of chronic wasting disease in the united states. *PLoS One* (2022) 17(12):e0278366. doi: 10.1371/journal.pone.0278366

15. Ritchie DL, Peden AH, Barria MA. Variant CJD: Reflections a quarter of a century on. *Pathogens* (2021) 10(11):1413. doi: 10.3390/pathogens10111413

16. Prusiner SB, Scott M, Foster D, Pan KM, Groth D, Mirenda C, et al. Transgenetic studies implicate interactions between homologous PrP isoforms in scrapie prion replication. *Cell* (1990) 63(4):673–86. doi: 10.1016/0092-8674(90)90134-z

17. Collinge J, Clarke AR. A general model of prion strains and their pathogenicity. *Science* (2007) 318(5852):930–6. doi: 10.1126/science.1138718

18. Sigurdson CJ, Nilsson KP, Hornemann S, Manco G, Fernández-Borges N, Schwarz P. A molecular switch controls interspecies prion disease transmission in mice. *J Clin Invest* (2010) 120(7):2590–9. doi: 10.1172/JCI42051

19. Myers R, Cembran A, Fernandez-Funez P. Insight from animals resistant to prion diseases: Deciphering the genotype - morphotype - phenotype code for the prion protein. *Front Cell Neurosci* (2020) 14:254. doi: 10.3389/fncel.2020.00254

20. Kurt TD, Jiang L, Fernández-Borges N, Bett C, Liu J, Yang T, et al. Human prion protein sequence elements impede cross-species chronic wasting disease transmission. *J Clin Invest* (2015) 125(4):1485–96. doi: 10.1172/JCI79408

21. Wilson R, Plinston C, Hunter N, Casalone C, Corona C, Tagliavini F, et al. Chronic wasting disease and atypical forms of bovine spongiform encephalopathy and scrapie are not transmissible to mice expressing wild-type levels of human prion protein. *J Gen Virol* (20122012) 93:1624–9. doi: 10.1099/vir.0.042507-0

22. Tamgüney G, Miller MW, Giles K, Lemus A, Glidden DV, DeArmond SJ, et al. Transmission of scrapie and sheep-passaged bovine spongiform encephalopathy prions to transgenic mice expressing elk prion protein. *J Gen Virol* (2009) 90:1035–47. doi: 10.1099/vir.0.007500-0

23. Wadsworth JDF, Joiner S, Linehan JM, Jack K, Al-Doujaily H, Costa H, et al. Humanised transgenic mice are resistant to chronic wasting disease prions from Norwegian reindeer and moose. *J Infect Dis* (2021) 226:933–7. doi: 10.1093/infdis/jiab033

24. Hamir AN, Kehrli MEJr, Kunkle RA, Greenlee JJ, Nicholson EM, Richt JA, et al. Experimental interspecies transmission studies of the transmissible spongiform encephalopathies to cattle: comparison to bovine spongiform encephalopathy in cattle. *J Vet Diagn Invest* (2011) 23(3):407–20. doi: 10.1177/1040638711403404

25. Di Bari MA, Nonno R, Castilla J, D'Agostino C, Pirisinu L, Riccardi G, et al. Chronic wasting disease in bank voles: characterisation of the shortest incubation time

model for prion diseases. *PLoS Pathog* (2013) 9(3):e1003219. doi: 10.1371/journal.ppat.1003219

26. Mathiason CK, Nalls AV, Seelig DM, Kraft SL, Carnes K, Anderson KR, et al. Susceptibility of domestic cats to chronic wasting disease. *J Virol* (2013) 87:1947–56. doi: 10.1128/JVI.02592-12

27. Moore SJ, West-Greenlee MH, Kondru N, Manne S, Smith JD, Kunkle RA, et al. Experimental transmission of the chronic wasting disease agent to swine after oral or intracranial inoculation. *J Virol* (2017) 91(19):e00926–17. doi: 10.1128/JVI.00926-17

28. Chiu A, Goddard E, Parlee B. Caribou consumption in northern Canadian communities. *J Toxicol Environ Health A* (2016) 79(16-17):762–97. doi: 10.1080/15287394.2016.1174011

29. Osterholm MT, Anderson CJ, Zabel MD, Scheftel JM, Moore KA, Appleby BS. Chronic wasting disease in cervids: Implications for prion transmission to humans and other animal species. *mBio* (2019) 10(4):e01091–19. doi: 10.1128/mBio.01091-19

30. Sikorska B, Knight R, Ironside JW, Liberski PP. Creutzfeldt-Jakob Disease. *Adv Exp Med Biol* (2012) 724:76–90. doi: 10.1007/978-1-4614-0653-2_6

31. Hannaoui S, Zemlyankina I, Chang SC, Arifin MI, Béringue V, McKenzie D, et al. Transmission of cervid prions to humanized mice demonstrates the zoonotic potential of CWD. *Acta Neuropathol* (2022) 144:767–84. doi: 10.1007/s00401-022-02482-9

32. Barria MA, Telling GC, Gambetti P, Mastrianni JA, Soto C. Generation of a new form of human PrP(Sc) *in vitro* by interspecies transmission from cervid prions. *J Biol Chem* (20112011) 286(9):7490–5. doi: 10.1074/jbc.M110.198465

33. Wang Z, Qin K, Camacho MV, Cali I, Yuan J, Shen P, et al. Generation of human chronic wasting disease in transgenic mice. *Acta Neuropathol Commun* (2021) 9(1):158. doi: 10.1186/s40478-021-01262-y

34. Race B, Meade-White KD, Phillips K, Striebel J, Race R, Chesebro B. Chronic wasting disease agents in nonhuman primates. *Emerg Infect Dis* (2014) 20(5):833–7. doi: 10.3201/eid2005.130778

35. Race B, Meade-White KD, Miller MW, Barbian KD, Rubenstein R, LaFauci G. Susceptibilities of nonhuman primates to chronic wasting disease. *Emerg Infect Dis* (2009) 2009) 15:1366–76. doi: 10.3201/eid1509.090253

36. Race B, Williams K, Orrú CD, Hughson AG, Lubke L, Chesebro B. Lack of transmission of chronic wasting disease to cynomolgus macaques. *J Virol* (2018) 92: e00550–18. doi: 10.1128/JVI.00550-18

37. Czub S, Schulz-Schaeffer W, Stahl-Hennig C, Beekes M, Schaetzl H, Motzkus D. First evidence of intracranial and perora transmission of chronic wasting disease (CWD) in cynomolgus macques: A work in progress. *Prion* (2017) 25:23–6.

38. Liberski PP, Gajos A, Sikorska B, Lindenbaum S. Kuru, the first human prion disease. *Viruses* (2019) 11(3):232. doi: 10.3390/v11030232

39. Smith PG, Bradley R. Bovine spongiform encephalopathy (BSE) and its epidemiology. *Br Med Bull* (2003) 66:185–98. doi: 10.1093/bmb/66.1.185

40. Nichols TA, Pulford B, Wyckoff AC, Meyerett C, Michel B, Gertig K, et al. Detection of protease-resistant cervid prion protein in water from a CWD-endemic area. *Prion* (2009) 3(3):171–83. doi: 10.4161/pri.3.3.9819

41. John TR, Schätzl HM, Gilch S. Early detection of chronic wasting disease prions in urine of pre-symptomatic deer by real-time quaking-induced conversion assay. *Prion* (2013) 7(3):253–8. doi: 10.4161/pri.24430

42. Kuznetsova A, McKenzie D, Banser P, Siddique T, Aiken JM. Potential role of soil properties in the spread of CWD in western Canada. *Prion* (2014) 8(1):92–9. doi: 10.4161/pri.28467

43. Pritzkow S, Morales R, Moda F, Khan U, Telling GC, Hoover E, et al. Grass plants bind, retain, uptake, and transport infectious prions. *Cell Rep* (2015) 11(8):1168–75. doi: 10.1016/j.celrep.2015.04.036

44. Bueler H, Aguzzi A, Sailer A, Greiner RA, Autenried P, Aguet M, et al. Mice devoid of PrP are resistant to scrapie. *Cell* (1993) 73:1339–47. doi: 10.1016/0092-8674(93)90360-3

45. Gilch S, Wopfner F, Renner-Müller I, Kremmer E, Bauer C, Wolf E, et al. Polyclonal anti-PrP auto-antibodies induced with dimeric PrP interfere efficiently with PrPSc propagation in prion-infected cells. *J Biol Chem* (2003) 278(20):18524–31. doi: 10.1074/jbc.M210723200

46. Abdelaziz DH, Thapa S, Abdulrahman B, Lu L, Jain S, Schatzyl HM. Immunization of cervidized transgenic mice with multimeric deer prion protein induces self-antibodies that antagonize chronic wasting disease infectivity *in vitro*. *Sci Rep* (2017) 7:10538. doi: 10.1038/s41598-017-11235-8

47. Mallucci G, Dickinson A, Linehan J, Klöhn PC, Brandner S Collinge J. Depleting neuronal PrP in prion infection prevents disease and reverses spongiosis. *Science* (2003) 302:871–4. doi: 10.1126/science.1090187

48. Kaiser-Schulz G, Heit A, Quintanilla-Martinez L, Hammerschmidt F, Hess S, Jennen L, et al. Polylactide-coglycolide microspheres co-encapsulating recombinant tandem prion protein with CpG-oligonucleotide break self-tolerance to prion protein in wild-type mice and induce CD4 and CD8 T cell responses. *J Immunol* (2007) 179 (5):2797–807. doi: 10.4049/jimmunol.179.5.2797

49. Nicoll AJ, Collinge J. Preventing prion pathogenicity by targeting the cellular prion protein. *Infect Disord Drug Targets* (2009) 9(1):48–57. doi: 10.2174/187152651090901004 8

50. Solforosi L, Criado JR, McGavern DB, Wirz S, Sánchez-Alavez M, Sugama S, et al. Cross-linking cellular prion protein triggers neuronal apoptosis in vivo. *Science* (2004) 303:1514–6. doi: 10.1126/science.1094273

51. Lefebvre-Roque M, Kremmer E, Gilch S, Zou WQ, Feraudet C, Gilles CM, et al. Toxic effects of intracerebral PrP antibody administration during the course of BSE infection in mice. *Prion* (2007) 1:198–206. doi: 10.4161/pri.1.3.4870

52. Klöhn PC, Farmer M, Linehan JM, O'Malley C, Fernandez de Marco M, Taylor W, et al. PrP antibodies do not trigger mouse hippocampal neuron apoptosis. *Science* (2012) 335(6064):52. doi: 10.1126/science.1215579

53. Cashman NR, Loertscher R, Nalbantoglu J, Shaw I, Kascsak RJ, Bolton DC, et al. Cellular isoform of the scrapie agent protein participates in lymphocyte activation. *Cell* (1990) 61:185–92. doi: 10.1016/0092-8674(90)90225-4

54. Mouillet-Richard S, Ermonval M, Chebassier C, Laplanche JL, Lehmann S, Launay JM, et al. Signal transduction through prion protein. *Science* (2000) 289:1925–8. doi: 10.1126/science.289.5486.1925

55. Sonati T, Reimann RR, Falsig J, Baral PK, O'Connor T, Hornemann S, et al. The toxicity of antiprion antibodies is mediated by the flexible tail of the prion protein. *Nature* (2013) 501:102–6. doi: 10.1038/nature12402

56. Isaacs JD, Jackson GS, Altmann DM. The role of the cellular prion protein in the immune system. *Clin Exp Immunol* (2006) 146(1):1–8. doi: 10.1111/j.1365-2249.2006.03194.x

57. Paramithiotis E, Pinard M, Lawton T, LaBoissiere S, Leathers V, Zou W, et al. A prion protein epitope selective for the pathologically misfolded conformation. *Nat Med* (2003) 9:893–9. doi: 10.1038/nm883

58. Hedlin P, Cashman N, Li L, Gupta J, Babiuk L, Potter A, et al. Design and delivery of a cryptic PrPC epitope for induction of PrPSc-specific antibody responses. *Vaccine* (2010) 28:981–8. doi: 10.1016/j.vaccine.2009.10.134

59. Cashman NR. *Antibodies and epitopes specific to misfolded prion protein*. United States patent US (2010).

60. Guest W, Cashman N, Plotkin S. Structure-based prediction of unstable regions in proteins: Applications to protein misfolding diseases. *Bull Am Phys Soc* (2009) 54: A40–013.

61. Gossert AD, Bonjour S, Lysek DA, Fiorito F, Wuthrich K. Prion protein NMR structures of elk and of mouse/elk hybrids. *Proc Natl Acad Sci USA* (2005) 102:646–50. doi: 10.1073/pnas.0409008102

62. Wang LQ, Zhao K, Yuan HY, Wang Q, Guan Z, Tao J, et al. Cryo-EM structure of an amyloid fibril formed by full-length human prion protein. *Nat Struct Mol Biol* (2020) 27:598–602. doi: 10.1038/s41594-020-0441-5

63. Kraus A, Hoyt F, Schwartz CL, Hansen B, Artikis E, Hughson AG, et al. High-resolution structure and strain comparison of infectious mammalian prions. *Mol Cell* (2021) 81(21):4540–51. doi: 10.1016/j.molcel.2021.08.011

64. Marciniuk K, Määttänen P, Taschuk R, Airey D, Potter A, Cashman NR, et al. Development of a multivalent, PrP^{Sc}-specific prion vaccine through rational optimization of three disease-specific epitopes. *Vaccine* (2014) 32:1988–97. doi: 10.1016/j.vaccine.2014.01.027

65. Taschuk R, van der Merwe J, Marciniuk K, Potter A, Cashman N, Griebel P, et al. *In vitro* neutralization of prions with PrP^{Sc}-specific antibodies. *Prion* (2015) 9:292–303. doi: 10.1080/19336896.2015.1071761

66. Taschuk R, Marciniuk K, Määttänen P, Madampage C, Hedlin P, Potter A. Safety, specificity and immunogenicity of a PrP(Sc)-specific prion vaccine based on the YYR disease specific epitope. *Prion* (2014) 8(1):51–9. doi: 10.4161/pri.27962

67. Wood ME, Griebel P, Huizenga ML, Lockwood S, Hansen C, Potter A, et al. Accelerated onset of chronic wasting disease in elk (Cervus canadensis) vaccinated with a PrPSc-specific vaccine and housed in a prion contaminated environment. *Vaccine* (2018) 36:7737–43. doi: 10.1016/j.vaccine.2018.10.057

68. Wille H, Requena JR. The structure of PrP^{Sc} prions. *Pathogens* (2018) 7(1):20. doi: 10.3390/pathogens7010020

69. Fleming M, Fang A, Tancowny B, Telling G, Wille H. Optimizing prion vaccination in a transgenic mouse model of gerstmann-Sträussler-Scheinker disease. *Prion* (2022) 16:95–253. doi: 10.1080/19336896.2022.2091286

70. Määttänen P, Taschuk R, Ross L, Marciniuk K, Bertram L, Potter A, et al. PrP^{Sc}-specific antibodies do not induce prion disease or misfolding of PrP^{C} in highly susceptible Tga20 mice. *Prion* (2013) 7:434–9. doi: 10.4161/pri.26639

71. Madampage C, Määttänen P, Marciniuk K, Brownlie R, Andrievskaia O, Potter A. Binding of bovine T194A PrP^{C} by PrP^{Sc}-specific antibodies. *Prion* (2013) 7:301–11. doi: 10.4161/pri.25148

72. Zabel MD. Avery AC Prions–not your immunologist's pathogen. *PLoS Pathog* (2015) 19:e1004624. doi: 10.1371/journal.ppat.1004624

73. Porter DD, Porter HG, Cox NA. Failure to demonstrate a humoral immune response to scrapie infection in mice. *J Immunol* (1973) 111:1407–10. doi: 10.4049/jimmunol.111.5.1407

74. Kasper KC, Stites DP, Bowman KA, Panitch H, Prusiner SB. Immunological studies of scrapie infection. *J Neuroimmunol* (1982) 3:187–20. doi: 10.1016/0165-5728(82)90022-4

75. Aucouturier P, Carnaud C. The immune system and prion diseases: a relationship of complicity and blindness. *J Leukoc Biol* (20022002) 72:1075–83. doi: 10.1189/jlb.72.6.1075

76. Aguzzi A. Prions and the immune system: a journey through gut, spleen, and nerves. *Adv Immunol* (2003) 81:123–71. doi: 10.1016/s0065-2776(03)81004-0

77. Mabbott NA, Alibhai JD, Manson J. The role of the immune system in prion infection. *Handb Clin Neurol* (2018) 153:85–107. doi: 10.1016/B978-0-444-63945-5.00005-2

78. Polymenidou M, Heppner FL, Pellicioli EC, Urich E, Miele G, Braun N, et al. Humoral immune response to native eukaryotic prion protein correlates with anti-prion protection. *Proc Natl Acad Sci USA* (2004) 101(Suppl. 2):14670–6. doi: 10.1073/pnas.0404772101

79. Ishibashi D, Yamanaka H, Yamaguchi N, Yoshikawa D, Nakamura R, Okimura N, et al. Immunization with recombinant bovine but not mouse prion protein delays the onset of disease in mice inoculated with a mouse-adapted prion. *Vaccine* (2007) 25 (6):985–92. doi: 10.1016/j.vaccine.2006.09.078

80. Heppner FL, Aguzzi A. Recent developments in prion immunotherapy. *Curr Opin Immunol* (2004) 16(5):594–8. doi: 10.1016/j.coi.2004.07.008

81. Tayebi M, Collinge J, Hawke S. Unswitched immunoglobulin m response prolongs mouse survival in prion disease. *J Gen Virol* (2009) 90:777–82. doi: 10.1099/vir.0.005041-0

82. Marciniuk K, Trost B, Napper S. EpIC: a rational pipeline for epitope immunogenicity characterization. *Bioinformatics* (2015) 31:2388–90. doi: 10.1093/bioinformatics/btv136

83. Taschuk R, Scruten E, Woodbury M, Cashman N, Potter A, Griebel P, et al. Induction of PrP^{Sc}-specific systemic and mucosal immune responses in white-tailed deer with an oral vaccine for chronic wasting disease. *Prion* (2017) 11(5):368–80. doi: 10.1080/19336896.2017.1367083

84. Pilon JL, Loiacono C, Okeson D, Lund S, Vercauteren K, Rhyan J, et al. Anti-prion activity generated by a novel vaccine formulation. *Neurosci Lett* (2007) 18:161–4. doi: 10.1016/j.neulet.2007.10.015

85. Bade S, Baier M, Boetel T, Frey A. Intranasal immunization of balb/c mice against prion protein attenuates orally acquired bovine spongiform encephalopathy. *Vaccine* (2006) 24:1242–53. doi: 10.1016/j.vaccine.2005.12.051

86. Yamanaka H, Ishibashi D, Yamaguchi N, Yoshikawa D, Nakamura R, Okimura N, et al. Enhanced mucosal immunogenicity of prion protein following fusion with b subunit of escherichia coli heat-labile enterotoxin. *Vaccine* (2006) 24(15):2815–23. doi: 10.1016/j.vaccine.2005.12.054

87. Koller MF, Grau T, Christen P. Induction of antibodies against murine full-length prion protein in wild-type mice. *J Neuroimmunol* (2002) 132:113–6. doi: 10.1016/S0165-5728(02)00316-8

88. Sakaguchi S, Arakawa T. Recent developments in mucosal vaccines against prion diseases. *Expert Rev Vaccines* (2007) 6(1):75–85. doi: 10.1586/14760584.6.1.75

89. Yarosh OK, Wandeler AI, Graham FL, Campbell JB, Prevec L. Human adenovirus type 5 vectors expressing rabies glycoprotein. *Vaccine* (1996) 14:1257–64. doi: 10.1016/S0264-410X(96)00012-6

90. Maki J, Guiot AL, Aubert M, Brochier B, Cliquet F, Hanlon CA, et al. Oral vaccination of wildlife using a vaccinia–rabies-glycoprotein recombinant virus vaccine (RABORAL V-RG®): a global review. *Vet Res* (2017) 48:57. doi: 10.1186/s13567-017-0459-9

91. Mahl P, Clinquet F, Guiot AL, Niin E, Fournials E, Saint-Jean N, et al. Twenty-year experience of the oral rabies vaccine SAG2 in wildlife: A global review. *Vet Res* (2014) 45:77. doi: 10.1186/s13567-014-0077-8.PMID:25106552

92. Buge SL, Richardson E, Alipanah S, Markham P, Cheng S, Kalyan N, et al. An adenovirus-simian immunodeficiency virus env vaccine elicits humoral, cellular, and mucosal immune responses in rhesus macaques and decreases viral burden following vaginal challenge. *J Virol* (1997) 71:8531–41. doi: 10.1128/jvi.71.11.8531-8541.1997

93. Alejo DM, Moraes MP, Liao X, Dias CC, Tulman ER, Diaz-San S, et al. An adenovirus vectored mucosal adjuvant augments protection of mice immunized intranasally with an adenovirus-vectored foot-and-mouth disease virus subunit vaccine. *Vaccine* (2013) 26:2302–09. doi: 10.1016/j.vaccine.2013.02.060

94. Matsuda K, Migueles SA, Huang J, Bolkhovitinov L, Stuccio S, Griesman T, et al. A replication-competent adenovirus-vectored influenza vaccine induces durable systemic and mucosal immunity. *J Clin Invest* (2021) 131(5):e140794. doi: 10.1172/JCI140794

95. Zhang Z, Dong L, Zhao C, Zheng P, Zhang X, Xu J. Vaccinia virus-based vector against infectious diseases and tumors. *Hum Vaccin Immunother* (20212021) 17 (6):1578–85. doi: 10.1080/21645515.2020.1840887

96. Hodyra-Stefaniak K, Miernikiewicz P, Drapala J, Drab M, Jonczyk-Matysiak E, Lecion D, et al. Mammalian host-Versus-Phage immune response determines phage fate *in vivo*. *Sci Rep* (2015) 5:14802. doi: 10.1038/srep14802

97. González-Cano P, Gamage L, Marciniuk K, Hayes C, Napper S, Hayes S, et al. Lambda display phage as a mucosal vaccine delivery vehicle for peptide antigens. *Vaccine* (2017) 35:7256–63. doi: 10.1016/j.vaccine.2017.11.010

98. Goni F, Knudsen E, Schreiber F, Scholtzova H, Pankiewicz J, Carp R, et al. Mucosal vaccination delays or prevents prion infection *via* an oral route. *Neurosci* (2005) 133:413–21. doi: 10.1016/j

99. Goni F, Prelli F, Schreiber F, Scholtzova H, Chung E, Kascsak R, et al. High titers of mucosal and systemic anti-PrP antibodies abrogate oral prion infection in mucosal-vaccinated mice. *Neuroscience* (2008) 15:679–86. doi: 10.1016/j

100. Goni F, Mathiason CK, Yim L, Wong K, Hayes-Klug J, Nalls A, et al. Mucosal immunization with an attenuated salmonella vaccine partially protects white-tailed deer from chronic wasting disease. *Vaccine* (2015) 33:726–33. doi: 10.1016/j.vaccine.2014.11.035

101. Ogra PL, Faden H, Welliver RC. Vaccination strategies for mucosal immune responses. *Clin Microbiol Rev* (2001) 14(2):430–45. doi: 10.1128/CMR.14.2.430-445.2001

102. Miller MW, Williams ES. Prion disease: horizontal prion transmission in mule deer. *Nature* (2003) 425:35–6. doi: 10.1038/425035a

103. Beekes M, McBride PA. The spread of prions through the body in naturally acquired transmissible spongiform encephalopathies. *FEBS J* (2007) 274:588–605. doi: 10.1111/j.1742-4658.2007.05631.x

104. Pilon JL, Rhyan JC, Wolfe LL, Davis TR, McCollum MP, O'Rourke KI, et al. Immunization with a synthetic peptide vaccine fails to protect mule deer (Odocoileus hemionus) from chronic wasting disease. *J Wildl Dis* (2013) 49:694–8. doi: 10.7589/2012-07-200

105. Poduslo JF, Curran GL, Wengenack TM, Malester B, Duff K. Permeability of proteins at the blood-brain barrier in the normal adult mouse and double transgenic mouse model of alzheimer's disease. *Neurobiol Dis* (2001) 8:555–67. doi: 10.1006/nbdi.2001.0402

106. Neuwelt EA, Bauer B, Fahlke C, Fricker G, Iadecola C, Janigro D, et al. Engaging neuroscience to advance translational research in brain barrier biology. *Nat Rev Neurosci* (2011) 12:169–82. doi: 10.1038/nrn2995

107. Katsinelos T, Tuck BJ, Mukadam AS, McEwan WA. The role of antibodies and their receptors in protection against ordered protein assembly in neurodegeneration. *Front Immunol* (2019) 10:1139. doi: 10.3389/fimmu.2019.01139

108. Gilch S. Chronic wasting disease - a prion disease through a one health lens. *Can Vet J* (2022) 63(4):431–3.

109. Saunders SE, Bartelt-Hunt SL, Bartz JC. Prions in the environment: occurrence, fate and mitigation. *Prion* (2008) 2:162–9. doi: 10.4161/pri.2.4.7951

frontiers | Frontiers in Immunology

TYPE Review
PUBLISHED 17 April 2023
DOI 10.3389/fimmu.2023.1172000

OPEN ACCESS

EDITED BY
Denis Archambault,
Université du Québec à Montréal, Canada

REVIEWED BY
Shafiqul Chowdhury,
Louisiana State University, United States
Tara Marlene Strutt,
University of Central Florida, United States

*CORRESPONDENCE
Dongwan Yoo
dyoo@illinois.edu

SPECIALTY SECTION
This article was submitted to Vaccines and Molecular Therapeutics, a section of the journal Frontiers in Immunology

RECEIVED 22 February 2023
ACCEPTED 03 April 2023
PUBLISHED 17 April 2023

CITATION
Su C-M, Du Y, Rowland RRR, Wang Q and Yoo D (2023) Reprogramming viral immune evasion for a rational design of next-generation vaccines for RNA viruses. *Front. Immunol.* 14:1172000. doi: 10.3389/fimmu.2023.1172000

Reprogramming viral immune evasion for a rational design of next-generation vaccines for RNA viruses

Chia-Ming Su[1], Yijun Du[2], Raymond R. R. Rowland[1], Qiuhong Wang[3,4] and Dongwan Yoo[1]*

[1]Department of Pathobiology, College of Veterinary Medicine, University of Illinois at Urbana-Champaign, Urbana, IL, United States, [2]Shandong Key Laboratory of Animal Disease Control and Breeding, Institute of Animal Science and Veterinary Medicine, Shandong Academy of Agricultural Sciences, Jinan, Shandong, China, [3]Center for Food Animal Health, Department of Animal Sciences, College of Food, Agricultural, and Environmental Sciences, The Ohio State University, Wooster, OH, United States, [4]Department of Veterinary Preventive Medicine, College of Veterinary Medicine, The Ohio State University, Columbus, OH, United States

Type I interferons (IFNs-α/β) are antiviral cytokines that constitute the innate immunity of hosts to fight against viral infections. Recent studies, however, have revealed the pleiotropic functions of IFNs, in addition to their antiviral activities, for the priming of activation and maturation of adaptive immunity. In turn, many viruses have developed various strategies to counteract the IFN response and to evade the host immune system for their benefits. The inefficient innate immunity and delayed adaptive response fail to clear of invading viruses and negatively affect the efficacy of vaccines. A better understanding of evasion strategies will provide opportunities to revert the viral IFN antagonism. Furthermore, IFN antagonism-deficient viruses can be generated by reverse genetics technology. Such viruses can potentially serve as next-generation vaccines that can induce effective and broad-spectrum responses for both innate and adaptive immunities for various pathogens. This review describes the recent advances in developing IFN antagonism-deficient viruses, their immune evasion and attenuated phenotypes in natural host animal species, and future potential as veterinary vaccines.

KEYWORDS

type I interferons (IFNs), NF-kappa B (NF-κB), IFN antagonism, live-attenuated vaccine, veterinary vaccine, viral immune evasion, next-generation vaccines, veterinary virology

1 Introduction

Virus-host interactions play a vital role during infection and determine pathogenic consequences, including host and tissue tropisms, viral elimination and persistence, tumorigenesis, and clinical outcomes. Physical and chemical barriers, innate immune systems, and various types of immune cells are considered the first line of defense of a host

against viral infections. Innate and adaptive immunities are two main surveillance systems to resolve viral infections. Immediately upon infection, the type I interferon (IFNs-α/β) production system is activated by recognizing viral components by host cell factors. It is the most effective cellular defense against viral infection in the early stage of infection (1). In turn, viruses have developed distinct immune-disarming abilities to facilitate replication. The modulation of IFN functions is an effective strategy for invading viruses to survive in the host (2). IFN suppression by viruses can also negatively impact the immunogenicity of live-attenuated vaccines (3). With the advances in the study of viral immune evasion mechanisms and reverse genetics technology, it is now possible to remove the IFN suppression function from target viruses and design new generation vaccines for diverse RNA viruses. Indeed, some engineered viruses have been constructed and examined in their natural host animal species for immunogenicity and clinical outcomes (4, 5). This article discusses the molecular mechanisms for viral IFN antagonism, generation of IFN antagonism-deficient viruses, their immunogenic consequences in animals following vaccination, and prospects as next-generation vaccines for veterinary diseases.

2 Innate immune response to viral infection

2.1 Type I interferons and innate immunity

Immune cells involved in the innate immune system represent monocytes, macrophages, eosinophils, neutrophils, and natural killer (NK) cells. IFNs-α/β are antiviral cytokines and constitute one of the most critical components in the innate immune system against invading viruses. The IFNs-α/β signaling triggers expression of a series of IFN-stimulated genes (ISGs) and contributes to the antiviral state of the cell (6). All nucleated cells can produce IFNs-α/β, but plasmacytoid dendritic cells (pDC) are the main type that produce type I IFNs most abundantly (7).

Once an RNA virus enters the cell, viral components trigger a series of intricate recognition mechanisms within the cell (8). The innate immune signaling cascade starts with the recognition of pathogen-associated molecular patterns (PAMPs) by pattern recognition receptors (PRRs) that are composed of fours groups of cellular proteins; nucleotide-binding oligomerization domain (NOD)-like receptors (NLRs), retinoic acid-inducible gene I (RIG-I)-like receptors (RLRs), C-type lectin receptors (CLRs), and Toll-like receptors (TLRs). NLRs, RLRs, and CLRs reside in the cytoplasm, whereas TLRs locate in the endosomal membrane (9). The viral RNA binds to RIG-I or melanoma differentiation-associated gene 5 (MDA5) and triggers conformational changes to expose its caspase activation and recruitment domain (CARD) at the N-terminus. CARD-CARD dimers are then formed and recruit the IFN-β promoter stimulator-1 (IPS-1) [also known as CARD adaptor inducing IFN-β (Cardif), mitochondrial antiviral-signaling protein (MAVS), or virus-induced signaling adaptor (VISA)] (10, 11). IPS-1 recruits the NF-kappa-B essential modulator (NEMO), tumor necrosis factor receptor-associated factor (TRAF) 3, and TRAF family-member-associated NF-κB activator (TANK) proteins, and its complex activates TANK binding kinase 1 (TBK1) and inhibitor of kappa B (IκB) kinase ϵ (IKKϵ). Subsequently, IFN regulatory factor 3 (IRF3) and IRF7 are phosphorylated in the TBK1- and IKKϵ-dependent manners (12). Then, phosphorylated IRF3 and IRF7 form a homodimer or heterodimer for translocation to the nucleus (13), where the IRF3- or IRF7-dimer forms an enhanceosome which binds to the positive regulatory domains (PRDs) I-III regions in the IFN promoters for IFN gene transcriptions (14, 15). IPS-1 may also activate IKKα and IKKβ to trigger the degradation of IkB to free up NF-κB. The released NF-κB binds to PRDs of respective IFN genes and proinflammatory cytokine promoters (15–17). Besides the RIG-I-mediated signaling cascades, TLR3 and TLR7 also recognize double-stranded RNA and single-stranded RNA, respectively, in the endosome (18). TLR3 can recruit the TRIF, nucleosome assembly protein 1 (NAP1), and TRAF3 adaptors and activates IRF3 for IFN expression and downstream signaling for many antiviral proteins (9, 15).

Once IFNs are produced, they are secreted from the cell and bind to their receptors, interferon alpha and beta receptor subunit 1 (IFNAR1) and IFNAR2, on the surface of the same cell (autocrine) or adjacent cells (paracrine). The binding of IFNs to their receptors triggers the Janus kinase (JAK)-signal transducers and activator of transcription (STAT) signaling pathway. The activation of JAK1 and tyrosine kinase 2 (Tyk2) is the first response to the IFN signaling and results in phosphorylation and dimerization of STAT1 and STAT2, followed by the recruitment of IRF9 to form the IFN-stimulated gene factor 3 (ISGF3) complex. The ISGF3 complex then translocates to the nucleus. It induces the expression of ISGs by binding to the IFN-stimulated regulatory response elements (ISRE) in the promoters of ISGs (19). More than 300 ISGs have been identified so far, and they are the major executors of IFNs acting as effector molecules for the antiviral response (19, 20).

2.2 Pleiotropic role of type I IFNs and activation of adaptive immunity

In addition to establishing an antiviral state, type I IFNs can enhance adaptive immunity by targeting dendritic cells (DCs), NK cells, T cells, and B cells (19). For DCs, type I IFNs play a key role in the generation and function of DCs (21), suggesting that type I IFNs represent a potent natural adjuvant for crossing the innate and adaptive immune systems. Type I IFNs enhance the ability of DCs to cross-present antigens to T cells and modulate antigen survival and processing (22, 23). IFNs regulate the DCs antigen presentation in an autocrine manner (24). Besides DCs, type I IFNs can promote the activation and survival of NK cells directly or indirectly *via* IL-15 *cis* and *trans* presentation (25) and regulate T cells directly through IFNARs on the surface of T cells. Type I IFNs are critical mediators for the spontaneous priming of antitumor CD8+ T cell response (26). In the herpesvirus-infected mouse model, type I IFNs have been shown to stimulate CD4+ T cells for undergoing clonal

expansion (27). The T cells primed by type I IFNs also show an increased ability to help B cells to enhance antibody secretion (28). The studies using lymphocytic choriomeningitis virus or West Nile virus as models have also demonstrated that type I IFNs upregulate the survival, maturation, cytotoxicity, and clonal expansion of CD8+ T cells during infection (29–34). In addition to effector CD8+ T cells, memory CD8+ T cells are also regulated by type I IFNs. Studies using vaccinia virus, vesicular stomatitis virus, and lymphocytic choriomeningitis virus have shown that type I IFNs promote the differentiation of memory CD8+ T cells by affecting the initial clonal expansion (31, 35). Furthermore, type I IFNs regulate B cell activation, antibody secretion, and isotype switching during the vesicular stomatitis virus and West Nile virus infections (36–38). By increasing the level of B-cell survival factors, type I IFNs can promote survival and activation of B cells and enhance autoantibody production (39). Thus, it is evident that the immunological functions of type I IFNs are much broader than establishing an antiviral state and play an important role in regulating adaptive immunity.

2.3 NF-κB signaling and cytokine responses to viral infection

Nuclear factor-κB (NF-κB) is a family of transcription factors and a key mediator for proinflammatory cytokine production. NF-κB consists of RelA (p65) and RelB, NF-κB1 (p50 and its precursor p105), NF-κB2 (p52 and its precursor p100), and c-Rel to form a homodimer or heterodimer with RelA or RelB. Numerous factors activate the NF-κB signaling including TLR ligands and cytokines such as tumor necrosis factor-α (TNF-α). Upon stimulation, upstream kinases IKKα and IKKβ are activated by phosphorylation. IKKβ then phosphorylates the IκB and degrades IκB through a proteasome-dependent manner. IκB is the negative regulator for NF-κB, and so the IκB degradation releases NF-κB, which is then phosphorylated. The activated NF-κB enters the nucleus and binds to the specific DNA locus, the κB site (40). NF-κB signaling triggers the expression of type I IFNs and various proinflammatory cytokines, including IL-1β, IL-6, IL-8, IL-15, and TNF-α (41). The expressed proinflammatory cytokines prompt the positive feedback loop to the NF-κB signaling in an autocrine manner (42). The protein inhibitor of activated STAT 1 (PIAS1) is the NF-κB negative regulator residing in the nucleus (43). PIAS1 prevents NF-κB dimers from binding to κB sites by binding to p65 in the nucleus (43). For respiratory viral infections, NF-κB is strongly activated in the lungs and results in the induction of proinflammatory cytokines and chemokines (44, 45).

3 Viral IFN antagonists and their mode of action

Many viruses code for viral proteins to antagonize the IFN pathway and often produce more than one antagonist (6, 46, 47). Viruses have evolved to employ diverse strategies to evade the IFN system, and some of the viral strategies and mechanisms of action are discussed below (Figure 1). For convenience, the signaling cascade for production of type I IFNs in virus-infected cells will be referred to as 'IFN production pathway', and the signaling mediated by IFNs for production of ISGs will be referred to as 'JAK-STAT signaling pathway'.

3.1 Inhibition of IFN production pathway

Some viruses suppress the IFN production pathway by disrupting IFN receptor functions, such as reducing receptor expression and degrading receptor molecules. For example, the influenza A virus disrupts IFN signaling by downregulating the expression of IFN receptor. The NS1 protein is a non-structural component encoded by influenza viruses A, B, and C. It counteracts the host antiviral responses by two primary mechanisms: inhibition of the activation of IRF3 and IFN transcription and inhibition of the processing of IFN pre-mRNAs (73). The NS1 protein binds the host cell RNA and forms complexes with RIG-I to antagonize IFN production (74). The NS1 protein also suppresses the expression of both chains of IFNAR receptor at the transcription level (75, 76). Epstein-Barr virus (EBV) establishes a latent infection in B lymphocytes. EBV expresses two isoforms of latent membrane protein 2 (LMP2). Of the two forms, LMP2A plays an essential role in viral latency and progression of EBV-related diseases such as Burkitt's lymphoma, nasopharyngeal carcinoma, and Hodgkin's lymphoma. The LMP2A and LMP2B proteins degrade IFN receptors and modulate both type I and type II IFN responses (77).

Activation of IRF3 is an essential step for downstream IFN production signaling (9, 15), and some viruses have developed mechanisms to manipulate the IRF3 activation. Hepatitis C virus NS3-4A is the viral serine protease and has a crucial role in the viral replication cycle. NS3-4A cleaves the polyprotein at four sequential sites to yield NS4A, NS4B, NS5A, and NS5B proteins. NS3-4A can cleave and inactivate the host proteins TRIF (TIR-domain-containing adapter-inducing interferon-β) and Cardif, which are essential adaptors in response to IFNs mediated by TLR3 and RIG-I, respectively. NS3/4A also cleaves IKK and inactivates IRF3 (78). Classical swine fever virus and bovine viral diarrhea virus are member viruses of the Pestivirus genus of the Flaviviridae family. For pestiviruses, N^{pro} is the N-terminal viral protease of the polyprotein and can degrade IRF3 for inactivation (79–81). Besides the direct degradation, IRF3 function may be inhibited by some other viruses. The rabies virus P protein and the hantavirus G1 protein have been determined to suppress IFN signaling by inhibiting IRF3 phosphorylation (82, 83). Rabies virus infects all species warm-blooded animals. It replicates in the cytoplasm of the cell, and the viral RNA is tightly encapsidated by the viral nucleoprotein and the RNA polymerase complex which consists of the phosphoprotein (P). The P protein is a cofactor of RNA polymerase by participating in viral genome transcription and replication. The P protein prevents IFN response in virus-infected cells by targeting TANK-binding kinase-1 (TBK1) and inhibiting phosphorylation and activation of IRF3. Sin Nombre virus, carried

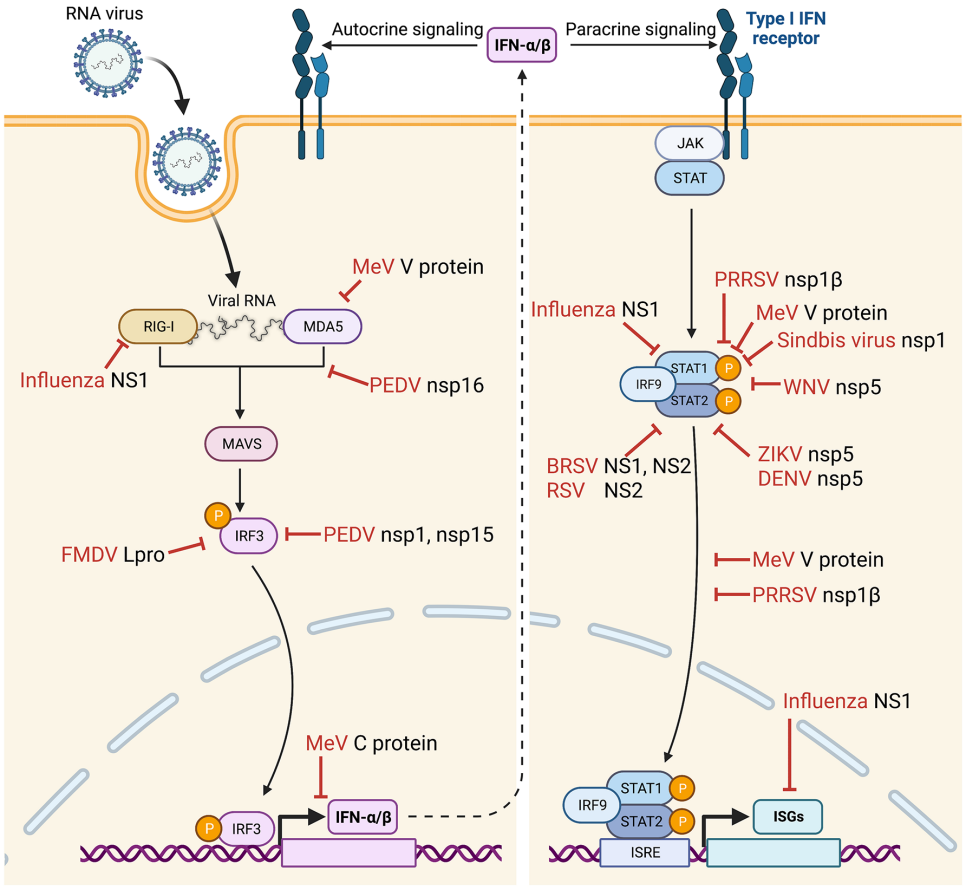

FIGURE 1
Suppression of IFNs-α/β production and IFN-stimulated gene (ISG) expression during infection by various animal viruses. IFN suppression-deficient viruses have been constructed, and their immunological and clinical outcomes have been examined in their natural host animal species. Vertical arrow (dotted line) divides the IFN signaling to "IFN production pathway" (left) and "IFN signaling JAK-STAT pathway" (right). Bars (red) indicate sites of action by specific viral proteins for IFN suppression. FMDV, foot-and-mouth disease virus (48–51); PEDV, porcine epidemic diarrhea virus (52); MeV, measles virus (53–59); PRRSV, porcine reproductive and respiratory syndrome virus (60–63); WNV, West Nile virus (64); ZIKV, Zika virus (65); DENV, Dengue virus (66); BRSV, bovine respiratory syncytial virus (67–70); RSV, respiratory syncytial virus (71, 72); IRF, interferon regulatory factor; ISRE, interferon stimulation response element; STAT, signal transducer and activator of transcription. Images were created with BioRender.com.

by rodents, is an etiologic agent for hantavirus pulmonary syndrome. With a pathogenic strain of hantavirus, the cytoplasmic tail of the G1 glycoprotein was shown to regulate the IFN response by inhibiting IRF3 phosphorylation at the level of the TBK1 complex (84). In contrast, the hantavirus G1-mediated IFN downregulation was absent in the Prospect Hill nonpathogenic strain, indicating that the IFN suppression is an important virulence factor for hantaviruses.

Coronaviruses (CoV) carry diverse strategies to inhibit IRF3 activation. CoV genomes are the largest among all RNA viruses and contain the positive-sense RNA of 25-32 kb in length. The viral genome codes for two large polyproteins, and the nsp1 protein is the N-terminal cleavage product of the polyprotein. The nsp1 protein of SARS-CoV-1 suppresses the IFN response *via* IRF3-dependent downregulation (85, 86), whereas the ORF8b and ORF8ab proteins induce IRF3 degradation *via* the ubiquitin-dependent proteasomal pathway (87). SARS-CoV-2 is an emerging virus with an unknown animal origin. As the causative agent for COVID-19 in humans, it has crossed the species barrier to infect other animal species, including cats, dogs, tigers, lions, mink, white-tail deer, monkeys, ferrets, and hamsters, to name a few (88). Humans can facilitate reverse-zoonotic transmission to animals, and the virus in infected animals may evolve to spill back to humans and other animal species. SARS-CoV-2 codes for nsp3 papain-like protease and nsp5 3C-like protease, and these two viral proteases are responsible for cleaving viral polyproteins for replication. The nsp3 protein cleaves IRF3 directly, and this finding explains the blunted type I IFN response seen in COVID-19 patients during infection (89). Although the nsp12 viral RNA polymerase of SARS-CoV-2 does not impair IRF3 activation, it attenuates type I IFN production by inhibiting IRF3 nuclear translocation (90). Meanwhile, the ORF7a protein decreases IRF3 phosphorylation by downregulating TBK1 expression (91, 92). Similarly, the viral spike (S) protein binds directly to IRF3 and further diminishes its expression, whereas the levels of NF-κB and STAT1 transcription factors remain intact (93). The murine coronavirus mouse hepatitis virus can also delay ISG production by limiting the IRF3 transcription (94).

Besides the direct regulation of IRF3, some viruses inhibit signaling adaptors and regulators in the IFN production pathway. For example, the swine arterivirus, porcine reproductive and respiratory syndrome virus (PRRSV), has been found to inhibit the IFN promoter activity

and impairs type I IFN production (60). The nsp1α protein of PRRSV downregulates IFN production by degrading the CREB (cyclic AMP response element-binding)-binding protein (CBP) *via* the ubiquitin-dependent proteasome pathway (95–97). PRRSV also suppresses the NF-κB activation and inhibits type I IFN production in the RIG-I dependent manner (98, 99). A recent study showed that nsp1β of PRRSV binds to nucleoporin 62 (Nup62) (100). Nup62 is a major structural component of the nuclear pore complex (NPC) on the nuclear membrane, and NPC functions as a gateway for nucleocytoplasmic trafficking of nuclear proteins and mRNAs. The binding of nsp1β to Nup62 disrupts the NPC integrity, causing the nuclear retention of host mRNAs and inhibiting the host cell protein production, including IFNs, ISGs, and IRF3 (100).

3.2 Inhibition of IFN signaling JAK-STAT pathway

IFNs-α/β are secretory cytokines. Once expressed in virus-infected cells and secreted, they bind to their receptors on the same cell or neighbor cells and activate the IFN signaling pathway, namely the JAK-STAT signaling. Some viruses have developed mechanisms to impair the JAK-STAT pathway by targeting STAT1 and STAT2. Paramyxoviruses disturb the STAT signaling by using diverse mechanisms, such as the direct binding of viral protein to STAT to prevent phosphorylation (101). The paramyxovirus V protein is of particular interest since it regulates the JAK-STAT pathway by degrading STAT1 and STAT2 and mediating their nuclear accumulations (53, 102–104). Sendai virus, a paramyxovirus, produces a set of four C proteins by mRNA editing of the P gene and inhibits IFN-induced tyrosine phosphorylation of STATs (101, 105, 106). All four C proteins bind to STAT1, but only the largest form of C induces the mono-ubiquitination of STAT1 and its degradation (106). Dengue virus (DENV) and Zika virus (ZIKV) in the family *Flaviviridae* have shown the ability to reduce the concentration of STATs in the cells (101, 107, 108). NS5 protein of ZIKV induces the degradation of STAT2 *via* the proteasomal pathway (65, 109).

Respiratory syncytial virus (RSV) has diverse mechanisms to inhibit the type 1 IFN response in different cell types (110). RSV degrades STATs in epithelial cells, whereas, in DCs, it inhibits STAT1 and STAT2 phosphorylation and nuclear accumulation (110, 111). Furthermore, RSV induces STAT2 downregulation through ubiquitin-proteasome degradation by the Elongin-Cullin E3 ligase (112, 113). The porcine arterivirus PRRSV nsp1β protein inhibits STAT1 phosphorylation, leading to inhibition of the JAK-STAT signaling pathway, resulting in the suppression of ISG expressions (60, 61). Other viruses can also block the IFN signaling by targeting IRF9. Such mechanisms are usually found in viruses that cause persistent infections and oncogeneses, such as human papillomavirus, porcine bocavirus, and human T-cell leukemia virus (114–116).

Viruses can block the nuclear accumulation of activated STATs and inhibit IFN signaling. For example, the paramyxovirus virus V protein binds to MDA-5 and decreases the IFN promoter activation (117), as well as binding to STAT1 and STAT2 and preventing their nuclear accumulation (118). The P protein of the rabies virus binds to the DNA-binding and coiled-coil domains of STAT1 to influence the IFN-induced transcription and impairs its nuclear translocation (119). The porcine arterivirus nsp1β protein inhibits STAT1 phosphorylation and further affects the nuclear translocation of ISGF3, thus inhibiting the JAK-STAT signaling pathway (60, 61). PRRSV nsp1β also degrades karyopherin-α1, one of the nuclear transporter proteins, and blocks the ISGF3 nuclear translocation to suppress ISG expressions (120).

4 Reprograming viral immune evasion and experimental infections in animals

Of various host immune surveillance systems, the innate immune system builds on a series of antiviral responses. Although the IFN inhibitory ability of a virus is not the only determinant for virulence, it is often one of the most critical virulence factors. Type I IFNs can also prime the activation and maturation of adaptive immune responses. Disturbed and delayed host responses against viral infection are attributed to the suppression of type I IFNs, suggesting that viral inhibition of IFN response may cause the unsatisfactory efficacy of certain vaccines. Thus, future vaccines should stimulate both innate and adaptive immune response. A large body of evidence demonstrates the importance of type I IFNs not only for innate immunity and antiviral function but also for the development of adaptive immunity. Murine norovirus infection in mice, of which type I IFN receptors are deficient, transforms an acute infection into a systemically persistent infection (121). Nevertheless, CD8+ T cell and antibody responses are still enhanced during persistent norovirus infection, suggesting that the deficiency of IFNs leads to viral persistence despite enhanced adaptive immunity (121). Many viruses suppressing the IFN response are known to cause insufficient protection upon vaccination, which makes many vaccines less effective (122).

4.1 IFNs as vaccine adjuvants

The potential of IFNs as vaccine adjuvants have been studied by many investigators. The results demonstrate that IFNs play a critical role in generating immune responses to vaccines. IFN treatment is the most effective therapy for controlling persistent hepatitis C virus infection (123–125). IFN-β is helpful for cancer vaccines that induce a greater expansion of tumor-specific CD8+ T cells (126). IFNs have been used as adjuvants coupled with veterinary vaccines. Replicating PRRSVs expressing various types of IFN increased the IFN levels in pigs and conferred protection against PRRSV challenges (127, 128). Recombinant porcine IFN (PoIFNα), used as an adjuvant in PRRSV vaccination, induces adaptive immune response in pigs (129). In other studies, PoIFNα, in combination with inactivated swine influenza virus, significantly upregulated the expression of various immunoregulatory cytokines and higher levels of HA-specific antibodies in 6-week-old pigs (130). Indeed,

type I IFNs is a potent adjuvant for influenza vaccines to induce an effective humoral response in mice (131, 132). PoIFNα coupled with a foot-and-mouth disease virus (FMDV) protein vaccine generated more robust immunogenicity and complete protection of pigs from virulent challenge (133). In other FMDV studies, IFNα was endogenously expressed in mice using an adenovirus vector, which improved the generation of T helper cells and the production of all classes of IgG immunoglobulins, especially IgG1 and IgG2a subtypes (134, 135). Endogenous IFNα expressed using a plasmid linked to the equine encephalitis virus (EEV) vaccine showed protection after being administered 24 hours before the challenge (136, 137). This result highlights that up to 24 hours is required to develop the IFN-mediated antiviral response. An IFN inducer coupled with a non-replicating vaccine for the rabies virus provided better protection in rhesus monkeys than the vaccine alone (138).

Taken together, such studies provide insights into the potential application of IFNs as an adjuvant for improving vaccine efficacy. Moreover, reprogramming the viral IFN evasion strategy has allowed the conceptual development of new vaccine designs. The approaches have proven useful in enhancing IFN response during vaccination and improving innate and adaptive immunities. Live attenuated vaccines are generally preferred in veterinary medicine and are considered more protective than inactivated vaccines. Live attenuated vaccines elicit both humoral and cellular immunities, whereas inactivated vaccines induce mainly antibody response. Removing IFN antagonism from viruses has been a strategy for developing both human and veterinary vaccines to achieve better immunogenicity and improved protection. In this article, however, we limit our discussions to only viruses that have been examined in the natural host animals, excluding human trials, as potential vaccine candidates against viral infections in animals.

4.2 Picornaviridae

4.2.1 Foot-and-mouth disease virus

FMDV is the prototype member of the *Aphthovirus* genus in the *Picornaviridae* family. FMDV is a highly contagious disease of cloven-hoofed animals in many livestock-producing countries worldwide. Despite the importance of the disease, difficulties in inducing and maintaining an adequate immune response in vaccinated animals have been an issue in controlling FMDV infection. FMDV can suppress the type I IFN response and persists in the tonsils of infected animals for up to 2 years (139). Among the viral proteins, the leader protein L^{pro} stands out as the most effective IFN suppressor of FMDV (Figure 1) (48–51). L^{pro} of FMDV is also a deubiquitinase (DUB) and deISGylase and interacts with ISG15 to induce its degradation (140). The FMDV mutant with modified deISGylase activity showed viral attenuation in mice (141). Deletion of L^{pro} from FMDV resulted in a slightly slower growth than wild-type virus in cells and was attenuated in mice (142). Therefore, L^{pro} is the target of the attenuated vaccine design for FMDV in natural host animal species. After removing the IFN suppression function from L^{pro}, the IFN suppression-negative FMDV induces higher levels of IFNs and ISGs with a robust neutralizing antibody response in vaccinated pigs (143, 144). Furthermore, pigs were completely protected from the high dose challenges of wild-type virus (143). Besides swine, the virulence of FMDV with L^{pro} mutation was investigated in bovine (145). In this study, a 57 nucleotide in-frame insertion was made in the region between two functional AUG initiation codons of L^{pro}. Both wild-type and insertional L^{pro} mutant viruses established primary infection in the nasopharyngeal mucosa with subsequent dissemination to the lungs of the cattle. Insertional L^{pro} mutant FMDV, however, replicated slower and showed quantitatively lower viral loads in secretions and infected tissues and reduced clinical disease, indicating the L^{pro} mutant FMDV was attenuated in cattle. In another study, a recombinant FMDV was generated to completely delete the L^{pro} gene. The L^{pro}-deficient FMDV provided 100% protection in cattle from challenges with wild-type virus (146), demonstrating the potential use of L^{pro} mutants in developing live attenuated vaccines for FMD.

4.3 Togaviridae

4.3.1 Sindbis virus

Alphavirus is the sole genus of the family *Togaviridae*, consisting of a group of positive-sense, single-stranded RNA viruses. Sindbis virus and Ross River virus are prototype viruses in the Alphavirus genus. Sindbis virus is one of the most widely distributed mosquito-borne viruses and is constantly found in insects and vertebrates. Sindbis virus infection causes polyarthritis, rash, and fever, although most infections are asymptomatic. It has been used as a model virus to study the molecular biology of togaviruses. The major virulence factor of the Sindbis virus is nsp1, which takes part in the inhibition of JAK-STAT signaling (Figure 1) (147). The neurovirulent strain AR86 inhibits tyrosine phosphorylation of STAT1 and STAT2, whereas two other closely-related strains, Girdwood and TR339, do not cause significant disease in adult mice and inhibit the JAK-STAT signaling pathway relatively inefficiently (147). Further, threonine at position 538 in the nsp1 protein of strain AR86 was identified as required for efficient disruption of STAT1 activation, while introducing threonine at position 538 to the Girdwood strain fully restored the ability to inhibit the JAK-STAT signaling and virulence in mice (147–149). A similar pathogenic effect has been demonstrated for the Ross River virus, a distantly related alphavirus, indicating that nsp1-mediated IFN suppression function can be removed from alphaviruses, and live-attenuated vaccine candidates can be developed (150–152).

4.4 Flaviviridae

4.4.1 West Nile virus and Zika virus

Flaviviruses are vector-borne viruses transmitted by arthropods. Flaviviruses cause a tremendous disease burden for humans and animals, causing millions of human infections annually. West Nile virus (WNV) can cause acute encephalitis and high morbidity

especially in horses and birds. The flaviviruses suppress host innate immune responses during infection, and the viral protein NS5 functions as an IFN antagonist by inhibiting the JAK-STAT signaling pathway (Figure 1) (64). NS5 inhibits IFN-dependent STAT1 phosphorylation or STAT2 degradation (153, 154). Kunjin virus is a naturally attenuated subtype of WNV. The molecular analyses of the Kunjin virus have identified serine 653 in NS5 as a potent amino acid residue that participates in viral attenuation and IFN modulation (154). After changing the amino acid residue S653 of NS5 to F653, the Kunjin virus restored the ability to downregulate JAK-STAT signaling. Similarly, the amino acid change from phenylalanine to serine in NS5 of the virulent strain of WNV resulted in the loss of the ability to inhibit the JAK-STAT signaling (154). In a mouse model, highly virulent WNV and WNV-like African Koutango virus infections produced severe neurological disease and higher morbidity. In addition, the enhanced virulence of WNV was associated with poor viral clearance and poor induction of neutralizing antibodies (155). Analogous to WNV, the virulence of the ZIKV results from the degradation of STAT2 mediated by NS5 (65). However, the IFN degradation by ZIKV NS5 is host species-restricted and functional for human and nonhuman primate but not for mouse (65). Like ZIKV, DENV NS5 does not antagonize IFN signaling in mice since the DENV NS5 protein does not bind to murine STAT2 (Figure 1) (66). Hence, the inability of the NS5 protein to bind to murine STAT2 induces IFN to greatly limit DENV replication in mice (66). Such studies highlight the importance of NS5 as a virulence factor and a target for constructing live attenuated flavivirus vaccines.

4.5 Paramyxoviridae

4.5.1 Bovine respiratory syncytial virus

Paramyxoviruses constitute a group of negative-sense, single-stranded, non-segmented RNA viruses. Bovine respiratory syncytial virus (BRSV) is classified in the Orthopneumovirus genus of the Paramyxoviridae family. BRSV is a significant cause of respiratory disease in cattle and a major contributor to the bovine respiratory disease (BRD) complex (156). Cattle vaccinated with the formalin-inactivated virus show enhanced severity when infected post-vaccination, suggesting the need for alternative BRSV vaccines (157). The genome of RSV codes for ten genes. NS1 and NS2 proteins have been identified as viral antagonists for the IFN system of hosts (67–70) (Figure 1). Various strategies using reverse genetics to remove viral IFN antagonists are being considered to generate attenuated BRSV vaccines (71). BRSV was engineered to delete the NS1 or NS2 gene, and the NS1 or NS2 gene-lacking BRSV induced higher levels IFNs than wild-type BRSV in bovine nasal fibroblasts and bronchoalveolar macrophages of immunized cattle (157). Furthermore, the recombinant BRSV was attenuated in IFN-competent cells *in vitro* and in calves, demonstrating that the NS1 and NS2 proteins are the critical determinants for the virulence of BRSV virulence. Recombinant BRSV lacking either NS1 or NS2 also induced higher BRSV-specific antibody titers in calves and greater priming of BRSV-specific, IFN-gamma-producing CD4(+) T cells for the protection against challenges with virulent BRSV (157). This finding delivers a prospect for developing a live attenuated BRSV vaccine.

The IFN antagonism has also been studied for human RSV as well. Recombinant human RSV with the NS2 deletion was highly attenuated in the lower respiratory tract in chimpanzees and induced significant resistance to challenges with wild-type RSV (71, 72) (Figure 1). These findings demonstrate that the deletion of an IFN antagonist from RSV is clinically attenuated and may provide increased protective immunity. However, controversial findings were reported in African green monkeys after evaluation of a series of recombinant human RSV. RSV with the NS2 deletion was not attenuated, whereas RSV with a double deletion of both NS1 and NS2 was over-attenuated and did not provide sufficient protection against wild-type RSV challenge (158). However, recombinant RSV with a double-deletion of M2-2 and NS2 exhibited attenuation and protection in monkeys. Despite the conflicting data, the results implicate the potential of IFN-deficient RSV as a live attenuated vaccine candidate (158, 159). The vaccine potential of IFN-suppression-deficient RSVs was further supported by the assessment in children (160–162). RSV/ΔNS2/Δ1313/I1314L contains three attenuating elements: deletion of the NS2 gene, deletion of codon 1313 in the RSV polymerase gene, and stabilizing missense mutation of I1314L in the polymerase. This triple mutant RSV was evaluated in RSV-seronegative children and shown to be restricted in replication but immunogenic and primed for potent antibody responses after natural exposure to wild-type RSV (161, 162). Taken together, the deletion of the NS2 gene leads to attenuation and immunogenicity of RSV. It validates the strategy to develop live attenuated vaccines by deleting the IFN-modulating function from RSV using reverse genetics.

4.5.2 Measles virus

The measles virus (MeV) in the *Morbillivirus* genus is a highly immunotropic pathogen that can cause significant childhood morbidity and mortality worldwide. MeV infection induces immunosuppression in the host contributing to secondary infections and mortality (163). The MeV P gene codes for three proteins by mRNA editing; P as an essential polymerase cofactor, and V and C that function as viral antagonists of the IFN pathways (164, 165). The V protein is a multi-functional protein inhibiting IFN responses (Figure 1). The V protein interferes with IFN signaling by blocking STAT1/STAT2 nuclear translocation (53–56). In addition, it inactivates STAT1 and Tyk2 phosphorylation (57) and blocks the JAK1 function for IFN suppression (58, 59). The V protein also interacts with MDA5 and the RIG-I/TRIM25 regulatory complex in the IFN production pathway and inhibits downstream signaling (166–168). Besides the V protein, the C protein has also been determined to interfere with IFN transcription.

Furthermore, the nuclear localization signal and efficient nuclear accumulation are critical for the C protein to downregulate IFN-β production (Figure 1). Compared to the wild-type virus, a mutation in the nuclear localization signal of the C protein is a marker common to all vaccine strains of MeV (169). Amino acids essential for preventing STAT1 nuclear translocation were examined in the V and P proteins by

screening the sequence of recombinant virus that could not antagonize STAT1 function, and three residues were identified in the shared domain of the P and V proteins; Y110, V112, and H115, with the Y110 being the most critical residue (164). A mutant virus was generated to harbor the three mutations and was used to assess the virulence in rhesus monkeys (170, 171). The inoculated monkeys showed a short duration of viremia and the absence of skin rash and other clinical signs observed with wild-type virus. This triple-amino acids mutant virus controlled the inflammatory response less efficiently, as measured by enhanced transcription of interleukin-6 and TNF-α in peripheral blood mononuclear cells from infected hosts. However, neutralizing antibody titers and virus-specific T-cell responses were equivalent in animals infected with either virus (172). These findings indicate that efficient MeV interactions with STAT1 are required to sustain virulence in a natural host by controlling the inflammatory response against the virus. Overall, these findings suggest that IFN-suppression defective MeV may have the potential as the vaccine for immunocompromised individuals.

4.5.3 Nipah virus

Nipah virus is an emerging zoonotic pathogen, causing encephalitis and respiratory illness in humans and pigs. It belongs to the *Henipavirus* genus of the family *Paramyxoviridae*. Similar to MeV, the P gene of the Nipah virus codes for four proteins by mRNA editing; phosphoprotein P and three accessory proteins W, V, and C (173). These proteins possess a distinct IFN-antagonist activity, including the W protein acting as the inhibitor of the TLR-3 pathway, whereas proteins V and C function on the IFN signaling by interacting with STAT1/STAT2 (102, 174–177). However, the recombinant Nipah virus lacking the V, C or W protein still suppressed the IFN response as with the wild-type virus, indicating that the lack of each accessory protein does not significantly affect the inhibition of IFN signaling (174). Ferret challenge studies using a recombinant Nipha virus with deletion of the STAT1-binding motif also demonstrated the minor role of P, V, and W proteins in inhibiting IFN signaling (178, 179).

4.6 Orthomyxoviridae

4.6.1 Human influenza virus

Influenza viruses belong to the family *Orthomyxoviridae* and contain single-stranded, negative-sense, eight segmented RNAs as the genome. Of seven genera of the family, influenza A and B viruses are of concern since they are frequently associated with respiratory disease in humans and animals. Two main subtypes are circulating in human population; H1N1 and H3N2. Of eight segments of the genomic RNA, segment 8 expresses two distinct proteins, nonstructural protein 1 (NS1) and nuclear export protein (NEP; also called NS2), using different reading frames from the same RNA segment. While NEP mediates the nuclear export of virion RNAs by acting as an adaptor between viral RNP complexes and the nuclear export machinery of the cell, NS1 is the viral antagonist for the IFN response of hosts (76, 180) (Figure 1). Influenza virus NS1 protein directly inhibits the production of IFNs by targeting RIG-I (180). In addition, the NS1 protein upregulates the inhibitors of JAK-STAT signaling and the suppressors of cytokine signaling (SOCS) family 1 and SOCS family 3 (76, 181), resulting in the downregulation of antiviral protein expression. NS1 protein also indirectly inhibits the IFN signal pathway and interacts with ISGs to antagonize the host's antiviral response (180). Based on such information, influenza viruses were engineered to modify the NS1 functions. The NS1-modified viruses appeared clinically attenuated and retained the immunogenicity in various species of animals, including mice (182–185), pigs (186–188), horses (189, 190), poultry (191–194), macaques (195) as well as in humans (196–198). Influenza A virus containing a partial deletion in the NS1 gene provides solid evidence for clinical attenuation in animals while providing protective immunity against virulent challenges with the wild-type virus (199). Influenza virus A/WSN/33 (H1N1) expressing the mutant NS1 R38A/K41A showed a robust reduction of viral titers in the lungs of mice but triggered high levels of IFN-α/β production in the lung tissues (200). In addition, the NS1 R38A/K41A NS1 mutant virus induced high titers of neutralizing antibodies against heterologous influenza A virus and provided 100% protection in a mouse model against wild-type virus (200). Immunization of mice with the H1N1 influenza virus containing a shortened NS1 gene also showed the enhancement of influenza-specific CD8+ T-cellular response in the lungs and the reduction of proinflammatory cytokines with a lower extent of leukocyte infiltration after heterologous challenges, indicating that NS1-truncated influenza virus modifies not only effector T-cells but also specific immunoregulatory mechanisms (185). Influenza B viruses with NS1 mutations were also attenuated in animals while inducing adequate protection against both homologous and heterologous subtype challenges with influenza B viruses in BALB/c and C57BL/6 PKR(-/-) mice (201). Furthermore, the influenza B viruses with a truncated NS1 gene induced comparable cellular and humoral immune responses in both aged and young mice (202). It should be noted that most inbred mouse strains have deletions or point mutations in ISG Mx1 (203) which is an important antiviral factor in influenza virus infection. Therefore, using mice as a model to study IFN-influenza virus interaction should be of concern. Taken all together, these data demonstrated that the IFN-deficient system is applicable for manufacturing the IFN-sensitive influenza vaccine viruses.

4.6.2 Swine influenza virus

Similar studies have been conducted for the swine influenza virus (SIV). Swine influenza is caused by the type A virus and regularly causes outbreaks in pigs. Swine influenza can cause high levels of illness in pig herds, but the mortality is low. Influenza viruses that circulate in swine are very different from influenza viruses circulating in people. Swine influenza viruses change genetically constantly. Pigs can be infected by avian influenza, human influenza, and swine influenza viruses. During the coinfection of pigs with influenza viruses from different species, the viruses can reassort, and new viruses can emerge as a mix of swine, human, and avian influenza viruses. Three main subtypes of influenza A virus have been isolated in pigs in the U.S.; H1N1, H3N2, and H1N2. Inactivated vaccines are less effective in

protecting pigs, and thus, live-attenuated vaccines have been licensed and available in the U.S (204).. The SIV strain A/Swine/Texas/4199-2/98 (TX/98) H3N2 was used to investigate the role of NS1 protein for virulence, and the swine influenza virus NS1 mutants were shown to be attenuated in pigs (186, 187). Immunization of pigs with SIV NS1 mutant *via* the intranasal route provided complete protection against homologous and antigenically variant heterologous challenges (205, 206). Moreover, H3N2 NS1 mutant SIV-inoculated pigs displayed attenuated clinical symptoms and reduced viral titers despite a minor reduction in lung lesions when challenged with H1N1 heterosubtype SIV (205). A chimeric virus between the bat influenza virus and SIV was constructed to express a truncated NS1 protein. This virus induced remarkably higher levels of mucosal IgA response and antigen-specific IFN-γ secreting cells against the challenge virus in the lungs of immunized pigs (207).

4.6.3 Avian influenza virus

The protective role of type I IFNs has also been studied for avian influenza virus in chickens. Avian influenza viruses continually circulate among wild birds and poultry worldwide, and the control of emerging influenza viruses for pandemic threats requires broadly protective vaccines. Influenza viruses with truncations in NS1 protein have shown broad-spectrum protection in birds and mammals, which has been correlated with the elevated IFN responses in vaccinated animals (208, 209). Immunologically improved strains of the avian influenza virus were identified by screening the subpopulation of viral vaccines (194). These strains appeared to have a small deletion in the NS1 protein or a single amino acid substitution in the polymerase 2 (PB2). These naturally occurring mutant viruses exhibited enhanced IFN-inducing phenotypes and protective immunity in chickens (194). Compared to an inactivated avian influenza vaccine, live-replicating NS1 mutant-avian influenza virus induced a more solid innate and highly cross-reactive serum antibody responses in immunologically immature chicken (210). Another study using H5N3 NS1 mutant virus also displayed similar levels of protection higher induction of IFN-β (211). However, the mutant virus reverted to wild-type phenotype within five back-passages in chickens, raising a concern about the stability of the NS1 mutant avian influenza vaccine (211). Taken all together, influenza viruses containing a truncated NS1 gene can boost a higher level of IFNs and adaptive immunity and confers protection from heterologous challenges in different species of animals. Such findings demonstrate that IFN-suppression negative mutant virus can be reprogramed to divert to an alternative vaccine candidate for veterinary diseases.

4.7 Coronaviridae

4.7.1 Porcine epidemic diarrhea virus

Coronaviruses (CoVs) infect humans and animals, causing a variety of diseases with varying severity. Emerging and reemerging CoVs include porcine epidemic diarrhea virus (PEDV), porcine delta-coronavirus (PDCoV), Middle East respiratory syndrome coronavirus (MERS-CoV), swine acute diarrhea syndrome coronavirus, canine-like alphacoronavirus, SARS-CoV-1, and SARS-CoV-2 (212, 213). CoVs are divided into four genera; Alpha-CoV, Beta-CoV, Gamma-CoV, and Delta-CoV. Among these, only alpha-CoVs and beta-CoVs harbor nonstructural protein 1 (nsp1), which inhibits antiviral host responses. The IFN antagonistic function has been removed from the Alpha-CoV transmissible gastroenteritis virus (TGEV) and PEDV and examined for the effect of IFN suppression on viral pathogenesis in pigs. A recombinant TGEV was constructed to alter the specific C-terminal motif of nsp1, based on the crystal structure. The nsp1 mutation did not affect viral replication in cells but significantly reduced clinical outcome and pathogenicity in pigs (214). PEDV is also a significant veterinary pathogen in swine that requires a better vaccine for control. PEDV infection results in enormous economic losses to the pork industry worldwide and has emerged in the U.S. in 2014. Multiple proteins of PEDV have been shown to inhibit IFN responses during infection (214–219). The nsp1 protein of PEDV is the most potent viral IFN antagonist (214), and three residues of F44, N93, and N95 of nsp1 are critical for both type I and type III IFN suppression (52, 220). PEDV nsp1 suppressed both types of IFN responses by interrupting the IRF3 and CREB-binding protein association and suppressing transcription factors (52) (Figure 1). A replication-competent PEDV mutant with an IFN inactive version of nsp1 induced IFN response in IFN-responsive cells (52). It was further demonstrated that PEDV carrying the nsp1 N93/95A mutation triggered a significantly higher level of IFN response and induced 100% protection from severe diarrhea and death in neonatal piglets post-challenge (220). These findings suggest that nsp1 is an essential virulence determinant for CoVs, providing a potential paradigm for the development of a new vaccine based on IFN modification.

Nonstructural protein 15 (nsp15) of PEDV is the viral endoribonuclease (EndoU) and has an additional function as the IFN antagonist. For PEDV nsp15, three residues of H226, H241, and K282 were identified as critical amino acids for endoribonuclease activity. PEDV nsp15 can directly degrade the RNA levels of TBK1 and IRF3 and suppress the production of IFNs and ISGs, demonstrating that PEDV antagonizes host's innate response to facilitate its replication (Figure 1). The endoribonuclease activity was removed from PEDV. The nsp15-modified PEDV reduced IFN antagonism with enhanced production of both type I and type III IFNs in cells and was clinically attenuated in infected piglets (216).

Nonstructural protein 16 (nsp16) of CoVs is 2'-*O*-methyltransferase (2'-*O*-MTase), and the nsp16 protein of PEDV also contains the methyltransferase. The methyltransferase activity was removed from nsp16 of PEDV. The nsp16 mutant PEDV increased type I IFN production in pigs and conferred complete protection following virulent PEDV challenge (221). Furthermore, infection with the inactive version of nsp1, nsp15, and nsp16 induced total and neutralizing antibody responses, and upon challenge with wild-type PEDV, no detectable clinical symptoms were observed in pigs (52). The pathogenic significance of 2'-*O*-MTase was also studied for SARS-CoV-1 and MERS-CoV. Both viruses with the nsp16 mutation resulted in IFN-based virulence attenuation and conferred the protection of mice from parental virus challenges (222, 223).

4.7.2 Mouse hepatitis virus

Among animal CoVs, mouse hepatitis virus (MHV) has extensively been investigated (212). MHV is a beta-CoV and has been a research model to understand CoV genome replication, transcription, and pathogenesis. Studies showed that removal of IFN antagonism yielded stronger immunity to MHV. The nsp14 protein of MHV is a multifunctional protein with the N7-methyltransferase (N7-MTase) activity and is highly conserved among different CoVs. A N7-MTase-deficient recombinant MHV was constructed by replacing aspartic acid at position 330 and tyrosine at position 414 of nsp14, each with alanine (224). The N7-MTase-deficient MHV was highly attenuated in mice and showed delayed IFN production *in vivo*. Furthermore, this nsp14 mutant MHV induced an improved and long-term humoral immune responses and conferred complete protection against a lethal-dose of MHV (224). This study demonstrates the potential application of IFN antagonism to the design of live attenuated vaccines against CoVs circulating in humans and animals.

4.8 Arteriviridae

4.8.1 Porcine reproductive and respiratory syndrome virus

Arteriviruses in the order *Nidovirales* infect a diverse species of mammals, including horses, pigs, possums, primates, and rodents (225). Arteriviruses have positive-sense, single-stranded RNA genomes and produce enveloped spherical particles. Porcine reproductive and respiratory syndrome virus (PRRSV) has evolved to carry various strategies for type I IFN antagonism and to evade host immune response. In PRRSV-infected pigs, the IFN response is meager and remains low in the lungs where the virus actively replicates (226, 227). In controlling PRRSV infection in pigs, viral suppression of innate immunity, delayed response of the adaptive immunity, and antigenic heterogeneity of PRRSV are the keys (228). Studies attempted to express various types of IFNs using PRRSV as a vector. IFN-expressing PRRSV increased the IFN levels in pigs after immunization and enhanced the protection against the secondary PRRSV challenge (127, 128). The porcine IFN-α-expressing plasmid as an adjuvant for PRRSV vaccines also induced a prolonged adaptive immune response in pigs (129). Instead of exogenous administration of IFNs, endogenous expression of IFNs seems to be a better way to enhance adaptive immunity. Indeed, a PRRSV strain of IFN-inducing phenotype PRRSV has been shown to improve the neutralizing antibody production (229).

The nsp1β protein of PRRSV is a potent IFN antagonist inhibiting both types I IFN production and downstream signaling (60–63) (Figure 1). Mutant PRRSVs were generated to remove IFN-suppression function from nsp1β, and pigs infected with nsp1β-mutant PRRSVs induced higher levels of IFN-α and ISGs (230, 231). The NK cell function and the IFN-γ level were increased in the lungs of pigs infected with the nsp1β mutant virus (230). Moreover, pigs inoculated with a nsp1β-mutant PRRSV exhibited shorter duration and lower titers of viremia, and a more robust PRRSV-specific antibody response. The neutralizing antibody titers were also higher than those of control pigs, indicating that the IFN-suppression-negative PRRSV mutants are clinically attenuated (231). These studies demonstrate the role of type I IFNs in priming the adaptive immune response in pigs and provide evidence that IFN antagonism-deficient PRRSV may be developed as a new vaccine candidate. Removing IFN antagonism from the virus is a reasonable strategy for developing next-generation vaccines.

4.8.2 Equine arteritis virus

Evidence is available for another arterivirus, the equine arteritis virus (EAV), for the removal of type I IFNs in developing adaptive immunity and viral clearance. The nsp2 protein of EAV contains DUB activity and is responsible for the viral suppression of innate immunity (232). Thus, a DUB-negative mutant EAV was constructed. Vaccination of horses with the DUB-negative mutant virus induced higher levels of IFNs and adaptive immune responses (233). Taken together, the removal of IFN antagonism is an important strategy for developing novel vaccines for arteriviruses.

5 Viral antagonist for NF-κB and as a potential target for attenuated vaccine development

NF-κB is a transcription factor and functions as a hub of complex signaling networks in the cell. NF-κB signaling contributes to immunity, inflammation, cell growth, development, cancer, and other cellular processes. The NF-κB pathway links pathogen and cellular signals and organizes cell resistance to invading pathogens. Many viruses have developed distinct mechanisms to suppress or activate the NF-κB signaling pathway to promote virus replication or cell proliferation (234). Virus-induced NF-κB activation is linked to overproduction and uncontrolled release of proinflammatory markers resulting in a "cytokine storm". SARS-CoV-2 activates the NF-κB signaling pathway and causes cytokine storm-like acute respiratory distress syndrome (235, 236). Targeting the NF-κB pathway has been considered a potential treatment for COVID-19 patients (236). The influenza virus can also activate NF-κB signaling and induces cytokine storm-like symptoms in infected hosts (237). Activation of NF-κB and production of proinflammatory cytokines are often synergistic during coinfection. Studies using PRRSV in pigs show that the virus can activate NF-κB signaling and elevate proinflammatory cytokine production when coinfected with Streptococcus suis. The cytokine storm-like production of inflammatory cytokines results in more severe clinical outcomes in coinfected animals (238). Thus, viral activation of NF-κB signaling and a cytokine storm-like event are additional concerns for attenuated viral vaccines. A study showed that the reduction of systemic inflammation and a boost of protective responses when combining an NF-κB inhibitor as an adjuvant with a vaccine in the influenza mice challenge model (239). Since the NF-κB signaling contributes to numerous cellular processes, potential off-target effects by NF-κB inhibition may be actuated and cause a systematically undesirable consequence. Thus, further research is required for developing NF-κB-activation-negative viruses as

feasible live-attenuated vaccines. Nevertheless, by the fine-tuning removal of the NF-κB activation, a newly generated virus is anticipated to relieve the clinical severity attributed to cytokine upregulations. By reprogramming the NF-κB activation, the newly generated virus is expected to relieve the clinical severity attributed to cytokine upregulation.

This concept is useful for pigs with PRRSV as a new approach to vaccine developments. For activation of NF-κB, the nucleocapsid (N) protein is the sole viral protein for PRRSV (240, 241). Studies show that the nuclear localization signal (NLS) in N is the essential domain for binding to PIAS1. PIAS1 is the negative regulator for NF-κB, so the binding of viral N protein to PIAS1 results in the release of p65 from PIAS1 and renders NF-κB activation (241). The NLS-modified N protein loses the ability for NF-κB activation and induces significantly lower levels of NF-κB-mediated inflammatory cytokines in cells (241). Studies using the NLS-null PRRSV infection show milder clinical signs and a shorter duration of viremia with higher titers of antibodies in infected pigs, demonstrating the association between the NLS motif of N protein and clinical attenuation of PRRSV infection (242–244). These studies provide evidence that NF-κB-activation-negative virus can induce milder clinical symptoms and higher humoral immune response than wild-type virus during coinfection of pigs. NF-κB activation function can be eliminated from RNA viruses using reverse genetics tools, and clinically attenuated vaccine candidates can be developed.

6 Conclusion

Numerous mechanisms for how viruses fight against the host immune system have been identified. Since type I IFNs are critical components of the host innate immunity and for the development and maturation of adaptive immunity, many attempts have been made to remove IFN suppression functions from different viruses. Such approaches may enhance the IFN response upon immunization. With the help of recent advances in molecular virology and reverse genetics technology, it is possible to construct mutant viruses of which phenotypes are IFN-suppression-deficient. Subsequently, IFN-suppression-negative viruses have shown to induce better immune responses and confer partial to complete protections from both homologous and heterologous challenges in the respective animal species, such as mice, pigs, chickens, and cattle (Table 1). Still remaining challenges include:

1) Identification of IFN-suppressive genes and active sites from target viruses: It requires an in-depth understanding of the

TABLE 1 The reprogramming of mutant viruses that their IFN evasion functions were eliminated by reverse genetics and the protective efficacies in natural host animal species following vaccination and virulent challenges.

Virus	Affected Animal Species	Disease and Risk	Viral IFN Antagonist	IFN Suppression Mechanism	Animal Vaccination	Protective Efficacy
FMDV	Cloven-hoofed animals	Blisters	L^{pro}	IRF3 ↓ ISG15 ↓	Mice (142) Pigs (143, 144) Cattle (145)	100% in pigs 100% in cattle
Sindbis virus	Mosquito, Avian	Rash-arthritis syndrome	Nsp1	JAK-STAT signaling ↓	Mice (147–149)	N/A
WNV	Mosquito, Avian	Encephalitis, Meningitis	NS5	STAT1 phosphorylation ↓	Mice (155)	N/A
BRSV	Bovine	Minimal to extreme respiratory diseases	NS1, NS2	JAK-STAT signaling ↓	Cattle (157)	↑ in cattle
RSV	Human, Primate	Bronchitis, Pneumonia	NS2	JAK-STAT signaling ↓	Chimpanzees (71, 72), Monkeys (158, 159)	↑ in chimpanzees No in monkeys
Measles virus	Human	Acute respiratory, Systemic illness	V	MDA5 and RIG-I/TRIM25 ↓ STATs nuclear translocation ↓ STAT1phosphorylation ↓ JAK1 function ↓	Rhesus monkeys (170, 171)	N/A
			C	IFN transcription ↓		
Nipah virus	Fruit Bat, Human	Acute respiratory, Encephalitis	W	TLR-3 pathway ↓	Ferrets (178, 179)	N/A
			V and C	STAT1/STAT2 ↓		
Influenza virus	Mammal, Avian	Respiratory	NS1	Targeting RIG-1 ↓ SOCS family ↑	Mice (182–185) Pigs (186–188, 205–207) Horses (189, 190)	100% in pigs ↑ in pigs ↑ in poultry

(Continued)

TABLE 1 Continued

Virus	Affected Animal Species	Disease and Risk	Viral IFN Antagonist	IFN Suppression Mechanism	Animal Vaccination	Protective Efficacy
					Poultry (191–194, 210) Macaques (195)	
PEDV	Swine	Enteritis in neonates	nsp1	IRF3 and CREB-binding protein ↓	Pigs (216, 220, 221)	100% in pigs
			nsp15	IRF3 ↓		
			nsp16	RIG-I and MDA5 ↓		
MHV	Murine	Enteritis, Neurologic, Hepatitis	nsp14	N/A	Mice (224)	100% in mice
PRRSV	Swine	Reproductive, Respiratory	nsp1β	ISGF3 nuclear translocation ↓ STAT1 phosphorylation ↓	Pigs (231)	↑ in pigs
EAV	Equine	Abortion, Respiratory	nsp2	ISG15 ↓	Horses (233)	↑ in horses

FMDV, foot-and-mouth disease virus; WNV, West Nile virus; BRSV, bovine respiratory syncytial virus; RSV, respiratory syncytial virus; PEDV, porcine epidemic diarrhea virus; MHV, mouse hepatitis virus; PRRSV, porcine reproductive and respiratory syndrome virus; EAV, equine arteritis virus.
↑ (up arrow) indicates "enhanced protection".
↓ (down arrow) indicates "down-regulation".
N/A indicates "Not available".

structure-function relationships of viral proteins and their role in the IFN signaling cascade.

2) Multigenic nature of viral IFN antagonists and introduction of multiple mutations: Viruses have evolved to equip with multiple proteins for IFN suppression such that their antagonism can be compensated even when one protein fails by evolutionary mutations. The strategy to overcome the multigenic nature of viral IFN antagonism is to introduce mutations to the most potent antagonist or simultaneous mutations to several antagonists.

3) Lethality of mutations for viral infectivity and viability: Many RNA viruses carry only a limited number of genes essential for replication and survival in a host. Deletion of a functional gene is often lethal for infectivity, and accurate measurements of the gene-wide mutations may be needed for the possible substitutions of amino acids and the removal of IFN antagonism.

4) Reversion of mutant viruses to virulence: RNA-dependent RNA polymerase lacks a proof-reading activity with an exception of coronaviruses that are found to contain an exonuclease as a proofreading enzyme. As a result, RNA viruses are prone to high rates of genetic mutations which may allow the reversion of IFN-negative attenuated viral mutants back to virulence. Deletion of the functional domain or amino acids instead of point mutations has been successful for some viruses to block their reversion to wild-type.

5) Over-attenuation of mutant viruses: Deletions or substitutions in a functional domain may confer over-attenuation of virus mutants. Continuous passages in cell culture have been attempted to increase viral titers. Cell culture passages in established lines may not provide immunological pressure but can allow viral adaptation for efficient replication and production of high viral titers.

The combination of research and new ideas will be vital in successfully developing future vaccines for veterinary diseases.

Author contributions

C-MS and DY contributed to developing concepts and design of the review article. C-MS performed the literature search, retrieved relevant articles, and prepared a draft of the original manuscript. C-MS and DY wrote the manuscript. YD, RR, and QW provided critical comments and revised the manuscript. All authors contributed to the article and approved the submitted version.

Funding

This project was supported by Agriculture and Food Research Initiative (AFRI) Competitive Grants nos. 2018-67015-28287 and 2023-67015-39710 from the U.S. Department of Agriculture (USDA) National Institute of Food and Agriculture (NIFA) to DY.

Conflict of interest

The authors declare that the research was conducted in the absence of any commercial or financial relationships that could be construed as a potential conflict of interest.

Publisher's note

References

1. Samuel CE. Antiviral actions of interferons. *Clin Microbiol Rev* (2001) 14:778–809. doi: 10.1128/CMR.14.4.778-809.2001

2. Katze MG, Fornek JL, Palermo RE, Walters K-A, Korth MJ. Innate immune modulation by RNA viruses: emerging insights from functional genomics. *Nat Rev Immunol* (2008) 8:644–54. doi: 10.1038/nri2377

3. Royer DJ, Carr MM, Chucair-Elliott AJ, Halford WP, Carr DJJ. Impact of type I interferon on the safety and immunogenicity of an experimental live-attenuated herpes simplex virus 1 vaccine in mice. *J Virol* (2017) 91:e02342–16. doi: 10.1128/JVI.02342-16

4. Ma Z, Li Z, Dong L, Yang T, Xiao S. Reverse genetic systems: rational design of coronavirus live attenuated vaccines with immune sequelae. *Adv Virus Res* (2020) 107:383–416. doi: 10.1016/bs.aivir.2020.06.003

5. Marsh G, Tannock G. The role of reverse genetics in the development of vaccines against respiratory viruses. *Expert Opin Biol Ther* (2005) 5:369–80. doi: 10.1517/14712598.5.3.369

6. Sadler AJ, Williams BRG. Interferon-inducible antiviral effectors. *Nat Rev Immunol* (2008) 8:559–68. doi: 10.1038/nri2314

7. Liu Y-J. IPC: professional type 1 interferon-producing cells and plasmacytoid dendritic cell precursors. *Annu Rev Immunol* (2005) 23:275–306. doi: 10.1146/annurev.immunol.23.021704.115633

8. Mogensen TH. Pathogen recognition and inflammatory signaling in innate immune defenses. *Clin Microbiol Rev* (2009) 22:240–73. doi: 10.1128/CMR.00046-08

9. Wu J, Chen ZJ. Innate immune sensing and signaling of cytosolic nucleic acids. *Annu Rev Immunol* (2014) 32:461–88. doi: 10.1146/annurev-immunol-032713-120156

10. Kawai T, Takahashi K, Sato S, Coban C, Kumar H, Kato H, et al. IPS-1, an adaptor triggering RIG-i- and Mda5-mediated type I interferon induction. *Nat Immunol* (2005) 6:981–8. doi: 10.1038/ni1243

11. Xu L-G, Wang Y-Y, Han K-J, Li L-Y, Zhai Z, Shu H-B. VISA is an adapter protein required for virus-triggered IFN-β signaling. *Mol Cell* (2005) 19:727–40. doi: 10.1016/j.molcel.2005.08.014

12. Akira S, Uematsu S, Takeuchi O. Pathogen recognition and innate immunity. *Cell* (2006) 124:783–801. doi: 10.1016/j.cell.2006.02.015

13. Lin R, Heylbroeck C, Pitha PM, Hiscott J. Virus-dependent phosphorylation of the IRF-3 transcription factor regulates nuclear translocation, transactivation potential, and proteasome-mediated degradation. *Mol Cell Biol* (1998) 18:2986–96. doi: 10.1128/MCB.18.5.2986

14. Dragan AI, Hargreaves VV, Makeyeva EN, Privalov PL. Mechanisms of activation of interferon regulator factor 3: the role of c-terminal domain phosphorylation in IRF-3 dimerization and DNA binding. *Nucleic Acids Res* (2007) 35:3525–34. doi: 10.1093/nar/gkm142

15. Honda K, Yanai H, Negishi H, Asagiri M, Sato M, Mizutani T, et al. IRF-7 is the master regulator of type-I interferon-dependent immune responses. *Nature* (2005) 434:772–7. doi: 10.1038/nature03464

16. Caamanão J, Hunter CA. NF-κB family of transcription factors: central regulators of innate and adaptive immune functions. *Clin Microbiol Rev* (2002) 15:414–29. doi: 10.1128/CMR.15.3.414-429.2002

17. Napetschnig J, Wu H. Molecular basis of NF-κB signaling. *Annu Rev Biophys* (2013) 42:443–68. doi: 10.1146/annurev-biophys-083012-130338

18. Baccala R, Hoebe K, Kono DH, Beutler B, Theofilopoulos AN. TLR-dependent and TLR-independent pathways of type I interferon induction in systemic autoimmunity. *Nat Med* (2007) 13:543–51. doi: 10.1038/nm1590

19. Schneider WM, Chevillotte MD, Rice CM. Interferon-stimulated genes: a complex web of host defenses. *Annu Rev Immunol* (2014) 32:513–45. doi: 10.1146/annurev-immunol-032713-120231

20. Ivashkiv LB, Donlin LT. Regulation of type I interferon responses. *Nat Rev Immunol* (2014) 14:36–49. doi: 10.1038/nri3581

21. Gessani S, Conti L, Del Cornò M, Belardelli F. Type I interferons as regulators of human antigen presenting cell functions. *Toxins (Basel)* (2014) 6:1696–723. doi: 10.3390/toxins6061696

22. Le Bon A, Etchart N, Rossmann C, Ashton M, Hou S, Gewert D, et al. Cross-priming of CD8+ T cells stimulated by virus-induced type I interferon. *Nat Immunol* (2003) 4:1009–15. doi: 10.1038/ni978

23. Spadaro F, Lapenta C, Donati S, Abalsamo L, Barnaba V, Belardelli F, et al. IFN-α enhances cross-presentation in human dendritic cells by modulating antigen survival, endocytic routing, and processing. *Blood* (2012) 119:1407–17. doi: 10.1182/blood-2011-06-363564

24. Baranek T, Vu Manh T-P, Alexandre Y, Maqbool MA, Cabeza JZ, Tomasello E, et al. Differential responses of immune cells to type I interferon contribute to host resistance to viral infection. *Cell Host Microbe* (2012) 12:571–84. doi: 10.1016/j.chom.2012.09.002

25. Paolini R, Bernardini G, Molfetta R, Santoni A. NK cells and interferons. *Cytokine Growth Fact Rev* (2015) 26:113–20. doi: 10.1016/j.cytogfr.2014.11.003

26. Fuertes MB, Woo S-R, Burnett B, Fu Y-X, Gajewski TF. Type I interferon response and innate immune sensing of cancer. *Trends Immunol* (2013) 34:67–73. doi: 10.1016/j.it.2012.10.004

27. Havenar-Daughton C, Kolumam GA, Murali-Krishna K. Cutting edge: the direct action of type I IFN on CD4 T cells is critical for sustaining clonal expansion in response to a viral but not a bacterial infection. *J Immunol* (2006) 176:3315–9. doi: 10.4049/jimmunol.176.6.3315

28. Le Bon A, Thompson C, Kamphuis E, Durand V, Rossmann C, Kalinke U, et al. Cutting edge: enhancement of antibody responses through direct stimulation of b and T cells by type I IFN. *J Immunol* (2006) 176:2074–8. doi: 10.4049/jimmunol.176.4.2074

29. Aichele P, Unsoeld H, Koschella M, Schweier O, Kalinke U, Vucikuja S. Cutting edge: CD8 T cells specific for lymphocytic choriomeningitis virus require type I IFN receptor for clonal expansion. *J Immunol* (2006) 176:4525–9. doi: 10.4049/jimmunol.176.8.4525

30. Curtsinger JM, Valenzuela JO, Agarwal P, Lins D, Mescher MF. Cutting edge: type I IFNs provide a third signal to CD8 T cells to stimulate clonal expansion and differentiation. *J Immunol* (2005) 174:4465–9. doi: 10.4049/jimmunol.174.8.4465

31. Kolumam GA, Thomas S, Thompson LJ, Sprent J, Murali-Krishna K. Type I interferons act directly on CD8 T cells to allow clonal expansion and memory formation in response to viral infection. *J Exp Med* (2005) 202:637–50. doi: 10.1084/jem.20050821

32. Urban SL, Berg LJ, Welsh RM. Type 1 interferon licenses naïve CD8 T cells to mediate anti-viral cytotoxicity. *Virology* (2016) 493:52–9. doi: 10.1016/j.virol.2016.03.005

33. Pinto AK, Daffis S, Brien JD, Gainey MD, Yokoyama WM, Sheehan KCF, et al. A temporal role of type I interferon signaling in CD8+ T cell maturation during acute West Nile virus infection. *PloS Pathog* (2011) 7:e1002407. doi: 10.1371/journal.ppat.1002407

34. Agarwal P, Raghavan A, Nandiwada SL, Curtsinger JM, Bohjanen PR, Mueller DL, et al. Gene regulation and chromatin remodeling by IL-12 and type I IFN in programming for CD8 T cell effector function and memory. *J Immunol* (2009) 183:1695–704. doi: 10.4049/jimmunol.0900592

35. Thompson LJ, Kolumam GA, Thomas S, Murali-Krishna K. Innate inflammatory signals induced by various pathogens differentially dictate the IFN-I dependence of CD8 T cells for clonal expansion and memory formation. *J Immunol* (2006) 177:1746–54. doi: 10.4049/jimmunol.177.3.1746

36. Bach P, Kamphuis E, Odermatt B, Sutter G, Buchholz CJ, Kalinke U. Vesicular stomatitis virus glycoprotein displaying retrovirus-like particles induce a type I IFN receptor-dependent switch to neutralizing IgG antibodies. *J Immunol* (2007) 178:5839–47. doi: 10.4049/jimmunol.178.9.5839

37. Fink K, Lang KS, Manjarrez-Orduno N, Junt T, Senn BM, Holdener M, et al. Early type I interferon-mediated signals on b cells specifically enhance antiviral humoral responses. *Eur J Immunol* (2006) 36:2094–105. doi: 10.1002/eji.200635993

38. Purtha WE, Chachu KA, Virgin HW, Diamond MS. Early b-cell activation after West Nile virus infection requires Alpha/Beta interferon but not antigen receptor signaling. *J Virol* (2008) 82:10964–74. doi: 10.1128/JVI.01646-08

39. Kiefer K, Oropallo MA, Cancro MP, Marshak-Rothstein A. Role of type I interferons in the activation of autoreactive b cells. *Immunol Cell Biol* (2012) 90:498–504. doi: 10.1038/icb.2012.10

40. Chen L-F, Greene WC. Shaping the nuclear action of NF-κB. *Nat Rev Mol Cell Biol* (2004) 5:392–401. doi: 10.1038/nrm1368

41. Vallabhapurapu S, Karin M. Regulation and function of NF-κB transcription factors in the immune system. *Annu Rev Immunol* (2009) 27:693–733. doi: 10.1146/annurev.immunol.021908.132641

42. Kagoya Y, Yoshimi A, Kataoka K, Nakagawa M, Kumano K, Arai S, et al. Positive feedback between NF-κB and TNF-α promotes leukemia-initiating cell capacity. *J Clin Invest* (2014) 124:528–42. doi: 10.1172/JCI68101

43. Liu B, Yang R, Wong KA, Getman C, Stein N, Teitell MA, et al. Negative regulation of NF-κB signaling by PIAS1. *Mol Cell Biol* (2005) 25:1113–23. doi: 10.1128/MCB.25.3.1113-1123.2005

44. Haeberle HA, Casola A, Gatalica Z, Petronella S, Dieterich H-J, Ernst PB, et al. IκB kinase is a critical regulator of chemokine expression and lung inflammation in respiratory syncytial virus infection. *J Virol* (2004) 78:2232–41. doi: 10.1128/JVI.78.5.2232-2241.2004

45. Tian B, Zhang Y, Luxon BA, Garofalo RP, Casola A, Sinha M, et al. Identification of NF-κB-Dependent gene networks in respiratory syncytial virus-infected cells. *J Virol* (2002) 76:6800–14. doi: 10.1128/JVI.76.13.6800-6814.2002

46. Xu Q, Tang Y, Huang G. Innate immune responses in RNA viral infection. *Front Med* (2021) 15:333–46. doi: 10.1007/s11684-020-0776-7

47. Bowie AG, Unterholzner L. Viral evasion and subversion of pattern-recognition receptor signalling. *Nat Rev Immunol* (2008) 8:911–22. doi: 10.1038/nri2436

48. Medina GN, Segundo FD-S, Stenfeldt C, Arzt J, de los Santos T. The different tactics of foot-and-Mouth disease virus to evade innate immunity. *Front Microbiol* (2018) 9:2644. doi: 10.3389/fmicb.2018.02644

49. Rodríguez Pulido M, Sáiz M. Molecular mechanisms of foot-and-Mouth disease virus targeting the host antiviral response. *Front Cell Infect Microbiol* (2017) 7:252. doi: 10.3389/fcimb.2017.00252

50. Peng J, Yi J, Yang W, Ren J, Wen Y, Zheng H, et al. Advances in foot-and-Mouth disease virus proteins regulating host innate immunity. *Front Microbiol* (2020) 11:2046. doi: 10.3389/fmicb.2020.02046

51. Sui C, Jiang D, Wu X, Liu S, Li F, Pan L, et al. Inhibition of antiviral innate immunity by foot-and-Mouth disease virus l pro through interaction with the n-terminal domain of swine RNase l. *J Virol* (2021) 95:e0036121. doi: 10.1128/JVI.00361-21

52. Deng X, Buckley AC, Pillatzki A, Lager KM, Faaberg KS, Baker SC. Inactivating three interferon antagonists attenuates pathogenesis of an enteric coronavirus. *J Virol* (2020) 94:e00565–20. doi: 10.1128/JVI.00565-20

53. Palosaari H, Parisien J-P, Rodriguez JJ, Ulane CM, Horvath CM. STAT protein interference and suppression of cytokine signal transduction by measles virus V protein. *J Virol* (2003) 77:7635–44. doi: 10.1128/JVI.77.13.7635-7644.2003

54. Ramachandran A, Parisien J-P, Horvath CM. STAT2 is a primary target for measles virus V protein-mediated Alpha/Beta interferon signaling inhibition. *J Virol* (2008) 82:8330–8. doi: 10.1128/JVI.00831-08

55. Caignard G, Bouraï M, Jacob Y, Tangy F, Vidalain P-O. Inhibition of IFN-α/β signaling by two discrete peptides within measles virus V protein that specifically bind STAT1 and STAT2. *Virology* (2009) 383:112–20. doi: 10.1016/j.virol.2008.10.014

56. Nagano Y, Sugiyama A, Kimoto M, Wakahara T, Noguchi Y, Jiang X, et al. The measles virus V protein binding site to STAT2 overlaps that of IRF9. *J Virol* (2020) 94:e01169-20. doi: 10.1128/JVI.01169-20

57. Chinnakannan SK, Nanda SK, Baron MD. Morbillivirus V proteins exhibit multiple mechanisms to block type 1 and type 2 interferon signalling pathways. *PloS One* (2013) 8:e57063. doi: 10.1371/journal.pone.0057063

58. Caignard G, Guerbois M, Labernardière J-L, Jacob Y, Jones LM, Wild F, et al. Measles virus V protein blocks Jak1-mediated phosphorylation of STAT1 to escape IFN-α/β signaling. *Virology* (2007) 368:351–62. doi: 10.1016/j.virol.2007.06.037

59. Yokota S, Saito H, Kubota T, Yokosawa N, Amano K, Fujii N. Measles virus suppresses interferon-α signaling pathway: suppression of Jak1 phosphorylation and association of viral accessory proteins, c and V, with interferon-α receptor complex. *Virology* (2003) 306:135–46. doi: 10.1016/S0042-6822(02)00026-0

60. Chen Z, Lawson S, Sun Z, Zhou X, Guan X, Christopher-Hennings J, et al. Identification of two auto-cleavage products of nonstructural protein 1 (nsp1) in porcine reproductive and respiratory syndrome virus infected cells: nsp1 function as interferon antagonist. *Virology* (2010) 398:87–97. doi: 10.1016/j.virol.2009.11.033

61. Patel D, Nan Y, Shen M, Ritthipichai K, Zhu X, Zhang Y-J. Porcine reproductive and respiratory syndrome virus inhibits type I interferon signaling by blocking STAT1/STAT2 nuclear translocation. *J Virol* (2010) 84:11045–55. doi: 10.1128/JVI.00655-10

62. Beura LK, Sarkar SN, Kwon B, Subramaniam S, Jones C, Pattnaik AK, et al. Porcine reproductive and respiratory syndrome virus nonstructural protein 1β modulates host innate immune response by antagonizing IRF3 activation. *J Virol* (2010) 84:1574–84. doi: 10.1128/JVI.01326-09

63. Wang R, Nan Y, Yu Y, Zhang Y-J. Porcine reproductive and respiratory syndrome virus Nsp1 inhibits interferon-activated JAK/STAT signal transduction by inducing karyopherin-1 degradation. *J Virol* (2013) 87:5219–28. doi: 10.1128/JVI.02643-12

64. Best SM. The many faces of the flavivirus NS5 protein in antagonism of type I interferon signaling. *J Virol* (2017) 91:e01970-16. doi: 10.1128/JVI.01970-16

65. Grant A, Ponia SS, Tripathi S, Balasubramaniam V, Miorin L, Sourisseau M, et al. Zika virus targets human STAT2 to inhibit type I interferon signaling. *Cell Host Microbe* (2016) 19:882–90. doi: 10.1016/j.chom.2016.05.009

66. Ashour J, Morrison J, Laurent-Rolle M, Belicha-Villanueva A, Plumlee CR, Bernal-Rubio D, et al. Mouse STAT2 restricts early dengue virus replication. *Cell Host Microbe* (2010) 8:410–21. doi: 10.1016/j.chom.2010.10.007

67. Ramaswamy M, Shi L, Monick MM, Hunninghake GW, Look DC. Specific inhibition of type I interferon signal transduction by respiratory syncytial virus. *Am J Respir Cell Mol Biol* (2004) 30:893–900. doi: 10.1165/rcmb.2003-0410OC

68. Spann KM, Tran K-C, Chi B, Rabin RL, Collins PL. Suppression of the induction of alpha, beta, and lambda interferons by the NS1 and NS2 proteins of human respiratory syncytial virus in human epithelial cells and macrophages. *J Virol* (2004) 78:6705–5. doi: 10.1128/JVI.78.12.6705.2004

69. Whelan JN, Tran KC, van Rossum DB, Teng MN. Identification of respiratory syncytial virus nonstructural protein 2 residues essential for exploitation of the host ubiquitin system and inhibition of innate immune responses. *J Virol* (2016) 90:6453–63. doi: 10.1128/JVI.00423-16

70. Yang P, Zheng J, Wang S, Liu P, Xie M, Zhao D. Respiratory syncytial virus nonstructural proteins 1 and 2 are crucial pathogenic factors that modulate interferon signaling and treg cell distribution in mice. *Virology* (2015) 485:223–32. doi: 10.1016/j.virol.2015.07.016

71. Collins PL. New generation live vaccines against human respiratory syncytial virus designed by reverse genetics. *Proc Am Thorac Soc* (2005) 2:166–73. doi: 10.1513/pats.200501-011AW

72. Whitehead SS, Bukreyev A, Teng MN, Firestone C-Y, St. Claire M, Elkins WR, et al. Recombinant respiratory syncytial virus bearing a deletion of either the NS2 or SH gene is attenuated in chimpanzees. *J Virol* (1999) 73:3438–42. doi: 10.1128/JVI.73.4.3438-3442.1999

73. Krug RM. Functions of the influenza a virus NS1 protein in antiviral defense. *Curr Opin Virol* (2015) 12:1–6. doi: 10.1016/j.coviro.2015.01.007

74. Min J-Y, Krug RM. The primary function of RNA binding by the influenza a virus NS1 protein in infected cells: inhibiting the 2′-5′ oligo (A) synthetase/RNase l pathway. *Proc Natl Acad Sci* (2006) 103:7100–5. doi: 10.1073/pnas.0602184103

75. Hale BG, Randall RE, Ortin J, Jackson D. The multifunctional NS1 protein of influenza a viruses. *J Gen Virol* (2008) 89:2359–76. doi: 10.1099/vir.0.2008/004606-0

76. Jia D, Rahbar R, Chan RWY, Lee SMY, Chan MCW, Wang BX, et al. Influenza virus non-structural protein 1 (NS1) disrupts interferon signaling. *PloS One* (2010) 5:e13927. doi: 10.1371/journal.pone.0013927

77. Shah KM, Stewart SE, Wei W, Woodman CBJ, O'Neil JD, Dawson CW, et al. The EBV-encoded latent membrane proteins, LMP2A and LMP2B, limit the actions of interferon by targeting interferon receptors for degradation. *Oncogene* (2009) 28:3903–14. doi: 10.1038/onc.2009.249

78. Luquin E, Larrea E, Civeira MP, Prieto J, Aldabe R. HCV structural proteins interfere with interferon-alpha Jak/STAT signalling pathway. *Antiviral Res* (2007) 76:194–7. doi: 10.1016/j.antiviral.2007.06.004

79. La Rocca SA, Herbert RJ, Crooke H, Drew TW, Wileman TE, Powell PP. Loss of interferon regulatory factor 3 in cells infected with classical swine fever virus involves the n-terminal protease, n pro. *J Virol* (2005) 79:7239–47. doi: 10.1128/JVI.79.11.7239-7247.2005

80. Baigent SJ, Zhang G, Fray MD, Flick-Smith H, Goodbourn S, McCauley JW. Inhibition of beta interferon transcription by noncytopathogenic bovine viral diarrhea virus is through an interferon regulatory factor 3-dependent mechanism. *J Virol* (2002) 76:8979–88. doi: 10.1128/JVI.76.18.8979-8988.2002

81. Gil LHVG, Ansari IH, Vassilev V, Liang D, Lai VCH, Zhong W, et al. The amino-terminal domain of bovine viral diarrhea virus n pro protein is necessary for Alpha/Beta interferon antagonism. *J Virol* (2006) 80:900–11. doi: 10.1128/JVI.80.2.900-911.2006

82. Brzoízka K, Finke S, Conzelmann K-K. Identification of the rabies virus Alpha/Beta interferon antagonist: phosphoprotein p interferes with phosphorylation of interferon regulatory factor 3. *J Virol* (2005) 79:7673–81. doi: 10.1128/JVI.79.12.7673-7681.2005

83. Prescott JB, Hall PR, Bondu-Hawkins VS, Ye C, Hjelle B. Early innate immune responses to sin nombre hantavirus occur independently of IFN regulatory factor 3, characterized pattern recognition receptors, and viral entry. *J Immunol* (2007) 179:1796–802. doi: 10.4049/jimmunol.179.3.1796

84. Alff PJ, Gavrilovskaya IN, Gorbunova E, Endriss K, Chong Y, Geimonen E, et al. The pathogenic NY-1 hantavirus G1 cytoplasmic tail inhibits RIG-i- and TBK-1-Directed interferon responses. *J Virol* (2006) 80:9676–86. doi: 10.1128/JVI.00508-06

85. Wathelet MG, Orr M, Frieman MB, Baric RS. Severe acute respiratory syndrome coronavirus evades antiviral signaling: role of nsp1 and rational design of an attenuated strain. *J Virol* (2007) 81:11620–33. doi: 10.1128/JVI.00702-07

86. Devaraj SG, Wang N, Chen Z, Chen Z, Tseng M, Barretto N, et al. Regulation of IRF-3-dependent innate immunity by the papain-like protease domain of the severe acute respiratory syndrome coronavirus. *J Biol Chem* (2007) 282:32208–21. doi: 10.1074/jbc.M704870200

87. Frieman M, Ratia K, Johnston RE, Mesecar AD, Baric RS. Severe acute respiratory syndrome coronavirus papain-like protease ubiquitin-like domain and catalytic domain regulate antagonism of IRF3 and NF-κB signaling. *J Virol* (2009) 83:6689–705. doi: 10.1128/JVI.02220-08

88. Yoo HS, Yoo D. COVID-19 and veterinarians for one health, zoonotic- and reverse-zoonotic transmissions. *J Vet Sci* (2020) 21:e51. doi: 10.4142/jvs.2020.21.e51

89. Moustaqil M, Ollivier E, Chiu H-P, Van Tol S, Rudolffi-Soto P, Stevens C, et al. SARS-CoV-2 proteases PLpro and 3CLpro cleave IRF3 and critical modulators of inflammatory pathways (NLRP12 and TAB1): implications for disease presentation

across species. *Emerg Microbes Infect* (2021) 10:178–95. doi: 10.1080/22221751.2020.1870414

90. Wang W, Zhou Z, Xiao X, Tian Z, Dong X, Wang C, et al. SARS-CoV-2 nsp12 attenuates type I interferon production by inhibiting IRF3 nuclear translocation. *Cell Mol Immunol* (2021) 18:945–53. doi: 10.1038/s41423-020-00619-y

91. Kouwaki T, Nishimura T, Wang G, Oshiumi H. RIG-I-Like receptor-mediated recognition of viral genomic RNA of severe acute respiratory syndrome coronavirus-2 and viral escape from the host innate immune responses. *Front Immunol* (2021) 12:700926. doi: 10.3389/fimmu.2021.700926

92. Sui L, Zhao Y, Wang W, Wu P, Wang Z, Yu Y, et al. SARS-CoV-2 membrane protein inhibits type I interferon production through ubiquitin-mediated degradation of TBK1. *Front Immunol* (2021) 12:662989. doi: 10.3389/fimmu.2021.662989

93. Freitas RS, Crum TF, Parvatiyar K. SARS-CoV-2 spike antagonizes innate antiviral immunity by targeting interferon regulatory factor 3. *Front Cell Infect Microbiol* (2022) 11:789462. doi: 10.3389/fcimb.2021.789462

94. Rose KM, Elliott R, Martiínez-Sobrido L, Garciía-Sastre A, Weiss SR. Murine coronavirus delays expression of a subset of interferon-stimulated genes. *J Virol* (2010) 84:5656–69. doi: 10.1128/JVI.00211-10

95. Han M, Du Y, Song C, Yoo D. Degradation of CREB-binding protein and modulation of type I interferon induction by the zinc finger motif of the porcine reproductive and respiratory syndrome virus nsp1α subunit. *Virus Res* (2013) 172:54–65. doi: 10.1016/j.virusres.2012.12.012

96. Kim O, Sun Y, Lai FW, Song C, Yoo D. Modulation of type I interferon induction by porcine reproductive and respiratory syndrome virus and degradation of CREB-binding protein by non-structural protein 1 in MARC-145 and HeLa cells. *Virology* (2010) 402:315–26. doi: 10.1016/j.virol.2010.03.039

97. Chen Z, Liu S, Sun W, Chen L, Yoo D, Li F, et al. Nuclear export signal of PRRSV NSP1α is necessary for type I IFN inhibition. *Virology* (2016) 499:278–87. doi: 10.1016/j.virol.2016.07.008

98. Song C, Krell P, Yoo D. Nonstructural protein 1α subunit-based inhibition of NF-κB activation and suppression of interferon-β production by porcine reproductive and respiratory syndrome virus. *Virology* (2010) 407:268–80. doi: 10.1016/j.virol.2010.08.025

99. Subramaniam S, Kwon B, Beura LK, Kuszynski CA, Pattnaik AK, Osorio FA. Porcine reproductive and respiratory syndrome virus non-structural protein 1 suppresses tumor necrosis factor-alpha promoter activation by inhibiting NF-κB and Sp1. *Virology* (2010) 406:270–9. doi: 10.1016/j.virol.2010.07.016

100. Ke H, Han M, Kim J, Gustin KE, Yoo D. Porcine reproductive and respiratory syndrome virus nonstructural protein 1 beta interacts with nucleoporin 62 to promote viral replication and immune evasion. *J Virol* (2019) 93:e00469–19. doi: 10.1128/JVI.00469-19

101. Gotoh B, Komatsu T, Takeuchi K, Yokoo J. Paramyxovirus strategies for evading the interferon response. *Rev Med Virol* (2002) 12:337–57. doi: 10.1002/rmv.357

102. Rodriguez JJ, Parisien J-P, Horvath CM. Nipah virus V protein evades alpha and gamma interferons by preventing STAT1 and STAT2 activation and nuclear accumulation. *J Virol* (2002) 76:11476–83. doi: 10.1128/JVI.76.22.11476-11483.2002

103. Rodriguez JJ, Wang L-F, Horvath CM. Hendra virus V protein inhibits interferon signaling by preventing STAT1 and STAT2 nuclear accumulation. *J Virol* (2003) 77:11842–5. doi: 10.1128/JVI.77.21.11842-11845.2003

104. Didcock L, Young DF, Goodbourn S, Randall RE. Sendai Virus and simian virus 5 block activation of interferon-responsive genes: importance for virus pathogenesis. *J Virol* (1999) 73:3125–33. doi: 10.1128/JVI.73.4.3125-3133.1999

105. Garcin D, Latorre P, Kolakofsky D. Sendai Virus c proteins counteract the interferon-mediated induction of an antiviral state. *J Virol* (1999) 73:6559–65. doi: 10.1128/JVI.73.8.6559-6565.1999

106. Garcin D, Marq J-B, Strahle L, le Mercier P, Kolakofsky D. All four Sendai virus c proteins bind Stat1, but only the larger forms also induce its mono-ubiquitination and degradation. *Virology* (2002) 295:256–65. doi: 10.1006/viro.2001.1342

107. Jones M, Davidson A, Hibbert L, Gruenwald P, Schlaak J, Ball S, et al. Dengue virus inhibits alpha interferon signaling by reducing STAT2 expression. *J Virol* (2005) 79:5414–20. doi: 10.1128/JVI.79.9.5414-5420.2005

108. Parisien J-P, Lau JF, Horvath CM. STAT2 acts as a host range determinant for species-specific paramyxovirus interferon antagonism and simian virus 5 replication. *J Virol* (2002) 76:6435–41. doi: 10.1128/JVI.76.13.6435-6441.2002

109. Le VTK, Trilling M, Wilborn M, Hengel H, Zimmermann A. Human cytomegalovirus interferes with signal transducer and activator of transcription (STAT) 2 protein stability and tyrosine phosphorylation. *J Gen Virol* (2008) 89:2416–26. doi: 10.1099/vir.0.2008/001669-0

110. Senft AP, Taylor RH, Lei W, Campbell SA, Tipper JL, Martinez MJ, et al. Respiratory syncytial virus impairs macrophage IFN-α/β– and IFN-γ–stimulated transcription by distinct mechanisms. *Am J Respir Cell Mol Biol* (2010) 42:404–14. doi: 10.1165/rcmb.2008-0229OC

111. Jie Z, Dinwiddie DL, Senft AP, Harrod KS. Regulation of STAT signaling in mouse bone marrow derived dendritic cells by respiratory syncytial virus. *Virus Res* (2011) 156:127–33. doi: 10.1016/j.virusres.2011.01.007

112. Ramaswamy M, Shi L, Varga SM, Barik S, Behlke MA, Look DC. Respiratory syncytial virus nonstructural protein 2 specifically inhibits type I interferon signal transduction. *Virology* (2006) 344:328–39. doi: 10.1016/j.virol.2005.09.009

113. Elliott J, Lynch OT, Suessmuth Y, Qian P, Boyd CR, Burrows JF, et al. Respiratory syncytial virus NS1 protein degrades STAT2 by using the elongin-cullin E3 ligase. *J Virol* (2007) 81:3428–36. doi: 10.1128/JVI.02303-06

114. Barnard P, McMillan NAJ. The human papillomavirus E7 oncoprotein abrogates signaling mediated by interferon-α. *Virology* (1999) 259:305–13. doi: 10.1006/viro.1999.9771

115. Zhang R, Fang L, Wang D, Cai K, Zhang H, Xie L, et al. Porcine bocavirus NP1 negatively regulates interferon signaling pathway by targeting the DNA-binding domain of IRF9. *Virology* (2015) 485:414–21. doi: 10.1016/j.virol.2015.08.005

116. Verweij MC, Wellish M, Whitmer T, Malouli D, Lapel M, Jonjić S, et al. Varicella viruses inhibit interferon-stimulated JAK-STAT signaling through multiple mechanisms. *PloS Pathog* (2015) 11:e1004901. doi: 10.1371/journal.ppat.1004901

117. Andrejeva J, Childs KS, Young DF, Carlos TS, Stock N, Goodbourn S, et al. The V proteins of paramyxoviruses bind the IFN-inducible RNA helicase, mda-5, and inhibit its activation of the IFN -β promoter. *Proc Natl Acad Sci* (2004) 101:17264–9. doi: 10.1073/pnas.0407639101

118. Hagmaier K, Stock N, Goodbourn S, Wang L-F, Randall R. A single amino acid substitution in the V protein of nipah virus alters its ability to block interferon signalling in cells from different species. *J Gen Virol* (2006) 87:3649–53. doi: 10.1099/vir.0.82261-0

119. Vidy A, Chelbi-Alix M, Blondel D. Rabies virus p protein interacts with STAT1 and inhibits interferon signal transduction pathways. *J Virol* (2005) 79:14411–20. doi: 10.1128/JVI.79.22.14411-14420.2005

120. Wang R, Nan Y, Yu Y, Zhang Y-J. Porcine reproductive and respiratory syndrome virus Nsp1β inhibits interferon-activated JAK/STAT signal transduction by inducing karyopherin-α1 degradation. *J Virol* (2013) 87:5219–28. doi: 10.1128/JVI.02643-12

121. Nice TJ, Osborne LC, Tomov VT, Artis D, Wherry EJ, Virgin HW. Type I interferon receptor deficiency in dendritic cells facilitates systemic murine norovirus persistence despite enhanced adaptive immunity. *PloS Pathog* (2016) 12:e1005684. doi: 10.1371/journal.ppat.1005684

122. Kimman TG, Cornelissen LA, Moormann RJ, Rebel JMJ, Stockhofe-Zurwieden N. Challenges for porcine reproductive and respiratory syndrome virus (PRRSV) vaccinology. *Vaccine* (2009) 27:3704–18. doi: 10.1016/j.vaccine.2009.04.022

123. Manns MP, McHutchison JG, Gordon SC, Rustgi VK, Shiffman M, Reindollar R, et al. Peginterferon alfa-2b plus ribavirin compared with interferon alfa-2b plus ribavirin for initial treatment of chronic hepatitis c: a randomised trial. *Lancet* (2001) 358:958–65. doi: 10.1016/S0140-6736(01)06102-5

124. Radkowski M, Gallegos-Orozco JF, Jablonska J, Colby TV, Walewska-Zielecka B, Kubicka J, et al. Persistence of hepatitis c virus in patients successfully treated for chronic hepatitis c. *Hepatology* (2005) 41:106–14. doi: 10.1002/hep.20518

125. Shiffman ML, Hofmann CM, Contos MJ, Luketic VA, Sanyal AJ, Sterling RK, et al. A randomized, controlled trial of maintenance interferon therapy for patients with chronic hepatitis c virus and persistent viremia. *Gastroenterology* (1999) 117:1164–72. doi: 10.1016/S0016-5085(99)70402-6

126. Audsley KM, Wagner T, Ta C, Newnes HV, Buzzai AC, Barnes SA, et al. IFNβ is a potent adjuvant for cancer vaccination strategies. *Front Immunol* (2021) 12:735133. doi: 10.3389/fimmu.2021.735133

127. Sang Y, Rowland RRR, Blecha F. Antiviral regulation in porcine monocytic cells at different activation states. *J Virol* (2014) 88:11395–410. doi: 10.1128/JVI.01714-14

128. Sang Y, Shi J, Sang W, Rowland RRR, Blecha F. Replication-competent recombinant porcine reproductive and respiratory syndrome (PRRS) viruses expressing indicator proteins and antiviral cytokines. *Viruses* (2012) 4:102–16. doi: 10.3390/v4010102

129. Meier WA, Husmann RJ, Schnitzlein WM, Osorio FA, Lunney JK, Zuckermann FA. Cytokines and synthetic double-stranded RNA augment the T helper 1 immune response of swine to porcine reproductive and respiratory syndrome virus. *Vet Immunol Immunopathol* (2004) 102:299–314. doi: 10.1016/j.vetimm.2004.09.012

130. Liu L, Fan W, Zhang H, Zhang S, Cui L, Wang M, et al. Interferon as a mucosal adjuvant for an influenza vaccine in pigs. *Virol Sin* (2019) 34:324–33. doi: 10.1007/s12250-019-00102-7

131. Bracci L, Canini I, Puzelli S, Sestili P, Venditti M, Spada M, et al. Type I IFN is a powerful mucosal adjuvant for a selective intranasal vaccination against influenza virus in mice and affects antigen capture at mucosal level. *Vaccine* (2005) 23:2994–3004. doi: 10.1016/j.vaccine.2004.12.006

132. Bracci L, Canini I, Venditti M, Spada M, Puzelli S, Donatelli I, et al. Type I IFN as a vaccine adjuvant for both systemic and mucosal vaccination against influenza virus. *Vaccine* (2006) 24:S56–7. doi: 10.1016/j.vaccine.2005.01.121

133. Cheng G, Zhao X, Yan W, Wang W, Zuo X, Huang K, et al. Alpha interferon is a powerful adjuvant for a recombinant protein vaccine against foot-and-mouth disease virus in swine, and an effective stimulus of *in vivo* immune response. *Vaccine* (2007) 25:5199–208. doi: 10.1016/j.vaccine.2007.04.089

134. Su C, Duan X, Zheng J, Liang L, Wang F, Guo L. IFN-α as an adjuvant for adenovirus-vectored FMDV subunit vaccine through improving the generation of T follicular helper cells. *PloS One* (2013) 8:e66134. doi: 10.1371/journal.pone.0066134

135. Chinsangaram J, Moraes MP, Koster M, Grubman MJ. Novel viral disease control strategy: adenovirus expressing alpha interferon rapidly protects swine from foot-and-Mouth disease. *J Virol* (2003) 77:1621–5. doi: 10.1128/JVI.77.2.1621-1625.2003

136. O'Brien L, Perkins S, Williams A, Eastaugh L, Phelps A, Wu J, et al. Alpha interferon as an adenovirus-vectored vaccine adjuvant and antiviral in Venezuelan equine encephalitis virus infection. *J Gen Virol* (2009) 90:874–82. doi: 10.1099/vir.0.006833-0

137. Wu JQH, Barabé ND, Huang Y-M, Rayner GA, Christopher ME, Schmaltz FL. Pre- and post-exposure protection against Western equine encephalitis virus after single inoculation with adenovirus vector expressing interferon alpha. *Virology* (2007) 369:206–13. doi: 10.1016/j.virol.2007.07.024

138. Baer GM, Moore SA, Shaddock JH, Levy HB. An effective rabies treatment in exposed monkeys: a single dose of interferon inducer and vaccine. *Bull World Health Organ* (1979) 57:807–13.

139. Hayer SS, Ranjan R, Biswal JK, Subramaniam S, Mohapatra JK, Sharma GK, et al. Quantitative characteristics of the foot-and-mouth disease carrier state under natural conditions in India. *Transbound Emerg Dis* (2018) 65:253–60. doi: 10.1111/tbed.12627

140. Swatek KN, Aumayr M, Pruneda JN, Visser LJ, Berryman S, Kueck AF, et al. Irreversible inactivation of ISG15 by a viral leader protease enables alternative infection detection strategies. *Proc Natl Acad Sci* (2018) 115:2371–6. doi: 10.1073/pnas.1710617115

141. Medina GN, Azzinaro P, Ramirez-Medina E, Gutkoska J, Fang Y, Diaz-San Segundo F, et al. Impairment of the DeISGylation activity of foot-and-Mouth disease virus lpro causes attenuation *In vitro* and *In vivo*. *J Virol* (2020) 94:e00341-20. doi: 10.1128/JVI.00341-20

142. Piccone ME, Rieder E, Mason PW, Grubman MJ. The foot-and-mouth disease virus leader proteinase gene is not required for viral replication. *J Virol* (1995) 69:5376–82. doi: 10.1128/jvi.69.9.5376-5382.1995

143. Díaz-San Segundo F, Weiss M, Pérez-Martín E, Dias CC, Grubman MJ, de los Santos T. Inoculation of swine with foot-and-Mouth disease SAP-mutant virus induces early protection against disease. *J Virol* (2012) 86:1316–27. doi: 10.1128/JVI.05941-11

144. Azzinaro PA, Medina GN, Rai D, Ramirez-Medina E, Spinard E, Rodriguez-Calzada M, et al. Mutation of FMDV lpro H138 residue drives viral attenuation in cell culture and *in vivo* in swine. *Front Vet Sci* (2022) 9:1028077. doi: 10.3389/fvets.2022.1028077

145. Arzt J, Pacheco JM, Stenfeldt C, Rodriguez LL. Pathogenesis of virulent and attenuated foot-and-mouth disease virus in cattle. *Virol J* (2017) 14:89. doi: 10.1186/s12985-017-0758-9

146. Uddowla S, Hollister J, Pacheco JM, Rodriguez LL, Rieder E. A safe foot-and-Mouth disease vaccine platform with two negative markers for differentiating infected from vaccinated animals. *J Virol* (2012) 86:11675–85. doi: 10.1128/JVI.01254-12

147. Simmons JD, Wollish AC, Heise MT. A determinant of sindbis virus neurovirulence enables efficient disruption of Jak/STAT signaling. *J Virol* (2010) 84:11429–39. doi: 10.1128/JVI.00577-10

148. Heise MT, Simpson DA, Johnston RE. A single amino acid change in nsP1 attenuates neurovirulence of the sindbis-group alphavirus S.A.AR86. *J Virol* (2000) 74:4207–13. doi: 10.1128/JVI.74.9.4207-4213.2000

149. Wollish AC, Ferris MT, Blevins LK, Loo Y-M, Gale M, Heise MT. An attenuating mutation in a neurovirulent sindbis virus strain interacts with the IPS-1 signaling pathway *in vivo*. *Virology* (2013) 435:269–80. doi: 10.1016/j.virol.2012.09.008

150. Cruz CC, Suthar MS, Montgomery SA, Shabman R, Simmons J, Johnston RE, et al. Modulation of type I IFN induction by a virulence determinant within the alphavirus nsP1 protein. *Virology* (2010) 399:1–10. doi: 10.1016/j.virol.2009.12.031

151. Jupille HJ, Oko L, Stoermer KA, Heise MT, Mahalingam S, Gunn BM, et al. Mutations in nsP1 and PE2 are critical determinants of Ross river virus-induced musculoskeletal inflammatory disease in a mouse model. *Virology* (2011) 410:216–27. doi: 10.1016/j.virol.2010.11.012

152. Stoermer Burrack KA, Hawman DW, Jupille HJ, Oko L, Minor M, Shives KD, et al. Attenuating mutations in nsP1 reveal tissue-specific mechanisms for control of Ross river virus infection. *J Virol* (2014) 88:3719–32. doi: 10.1128/JVI.02609-13

153. Best SM, Morris KL, Shannon JG, Robertson SJ, Mitzel DN, Park GS, et al. Inhibition of interferon-stimulated JAK-STAT signaling by a tick-borne flavivirus and identification of NS5 as an interferon antagonist. *J Virol* (2005) 79:12828–39. doi: 10.1128/JVI.79.20.12828-12839.2005

154. Laurent-Rolle M, Boer EF, Lubick KJ, Wolfinbarger JB, Carmody AB, Rockx B, et al. The NS5 protein of the virulent West Nile virus NY99 strain is a potent antagonist of type I interferon-mediated JAK-STAT signaling. *J Virol* (2010) 84:3503–15. doi: 10.1128/JVI.01161-09

155. Prow NA, Setoh YX, Biron RM, Sester DP, Kim KS, Hobson-Peters J, et al. The West Nile virus-like flavivirus koutango is highly virulent in mice due to delayed viral clearance and the induction of a poor neutralizing antibody response. *J Virol* (2014) 88:9947–62. doi: 10.1128/JVI.01304-14

156. Jim K. Impact of bovine respiratory disease (BRD) from the perspective of the Canadian beef producer. *Anim Heal Res Rev* (2009) 10:109–10. doi: 10.1017/S1466252309990119

157. Valarcher J-F, Furze J, Wyld S, Cook R, Conzelmann K-K, Taylor G. Role of Alpha/Beta interferons in the attenuation and immunogenicity of recombinant bovine respiratory syncytial viruses lacking NS proteins. *J Virol* (2003) 77:8426–39. doi: 10.1128/JVI.77.15.8426-8439.2003

158. Jin H, Cheng X, Traina-Dorge VL, Park HJ, Zhou H, Soike K, et al. Evaluation of recombinant respiratory syncytial virus gene deletion mutants in African green monkeys for their potential as live attenuated vaccine candidates. *Vaccine* (2003) 21:3647–52. doi: 10.1016/S0264-410X(03)00426-2

159. Jin H, Zhou H, Cheng X, Tang R, Munoz M, Nguyen N. Recombinant respiratory syncytial viruses with deletions in the NS1, NS2, SH, and M2-2 genes are attenuated in vitro and in vivo. *Virology* (2000) 273:210–8. doi: 10.1006/viro.2000.0393

160. Wright PF, Karron RA, Madhi SA, Treanor JJ, King JC, O'Shea A, et al. The interferon antagonist NS2 protein of respiratory syncytial virus is an important virulence determinant for humans. *J Infect Dis* (2006) 193:573–81. doi: 10.1086/499600

161. Karron RA, Luongo C, Mateo JS, Wanionek K, Collins PL, Buchholz UJ. Safety and immunogenicity of the respiratory syncytial virus vaccine RSV/ΔNS2/Δ1313/I1314L in RSV-seronegative children. *J Infect Dis* (2020) 222:82–91. doi: 10.1093/infdis/jiz408

162. Cunningham CK, Karron RA, Muresan P, Kelly MS, McFarland EJ, Perlowski C, et al. Evaluation of recombinant live-attenuated respiratory syncytial virus (RSV) vaccines RSV/ΔNS2/Δ1313/I1314L and RSV/276 in RSV-seronegative children. *J Infect Dis* (2022) 226:2069–78. doi: 10.1093/infdis/jiac253

163. Griffin DE. Measles virus-induced suppression of immune responses. *Immunol Rev* (2010) 236:176–89. doi: 10.1111/j.1600-065X.2010.00925.x

164. Devaux P, von Messling V, Songsungthong W, Springfeld C, Cattaneo R. Tyrosine 110 in the measles virus phosphoprotein is required to block STAT1 phosphorylation. *Virology* (2007) 360:72–83. doi: 10.1016/j.virol.2006.09.049

165. Gerlier D, Valentin H. Measles virus interaction with host cells and impact on innate immunity. *Curr Top Microbiol Immunol* (2009) 329:163–91. doi: 10.1007/978-3-540-70523-9_8

166. Parisien J-P, Bamming D, Komuro A, Ramachandran A, Rodriguez JJ, Barber G, et al. A shared interface mediates paramyxovirus interference with antiviral RNA helicases MDA5 and LGP2. *J Virol* (2009) 83:7252–60. doi: 10.1128/JVI.00153-09

167. Motz C, Schuhmann KM, Kirchhofer A, Moldt M, Witte G, Conzelmann K-K, et al. Paramyxovirus V proteins disrupt the fold of the RNA sensor MDA5 to inhibit antiviral signaling. *Sci (80-)* (2013) 339:690–3. doi: 10.1126/science.1230949

168. Sánchez-Aparicio MT, Feinman LJ, García-Sastre A, Shaw ML. Paramyxovirus V proteins interact with the RIG-I/TRIM25 regulatory complex and inhibit RIG-I signaling. *J Virol* (2018) 92:e01960-17. doi: 10.1128/JVI.01960-17

169. Sparrer KMJ, Pfaller CK, Conzelmann K-K. Measles virus c protein interferes with beta interferon transcription in the nucleus. *J Virol* (2012) 86:796–805. doi: 10.1128/JVI.05899-11

170. de Vries RD, Lemon K, Ludlow M, McQuaid S, Yüksel S, van Amerongen G, et al. *In vivo* tropism of attenuated and pathogenic measles virus expressing green fluorescent protein in macaques. *J Virol* (2010) 84:4714–24. doi: 10.1128/JVI.02633-09

171. Devaux P, Hodge G, McChesney MB, Cattaneo R. Attenuation of V- or c-defective measles viruses: infection control by the inflammatory and interferon responses of rhesus monkeys. *J Virol* (2008) 82:5359–67. doi: 10.1128/JVI.00169-08

172. Devaux P, Hudacek AW, Hodge G, Reyes-del Valle J, McChesney MB, Cattaneo R. A recombinant measles virus unable to antagonize STAT1 function cannot control inflammation and is attenuated in rhesus monkeys. *J Virol* (2011) 85:348–56. doi: 10.1128/JVI.00802-10

173. Chua KB, Bellini WJ, Rota PA, Harcourt BH, Tamin A, Lam SK, et al. Nipah virus: a recently emergent deadly paramyxovirus. *Sci (80-)* (2000) 288:1432–5. doi: 10.1126/science.288.5470.1432

174. Yoneda M, Guillaume V, Sato H, Fujita K, Georges-Courbot M-C, Ikeda F, et al. The nonstructural proteins of nipah virus play a key role in pathogenicity in experimentally infected animals. *PloS One* (2010) 5:e12709. doi: 10.1371/journal.pone.0012709

175. Keiffer TR, Ciancanelli MJ, Edwards MR, Basler CF. Interactions of the nipah virus p, V, and W proteins across the STAT family of transcription factors. *mSphere* (2020) 5:e00449-20. doi: 10.1128/mSphere.00449-20

176. Uchida S, Horie R, Sato H, Kai C, Yoneda M. Possible role of the nipah virus V protein in the regulation of the interferon beta induction by interacting with UBX domain-containing protein1. *Sci Rep* (2018) 8:7682. doi: 10.1038/s41598-018-25815-9

177. Rodriguez JJ, Cruz CD, Horvath CM. Identification of the nuclear export signal and STAT-binding domains of the nipah virus V protein reveals mechanisms underlying interferon evasion. *J Virol* (2004) 78:5358–67. doi: 10.1128/JVI.78.10.5358-5367.2004

178. Satterfield BA, Cross RW, Fenton KA, Agans KN, Basler CF, Geisbert TW, et al. The immunomodulating V and W proteins of nipah virus determine disease course. *Nat Commun* (2015) 6:7483. doi: 10.1038/ncomms8483

179. Satterfield BA, Borisevich V, Foster SL, Rodriguez SE, Cross RW, Fenton KA, et al. Antagonism of STAT1 by nipah virus p gene products modulates disease course but not lethal outcome in the ferret model. *Sci Rep* (2019) 9:16710. doi: 10.1038/s41598-019-53037-0

180. Ji Z, Wang X, Liu X. NS1: a key protein in the "Game" between influenza a virus and host in innate immunity. *Front Cell Infect Microbiol* (2021) 11:670177. doi: 10.3389/fcimb.2021.670177

181. Pauli E-K, Schmolke M, Wolff T, Viemann D, Roth J, Bode JG, et al. Influenza a virus inhibits type I IFN signaling *via* NF-κB-Dependent induction of SOCS-3 expression. *PloS Pathog* (2008) 4:e1000196. doi: 10.1371/journal.ppat.1000196

182. Nogales A, Baker SF, Ortiz-Riaño E, Dewhurst S, Topham DJ, Martínez-Sobrido L. Influenza a virus attenuation by codon deoptimization of the NS gene for vaccine development. *J Virol* (2014) 88:10525–40. doi: 10.1128/JVI.01565-14

183. Mueller SN, Langley WA, Carnero E, Garciía-Sastre A, Ahmed R. Immunization with live attenuated influenza viruses that express altered NS1 proteins results in potent and protective memory CD8 + T-cell responses. *J Virol* (2010) 84:1847–55. doi: 10.1128/JVI.01317-09

184. Wang P, Zheng M, Lau S-Y, Chen P, Mok BW-Y, Liu S, et al. Generation of DelNS1 influenza viruses: a strategy for optimizing live attenuated influenza vaccines. *MBio* (2019) 10:e02180-19. doi: 10.1128/mBio.02180-19

185. Vasilyev K, Shurygina A-P, Sergeeva M, Stukova M, Egorov A. Intranasal immunization with the influenza a virus encoding truncated NS1 protein protects mice from heterologous challenge by restraining the inflammatory response in the lungs. *Microorganisms* (2021) 9:690. doi: 10.3390/microorganisms9040690

186. Soloírzano A, ebby WRJ, Lager KM, Janke BH, Garciía-Sastre A, Richt JA. Mutations in the NS1 protein of swine influenza virus impair anti-interferon activity and confer attenuation in pigs. *J Virol* (2005) 79:7535–43. doi: 10.1128/JVI.79.12.7535-7543.2005

187. Vandoorn E, Stadejek W, Parys A, Chepkwony S, Chiers K, Van Reeth K. Pathobiology of an NS1-truncated H3N2 swine influenza virus strain in pigs. *J Virol* (2022) 96:e00519–22. doi: 10.1128/jvi.00519-22

188. Nogales A, DeDiego ML, Martínez-Sobrido L. Live attenuated influenza a virus vaccines with modified NS1 proteins for veterinary use. *Front Cell Infect Microbiol* (2022) 12:954811. doi: 10.3389/fcimb.2022.954811

189. Chambers TM, Quinlivan M, Sturgill T, Cullinane A, Horohov DW, Zamarin D, et al. Influenza a viruses with truncated NS1 as modified live virus vaccines: pilot studies of safety and efficacy in horses. *Equine Vet J* (2009) 41:87–92. doi: 10.2746/042516408X371937

190. Quinlivan M, Zamarin D, Garciía-Sastre A, Cullinane A, Chambers T, Palese P. Attenuation of equine influenza viruses through truncations of the NS1 protein. *J Virol* (2005) 79:8431–9. doi: 10.1128/JVI.79.13.8431-8439.2005

191. Chen S, Zhu Y, Yang D, Yang Y, Shi S, Qin T, et al. Efficacy of live-attenuated H9N2 influenza vaccine candidates containing NS1 truncations against H9N2 avian influenza viruses. *Front Microbiol* (2017) 8:1086. doi: 10.3389/fmicb.2017.01086

192. Steel J, Lowen AC, Pena L, Angel M, Soloírzano A, Albrecht R, et al. Live attenuated influenza viruses containing NS1 truncations as vaccine candidates against H5N1 highly pathogenic avian influenza. *J Virol* (2009) 83:1742–53. doi: 10.1128/JVI.01920-08

193. Wang L, Suarez DL, Pantin-Jackwood M, Mibayashi M, García-Sastre A, Saif YM, et al. Characterization of influenza virus variants with different sizes of the non-structural (NS) genes and their potential as a live influenza vaccine in poultry. *Vaccine* (2008) 26:3580–6. doi: 10.1016/j.vaccine.2008.05.001

194. Ghorbani A, Abundo MC, Ji H, Taylor KJM, Ngunjiri JM, Lee C-W. Viral subpopulation screening guides in designing a high interferon-inducing live attenuated influenza vaccine by targeting rare mutations in NS1 and PB2 proteins. *J Virol* (2020) 95:e01722-20. doi: 10.1128/JVI.01722-20

195. Baskin CR, Bielefeldt-Ohmann H, Garciía-Sastre A, Tumpey TM, Van Hoeven N, Carter VS, et al. Functional genomic and serological analysis of the protective immune response resulting from vaccination of macaques with an NS1-truncated influenza virus. *J Virol* (2007) 81:11817–27. doi: 10.1128/JVI.00590-07

196. Wacheck V, Egorov A, Groiss F, Pfeiffer A, Fuereder T, Hoeflmayer D, et al. A novel type of influenza vaccine: safety and immunogenicity of replication-deficient influenza virus created by deletion of the interferon antagonist NS1. *J Infect Dis* (2010) 201:354–62. doi: 10.1086/649428

197. Mössler C, Groiss F, Wolzt M, Wolschek M, Seipelt J, Muster T. Phase I/II trial of a replication-deficient trivalent influenza virus vaccine lacking NS1. *Vaccine* (2013) 31:6194–200. doi: 10.1016/j.vaccine.2013.10.061

198. Nicolodi C, Groiss F, Kiselev O, Wolschek M, Seipelt J, Muster T. Safety and immunogenicity of a replication-deficient H5N1 influenza virus vaccine lacking NS1. *Vaccine* (2019) 37:3722–9. doi: 10.1016/j.vaccine.2019.05.013

199. Talon J, Salvatore M, O'Neill RE, Nakaya Y, Zheng H, Muster T, et al. Influenza a and b viruses expressing altered NS1 proteins: a vaccine approach. *Proc Natl Acad Sci* (2000) 97:4309–14. doi: 10.1073/pnas.070525997

200. Chen C, Fan W, Li J, Zheng W, Zhang S, Yang L, et al. A promising IFN-deficient system to manufacture IFN-sensitive influenza vaccine virus. *Front Cell Infect Microbiol* (2018) 8:127. doi: 10.3389/fcimb.2018.00127

201. Hai R, Martiínez-Sobrido L, Fraser KA, Ayllon J, Garciía-Sastre A, Palese P. Influenza b virus NS1-truncated mutants: live-attenuated vaccine approach. *J Virol* (2008) 82:10580–90. doi: 10.1128/JVI.01213-08

202. Pica N, Langlois RA, Krammer F, Margine I, Palese P. NS1-truncated live attenuated virus vaccine provides robust protection to aged mice from viral challenge. *J Virol* (2012) 86:10293–301. doi: 10.1128/JVI.01131-12

203. Staeheli P, Grob R, Meier E, Sutcliffe JG, Haller O. Influenza virus-susceptible mice carry mx genes with a large deletion or a nonsense mutation. *Mol Cell Biol* (1988) 8:4518–23. doi: 10.1128/mcb.8.10.4518-4523.1988

204. Loving CL, Lager KM, Vincent AL, Brockmeier SL, Gauger PC, Anderson TK, et al. Efficacy in pigs of inactivated and live attenuated influenza virus vaccines against infection and transmission of an emerging H3N2 similar to the 2011-2012 H3N2v. *J Virol* (2013) 87:9895–903. doi: 10.1128/JVI.01038-13

205. Vincent AL, Ma W, Lager KM, Janke BH, Webby RJ, García-Sastre A, et al. Efficacy of intranasal administration of a truncated NS1 modified live influenza virus vaccine in swine. *Vaccine* (2007) 25:7999–8009. doi: 10.1016/j.vaccine.2007.09.019

206. Artiaga BL, Morozov I, Ransburgh R, Kwon T, Balaraman V, Indran SV, et al. Evaluating α-galactosylceramide as an adjuvant for live attenuated influenza vaccines in pigs. *Anim Dis* (2022) 2:19. doi: 10.1186/s44149-022-00051-x

207. Lee J, Li Y, Li Y, Cino-Ozuna AG, Duff M, Lang Y, et al. Bat influenza vectored NS1-truncated live vaccine protects pigs against heterologous virus challenge. *Vaccine* (2021) 39:1943–50. doi: 10.1016/j.vaccine.2021.02.077

208. Jang H, Ngunjiri JM, Lee C-W. Association between interferon response and protective efficacy of NS1-truncated mutants as influenza vaccine candidates in chickens. *PloS One* (2016) 11:e0156603. doi: 10.1371/journal.pone.0156603

209. Ngunjiri JM, Ali A, Boyaka P, Marcus PI, Lee CW. *In vivo* assessment of NS1-truncated influenza virus with a novel SLSYSINWRH motif as a self-adjuvanting live attenuated vaccine. *PloS One* (2015) 10:e0118934. doi: 10.1371/journal.pone.0118934

210. Jang H, Elaish M KCM, Abundo MC, Ghorbani A, Ngunjiri JM, Lee C-W. Efficacy and synergy of live-attenuated and inactivated influenza vaccines in young chickens. *PloS One* (2018) 13:e0195285. doi: 10.1371/journal.pone.0195285

211. Brahmakshatriya VR, Lupiani B, Reddy SM. Characterization and evaluation of avian influenza NS1 mutant virus as a potential live and killed DIVA (differentiating between infected and vaccinated animals) vaccine for chickens. *Vaccine* (2010) 28:2388–96. doi: 10.1016/j.vaccine.2009.12.074

212. Zhang G, Li B, Yoo D, Qin T, Zhang X, Jia Y, et al. Animal coronaviruses and SARS-CoV-2. *Transbound Emerg Dis* (2021) 68:1097–110. doi: 10.1111/tbed.13791

213. Vlasova AN, Toh T-H, Lee JS-Y, Poovorawan Y, Davis P, Azevedo MSP, et al. Animal alphacoronaviruses found in human patients with acute respiratory illness in different countries. *Emerg Microbes Infect* (2022) 11:699–702. doi: 10.1080/22221751.2022.2040341

214. Zhang Q, Shi K, Yoo D. Suppression of type I interferon production by porcine epidemic diarrhea virus and degradation of CREB-binding protein by nsp1. *Virology* (2016) 489:252–68. doi: 10.1016/j.virol.2015.12.010

215. Zhang Q, Ke H, Blikslager A, Fujita T, Yoo D. Type III interferon restriction by porcine epidemic diarrhea virus and the role of viral protein nsp1 in IRF1 signaling. *J Virol* (2018) 92:e01677-17. doi: 10.1128/JVI.01677-17

216. Deng X, van Geelen A, Buckley AC, O'Brien A, Pillatzki A, Lager KM, et al. Coronavirus endoribonuclease activity in porcine epidemic diarrhea virus suppresses type I and type III interferon responses. *J Virol* (2019) 93:e02000-18. doi: 10.1128/JVI.02000-18

217. Xu X, Zhang H, Zhang Q, Dong J, Liang Y, Huang Y, et al. Porcine epidemic diarrhea virus e protein causes endoplasmic reticulum stress and up-regulates interleukin-8 expression. *Virol J* (2013) 10:26. doi: 10.1186/1743-422X-10-26

218. Ding Z, Fang L, Jing H, Zeng S, Wang D, Liu L, et al. Porcine epidemic diarrhea virus nucleocapsid protein antagonizes beta interferon production by sequestering the interaction between IRF3 and TBK1. *J Virol* (2014) 88:8936–45. doi: 10.1128/JVI.00700-14

219. Wang D, Fang L, Shi Y, Zhang H, Gao L, Peng G, et al. Porcine epidemic diarrhea virus 3C-like protease regulates its interferon antagonism by cleaving NEMO. *J Virol* (2016) 90:2090–101. doi: 10.1128/JVI.02514-15

220. Niu X, Kong F, Xu J, Liu M, Wang Q. Mutations in porcine epidemic diarrhea virus nsp1 cause increased viral sensitivity to host interferon responses and attenuation *In vivo*. *J Virol* (2022) 96:e0046922. doi: 10.1128/jvi.00469-22

221. Hou Y, Ke H, Kim J, Yoo D, Su Y, Boley P, et al. Engineering a live attenuated porcine epidemic diarrhea virus vaccine candidate *via* inactivation of the viral 2'- O -methyltransferase and the endocytosis signal of the spike protein. *J Virol* (2019) 93: e00406-19. doi: 10.1128/JVI.00406-19

222. Menachery VD, Gralinski LE, Mitchell HD, Dinnon KH, Leist SR, Yount BL, et al. Middle East respiratory syndrome coronavirus nonstructural protein 16 is necessary for interferon resistance and viral pathogenesis. *mSphere* (2017) 2:e00346-17. doi: 10.1128/mSphere.00346-17

223. Menachery VD, Yount BL, Josset L, Gralinski LE, Scobey T, Agnihothram S, et al. Attenuation and restoration of severe acute respiratory syndrome coronavirus mutant lacking 2′-O-Methyltransferase activity. *J Virol* (2014) 88:4251–64. doi: 10.1128/JVI.03571-13

224. Zhang Z, Liu Q, Sun Y, Li J, Liu J, Pan R, et al. Live attenuated coronavirus vaccines deficient in N7-methyltransferase activity induce both humoral and cellular immune responses in mice. *Emerg Microbes Infect* (2021) 10:1626–37. doi: 10.1080/22221751.2021.1964385

225. Snijder EJ, Kikkert M, Fang Y. Arterivirus molecular biology and pathogenesis. *J Gen Virol* (2013) 94:2141–63. doi: 10.1099/vir.0.056341-0

226. Albina E, Piriou L, Hutet E, Cariolet R, L'Hospitalier R. Immune responses in pigs infected with porcine reproductive and respiratory syndrome virus (PRRSV). *Vet Immunol Immunopathol* (1998) 61:49–66. doi: 10.1016/S0165-2427(97)00134-7

227. Van Reeth K, Labarque G, Nauwynck H, Pensaert M. Differential production of proinflammatory cytokines in the pig lung during different respiratory virus infections:

correlations with pathogenicity. *Res Vet Sci* (1999) 67:47–52. doi: 10.1053/rvsc.1998.0277

228. Ke H, Yoo D. The viral innate immune antagonism and an alternative vaccine design for PRRS virus. *Vet Microbiol* (2017) 209:75–89. doi: 10.1016/j.vetmic.2017.03.014

229. Wang R, Xiao Y, Opriessnig T, Ding Y, Yu Y, Nan Y, et al. Enhancing neutralizing antibody production by an interferon-inducing porcine reproductive and respiratory syndrome virus strain. *Vaccine* (2013) 31:5537–43. doi: 10.1016/j.vaccine.2013.09.023

230. Li Y, Shyu D-L, Shang P, Bai J, Ouyang K, Dhakal S, et al. Mutations in a highly conserved motif of nsp1β protein attenuate the innate immune suppression function of porcine reproductive and respiratory syndrome virus. *J Virol* (2016) 90:3584–99. doi: 10.1128/JVI.03069-15

231. Ke H, Han M, Zhang Q, Rowland R, Kerrigan M, Yoo D. Type I interferon suppression-negative and host mRNA nuclear retention-negative mutation in nsp1β confers attenuation of porcine reproductive and respiratory syndrome virus in pigs. *Virology* (2018) 517:177–87. doi: 10.1016/j.virol.2018.01.016

232. van Kasteren PB, Bailey-Elkin BA, James TW, Ninaber DK, Beugeling C, Khajehpour M, et al. Deubiquitinase function of arterivirus papain-like protease 2 suppresses the innate immune response in infected host cells. *Proc Natl Acad Sci* (2013) 110:E838–47. doi: 10.1073/pnas.1218464110

233. van Kasteren PB, Knaap RCM, van den Elzen P, Snijder EJ, Balasuriya UBR, van den Born E, et al. *In vivo* assessment of equine arteritis virus vaccine improvement by disabling the deubiquitinase activity of papain-like protease 2. *Vet Microbiol* (2015) 178:132–7. doi: 10.1016/j.vetmic.2015.04.018

234. Rahman MM, McFadden G. Modulation of NF-κB signalling by microbial pathogens. *Nat Rev Microbiol* (2011) 9:291–306. doi: 10.1038/nrmicro2539

235. Su C-M, Wang L, Yoo D. Activation of NF-κB and induction of proinflammatory cytokine expressions mediated by ORF7a protein of SARS-CoV-2. *Sci Rep* (2021) 11:13464. doi: 10.1038/s41598-021-92941-2

236. Kircheis R, Haasbach E, Lueftenegger D, Heyken WT, Ocker M, Planz O. NF-κB pathway as a potential target for treatment of critical stage COVID-19 patients. *Front Immunol* (2020) 11:598444. doi: 10.3389/fimmu.2020.598444

237. Gu Y, Zuo X, Zhang S, Ouyang Z, Jiang S, Wang F, et al. The mechanism behind influenza virus cytokine storm. *Viruses* (2021) 13:1362. doi: 10.3390/v13071362

238. Auray G, Lachance C, Wang Y, Gagnon CA, Segura M, Gottschalk M. Transcriptional analysis of PRRSV-infected porcine dendritic cell response to streptococcus suis infection reveals up-regulation of inflammatory-related genes expression. *PloS One* (2016) 11:e0156019. doi: 10.1371/journal.pone.0156019

239. Moser BA, Steinhardt RC, Escalante-Buendia Y, Boltz DA, Barker KM, Cassaidy BJ, et al. Increased vaccine tolerability and protection *via* NF-κB modulation. *Sci Adv* (2020) 6:eaaz8700. doi: 10.1126/sciadv.aaz8700

240. Wang G, Li L, Yu Y, Tu Y, Tong J, Zhang C, et al. Highly pathogenic porcine reproductive and respiratory syndrome virus infection and induction of apoptosis in bone marrow cells of infected piglets. *J Gen Virol* (2016) 97:1356–61. doi: 10.1099/jgv.0.000454

241. Ke H, Lee S, Kim J, Liu H-C, Yoo D. Interaction of PIAS1 with PRRS virus nucleocapsid protein mediates NF-κB activation and triggers proinflammatory mediators during viral infection. *Sci Rep* (2019) 9:11042. doi: 10.1038/s41598-019-47495-9

242. Lee C, Hodgins D, Calvert JG, Welch S-KW, Jolie R, Yoo D. Mutations within the nuclear localization signal of the porcine reproductive and respiratory syndrome virus nucleocapsid protein attenuate virus replication. *Virology* (2006) 346:238–50. doi: 10.1016/j.virol.2005.11.005

243. Lee C, Hodgins DC, Calvert JG, Welch S-KW, Jolie R, Yoo D. The nuclear localization signal of the PRRS virus nucleocapsid protein viral replication *in vitro* and antibody response *in vivo*. *Adv Exp Med Biol* (2006) 581:145–8. doi: 10.1007/978-0-387-33012-9_25

244. Pei Y, Hodgins DC, Lee C, Calvert JG, Welch S-KW, Jolie R, et al. Functional mapping of the porcine reproductive and respiratory syndrome virus capsid protein nuclear localization signal and its pathogenic association. *Virus Res* (2008) 135:107–14. doi: 10.1016/j.virusres.2008.02.012

frontiers | Frontiers in Immunology

TYPE Original Research
PUBLISHED 15 May 2023
DOI 10.3389/fimmu.2023.1143451

OPEN ACCESS

EDITED BY
Brad Pickering,
National Centre for Foreign Animal Disease (NCFAD), Canada

REVIEWED BY
Tamiru N. Alkie,
Canadian Food Inspection Agency (CFIA), Canada
Harvinder Gill,
Texas Tech University, United States

*CORRESPONDENCE
Eric A. Weaver
Eweaver2@unl.edu

RECEIVED 13 January 2023
ACCEPTED 28 April 2023
PUBLISHED 15 May 2023

CITATION
Petro-Turnquist E, Pekarek M, Jeanjaquet N, Wooledge C, Steffen D, Vu H and Weaver EA (2023) Adenoviral-vectored epigraph vaccine elicits robust, durable, and protective immunity against H3 influenza A virus in swine. *Front. Immunol.* 14:1143451. doi: 10.3389/fimmu.2023.1143451

Adenoviral-vectored epigraph vaccine elicits robust, durable, and protective immunity against H3 influenza A virus in swine

Erika Petro-Turnquist[1,2], Matthew Pekarek[1,2], Nicholas Jeanjaquet[1,2], Cedric Wooledge[3], David Steffen[4], Hiep Vu[1,5] and Eric A. Weaver[1,2]*

[1]Nebraska Center for Virology, University of Nebraska-Lincoln, Lincoln, NE, United States, [2]School of Biological Sciences, University of Nebraska-Lincoln, Lincoln, NE, United States, [3]Office of Research and Development, University of Nebraska-Lincoln, Lincoln, NE, United States, [4]Nebraska Veterinary Diagnostic Center, Lincoln, NE, United States, [5]Department of Animal Science, University of Nebraska-Lincoln, Lincoln, NE, United States

Current methods of vaccination against swine Influenza A Virus (IAV-S) in pigs are infrequently updated, induce strain-specific responses, and have a limited duration of protection. Here, we characterize the onset and duration of adaptive immune responses after vaccination with an adenoviral-vectored Epigraph vaccine. In this longitudinal study we observed robust and durable antibody responses that remained above protective titers six months after vaccination. We further identified stable levels of antigen-specific T cell responses that remained detectable in the absence of antigen stimulation. Antibody isotyping revealed robust class switching from IgM to IgG induced by Epigraph vaccination, while the commercial comparator vaccine failed to induce strong antibody class switching. Swine were challenged six months after initial vaccination, and Epigraph-vaccinated animals demonstrated significant protection from microscopic lesion development in the trachea and lungs, reduced duration of viral shedding, lower presence of infectious virus and viral antigens in the lungs, and significant recall of antigen-specific T cell responses following challenge. The results obtained from this study are useful in determining the kinetics of adaptive immune responses after vaccination with adjuvanted whole inactivated virus vaccines compared to adenoviral vectored vaccines and contribute to the continued efforts of creating a universal IAV-S vaccine.

KEYWORDS

adenoviral (Ad) vector, epigraph, swine influenza, vaccine, duration, transmission, pathology

1 Introduction

Swine Influenza A Virus (IAV-S) is a significant pathogen that affects swine populations around the world (1) and imposes a significant burden on the pork industry. Economic losses to the U.S. pork industry can cost nearly $700,000,000 per year (2), and are due to reduced weight gain, delayed production, and increased susceptibility to secondary infections leading to greater veterinary costs (3–5). At present IAV-S in swine is considered one of the three top health challenges to the swine industry (6) and affects swine in all phases of production (7). Three main subtypes of IAV-S currently circulate in U.S. swine populations: H1N1, H1N2, and H3N2 (8). Though a large proportion of circulating strains are of the H1N1 subtype, recent epidemiological surveys indicate an increased incidence of H3N2 IAV-S detected in U.S. swine (9). IAV-S causes acute respiratory disease that typically resolves 3-7 days after infection (10) but can cause up to 100% morbidity in infected herds. Additionally, swine are susceptible to swine, avian, and human influenzas due to the distribution of α2, 3- and α2, 6-linked sialic acid receptors in the respiratory tract (11, 12). Because of this, swine are considered "mixing vessels" and can foster reassortment of influenza during co-infections with multiple strains, resulting in the evolution of antigenically distinct and potentially pandemic strains of IAV (3, 13). Interspecies transmission of IAV between swine and humans has been described to occur at slaughterhouses, swine production barns, live animal markets, and even agricultural fairs (14, 15). Zoonotic emergence of IAV was recently named a top priority of the One Health workshop for disease prevention in the United States. More specifically, swine were considered a significant intermediate reservoir in IAV infections and pose the greatest risk of zoonotic transmission of IAV into humans (6). One such example occurred in 2009 and was termed the "swine flu" pandemic. This novel swine influenza isolate initially arose in Mesoamerica, but quickly spread and infected ~24% of the global population within the first year (16). Importantly, this zoonotic transmission event paved the way for the establishment of a new and stable lineage of H1 influenza in humans, now known as H1N1pdm09, and is the most predominantly circulating lineage of H1N1 in humans today (17, 18). Due to the significant role swine play in the evolution and transmission of potentially pandemic strains of influenza and the substantial economic impacts of IAV-S, it is imperative that efforts be made towards the development of more effective vaccination strategies in vulnerable pig populations.

Current methods of controlling IAV-S in swine include commercially available whole-inactivated virus (WIV) vaccines, autogenous herd-specific virus vaccines, and live attenuated influenza virus (LAIV) vaccines. Commercially available WIV vaccines, such as FluSure XP, incorporate 2 strains of H1 and 2 strains of H3 IAV-S and are often supplemented with an oil-in-water adjuvant. While WIV vaccines have shown to induce robust protection after homologous challenge (19–22), interface with antigenically divergent IAV-S can result in dampened cross protection (20). Further, this method of vaccination has been linked with the induction of vaccine-associated enhanced respiratory disease (VAERD) after heterologous challenge (20, 23). This phenomenon is characterized by the presence of cross-reactive, but non-neutralizing antibodies directed towards the HA2 stalk domain of a hemagglutinin protein (24). In the absence of neutralizing antibodies against the HA1 head domain, these antibodies have been described to facilitate enhanced viral infection of MDCK cells *in vitro* and rapidly induce dysregulated levels of proinflammatory cytokines in the lungs (25). Further recruitment of inflammatory cell populations results in collateral damage in the lungs and enhanced respiratory disease. Because the process of producing and licensing a WIV vaccine is time-consuming and expensive, the commercial WIV is not updated fast enough to cope with the continually evolving swine influenza virus. In light of these challenges, autogenous herd-specific WIV vaccines are gaining popularity, with a staggering estimate of 50% of IAV-S vaccines employed in the United States being autogenous WIV vaccines in 2008 (26, 27). However, autogenous WIV vaccines have multiple drawbacks, including labor intensive laboratory techniques for diagnosis, isolation, virus growth, purification, and efficacy testing. This leads to a significant lag period before administration of the vaccine to a given herd. LAIV vaccines have recently been approved for clinical application in swine and promisingly induce heterologous protection where WIV have failed (28, 29). However, evidence of reassortment between the LAIV strain and field IAV-S calls to question the safety of the LAIV platform (30). The inherent difficulties of producing a seasonal vaccine for swine demonstrates that a safe and universal swine influenza vaccine that induces durable and broadly cross-reactive immunity to all divergent strains is needed.

Adenoviruses (Ad) are present in several mammalian species including cows, sheep, pigs, chimpanzees, and humans, and have the ability to naturally infect and replicate in a broad spectrum of cells (31, 32). Infection of epithelial cells at mucosal surfaces and dendritic cells can results in efficient antigen presentation and elicit potent immune responses. Ad has a stable double-stranded DNA genome that is maintained as an episome in an infected cell (33), mitigating the risk of insertional mutagenesis (31). Further, Ads can be made replication-defective by deleting the early E1 gene and replacing it with a gene of interest (34). Ads can be further modified to increase packaging capacity of a desired transgene by deletion of the E3 gene (34), which modulates the host immune response during an infection. Both replication-competent and replication-defective Ad vectors have been investigated as potential vaccine candidates and are superior to inactivated virus vaccines by mimicking a natural viral infection. The induction of cytokines and costimulatory molecules provide a potent adjuvant effect *in vivo* and can elicit robust adaptive immune responses to a delivered transgene. Further, amplification of replication-defective Ad amplification is easily scalable by expansion in E1-complementing cell lines in large bioreactors, and rapid ultracentrifugation purification techniques (32). A recent estimate indicates that large-scale production of Ad-vectored vaccines can cost as little as $1.25/dose (35). However, a common concern with using an adenovirus as a viral vector for vaccine development is the presence of preexisting immunity that neutralizes the vector and causes dampened immunity to the delivered transgene (36). Using adenovirus serotypes with low seroprevalence and non-human

adenoviral vectors can address this concern when developing vaccines and therapies for humans. Congruently, the same tactic can be used when creating adenoviral-vectored vaccines for non-human mammalian species. Human adenovirus type 5 (Ad5) has been well described in the swine animal model to prevent foot and mouth disease (FMD) (37), porcine respiratory and reproductive syndrome virus (PRRSV) (38), and pseudorabies virus (PrV) (39, 40), and can serve as an attractive viral vector for a universal vaccine against IAV-S.

To address the need for improved vaccination methods in swine, our group has recently characterized the use of a replication-defective adenoviral-vectored Epigraph vaccine against swine H3 influenza A virus in mice and swine (41). The Epigraph platform uses a computational algorithm to determine the frequency of potential T cell epitopes in a target population of sequences and incorporates the highest frequency epitopes into a synthetic immunogen for optimal T cell activation after immunization (42, 43). Indeed, we have previously shown that this platform induces significantly higher cross-reactive antibodies, robust T cell activation, and protection against divergent swine and human H3 influenza challenge in mice compared to a WT immunogen and the commercial comparator WIV vaccine, FluSure XP (41). However, to the best of our knowledge, no studies have performed a longitudinal study analyzing the onset and duration of immune responses elicited after vaccination with an adenoviral-vectored vaccine and compared these results to a WIV vaccine in swine.

Here, we evaluated the kinetics of antibody and T cell response generation after vaccination with an adenoviral-vectored Epigraph vaccine (Ad-swH3-Epi) and compare the responses observed to vaccination with a commonly used WIV vaccine, FluSure XP. We further characterize the differences in antibody class switching after vaccination with these different platforms. Finally, we assessed protection against challenge 6 months after the initial vaccination to evaluate the extent of the protective responses in a clinically relevant model, as the average lifespan of standard market pig in the pork industry is 6-7 months of age. The data observed in this study support the use of Ad-swH3-Epi for robust and durable protection against H3 IAV-S in swine.

2 Materials and methods

2.1 Ethics statement

All procedures in this study were approved by the Institutional Biosafety Committee at the University of Nebraska-Lincoln (IBC #619). Fifteen 3-week-old cross bred female Yorkshire pigs serologically negative for prior influenza exposure were obtained from Midwest Research Farms and randomly allocated into three immunization groups. All pigs were housed at the University of Nebraska-Lincoln Life Science Annex under animal biosafety level 2 (ABSL2) conditions (IACUC #2167) as per the Association for Assessment and Accreditation of Laboratory Animal Care International (AAALAC) guidelines with access to food and water *ad libitum* and were allowed to acclimate for one week prior to immunization.

2.2 Cells and viruses

The following swine influenza A virus was a generous gift from our collaborator: A/swine/Kansas/11-110529/2011 (sw/KS/11) from Dr. Wenjun Ma. The following viruses were obtained from the Biodefense and Emerging Infectious Diseases Repository: A/swine/Ohio/11SW87/2011 (sw/OH/11) [NR-36715] and A/swine Manitoba/00446/2005 (sw/Man/05) [NR-43049]. The following isolates were obtained from the USDA Swine Surveillance Influenza A virus repository: A/swine/Texas/4199-2/1998 (sw/TX/98), A/swine/Colorado/23619/1999 (sw/CO/99), A/swine/Wyoming/A01444562/2013 (sw/WY/13), A/swine/Minnesota/A01432544/2013 (sw/MN/13), A/swine/Indiana/A01202866/2011 (sw/IN/11), and A/swine/Texas/A01785781/2018 (sw/TX/18). All swine influenza viruses were grown in specific pathogen-free embryonated chicken eggs, quantified by hemagglutination assay (HA) and $TCID_{50}$, and quantified virus from the chorioallantoic fluid was stored at -80°C for subsequent assays.

Madin-Darby Canine Kidney-London strain (MDCK-Ln) cells used in $TCID_{50}$ assays were cultured in DMEM supplemented with 5% FBS and 1% penicillin-streptomycin at 37°C, 5% CO2 in a humidified incubator.

2.3 Animal immunization and sampling

Production of the Epigraph immunogens has been described previously (41). Briefly, all unique and full-length swine H3 strains as of April 25th, 2017 were downloaded from the Influenza Research Database, aligned using ClustalW, and submitted to the Epigraph Vaccine Designer at the Los Alamos National Laboratories with the following parameters: cocktail size: 3, epitope length: 9. On study day 0 (D0), pigs in the Ad-swH3-Epi group were intramuscularly immunized with 10^{11} viral particles (vp) (the cocktail of three epigraph immunogens at equal ratios ($3.33x10^{10}$ vp per epigraph) to a total of 10^{11} vp (41)) diluted in 1 mL DPBS, then boosted three weeks after the prime immunization (D21). Pigs in the FluSure XP group were intramuscularly immunized according to manufacturer's instructions with 2 mL on D0, then boosted on D21. A group of five pigs served as a negative control group and received a 2 mL intramuscular injection of DPBS on D0 and D21. Whole blood was collected by external jugular vein puncture every 7 days for the first month, every 30 days for the subsequent 5 months, and 5 days after influenza challenge. Serum was isolated from whole blood using BD Vacutainer Separator Tubes (Becton Dickinson) on D0, D7, D14, D21, D28, D60, D90, D120, D150, and D180 post-vaccination (Figure 1A). PBMCs were isolated on D0, D21, D60, D120, D150, D180, and 5 days post infection (5dpi) by diluting whole blood 1:1 with sterile DPBS then gently layering diluted blood on top of lymphocyte separation media (Corning #25072CV) and centrifuging diluted blood at 400g for 30 minutes. The PBMC layer was collected, washed with RPMI containing 5% FBS and 1% penicillin streptomycin, and residual red blood cells were lysed with ACK lysis buffer for 5 minutes before quenching with complete RPMI. Cells were resuspended in complete RPMI, counted on a

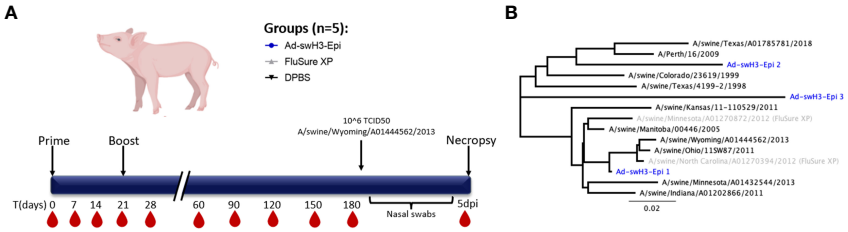

FIGURE 1
Study timeline and phylogenetic analysis of strains used in study. **(A)** Groups of three-week-old swine (n=5/group) were immunized with Ad-swH3-Epi, FluSure XP, or DPBS as a negative control group at D0 and boosted at D21. Blood samples were collected every 7 days for the first month, then every 30 days for the subsequent 5 months for a total duration study of 6 months. Six months after the initial immunization all pigs were subjected to challenge with a divergent Cluster IV(A) IAV-S isolate, A/swine/Wyoming/A01444562/2013. Nasal swabs were taken every other day after challenge, then at 5 days post infection pigs were humanely bled, euthanized, and samples were taken for analysis. **(B)** Phylogenetic divergence of strains used for serological analysis, T cell analysis, and challenge (black) compared to Epigraph immunogens (blue) and strains incorporated in FluSure XP WIV vaccine (grey).

Coulter Counter (Beckman Coulter), then cryopreserved in freezing medium containing 50% RPMI, 45% FBS, and 5% DMSO.

2.4 Hemagglutination inhibition assay

Sera from whole blood was used for hemagglutination inhibition (HI) activity according to previously described methods (44). Briefly, sera were treated in a 1:3 ratio with receptor destroying enzyme (RDE; Denka Seiken) at 37°C for 18 hours. RDE was then heat-inactivated at 56°C for 1 hour, and serum was diluted to a final 1:10 dilution in sterile DPBS. Sera were then serially diluted 2-fold in a 96-well V-bottom plate, and 4 hemagglutination units (HA) of representative swine influenza virus from Cluster I, II, IV, IV(A), IV(B), IV(C), IV(F), or the 2010.1 human-like cluster (Figure 1B) added to the serum dilutions and incubated at room temperature for 1 hour. 50µL of 0.5% chicken red blood cells was added to each well and hemagglutination patterns were read after 30 minutes.

2.5 IgM and IgG antibody isotyping by recombinant protein ELISA

IgM and IgG antibody responses were analyzed against A/Perth/16/2009 HA protein by ELISA. Briefly, flat-bottomed 96-well plates (Immunolon 4 HBX; VWR) were coated overnight at 4°C with 100µL (150ng/well) of recombinant A/Perth/16/2009 HA protein (NR-49734) diluted in carbonate/bicarbonate coating buffer. Wells were washed 4 times with PBS containing 0.1% Tween 20 (PBS-T) then blocked at room temperature with blocking buffer (10% skim milk diluted in PBS-T) for 2 hours. Sera samples were heat-inactivated at 56°C for 1 hour, then serially diluted two-fold in 5% skim milk in PBS-T and 100µL of each dilution was added to the coated wells and incubated at room temperature for 1 hour. Plates were washed 5 times with PBS-T then HRP-conjugated goat anti-pig IgM (Cat. No. AAI48P; BioRad) or IgG (Cat. No. AHP865P; BioRad) antibody diluted to 1:5000 in 5% skim milk in PBS-T were added to wells and incubated at room temperature for 30 minutes. Plates were washed 5 times with PBS-T then developed with 1-Step Ultra TMB-ELISA (Thermo Fisher) and the reaction was stopped with 2M sulfuric acid. Absorbance values were evaluated at OD450 on a SpectraMax i3x Multi-Mode automatic microplate reader (Molecular Devices). Endpoint titers were calculated as equivalent to the mean plus three standard deviations of the OD values from the PBS-immunized control animals at each timepoint.

2.6 IFN-γ ELISPOT analysis

PBMCs were analyzed for T cell responses by IFN-γ ELISpot assay. An overlapping peptide array spanning the entire length of A/swine/Ohio/11SW87/2011 HA protein was synthesized by Genscript as individual 17-mer peptides with 10 amino acid overlaps. 96-well polyvinylidene difluoride-backed plates (MultiScreen-IP, Millipore) were coated with anti-porcine IFN-γ mAb pIFN-γ (5µg/mL; Mabtech) at 4°C overnight. Plates were washed three times with DPBS then blocked with RPMI containing 10% FBS and 1% penicillin and streptomycin for 2 hours at 37°C. Single-cell suspensions of $2.5x10^5$ PBMCs 2.5×10^5 cells were stimulated overnight at 37°C, 5% CO2 with 5µg/mL peptide, concanavalin A (ConA; 5µg/mL), or RPMI, in duplicate. After overnight incubation, plates were washed three times with DPBS + 0.10% Tween-20, then incubated at room temperature with 50µL of biotinylated anti-porcine IFN-γ mAb P2C11 (1:1000; Mabtech). Plates were washed six times with DPBS + 0.10% Tween-20 then incubated with 100µL of 1:1000 streptavidin-alkaline phosphatase conjugate (1:1000 dilution; Mabtech). After 1hr incubation at room temperature, plates were washed six times with DPBS + 0.10% Tween-20 then developed by adding 100µL of BCIP/NBT (Plus) alkaline phosphatase substrate (Thermo Fisher). Development was stopped by washing several times with dH2O after spots appeared in the ConA positive control wells, the plates were air dried, and spots were enumerated on an automated ELISpot plate reader (Cellular Technology Ltd.). Results are expressed as number of spot-forming units (SFU) per 10^6 PBMCs.

2.7 Influenza challenge and tissue collection

Six months after the initial immunization (D180) all swine were subjected to split intratracheal and intranasal inoculation (45) of a divergent IAV-S isolate under telazol (Zoetis), zolazepam (Zoetis), ketamine (Zoetis), and xylazine (Vet One) induced anesthesia. Swine were inoculated intratracheally with 2mL of $2.5x10^5$ $TCID_{50}$/mL of A/swine/Wyoming/A01444562/2013 (sw/WY/13), and intranasally with 1mL $2.5x10^5$ $TCID_{50}$/mL of virus per nostril for a total dose of $1x10^6$ $TCID_{50}$ of virus. Swine were inoculated through both the intratracheal and intranasal route to ensure infection of both the upper and lower respiratory tract. Clinical disease was observed for the subsequent 4 days and scored by an experience veterinarian blinded to the treatment groups according to a previously established scoring system (46). Rectal temperatures were collected on 0-, 1-, 2-, 3-, and 4- days post infection and nasal swabs were collected on 1-, 3-, and 5-days post infection. Nasal swabs were placed in UniTranz-RT Universal Transport Medium (Puritan) then aliquoted and stored at -80°C. At 5dpi, all animals were euthanized with an overdose of sodium pentobarbital Fatal-Plus (Vortech), and lungs were removed for a bronchioalveolar lavage (BAL) wash and infectious virus quantification. One-centimeter-thick tissues were samples from the middle trachea, apical, middle, and caudal right lung was excised and stored in 10% neutral buffered formalin for H&E staining, histopathological analysis, and IHC against the conserved nucleoprotein (NP) viral antigen using a rabbit anti-Influenza A virus NP antibody (Cat. No. PA5-32242; Invitrogen). The formalin-fixed tissues were processed routinely for histologic examination after 72 hours fixation, sectioned at 4-5µm, and stained with hematoxylin and eosin and examined by an ACVP certified pathologist according to previously established scoring protocols (47). Tracheas were scored as 0, normal; 1, focal inflammation with cilia present; 2, diffuse inflammation and multi focal cilia loss; 3, widespread inflammation and cilia loss. Lung consolidation percentage was scored for apical, middle, and caudal lobes. Score were 0 normal, 1 <5%, 1.5 5-25%, 2.0 25-50%, 2.5 50-75%, 3.0 >75%. Scoring for bronchiolar necrosis, bronchiolar inflammation, septal inflammation, and perivascular cuffing was done on the lung sections with the highest consolidation score from each pig. The score 0-3 were used and reflected percentages of lung affected as described for other histologic lesions. IAV-S NP Immunohistochemistry distribution was scored on trachea and the apical lung lobe. Scores were 0 no stain, 1 trachea only, 2 trachea + bronchi, 3 trachea + bronchioles, and 4 trachea + bronchi + bronchioles.

2.8 RT-qPCR analysis in nasal swabs

Viral RNA was extracted from nasal swabs at 1-, 3-, and 5-dpi using the PureLink Viral RNA/DNA Extraction Kit according to manufacturer's instructions (Invitrogen). Reverse-transcription qPCR was performed using the Luna Universal Prone One-Step RT-qPCR Kit (NEB) and analyzed on a QuantStudio 3 Real-Time PCR System (Applied Biosystems). The following cycling conditions were used: 55°C for 30 mins, 95°C for 2 mins, and 40 cycles of 95°C for 15 secs and 60°C for 30 secs. The universal primer-probe set for Influenza A Virus was used (BEI Resources, NR-15593, NR-15594, and NR-15595) and viral RNA quantification was calculated based on a standard curve created using RNA extracted from a known quantity of infectious virus of A/swine/Wyoming/A01444562/2013.

2.9 Tissue culture infectious dose

Presence of infectious virus in nasal swabs and bronchioalveolar lavage (BAL) was determined by titration on MDCK-Ln cells. Nasal swab and BAL samples were serially diluted in DMEM containing 5% FBS and 1% penicillin streptomycin then $2x10^5$ cells were added to virus dilutions and incubated for 24 hours. The next day, plates were washed twice with DPBS and DMEM containing 2µg/mL of TPCK-trypsin was added before incubating plates for 72 hours. After three days of incubation, 50µL of 0.5% chicken red blood cells were added and agglutination patterns were read after a 45-minute incubation at room temperature. All nasal swab samples and BAL samples were independently run with four technical replicates per sample.

2.10 Statistical analysis

All statistical analysis and data representation was carried out using GraphPad Prism 9. Data are expressed as the mean with standard error (SEM). HI titers, ELISA endpoint titers, T cell analysis, and $TCID_{50}$ results were analyzed by one-way ANOVA with Tukey's multiple comparisons. A p value <0.05 was considered statistically significant ($^*p < 0.05$; $^{**}p < 0.01$; $^{***}p < 0.001$; $^{****}p < 0.0001$).

3 Results

3.1 Ad-swH3-epigraph vaccination generates rapid and durable antibody responses

To evaluate the onset and duration of antibody responses, groups of three-week-old cross-bred Yorkshire pigs were intramuscularly immunized with Ad-swH3-Epi and responses over time were compared to swine immunized with the commercial vaccine, FluSure XP, or DPBS as a negative control immunization group (Figure 1A). The breadth and duration of antibody responses were examined by hemagglutination inhibition (HI) assay against a panel of divergent IAV-S strains that represent Cluster I, Cluster II, Cluster IV (A-F), and the human-like Cluster of H3 IAV-S (Figure 1B). Immunization with FluSure XP and Ad-swH3-Epi induced moderate HI antibody responses against isolates representing Cluster I (Figure 2A) and Cluster II (Figure 2B) IAV-S. The responses to

10.3389/fimmu.2023.1143451

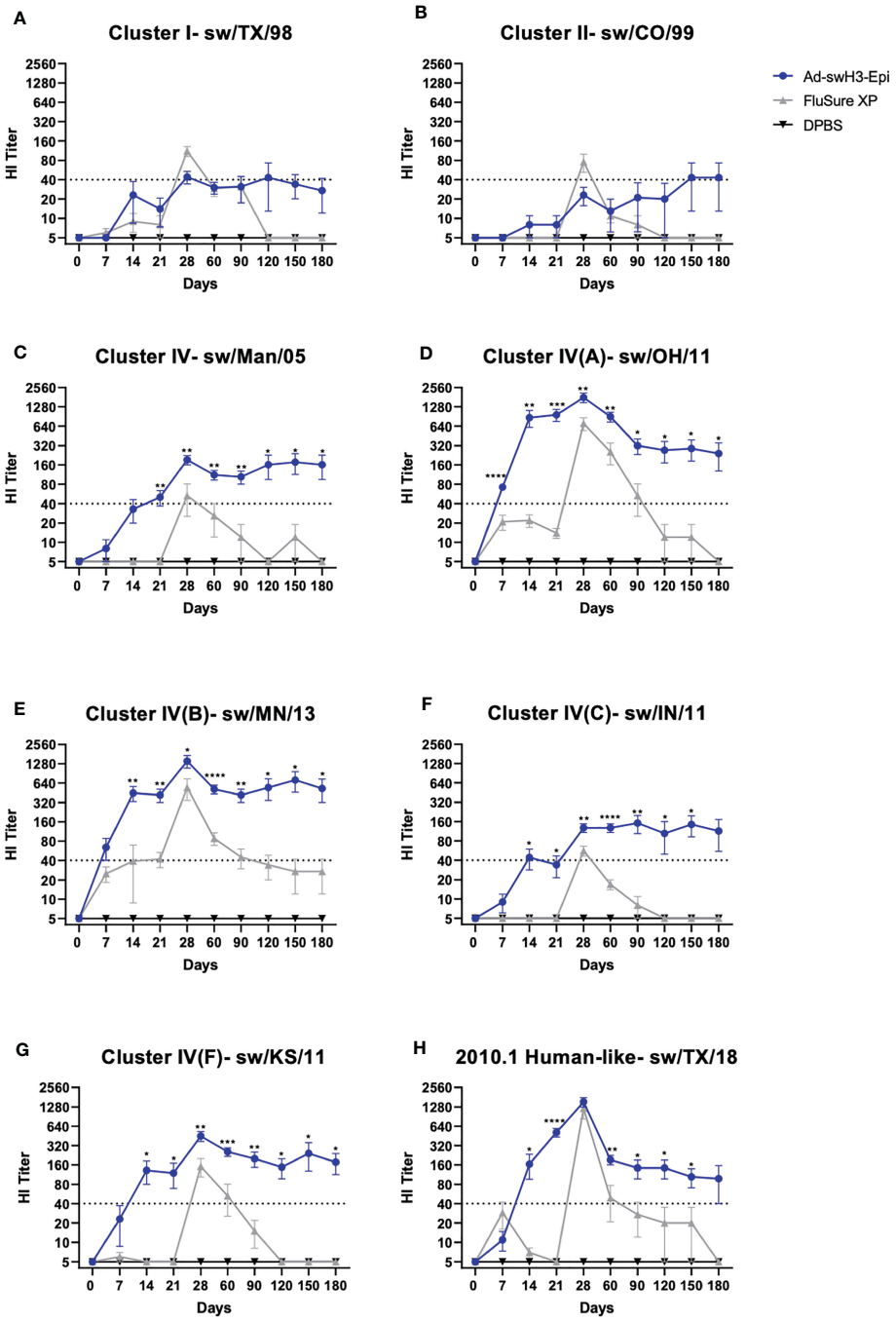

FIGURE 2
Vaccination with Ad-swH3-Epi rapidly induces durable antibody responses. Cross-reactive antibodies against Cluster I, Cluster II, and Cluster IV(A-F) and the human-like Cluster swine H3 strains were screened by hemagglutination inhibition (HI) assay. **(A)** Cluster I- sw/TX/98, **(B)** Cluster II- sw/CO/99, **(C)** Cluster IV- sw/Man/05, **(D)** Cluster IV(A)- sw/OH/11, **(E)** Cluster IV(B)- sw/MN/13, **(F)** Cluster IV(C)- sw/IN/11, **(G)** Cluster IV(F)- sw/KS/11, and **(H)** 2010.1 human-like Cluster- sw/TX/18. A protective titer of ≥1:40 is indicated as a dashed line on each graph. Data are represented as the mean ± SEM. (n=5; one-way ANOVA with Tukey's multiple comparison; *$p < 0.05$, **$p < 0.01$, ***$p < 0.005$, ****$p < 0.0001$).

these cluster representatives exhibited similar kinetics of development and retraction over time with no statistically significant differences observed between FluSure XP and Ad-swH3-Epi immunized animals at any timepoints. Analysis of more recently circulating isolates from Cluster IV, Cluster IV subclusters A-F, and the 2010.1 cluster "human-like" IAV-S revealed that, while FluSure XP induced cross-reactive antibody responses after boost immunization, vaccination with Ad-swH3-Epi was able to rapidly elicit protective HI titers, represented by endpoint titers _ 40 (48–50), as early as two weeks after prime immunization (D14). HI titers induced by Ad-swH3-Epi

vaccination were significantly higher than those observed in the FluSure XP immunized animals by 14 days post immunization (Figures 2C-H). Peak responses in the Ad-swH3-Epi immunized group were seen one week after the boost immunization (D28), and these responses were significantly higher than vaccination with FluSure XP against representative IAV-S isolates from Cluster IV (Figure 2C), Cluster IV(A) (Figure 2D), Cluster IV(B) (Figure 2E), Cluster IV(C) (Figure 2F), and Cluster IV(F) (Figure 2G). Notably, while protective responses _ 40 were observed after boosting in the FluSure XP immunized group, these responses rapidly dropped two months after the boost immunization (D90) to at or below the protective titer, and responses against sw/Man/05, sw/OH/11, sw/IN/11, sw/KS/11, and sw/TX/18 dropping to undetectable levels by the completion of the 6-month analysis. In comparison, pigs immunized with Ad-swH3-Epi had significantly more durable responses, with HI antibody levels gradually retracting over the course of 6 months (D180) and responses against sw/Man/05, sw/OH/11, sw/MN/13, sw/IN/11, sw/KS/11, and sw/TX/18 persisting at a level of _ 40 (Figures 2C-H) by the end of the 6-month study. These data suggest an exciting result because the average lifespan of a standard market pig is 6 to 7 months of age, and our vaccine demonstrates the ability to induce lasting protection against divergent IAV-S, potentially lasting the entire lifespan of market animals.

3.2 Ad-swH3-epigraph induces robust and durable T cell responses

T cell responses have been shown to play an important role in viral clearance during influenza infection (51–53). In congruence with this, we evaluated the onset and duration of circulating T cell responses by IFN-γ ELISPOT against a Cluster IV(A) strain, A/swine/Ohio/11SW87/2011. An overlapping peptide array consisting of 17-mer peptides with 10 amino acid overlap was constructed, and responses were considered positive if greater than 50 spot forming units (SFU) were obtained per million cells analyzed (54). By D21, vaccination with Ad-swH3-Epi resulted in 7.6-fold higher levels of IFN-γ secreting T cells compared to FluSure XP immunized animals (mean 838 SFU/10^6 cells compared to mean 110 SFU/10^6 cells,

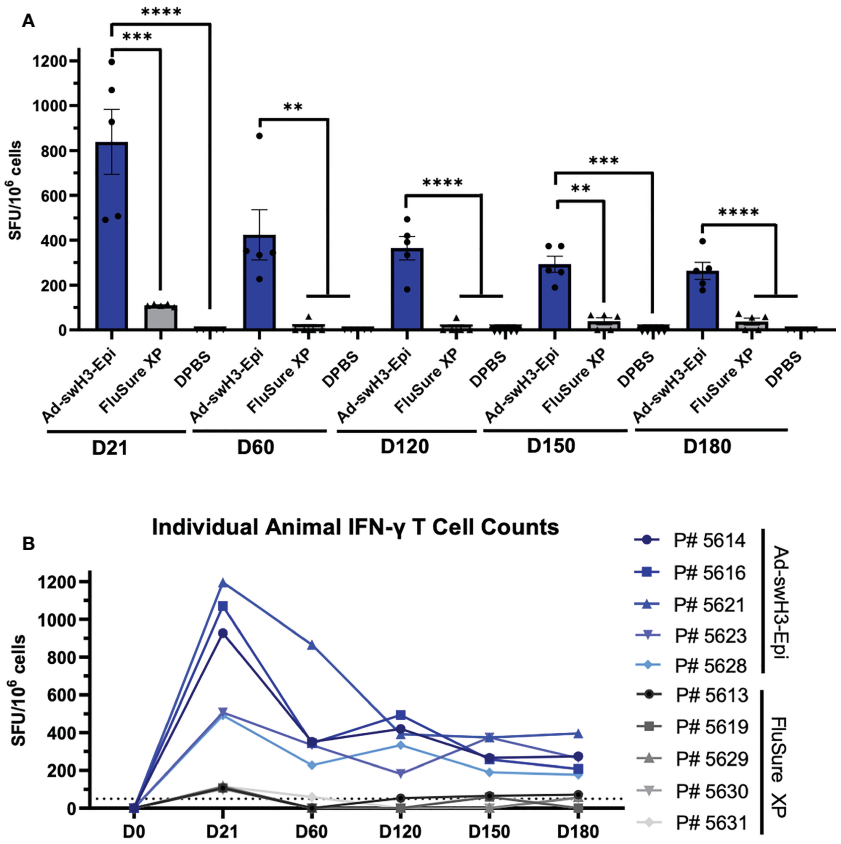

FIGURE 3
Vaccination with Ad-swH3-Epi elicits lasting T cell responses. PBMCs were isolated from peripheral blood at D0, D21, D60, D120, D150, and D180 and screened for antigen-specific T cells by IFN-γ ELISPOT. PBMCs were stimulated with an overlapping peptide array containing individual 17-mer peptides with 10 amino acid overlap spanning the entire length of A/swine/Ohio/11SW87/2011 HA protein. Peptide responses of ≥ 50 spot forming units (SFUs) per million PBMCs were considered positive. **(A)** Mean total T cell responses from D21 to D180 after vaccination with Ad-swH3-Epi, FluSure XP, or DPBS. Data are presented as the mean ± SEM (n=5 pigs/group; one-way ANOVA with Tukey's multiple comparison; $^{**}p < 0.01$, $^{***}p < 0.005$, $^{****}p < 0.0001$). **(B)** T cell responses of individual animals in Ad-swH3-Epi (blue) and FluSure XP (grey) immunized groups analyzed over the study duration.

respectively) (Figure 3A). While the circulating T cells of the pigs vaccinated with FluSure XP rapidly declined to undetectable or nearly undetectable levels by D60, circulating T cells induced by vaccination with Ad-swH3-Epi gradually retracted over time (D60 mean: 425 SFU/10^6 cells; D120 mean: 364 SFU/10^6 cells; D150 mean: 292 SFU/10^6 cells; D180: 264 SFU/10^6 cells) (Figure 3A), consistent with retraction of T cells in the absence of antigen stimulation over time. Individual analysis of each pig in the Ad-swH3-Epi and FluSure XP immunized groups showed peak responses at D21 for both groups, and all pigs in the Ad-swH3-Epi group maintained detectable T cell responses by D180 (Figure 3B). As expected, pigs in the DPBS immunization group did not produce any antigen-specific T cell responses (Figure 3A). Overall, we observed that vaccination with Ad-swH3-Epi induced strong circulating T cell responses that were significantly higher and more durable than those induced by vaccination with FluSure XP.

3.3 Ad-swH3-epigraph elicits faster and more robust class-switched IgG levels against a divergent human IAV hemagglutinin

We next assessed the kinetics of antibody class switching to detect antigen-specific IgM and IgG antibodies in the peripheral blood. Antibodies from Ad-swH3-Epi, FluSure XP, and DPBS immunized pigs were screened by ELISA against a divergent human H3 IAV recombinant HA protein, A/Perth/16/2009. We observed a similar onset and duration of IgM antibody responses mounted between the Ad-swH3-Epi and FluSure XP immunized animals with no statistically significant differences in IgM antibody levels at D7, D14, D21, or D28 (Figure 4A), showing that the rate of IgM antibody development was not different between these two vaccination platforms. DPBS immunized animals did not develop any IgM antibody responses, as expected (Figure 4A). However, when we assessed the levels of class-switched antigen-specific IgG antibody levels, we observed that pigs vaccinated with Ad-swH3-Epi developed antigen-specific IgG antibodies sooner than those observed in the FluSure XP immunized pigs (Figure 4B). Similarly, these responses were elicited at significantly higher levels than those induced after vaccination with FluSure XP, which retracted by D90 and were not significantly higher than unimmunized pigs from D90 to D150. The similar kinetics of IgM levels between Ad-swH3-Epi and FluSure XP immunized pigs but differences in mounted of antigen-specific IgG levels is likely due to a stronger T cell development in Ad-swH3-Epi vaccinated pigs (Figure 3), which are crucial in triggering class-switch recombination and strong plasma cell development and subsequently IgG antibody development (55, 56). These results suggest that development of robust and broadly reactive IgG antibody responses can be achieved by vaccination with Ad-swH3-Epi, and that these responses are significantly higher than those observed with the whole inactivated virus vaccine, FluSure XP.

3.4 Ad-swH3-epigraph vaccination reduces viral shedding after heterologous challenge

We next wanted to assess the ability of Ad-swH3-Epi and FluSure XP to provide protection against heterologous challenge six months after the initial vaccination (D180). This objective is particularly important because the average time to grow and procure a market pig is typically 6-7 months (57) and, given that IAV-S affects swine at all stages of pork production, providing protection against challenge for six months could greatly impact pork production outcomes and limit the spread of IAV-S among pigs during production. All pigs were challenged with 10^6 $TCID_{50}$ of a Cluster IV(A) IAV-S isolate, A/swine/Wyoming/A01444562/2013 (Figure 1A), by split intratracheal and intranasal inoculation (45) under anesthesia. This strain was chosen based on epidemiological analysis of recently circulating strains within the United States (9) and may represent isolates that swine could interface in the field.

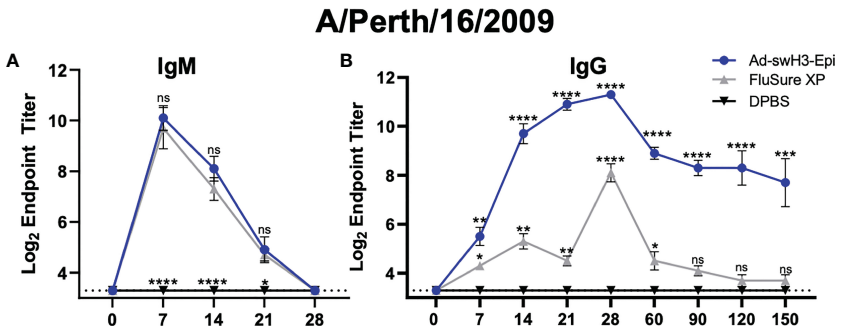

FIGURE 4
Vaccination with Ad-swH3-Epi allows for more robust class switching of IgM to IgG against a human H3 IAV strain. Sera from vaccinated pigs were isolated and used for antibody isotyping of IgM **(A)** and IgG **(B)** over time. Endpoint titers are represented as $\log_2$ of the reciprocal of the highest sera dilution that were positive against A/Perth/16/2009 recombinant protein. Samples were considered positive if the OD value was three standard deviations above the mean OD values measured from negative control immunized animals. Data are represented as the mean ± SEM (n=5 pigs/group; one-way ANOVA with Tukey's multiple comparison; *p<0.05, **$p < 0.01$, ***$p < 0.005$, ****$p < 0.0001$). All statistical significance shown in the Ad-swH3-Epi group are compared to FluSure XP immunized pigs. All statistical significance shown in the FluSure XP group are compared the DPBS immunized pigs. ns, not significant.

Clinical disease was scored by an experienced veterinarian blinded to the treatment groups and rectal temperatures were collected daily. No significant differences in clinical disease or change in body temperature was observed between the three vaccination groups (Supplementary Figure 1A, B), which is likely due to the advanced age of the pigs at the time of challenge (45). Nasal swabs were collected at 1 day post infection (dpi), 3dpi, and 5dpi. Presence of viral RNA was assessed by RT-qPCR and quantification of infectious virus was enumerated by $TCID_{50}$. At 1dpi, 3dpi, and 5dpi similar levels of viral RNA was detected among all groups, with no statistically significant differences observed at any timepoint (Figure 5A). When analyzing the presence of infectious virus by $TCID_{50}$ a trend of lower levels of infectious virus were seen at 1dpi in Ad-swH3-Epi group compared to FluSure XP and DPBS immunized animals, though this did not reach statistical significance (Figure 5B). Similar levels of infectious virus were present at 3dpi, with no statistically significant differences observed between the three immunization groups. Importantly, at 5dpi pigs vaccinated with Ad-swH3-Epi showed to have significantly lower presence of infectious virus in nasal secretions compared to DPBS immunized pigs, while FluSure XP immunized pigs had similar levels of infectious virus as DPBS immunized pigs (Figure 5B). This result suggests that vaccination with Ad-swH3-Epi can resolve viral shedding earlier and lower the risk of transmission of infectious virus through nasal secretions.

3.5 Ad-swH3-epigraph reduces microscopic lesion development, lowers presence of infectious virus and viral antigen in the lungs, and provides strong reactivation of circulating antigen-specific T cells after challenge

Lastly, all pigs were humanely bled and euthanized at 5 days post infection for histopathological analysis of lung and tracheal tissues, quantification of viral antigen and infectious virus in the lungs, and evaluation of recall T cell responses. Gross lesions were observed on the lungs of one FluSure XP immunized pig (Supplementary Figure 2) and were not present in any other vaccine group. Histopathological analysis of trachea samples (Figure 6A) showed that pigs vaccinated with Ad-swH3-Epi displayed healthy submucosal tissues with minimal infiltration of inflammatory cells and respiratory epithelial cells that were columnar and ciliated. In contrast, vaccination with FluSure XP resulted in inflammatory cell infiltrates into the submucosa and mucosal epithelium with rounded and cuboidal respiratory epithelial cells and reduction in cilia at the epithelial surface. DPBS immunized pigs showed significant inflammatory cell infiltrates coupled with disrupted and thinned surface epithelium and complete loss of cilia. This resulted in a trend of decreased tracheitis scoring in the Ad-swH3-Epi group compared to FluSure XP and DPBS immunized pigs (Figure 6D). Further analysis of sectioned bronchioles revealed that

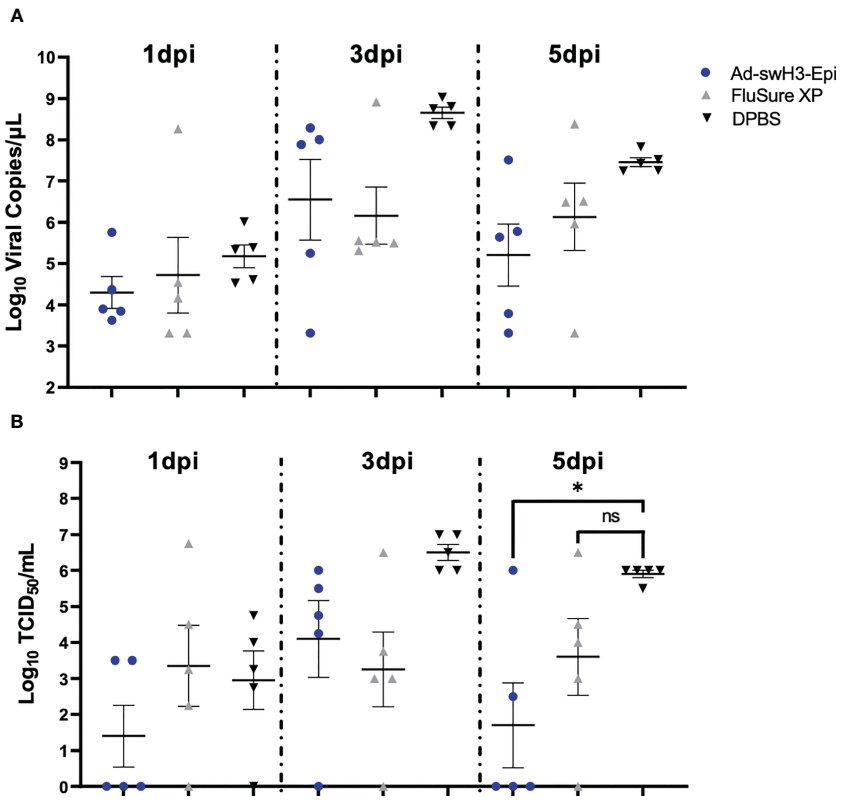

FIGURE 5
Ad-swH3-Epi reduces viral shedding at 5 days post infection. Swine were challenged with 10^6 $TCID_{50}$ of A/swine/Wyoming/A01444562/2013 by split intratracheal and intranasal inoculation. Nasal swabs were collected at 1-, 3-, and 5-days post infection and amount of viral RNA was quantified by RT-qPCR **(A)** and levels of infectious virus were measured by $TCID_{50}$ **(B)**. Data are presented as the mean ± SEM (n=5 pigs/group; one-way ANOVA with Tukey's multiple comparison; *p<0.05). ns, not significant.

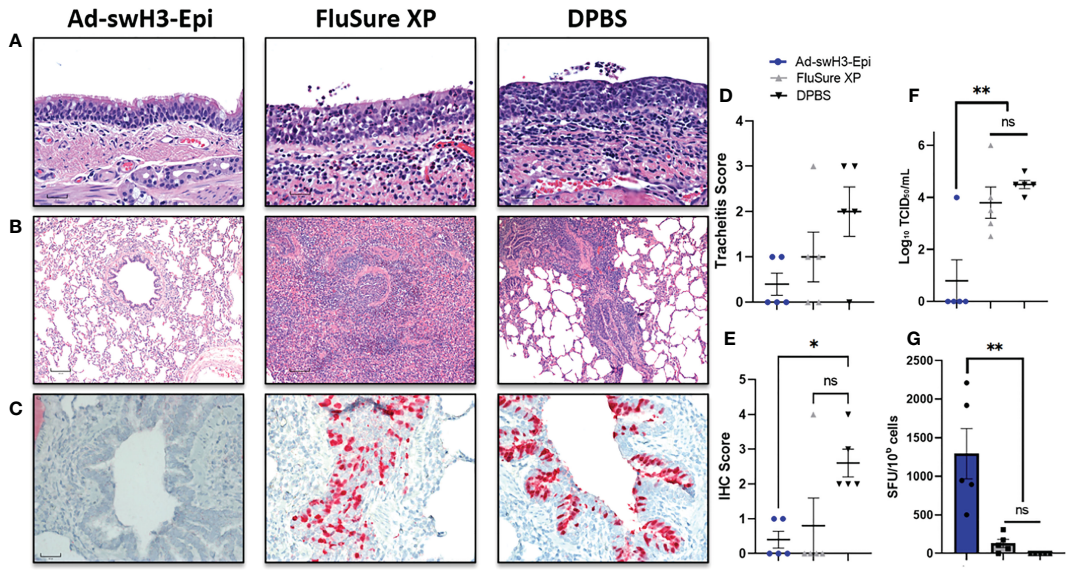

FIGURE 6
Ad-swH3-Epi provides protection against challenge with a divergent IAV-S. Five days after challenge lungs and tracheas were removed for histopathological analysis. H&E staining of representative trachea samples are shown **(A)** and representative bronchioles from lungs are shown in **(B)**. Immunohistochemistry of bronchioles against the conserved NP viral protein **(C)**. Tracheas shown in **(A)** were scored for tracheitis by a board-certified pathologist blinded to the treatment groups **(D)**. IHC distribution was recorded; higher scores correlate with deeper pulmonary infection **(E)**. Levels of infectious virus present in the bronchioalveolar lavage was enumerated by tissue culture infectious dose ($TCID_{50}$) **(F)** and recall T cell responses were analyzed by IFN-γ ELISPOT **(G)**. Scale bars in **(A–C)** are 30μM, 120μM, and 60μM, respectively. Data are presented as the mean ± SEM (n=5; one-way ANOVA with Tukey's multiple comparison; $*p < 0.05$ and $**p < 0.01$). ns, not significant.

vaccination with Ad-swH3-Epi was able to protect against bronchiolar necrosis, inflammation, and perivascular cuffing (Figure 6B). In comparison, FluSure XP and DPBS immunization demonstrated significant suppurative bronchitis and inflammatory cell infiltration into the bronchiole (Figure 6B). Immunohistochemical (IHC) analysis against the conserved influenza nucleoprotein (NP) antigen showed many viral infected cells within the epithelium of bronchi and bronchioles of pigs immunized with FluSure XP or DPBS (Figure 6C) leading to a higher IHC score in these groups (Figure 6E). A bronchioalveolar lavage (BAL) was performed during necropsy to evaluated levels of infectious virus present in the lungs by $TCID_{50}$. High titers of infectious virus were present in the BAL obtained from pigs immunized with FluSure XP and DPBS (FluSure XP mean: $10^{3.8}$ $TCID_{50}$/mL; DPBS mean: $10^{4.5}$ $TCID_{50}$/mL) (Figure 6F). In contrast, only one pig in the Ad-swH3-Epi immunization group had detectable levels of infectious virus present in the BAL (Ad-swH3-Epi mean: $10^{0.8}$ $TCID_{50}$/mL) while all other pigs had cleared the virus from the lungs by 5 days post infection (Figure 6F). Finally, we evaluated the recall T cell responses elicited after challenge by assessing levels of antigen-specific T cells present in the peripheral blood at 5dpi by IFN-γ ELISPOT against the same overlapping peptide array previously used to assess the development and duration of T cell responses after vaccination (Figure 3). We observed a strong reactivation of circulating antigen-specific T cell responses (Figure 6G) that were higher than those observed at D21 after vaccination (Figure 3A) (D21 mean: 838 SFU/10^6 and 5dpi mean: 1293 SFU/10^6 cells). This demonstrates that antigen encounter after challenge was able to robustly reactivate memory T cells and likely played a crucial role in the clearance of viral infected cells after challenge. Collectively, we have demonstrated that the immune responses elicited after immunization with Ad-swH3-Epi can protect against challenge with a heterologous IAV-S isolate 6 months after vaccination and this protection is significantly better than the protection observed after immunization with WIV vaccine, FluSure XP.

4 Discussion

In this study, we characterized the onset and duration of immune responses elicited after vaccination with Ad-swH3-Epigraph and compared these responses to a commonly used WIV vaccine, FluSure XP. An ideal vaccine for use against IAV-S in pigs would elicit lifelong responses that provide protection against a broad range of antigenically distinct viruses. However, current methods of vaccination fail to provide durable and broadly protective responses and can induce vaccine-associated enhanced respiratory disease (VAERD) after heterologous challenge. Here, we demonstrate that vaccination with Ad-swH3-Epi rapidly induced robust and durable antibody responses against recently circulating IAV-S isolates that remained above protective levels (_ 40) for 6 months after vaccination. In comparison, FluSure XP did not induce protective titers until after boost immunization, corroborating previously identified results (41). Further, antibody levels in the FluSure XP immunized pigs quickly diminished to below protective titers 30-60 days after boost vaccination, indicating that this vaccine platform may induce a short duration of antibody-mediated protection. The duration of these responses has significant

clinical relevance, as the average lifespan of a standard market pig in the pork industry is 6-7 months of age, and IAV-S affects swine at all stages of pork production. Interestingly, we also saw modest antibody responses against the representative Clade I and Clade II IAV-S isolates, sw/TX/98 and sw/CO/99, in the Ad-swH3-Epi immunization group. Indeed, we have previously observed lower responses to these clades (41), which is likely due to the limited representation of these strains in the Epigraph immunogen design.

Importantly, we also observed robust and durable antigen-specific T cell development after vaccination with Ad-swH3-Epi. While FluSure XP immunized pigs developed modest T cell responses that quickly retracted by D60, Ad-swH3-Epi was able to induce lasting responses that were detectable 6 months after vaccination. Given that T cells play a pivotal role in the clearance of viral infected cells, B-cell activation, and class-switching during affinity maturation, we hypothesize that the strong induction of T cell responses likely played an important role in the development of class-switched antigen-specific IgG antibody levels as well as the viral clearance observed after challenge. While we observed similar kinetics of IgM development between the two immunization groups, we also observed reduced levels of class-switched IgG antibodies with a delayed onset in the FluSure XP immunized pigs compared to Ad-swH3-Epi immunized animals. This observation, coupled with the kinetics of robust T cell activation, suggests that the enhanced levels and duration of antibody responses seen in the Ad-swH3-Epi group were due to a balanced induction of both B and T cell responses.

Recent epidemiological analysis of U.S. swine herds indicates high circulation of Cluster IV(A) H3 IAV-S (9). In accordance with this, we chose to challenge the pigs with a high dose of divergent IAV-S isolate, A/swine/Wyoming/A01444562/2013, 6 months after the initial vaccination. We hypothesized this challenge study design closely recapitulates relevant field conditions. Further, this isolate was not screened for antibody or T cell responses prior to challenge to prevent bias in choosing the challenge strain. Analysis of nasal swabs indicated that vaccination with Ad-swH3-Epi was able to reduce the duration of viral shedding, as 3/5 pigs had completely abrogated levels of infectious virus present in the nose by 5dpi. This is important because reduction of infectious virus in the nose can reduce transmission and spread of IAV-S between pigs within a herd and lower the potential of zoonotic transmission of IAV-S into humans at swine-to-human interfaces (58). Further analysis of the lungs and trachea indicated that the durable immune responses elicited by Ad-swH3-Epi immunization was able rapidly clear infected cells, as pigs exhibited reduce levels of tracheitis, healthy bronchioles, and reduced viral antigen detected by IHC. This was coupled with significant reduction of infectious virus in the lungs by 5dpi. We further characterized that influenza challenge was able to activate robust recall T cell responses in the Ad-swH3-Epi immunized animals, corroborating the crucial role of T cells during protection against IAV-S in swine. Here, we observed that Ad-swH3-Epi induced broad and durable protection that was significantly superior to a commonly used WIV vaccine, FluSure XP.

Recent advances in gene delivery by viral vectors have paved the way for improved safety and immunogenicity profiles of viral vectors. In light of the recent COVID-19 pandemic, two adenoviral-vectored vaccines have recently made it to the market for use in humans (59–61). Utility of a species C human adenovirus type 5 (Ad5) viral vector has been well described in both humans and swine against a variety of infectious diseases. Notably, the tissue tropism of Ad5 in swine has been identified as lung epithelial cells (62, 63) and pulmonary intravascular macrophage cells (64, 65), which is an optimal location to elicit both antibody and cellular-mediated immune responses against a respiratory pathogen such as influenza. Despite the substantial advances in adenoviral-vectored vaccine development, there is still a concern of dampened responses due to preexisting immunity to the delivered vector after boosting with a homologous adenovirus serotype. By utilizing a human adenovirus as our vaccine vector, we minimize the risk of swine having previously been exposed to the vector through natural infection mechanisms. Further, while we observed peak antibody responses after boosting, it is possible that boosting with a heterologous adenovirus serotype would have elicited higher levels of antibody responses and T cell responses. Additional studies investigating heterologous adenovirus prime-boosting strategies in swine are needed to fully elucidate the potential to induce stronger responses than those observed in this study.

The results obtained in this study have significant impact to the field of vaccine development and details the kinetics of immune responses elicited after vaccination with WIV vaccines compared to viral-vectored vaccination strategies. Notably, standard methods of vaccine efficacy testing typically analyze and report short durations of immune responses and perform *in vivo* challenges shortly after vaccination during peak responses. Here, we chose to sequentially analyze immune responses in a longitudinal study to mitigate possible biases in vaccine efficacy testing. However, completing a longitudinal study in swine can have several limitations. One such limitation is the rapid growth of domestic swine, which requires advanced containment facilities, enhanced biocontainment practices after challenge, and specially trained personnel for animal handling. An additional limitation is that older swine have been characterized to be less susceptible to IAV-S infection compared to younger pigs (45). To overcome these challenges, we chose to use a high dose of IAV-S inoculation to ensure adequate infection in our *in vivo* infection model and were able to collect infectious virus from DPBS immunized pigs at 5dpi, indicating that these older pigs were susceptible to IAV-S infection. A final limitation of this study was that we were only able to perform a challenge using one virus. Though our challenge strain was chosen to represent recently circulating strains, reverse-zoonotic transmission of IAV from humans to swine has established a stable cluster of IAV-S, known as the 2010.1 cluster, that has recently emerged as an endemic clade within U.S. swine herds (66). While we were unable to perform an additional challenge in this longitudinal study, we hypothesize that we would see similar protection against this clade, as we observed robust and durable HI antibody responses to the representative 2010.1 strain, sw/TX/18. However, further challenge studies are required to confirm this hypothesis.

Here, we characterized the onset and duration of immunity elicited by vaccination with an adenoviral vectored Epigraph vaccine and compared these responses to a commonly used WIV vaccine, FluSure XP. We observed that vaccination with Ad-swH3-Epi induced durable and protective levels of antibody and T cell responses that remained detectable for 6 months, and a faster evolution of class-switched IgG antibody responses compared to FluSure XP. We further identified that these responses lead to significantly reduced viral

shedding by 5dpi, enhanced viral clearance from the lungs, and prevented the development of lesions in the trachea and lungs after challenge 6 months post-vaccination. The results obtained in this study can enhance to our understanding of immune responses elicited after vaccination in swine and contribute to the development of a universal swine influenza virus vaccine.

Data availability statement

The original contributions presented in the study are included in the article/Supplementary Material, Further inquiries can be directed to the corresponding author.

Ethics statement

The animal study was reviewed and approved by University of Nebraska - Lincoln, Institute of Animal Care and Use Committee (Protocol: 2167).

Author contributions

EP-T, MP, NJ, and CW provided technical expertise and performed sampling, animal husbandry and management, performed assays and data collection. EP-T, MP, and CW performed immune assays and curated samples collected during the studies. EP-T, DS and HV performed the swine challenge experiments, collected data, and analyzed data. EP-T collected all data and performed extensive analyses and statistics. EP-T, DS and HV interpreted the histology and EAW designed, managed, supervised and procured funding for the research study. EP-T and MP wrote the manuscript. All authors contributed to the article and approved the submitted version.

Funding

This research was supported by the United States Department of Agriculture (USDA) (Grant number 2020-06448) and the National Institutes of Health under Ruth Kirchstein National Research Service Award 1 T32 5T32AI125207-05. The funding source was not involved in the design or execution of the study, analysis, or interpretation of the data, or writing and submission of the manuscript. Funded by National Institutes of Health - NIAID (1R01AI147109-01A1).

Acknowledgments

We would like to thank the Biodefense and Emerging Infectious Disease (BEI) Repository and the USDA Swine Surveillance Influenza A virus isolates repository for the viruses used in this study. We would also like to thank the highly skilled members of the UNL Life Science Annex for their expertise in animal handling and help with sampling throughout the duration of this study.

Conflict of interest

The authors declare that the research was conducted in the absence of any commercial or financial relationships that could be construed as a potential conflict of interest.

Publisher's note

Supplementary material

The Supplementary Material for this article can be found online at: https://www.frontiersin.org/articles/10.3389/fimmu.2023.1143451/full#supplementary-material

SUPPLEMENTARY FIGURE 1
Daily rectal temperatures and daily clinical disease scoring after infection. **(A)** Daily rectal temperatures were collected after infection. A dashed line at 38.4° C indicates normal body temperatures of swine. A dashed line at 39.5°C indicates pyrexia in swine. **(B)** Daily clinical disease scoring was done by an experienced vet blinded to the treatment groups. A previously established scoring scale from 1-5 was used.

SUPPLEMENTARY FIGURE 2
Gross lesion analysis of lungs 5 days after challenge. Lungs were removed at 5dpi and representative lungs from each vaccination group are shown. Lungs were observed for purple-red consolidation on the lobes and minor consolidation was noted on one animal in the FluSure XP immunization group (yellow arrows).

References

1. Lewis NS, Russell CA, Langat P, Anderson TK, Berger K, Bielejec F, et al. The global antigenic diversity of swine influenza a viruses. *Elife* (2016) 5:e12217. doi: 10.7554/eLife.12217

2. Channing S, Kitikoon P, Donovan T. Influenza isolate selection methodology for timely autogenous vaccine use. In: *50th American Association of Swine Veterinarians Annual Meeting*. 2019 March 9-12; Orlando, FL. American Association of Swine Veterinarians (2019) p. 242–244.

3. Ma W, Lager KM, Vincent AL, Janke BH, Gramer MR, Richt JA. The role of swine in the generation of novel influenza viruses. *Zoonoses Public Health* (2009) 56(6-7):326–37. doi: 10.1111/j.1863-2378.2008.01217.x

4. Kyriakis CS, Brown IH, Foni E, Kuntz-Simon G, Maldonado J, Madec F, et al. Virological surveillance and preliminary antigenic characterization of influenza viruses in pigs in five European countries from 2006 to 2008. *Zoonoses Public Health* (2011) 58 (2):93–101. doi: 10.1111/j.1863-2378.2009.01301.x

5. Kyriakis CS, Zhang M, Wolf S, Jones LP, Shim BS, Chocallo AH, et al. Molecular epidemiology of swine influenza a viruses in the southeastern united states, highlights regional differences in circulating strains. *Vet Microbiol* (2017) 211:174–9. doi: 10.1016/j.vetmic.2017.10.016

6. CDC. *Prioritizing zoonotic diseases for multisectoral, one health collaboration in the united states* (2018). Available at: https://www.cdc.gov/onehealth/pdfs/us-ohzdp-report-508.pdf.

7. USDA. *Influenza a virus in swine surveillance quarterly report for fiscal year 2022* (2021). Available at: https://www.aphis.usda.gov/animal_health/animal_dis_spec/swine/downloads/fy2022quarter3swinereport.pdf.

8. Walia RR, Anderson TK, Vincent AL. Regional patterns of genetic diversity in swine influenza a viruses in the united states from 2010 to 2016. *Influenza Other Respir Viruses* (2019) 13(3):262–73. doi: 10.1111/irv.12559

9. Zeller MA, Anderson TK, Walia RW, Vincent AL, Gauger PC. ISU FLUture: a veterinary diagnostic laboratory web-based platform to monitor the temporal genetic patterns of influenza a virus in swine. *BMC Bioinf* (2018) 19(1):397. doi: 10.1186/s12859-018-2408-7

10. Hemmink JD, Morgan SB, Aramouni M, Everett H, Salguero FJ, Canini L, et al. Distinct immune responses and virus shedding in pigs following aerosol, intra-nasal and contact infection with pandemic swine influenza a virus, A(H1N1)09. *Vet Res* (2016) 47(1):103. doi: 10.1186/s13567-016-0390-5

11. Suzuki Y, Ito T, Suzuki T, Holland REJr., Chambers TM, Kiso M, et al. Sialic acid species as a determinant of the host range of influenza a viruses. *J Virol* (2000) 74 (24):11825–31. doi: 10.1128/JVI.74.24.11825-11831.2000

12. Ito T, Couceiro JN, Kelm S, Baum LG, Krauss S, Castrucci MR, et al. Molecular basis for the generation in pigs of influenza a viruses with pandemic potential. *J Virol* (1998) 72(9):7367–73. doi: 10.1128/JVI.72.9.7367-7373.1998

13. Ma W, Kahn RE, Richt JA. The pig as a mixing vessel for influenza viruses: human and veterinary implications. *J Mol Genet Med* (2008) 3(1):158–66.

14. Bowman AS, Walia RR, Nolting JM, Vincent AL, Killian ML, Zentkovich MM, et al. Influenza A(H3N2) virus in swine at agricultural fairs and transmission to humans, Michigan and Ohio, USA, 2016. *Emerg Infect Dis* (2017) 23(9):1551–5. doi: 10.3201/eid2309.170847

15. Anderson TK, Chang J, Arendsee ZW, Venkatesh D, Souza CK, Kimble JB, et al. Swine influenza a viruses and the tangled relationship with humans. *Cold Spring Harb Perspect Med* (2021) 11(3). doi: 10.1101/cshperspect.a038737

16. Van Kerkhove MD, Hirve S, Koukounari A, Mounts AWgroup HNpsw. Estimating age-specific cumulative incidence for the 2009 influenza pandemic: a meta-analysis of A(H1N1)pdm09 serological studies from 19 countries. *Influenza Other Respir Viruses* (2013) 7(5):872–86. doi: 10.1111/irv.12074

17. Smith GJ, Vijaykrishna D, Bahl J, Lycett SJ, Worobey M, Pybus OG, et al. Origins and evolutionary genomics of the 2009 swine-origin H1N1 influenza a epidemic. *Nature* (2009) 459(7250):1122–5. doi: 10.1038/nature08182

18. CDC. *ILI and viral surveillance: FluView*. (2022). Available at: https://www.cdc.gov/flu/weekly/usmap.htm

19. Krammer F. The human antibody response to influenza a virus infection and vaccination. *Nat Rev Immunol* (2019) 19(6):383–97. doi: 10.1038/s41577-019-0143-6

20. Vincent AL, Lager KM, Janke BH, Gramer MR, Richt JA. Failure of protection and enhanced pneumonia with a US H1N2 swine influenza virus in pigs vaccinated with an inactivated classical swine H1N1 vaccine. *Vet Microbiol* (2008) 126(4):310–23. doi: 10.1016/j.vetmic.2007.07.011

21. Vincent AL, Ciacci-Zanella JR, Lorusso A, Gauger PC, Zanella EL, Kehrli MEJr., et al. Efficacy of inactivated swine influenza virus vaccines against the 2009 A/H1N1 influenza virus in pigs. *Vaccine* (2010) 28(15):2782–7. doi: 10.1016/j.vaccine.2010.01.049

22. Kitikoon P, Gauger PC, Anderson TK, Culhane MR, Swenson S, Loving CL, et al. Swine influenza virus vaccine serologic cross-reactivity to contemporary US swine H3N2 and efficacy in pigs infected with an H3N2 similar to 2011-2012 H3N2v. *Influenza Other Respir Viruses* (2013) 7(Suppl 4):32–41. doi: 10.1111/irv.12189

23. Gauger PC, Vincent AL, Loving CL, Lager KM, Janke BH, Kehrli MEJr., et al. Enhanced pneumonia and disease in pigs vaccinated with an inactivated human-like (delta-cluster) H1N2 vaccine and challenged with pandemic 2009 H1N1 influenza virus. *Vaccine* (2011) 29(15):2712–9. doi: 10.1016/j.vaccine.2011.01.082

24. Khurana S, Loving CL, Manischewitz J, King LR, Gauger PC, Henningson J, et al. Vaccine-induced anti-HA2 antibodies promote virus fusion and enhance influenza virus respiratory disease. *Sci Transl Med* (2013) 5(200):200ra114. doi: 10.1126/scitranslmed.3006366

25. Wymore Brand M, Anderson TK, Kitikoon P, Brian Kimble J, Otis N, Gauger PC, et al. Bivalent hemagglutinin and neuraminidase influenza replicon particle vaccines protect pigs against influenza a virus without causing vaccine associated enhanced respiratory disease. *Vaccine* (2022) 40(38):5569–78. doi: 10.1016/j.vaccine.2022.07.042

26. Yoo SJ, Kwon T, Lyoo YS. Challenges of influenza a viruses in humans and animals and current animal vaccines as an effective control measure. *Clin Exp Vaccine Res* (2018) 7(1):1–15. doi: 10.7774/cevr.2018.7.1.1

27. Sandbulte MR, Spickler AR, Zaabel PK, Roth JA. Optimal use of vaccines for control of influenza a virus in swine. *Vaccines (Basel)* (2015) 3(1):22–73. doi: 10.3390/vaccines3010022

28. Kappes MA, Sandbulte MR, Platt R, Wang C, Lager KM, Henningson JN, et al. Vaccination with NS1-truncated H3N2 swine influenza virus primes T cells and confers cross-protection against an H1N1 heterosubtypic challenge in pigs. *Vaccine* (2012) 30(2):280–8. doi: 10.1016/j.vaccine.2011.10.098

29. Vincent AL, Ma W, Lager KM, Richt JA, Janke BH, Sandbulte MR, et al. Live attenuated influenza vaccine provides superior protection from heterologous infection in pigs with maternal antibodies without inducing vaccine-associated enhanced respiratory disease. *J Virol* (2012) 86(19):10597–605. doi: 10.1128/JVI.01439-12

30. Sharma A, Zeller MA, Li G, Harmon KM, Zhang J, Hoang H, et al. Detection of live attenuated influenza vaccine virus and evidence of reassortment in the U.S. swine population. *J Vet Diagn Invest* (2020) 32(2):301–11. doi: 10.1177/1040638720907918

31. Ribacka C, Pesonen S, Hemminki A. Cancer, stem cells, and oncolytic viruses. *Ann Med* (2008) 40(7):496–505. doi: 10.1080/07853890802021342

32. Hitt MM, Addison CL, Graham FL. Human adenovirus vectors for gene transfer into mammalian cells. *Adv Pharmacol* (1997) 40:137–206. doi: 10.1016/S1054-3589(08)60140-4

33. Harui A, Suzuki S, Kochanek S, Mitani K. Frequency and stability of chromosomal integration of adenovirus vectors. *J Virol* (1999) 73(7):6141–6. doi: 10.1128/JVI.73.7.6141-6146.1999

34. Imler JL. Adenovirus vectors as recombinant viral vaccines. *Vaccine* (1995) 13 (13):1143–51. doi: 10.1016/0264-410X(95)00032-V

35. Ferreira RG, Gordon NF, Stock R, Petrides D. Adenoviral vector COVID-19 vaccines: process and cost analysis. *MDPI Processes* (2021) 8(9):1430. doi: 10.3390/pr9081430

36. Casimiro DR, Chen L, Fu TM, Evans RK, Caulfield MJ, Davies ME, et al. Comparative immunogenicity in rhesus monkeys of DNA plasmid, recombinant vaccinia virus, and replication-defective adenovirus vectors expressing a human immunodeficiency virus type 1 gag gene. *J Virol* (2003) 77(11):6305–13. doi: 10.1128/JVI.77.11.6305-6313.2003

37. Mayr GA, Chinsangaram J, Grubman MJ. Development of replication-defective adenovirus serotype 5 containing the capsid and 3C protease coding regions of foot-and-mouth disease virus as a vaccine candidate. *Virology* (1999) 263(2):496–506. doi: 10.1006/viro.1999.9940

38. Gagnon CA, Lachapelle G, Langelier Y, Massie B, Dea S. Adenoviral-expressed GP5 of porcine respiratory and reproductive syndrome virus differs in its cellular maturation from the authentic viral protein but maintains known biological functions. *Arch Virol* (2003) 148(5):951–72. doi: 10.1007/s00705-002-0943-y

39. Eloit M, Gilardi-Hebenstreit P, Toma B, Perricaudet M. Construction of a defective adenovirus vector expressing the pseudorabies virus glycoprotein gp50 and its use as a live vaccine. *J Gen Virol* (1990) 71(Pt 10):2425–31. doi: 10.1099/0022-1317-71-10-2425

40. Monteil M, Le Pottier MF, Ristov AA, Cariolet R, L'Hospitalier R, Klonjkowski B, et al. Single inoculation of replication-defective adenovirus-vectored vaccines at birth in piglets with maternal antibodies induces high level of antibodies and protection against pseudorabies. *Vaccine* (2000) 18(17):1738–42. doi: 10.1016/S0264-410X(99)00545-9

41. Bullard BL, Corder BN, DeBeauchamp J, Rubrum A, Korber B, Webby RJ, et al. Epigraph hemagglutinin vaccine induces broad cross-reactive immunity against swine H3 influenza virus. *Nat Commun* (2021) 12(1):1203. doi: 10.1038/s41467-021-21508-6

42. Theiler J, Korber B. Graph-based optimization of epitope coverage for vaccine antigen design. *Stat Med* (2018) 37(2):181–94. doi: 10.1002/sim.7203

43. Theiler J, Yoon H, Yusim K, Picker LJ, Fruh K, Korber B. Epigraph: a vaccine design tool applied to an HIV therapeutic vaccine and a pan-filovirus vaccine. *Sci Rep* (2016) 6:33987. doi: 10.1038/srep33987

44. Kitikoon P, Gauger PC, Vincent AL. Hemagglutinin inhibition assay with swine sera. *Methods Mol Biol* (2014) 1161:295–301. doi: 10.1007/978-1-4939-0758-8_24

45. Lager KM, Vincent AL. *In vivo* models for pathotyping and vaccine efficacy for swine influenza. *Methods Mol Biol* (2020) 2123:345–51. doi: 10.1007/978-1-0716-0346-8_25

46. Brookes SM, Nunez A, Choudhury B, Matrosovich M, Essen SC, Clifford D, et al. Replication, pathogenesis and transmission of pandemic (H1N1) 2009 virus in non-immune pigs. *PloS One* (2010) 5(2):e9068. doi: 10.1371/journal.pone.0009068

47. Gauger PC, Vincent AL, Loving CL, Henningson JN, Lager KM, Janke BH, et al. Kinetics of lung lesion development and pro-inflammatory cytokine response in pigs with vaccine-associated enhanced respiratory disease induced by challenge with pandemic (2009) A/H1N1 influenza virus. *Vet Pathol* (2012) 49(6):900–12. doi: 10.1177/0300985812439724

48. Coudeville L, Bailleux F, Riche B, Megas F, Andre P, Ecochard R. Relationship between haemagglutination-inhibiting antibody titres and clinical protection against influenza: development and application of a bayesian random-effects model. *BMC Med Res Methodol* (2010) 10:18. doi: 10.1186/1471-2288-10-18

49. Black S, Nicolay U, Vesikari T, Knuf M, Del Giudice G, Della Cioppa G, et al. Hemagglutination inhibition antibody titers as a correlate of protection for inactivated influenza vaccines in children. *Pediatr Infect Dis J* (2011) 30(12):1081–5. doi: 10.1097/INF.0b013e3182367662

50. Hobson D, Curry RL, Beare AS, Ward-Gardner A. The role of serum haemagglutination-inhibiting antibody in protection against challenge infection with influenza A2 and b viruses. *J Hyg (Lond)* (1972) 70(4):767–77. doi: 10.1017/S0022172400022610

51. Graham MB, Braciale TJ. Resistance to and recovery from lethal influenza virus infection in b lymphocyte-deficient mice. *J Exp Med* (1997) 186(12):2063–8. doi: 10.1084/jem.186.12.2063

52. Edmans M, McNee A, Porter E, Vatzia E, Paudyal B, Martini V, et al. Magnitude and kinetics of T cell and antibody responses during H1N1pdm09 infection in inbred babraham pigs and outbred pigs. *Front Immunol* (2020) 11:604913. doi: 10.3389/fimmu.2020.604913

53. Heinen PP, de Boer-Luijtze EA, Bianchi ATJ. Respiratory and systemic humoral and cellular immune responses of pigs to a heterosubtypic influenza a virus infection. *J Gen Virol* (2001) 82(Pt 11):2697–707. doi: 10.1099/0022-1317-82-11-2697

54. Samri A, Durier C, Urrutia A, Sanchez I, Gahery-Segard H, Imbart S, et al. Evaluation of the interlaboratory concordance in quantification of human immunodeficiency virus-specific T cells with a gamma interferon enzyme-linked immunospot assay. *Clin Vaccine Immunol* (2006) 13(6):684–97. doi: 10.1128/CVI.00387-05

55. Sundling C, Lau AWY, Bourne K, Young C, Laurianto C, Hermes JR, et al. Positive selection of IgG(+) over IgM(+) b cells in the germinal center reaction. *Immunity* (2021) 54(5):988–1001 e5. doi: 10.1016/j.immuni.2021.03.013

56. Inoue T, Shinnakasu R, Kurosaki T. Generation of high quality memory b cells. *Front Immunol* (2021) 12:825813. doi: 10.3389/fimmu.2021.825813

57. USDA. *The biological hog cycle* (2022). Available at: https://www.ers.usda.gov/topics/animal-products/hogs-pork/sector-at-a-glance/#:~:text=In%20a%20farrow-to-finish%20operation%2C%2022-26%20weeks%20%28starting%20at,This%20is%20the%20farrow-to-wean%20phase%20of%20hog%20production.

58. Lorbach JN, Nelson SW, Lauterbach SE, Nolting JM, Kenah E, McBride DS, et al. Influenza vaccination of swine reduces public health risk at the swine-human interface. *mSphere* (2021) 6(3):e0117020. doi: 10.1128/mSphere.01170-20

59. Falsey AR, Sobieszczyk ME, Hirsch I, Sproule S, Robb ML, Corey L, et al. Phase 3 safety and efficacy of AZD1222 (ChAdOx1 nCoV-19) covid-19 vaccine. *N Engl J Med* (2021) 385(25):2348–60. doi: 10.1056/NEJMoa2105290

60. Sadoff J, Le Gars M, Shukarev G, Heerwegh D, Truyers C, de Groot AM, et al. Interim results of a phase 1-2a trial of Ad26.COV2.S covid-19 vaccine. *N Engl J Med* (2021) 384(19):1824–35. doi: 10.1056/NEJMoa2034201

61. Voysey M, Clemens SAC, Madhi SA, Weckx LY, Folegatti PM, Aley PK, et al. Safety and efficacy of the ChAdOx1 nCoV-19 vaccine (AZD1222) against SARS-CoV-2: an interim analysis of four randomised controlled trials in Brazil, south Africa, and the UK. *Lancet* (2021) 397(10269):99–111. doi: 10.1016/S0140-6736(20)32661-1

62. Torres JM, Alonso C, Ortega A, Mittal S, Graham F, Enjuanes L. Tropism of human adenovirus type 5-based vectors in swine and their ability to protect against transmissible gastroenteritis coronavirus. *J Virol* (1996) 70(6):3770–80. doi: 10.1128/jvi.70.6.3770-3780.1996

63. Jogler C, Hoffmann D, Theegarten D, Grunwald T, Uberla K, Wildner O. Replication properties of human adenovirus *in vivo* and in cultures of primary cells from different animal species. *J Virol* (2006) 80(7):3549–58. doi: 10.1128/JVI.80.7.3549-3558.2006

64. Hackett NR, El Sawy T, Lee LY, Silva I, O'Leary J, Rosengart TK, et al. Use of quantitative TaqMan real-time PCR to track the time-dependent distribution of gene transfer vectors in vivo. *Mol Ther* (2000) 2(6):649–56. doi: 10.1006/mthe.2000.0203

65. Koodie L, Robertson MG, Chandrashekar M, Ruth G, Dunning M, Bianco RW, et al. Rodents versus pig model for assessing the performance of serotype chimeric Ad5/3 oncolytic adenoviruses. *Cancers (Basel)* (2019) 11(2):198. doi: 10.3390/cancers11020198

66. Sharma A, Zeller MA, Souza CK, Anderson TK, Vincent AL, Harmon K, et al. Characterization of a 2016-2017 human seasonal H3 influenza a virus spillover now endemic to U.S. swine. *mSphere* (2022) 7(1):e0080921. doi: 10.1128/msphere.00809-21

frontiers | Frontiers in Immunology

TYPE Brief Research Report
PUBLISHED 29 June 2023
DOI 10.3389/fimmu.2023.1192715

OPEN ACCESS

EDITED BY
Christophe Chevalier,
Institut National de Recherche pour l'agriculture, l'alimentation et l'environnement (INRAE), France

REVIEWED BY
Juliana Cassataro,
National University of General San Martín, Argentina
Heather Lynne Wilson,
International Vaccine Centre (VIDO-InterVac), Canada

*CORRESPONDENCE
Bert Devriendt
b.devriendt@ugent.be

RECEIVED 23 March 2023
ACCEPTED 16 June 2023
PUBLISHED 29 June 2023

CITATION
Van der Weken H, Jahantigh HR, Cox E and Devriendt B (2023) Targeted delivery of oral vaccine antigens to aminopeptidase N protects pigs against pathogenic *E. coli* challenge infection.
Front. Immunol. 14:1192715.
doi: 10.3389/fimmu.2023.1192715

Targeted delivery of oral vaccine antigens to aminopeptidase N protects pigs against pathogenic *E. coli* challenge infection

Hans Van der Weken[1], Hamid Reza Jahantigh[2,3], Eric Cox[1] and Bert Devriendt[1]*

[1]Laboratory of Immunology, Department of Translational Physiology, Infectiology and Public Health, Faculty of Veterinary Medicine, Ghent University, Merelbeke, Belgium, [2]Department of Pathology, Faculty of Medicine, Emory University, Atlanta, GA, United States, [3]Interdisciplinary Department of Medicine – Section of Occupational Medicine, University of Bari, Bari, Italy

Oral subunit vaccines are an interesting alternative strategy to traditional live-attenuated or inactivated vaccines for conferring protection against gut pathogens. Despite being safer and more cost-effective, the development of oral subunit vaccines remains challenging due to barriers imposed by the gastrointestinal tract, such as digestive enzymes, a tolerogenic immune environment and the inability of larger proteins to cross the epithelial barrier. Recent advances have focused on overcoming these barriers by using potent mucosal adjuvants or pH-responsive delivery vehicles to protect antigens from degradation and promote their release in the intestinal lumen. A promising approach to allow vaccine antigens to pass the epithelial barrier is by their targeting towards aminopeptidase N (APN; CD13), an abundant membrane protein present on small intestinal enterocytes. APN is a peptidase involved in digestion, but also a receptor for several enteric pathogens. In addition, upon antibody-mediated crosslinking, APN facilitated the transport of antibody-antigen fusion constructs across the gut epithelium. This epithelial transport resulted in antigen-specific immune responses. Here, we present evidence that oral administration of APN-specific antibody-antigen fusion constructs comprising the porcine IgA Fc-domain and the FedF tipadhesin of F18-fimbriated *E. coli* elicited both mucosal and systemic immune responses and provided at least partial protection to piglets against a subsequent challenge infection with an F18-fimbriated STEC strain. Altogether, these findings will contribute to the further development of new oral subunit vaccines and provide a first proof-of-concept for the protective efficacy of APN-targeted vaccine antigens.

KEYWORDS

oral vaccination, challenge infection, E. coli, aminopeptidase N, epithelial targeting, mucosal immunity, recombinant antibody, subunit vaccine

1 Introduction

Oral subunit vaccines hold great promise to protect against gut pathogens in a safer and more cost-effective manner than traditional live-attenuated or inactivated vaccines. However, the development of oral subunit vaccines remains challenging due to the barriers imposed by the gastrointestinal tract. The presence of digestive enzymes, the tolerogenic immune environment pervading the gut and the inability of larger proteins to cross the gut epithelial barrier all contribute to a poor bioavailability and immunogenicity of oral subunit vaccines. Several strategies have been developed in recent years to overcome these barriers, including the use of potent mucosal adjuvants to circumvent the tolerogenic environment and pH-responsive delivery vehicles, such as nanoparticles, that protect the vaccine antigens from degradation in the gastrointestinal tract and promote their release in the intestinal lumen (1, 2).

Despite these advances, a major issue holding back the development of new oral subunit vaccines is their inability to cross the small intestinal epithelial barrier. As a result, most oral vaccine candidates induce weak mucosal immune responses. One promising approach to overcome this challenge is to target the vaccine antigens towards receptors present on the apical side of gut epithelial cells that facilitate transport across the gut epithelium (3). Two examples include glycoprotein 2 (GP2) present on Peyer's patch M cells and the neonatal Fc receptor (FcRn) present on absorptive enterocytes. GP2 specifically recognizes FimH, a component of type I pili of certain Gram-negative enterobacteria, and promotes the uptake of $FimH^+$ bacteria, resulting in specific mucosal immune responses in mice (4). Oral administration of a biotinylated ovalbumin peptide conjugated with an anti-GP2-streptavidin fusion antibody was able to induce ovalbumin-specific mucosal immune responses in mice by targeting the peptide towards GP2 (5). One downside of targeting M-cells is their relative low abundance in the gut epithelium. In contrast, enterocytes are by far the most abundant epithelial cell type in the intestine and express FcRn. This receptor interacts with the Fc domain of IgG in a pH-specific manner and allows for bi-directional transport through the intestinal epithelium (6–9). Oral administration of IgG Fc domain-coupled prepro-insulin in mice resulted in efficient transport through the intestinal epithelium and was taken up by antigen-presenting cells and transported to the spleen and thymus (10). Furthermore, oral delivery of recombinant *Lactobacillus plantarum* expressing the influenza viral protein M2e fused to an IgG Fc domain resulted in protective immunity against subsequent infection with influenza viruses in mice (11).

Another attractive target receptor expressed by small intestinal epithelial cells is aminopeptidase N (APN; CD13). This highly glycosylated, homodimeric membrane protein plays a role in cholesterol uptake and in the final digestion of peptides (12, 13). APN is also expressed on conventional dendritic cells, where it plays a role in antigen processing and presentation (14). Due to its highly conserved nature across different species, including pig and human, it represents an interesting target for the oral delivery of vaccine antigens. We previously demonstrated that antibody-mediated targeting of antigens and microparticles to APN triggered their transcytosis through the gut epithelial barrier (15–18). This resulted in their uptake by small intestinal antigen-presenting cells, subsequent transport to the mesenteric lymph nodes and the induction of robust intestinal IgA responses. Recently, we fused the FedF tipadhesin from F18-fimbriated *E. coli* to porcinized APN-specific monoclonal antibodies. Upon oral administration to piglets both systemic and intestinal FedF-specific antibody responses were elicited. However, it remained unresolved whether these immune responses were sufficient to protect animals against infection with F18-fimbriated *E. coli* (15).

Post-weaning diarrhea and edema disease are important causes of illness in recently weaned piglets, leading to growth retardation, mortality and significant economic losses. The primary causative agents of these diseases are F4- and F18-fimbriated enterotoxigenic *Escherichia coli* (ETEC) and F18-fimbriated Shiga-toxin producing *E. coli* (STEC) strains (19). Current strategies for preventing infections in weaned piglets rely on good sanitation practices and the use of antimicrobial agents, such as antibiotics and zinc oxide. Due to concerns on increased antibiotic resistance, the preventive use of antibiotics in the pig industry has been banned in Europe since 2006, while the use of zinc oxide has also been restricted since 2022. For these reasons, the development of alternative strategies, like vaccines, to prevent disease is of utmost importance (20, 21). Currently, a live oral vaccine against F4- and F18-fimbriated ETEC, Coli-protec, is marketed (22). While live vaccines are efficient at preventing disease, some concerns have been raised on uncontrolled replication, severe inflammatory reactions, and the risk of reversion to virulence (23, 24). Additionally, the use of live vaccines precludes their use with other interventions that are aimed at preventing bacterial infections during the post-weaning period, such as antimicrobial compounds or feed supplements. For these reasons, there is currently a high need for the development of new oral vaccination strategies to prevent these bacterial infections in weaned piglets. Here, we further investigated the protective efficacy of our APN targeted vaccine candidate by challenging immunized piglets with an F18-fimbriated STEC strain.

2 Methods

2.1 Production of recombinant antibodies

The chimeric αAPN-pIgA-FedF fusion antibody was generated as previously described, using the variable regions of the porcine APN-specific IMM013 clone (mouse antibody) and the porcine constant light (AAA03520.1) and porcine IgA heavy (AAA65943.1) chains. The heavy chain was genetically fused to the tipadhesin $FedF_{15\text{-}165}$ of F18 fimbriae (PDB entry: 4B4P) using a $(G_4S)_3$-flexible linker (25). Recombinant antibodies were secreted by CHO and subsequently purified using ammonium sulphate precipitation between 43 and 47% saturation and dialyzed against PBS. The final formulation of the purified product contained 600 µg/ml of the αAPN-pIgA-FedF fusion antibody and 20 mg/ml BSA, which serves as a decoy protein for proteolytic degradation in the small intestine (Figure S1).

2.2 Animals and immunization procedures

Sixteen conventionally reared piglets (Belgian Landrace x Pietrain) from a Belgian farm were weaned at 3 weeks and transported to our facilities. These animals were screened to be F18 fimbriae seronegative and F18 receptor positive using FUT1 genotyping (26). The piglets were housed in isolation units and treated with colistin (Colivet quick pump®, 6.4 mg/kg bodyweight) for 5 days before the start of the experiment. Animals were randomly divided in 2 groups of 8 animals and housed in a single unit. The piglets were orally immunized for 3 consecutive days, followed by a booster immunization 14 days post primary immunization (dppi). The gastric pH was neutralized by administration of Omeprazole (20 mg) 24 hours before each immunization and animals were deprived of feed and water 3 hours before and 1 hour after each immunization. Animals were immunized by oral administration with a syringe containing 3 mg of the recombinant αAPN-pIgA-FedF fusion antibody, 10 mg BSA as a decoy protein and adjuvanted with 50 µg cholera toxin (Merck, C8052) in 10 ml PBS for the vaccine group or 10 ml PBS for the control group. Blood was collected at 0, 14, 21, 28, 35, 42 and 49 dppi to analyze antigen-specific serum responses. The animals were euthanized at 49 dppi by intravenous injection of sodium pentobarbital 20% (60 mg/2.5 kg BW; Kela) and upon exsanguination, intestinal content was collected from the ileum for detection of antigen-specific IgA antibodies.

2.3 Challenge infection

Piglets were infected with an F18-fimbriated Shiga toxin-producing *Escherichia coli* (STEC) strain 2 weeks after the booster immunization (28 dppi). Therefore, the piglets were first sedated intramuscularly with Stressnil (2 mg/kg body weight), after which the pH of the stomach was neutralized with 62 ml $NaHCO_3$ (1.4% w/v; intragastric administration). A half hour later, piglets were infected with 10^{11} $F18^+$ STEC (F107/86 strain (O139:H1; $F18ab^+$; $Stx2e^+$; Streptomycin-resistant) in 10 ml PBS. The piglets were deprived of feed and water 3 hours before and 2 hours after the infection. Feces were subsequently collected for 12 consecutive days to monitor bacterial excretion. Therefore, fecal serial dilutions (5 to 0.00001%; w/v) were made in sterile PBS and plated onto blood agar (BBL™ Blood agar base infusion agar; BD Biosciences) plates containing 1 mg/ml streptomycin.

F18 fimbriae expression by the colonies was confirmed by dot blot. Briefly, PVDF membranes (Amersham™ Hybond™; Cytiva) were incubated in methanol for 10 minutes, washed in UP water, placed on the colony-containing bacterial plates and incubated for 2 hours. After an overnight blocking step in PBS + 5% milk + 0.2% Tween-80, the membranes were subsequently incubated for 1 hour at room temperature with a FedA-specific mouse monoclonal antibody (IMM02; in-house), followed by a 1 h incubation step with an anti-mouse IgG-HRP (P0260, dako). Membranes were washed with PBS 3 times for 5 min in between each incubation step. Positive colonies were subsequently detected by developing the membrane with 3-amino-9-ethylcarbazole (AEC). The reaction was stopped with UP water.

2.4 FedF-specific immune responses

Blood was collected from the jugular vein into a gel and clot activator tube (Vacutest, Kima). After 1h incubation at RT, tubes were centrifuged and serum was collected, inactivated at 56°C for 30 minutes and treated with kaolin to reduce background levels in ELISA. Serum samples were stored at -20°C until use. After euthanasia and exsanguination, intestinal content was collected from the ileum (0.25 g) and further homogenized in 5 ml ice-cold extraction buffer (0.1% BSA, 0.05% Tween-20 and Complete protease inhibitor cocktail (Sigma)) using glass beads. The supernatant (4 ml) was subsequently mixed with 1.25 ml glycerol and heated for 10 minutes at 56°C after which the samples were snap-frozen in liquid N_2 and stored at -20°C for further analysis.

Maxisorp microtiter plates (96-well, Life Technologies) were coated with FedF (5 µg/ml; in-house) in PBS for 2h at 37°C (18). After overnight blocking at 4°C with PBS + 3% BSA + 0.2% Tween-80, different dilutions of serum or intestinal content were added in dilution buffer (PBS + 3% BSA + 0.2% Tween-20) to the wells. The serum was serially diluted starting at 1/25 dilution, while the intestinal content was diluted 1/2. After incubation for 1 h at 37°C, plates were washed and incubated for 1 h with HRP-conjugated mouse anti-pig IgG (1/1000; MabTech) or IgA (1/10000; Bethyl). Following 3 washes, ABTS was added and the optical density was measured at 405nm after 60 minutes incubation at 37°C using a spectrophotometer (Tecan SpectraFluor).

2.5 *In vitro* villous adhesion assay

An *in vitro* adhesion assay on small intestinal villi was performed as described previously (27). Briefly, jejunal villi were collected at euthanasia for all piglets and the binding of the F18-fimbriated STEC strain F107/86 to the villi was tested by adding $4x10^8$ bacteria to an average of 50 villi in 500 µl PBS while gently shaking for 1h at room temperature. The villi were subsequently examined by phase-contrast microscopy at a 600x magnification. The mean number of bacteria adhering to the brush border were counted for 15 randomly selected places of 50 µm in length for each piglet (Figure S2).

2.6 Ethical statement

All animal procedures were reviewed and approved by the Ethical Committee of the Faculty of Veterinary Medicine of Ghent University (EC2021-025).

2.7 Data analysis

The data were analyzed using Graphpad Prism software version 9. Serum IgG responses and bacterial excretion numbers were analyzed using two-way ANOVA (mixed-effects model) with repeated measures. IgA responses between groups in the ileal content were analyzed using the Mann-Whitney test. Homogeneity of variances was assessed with Levene's test. Multiple comparisons were corrected using the Two-stage linear step-up procedure of Benjamini, Krieger and Yekutieli. Differences were considered significant when the adjusted p-value <.05.

3 Results

3.1 Systemic and local immune responses after oral immunization with APN-targeted antigen

To evaluate the ability of the APN-targeted antibody-antigen fusion construct to provide protection against infection, a challenge infection experiment was performed (Figure 1A). To this end, piglets (n=8 per group) received orally the chimeric APN-specific porcine IgA-FedF fusion construct (Figure 1B; αAPN-pIgA-FedF) adjuvanted with cholera toxin in a prime-boost regime. Animals in the control group received PBS. The ability to elicit FedF-specific systemic and local immune responses was subsequently evaluated by ELISA (Figure 1C, D). Here, we showed increased FedF-specific serum IgG responses 28, 35, 42 and 49 days post primary immunization (dppi) for the APN-targeted fusion construct as compared to the control group (Figure 1C). No increased FedF-specific serum IgA responses were observed (data not shown). More importantly, FedF-specific IgA antibodies were increased in the ileal content (49 dppi) of piglets orally immunized with the APN-targeted fusion construct in comparison with the control group (Figure 1D). To confirm effective delivery of the oral vaccine, the IgG serum response against the adjuvant cholera toxin was also evaluated. As shown in Figure 1E, a strong increase could be observed for the immunized animals compared to the control group starting from 14 dppi (Figure 1E). Since the vaccine construct contained the Fc domain of pig IgA and CT is a potent mucosal adjuvant, we wondered whether antibody responses against pig IgA were induced. Using ELISA, pig IgA-specific IgG serum responses were not observed (Figure S3). These data show that the oral immunization with the APN-targeted FedF primed the immune system, which boosted the FedF-specific systemic and local immune responses upon challenge infection with an F18-fimbriated *E. coli* strain.

3.2 Rapid reduction and clearance of F18+ STEC after challenge infection

To assess whether the induced immune responses were sufficient to provide protection against infection, the piglets were challenged with an F18-fimbriated STEC strain at 28 dppi (Figure 1A). The bacterial excretion was monitored for 12 consecutive days. Here, a significant reduction (200-fold) in the bacterial excretion between the immunized animals and the control group could be observed starting from 7 days post challenge (dpc) (Figure 2A). Furthermore, the excretion levels of the infection strain dropped below the detection limit ($2x10^2$ CFU/g feces) in 62.5% of piglets in the immunization group at 9 dpc, compared to none of the piglets in the control group (Figure 2B). At the end of the fecal collection period (12 dpc), the percentage of piglets where the infection strain was no longer detectable increased to 87.5% for the immunized animals as opposed to 14.3% for the control group. These data clearly show that the immune responses elicited by oral administration of the APN-targeted antibody-antigen vaccine construct resulted in a more rapid reduction and clearance of the pathogen and partially protected the piglets from infection. This is further highlighted by the observation of severe symptoms of edema disease in one piglet of the control group, which had to be euthanized at 6 dpc. All animals were shown to be susceptible to $F18^+$ *E. coli* infection postmortem using a villous adhesion assay.

4 Discussion

We have previously identified APN as an interesting target for the oral delivery of vaccine antigens, as binding of APN-specific antibodies towards APN leads to transcytosis through the intestinal epithelium and subsequent uptake by antigen-presenting cells. Targeting of the tipadhesin FedF, a protective antigen for F18-fimbriated *E. coli*, to APN using chimeric porcinized IgA antibody-antigen fusion constructs led to both systemic and mucosal immune responses after oral delivery and gave a first indication that APN targeting could be used for the development of new oral subunit vaccines (15–18).

In this study, we further explored the potential of APN targeting in oral vaccination and showed that the observed immune responses were sufficient to confer at least partial protection against infection by an F18-fimbriated STEC strain. A 200-fold reduction in bacterial excretion could be observed 7 days after the challenge infection for immunized piglets in comparison with control animals. Furthermore, the immunized piglets were able to clear the pathogen more rapidly. In 62.5% of the immunized piglets, the infection pathogen could no longer be detected 9 days after infection, increasing to 87.5% at the end of the fecal collection period (day 12). On the other hand, in the control group, not a single animal was able to clear the pathogen on day 9 and only one animal had completely cleared the pathogen at the end of the experiment. These results clearly indicate that the immunized animals were partially protected against infection. Furthermore, only in the control group, one animal suffered from severe symptoms of edema disease and had to be euthanized. Although morbidity rates can vary a lot between strains and usually remain low, mortality rates of affected piglets can go as high as 50 to 90% (28–31). Unfortunately, no firm conclusions can be drawn regarding protection against morbidity or mortality as the group sizes were too small and this was not the aim of the experiment. Further efforts should include a field trial to assess

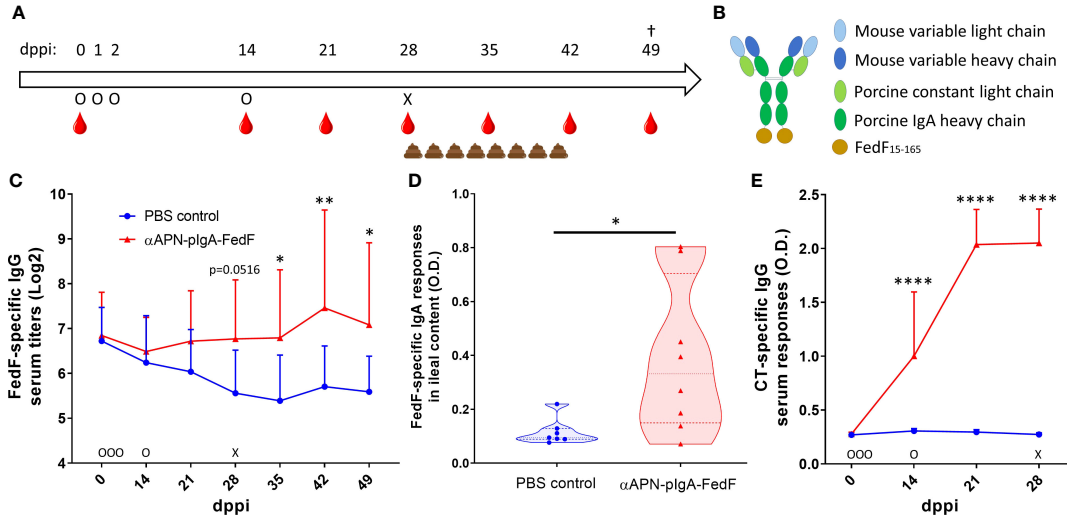

FIGURE 1
Increased FedF-specific immune responses after oral immunization with an APN-specific antibody-antigen fusion construct. **(A)** Timeline of the experiment with days of oral immunization (O), challenge infection with an F18-fimbriated STEC strain (X), feces collection and blood collection time points. **(B)** schematic structure of the antibody-antigen fusion construct. **(C)** FedF-specific IgG serum responses from 0 to 49 days post primary immunization (dppi) and **(D)** FedF-specific IgA antibodies in the ileal content at the day of euthanization (49 dppi). **(E)** CT-specific IgG serum responses from 0 to 28 dppi. *Indicates a significant difference compared to the PBS control group. *: p <.05, **: p <.01, ****: p <.0001, n = 8 per group.

the efficacy of this vaccine candidate in preventing disease symptoms and mortality.

Although the induced immune responses were not sufficient to completely prevent pathogen colonization, this is not necessary to protect infected animals from severe disease symptoms and mortality. As was shown by Nadeau et al., a strong reduction in bacterial excretion levels can be sufficient to reduce the infection burden and resulting symptoms of ETEC/STEC infection (22). In that study, animals were orally vaccinated with the live-attenuated Coli-protec vaccine and infected with an F18-fimbriated *E. coli* strain, producing multiple toxins (9910297-^{2STM}; STb$^+$, LT$^+$, East-1$^+$, Stx2e$^+$, F18ab$^+$). Their results indicated that a reduction to around 10^6 CFU/g stool seemed to be sufficient to prevent most signs of infection, including mild to moderate diarrhea. In our experiment, the infection burden peaked within the first 5 days of infection, after which excretion levels dropped drastically. This indicates the presence of local immune responses sufficient to clear the pathogen. Although not significant, the peak excretion levels for the immunized animals also appear to be lower compared to the control animals, which reached peak excretion levels exceeding 10^8 CFU/g feces for three consecutive days. A further reduction of the peak bacterial excretion in the vaccinated animals by a factor 10 would result in excretion levels reaching 10^6 CFU/g, which would be similar to the results of Nadeau et al. and should be

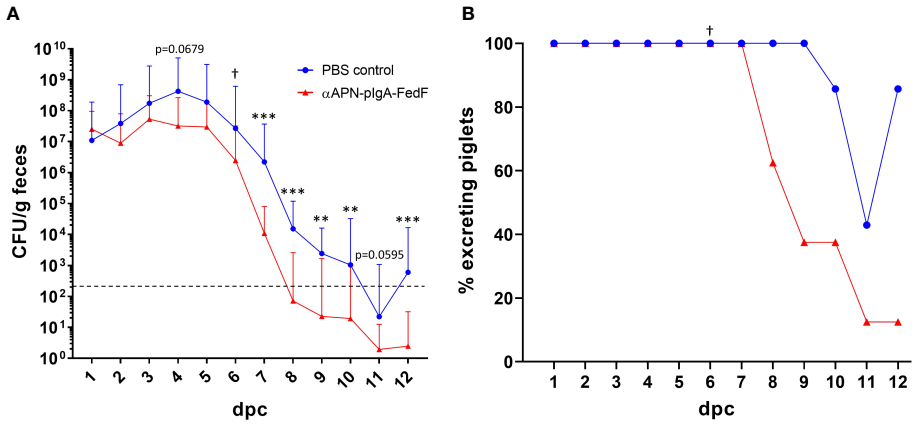

FIGURE 2
Rapid reduction and clearance of the pathogen after challenge infection. **(A)** Mean bacterial excretion over time after a challenge infection with an F18-fimbriated STEC strain. Error bars represent the standard deviation. The dashed line represents the detection limit (200 CFU/g feces). **(B)** The percentage of piglets with detectable excretion levels of the F18+ STEC strain over time. CFU: Colony forming units. dpc: days post challenge. *Indicates significant differences compared to the control group. **: p <.01, ***: p <.001. †one piglet in the control group was euthanized due to severe symptoms of edema disease. n = 8 per group.

sufficient to prevent disease symptoms. Of note, vaccines that fail to completely block transmission of the target pathogen might be a risk for the emergence of vaccine-escape mutants.

The observed reduction in bacterial excretion could be further strengthened by increasing the local antibody immune response against the vaccine antigen. It is known that FedF has a poor immunogenicity and we previously showed this can be attributed to its immune suppressive properties by decreasing the antigen-presenting capacity of intestinal antigen-presenting cells (15). This is further highlighted by the fact that no significant increases in FedF-specific serum IgG and IgA in the ileal content could be observed in the control group 3 weeks after the challenge infection. Besides targeting towards APN, the immunogenicity of FedF could be further improved by multimerization. This strategy is known to promote antigen recognition of low affinity B-cells and promote their differentiation to antibody-secreting plasma cells (32). What is also worth considering is that subunit vaccines based on a single antigen might fail to provide sufficient protection, even if strong immune responses to the target antigen are induced. Therefore, it might be interesting to develop a multivalent vaccine. In particular for targeting F18-fimbriated ETEC/STEC infections, the major fimbrial subunit FedA might provide another interesting candidate as a vaccine antigen. A multivalent vaccine approach would also have the advantage that different strains can be targeted. For example, by combining the FaeG subunit of F4 fimbriae and the FedF subunit of F18 fimbriae, a multivalent subunit vaccine targeting the two most common causative agents of post-weaning diarrhea and edema disease could be developed. Our vaccine candidate contained cholera toxin (CT). While CT is a potent mucosal adjuvant, it is also toxic to humans. As such, adjuvating our vaccine candidate with CT might pose a risk for personnel and detoxified mmCT might be a better alternative (33).

Because our vaccine candidate uses a porcine IgA Fc domain, the antibody-antigen fusion construct might be recognized by FcαRI (CD89) expressed by myeloid cells, such as monocytes, macrophages and specific dendritic cell subsets (34, 35). FcαRI binds IgA at the CH2-CH3 interface. While the $FedF_{15\text{-}165}$ antigen is fused to the CH3 domain, it most likely does not block recognition of IgA by FcαRI, as fusing FedF to mouse IgG1 did not interfere with protein G-mediated purification (15). Protein G binds the Fc domain of IgG at the CH2-CH3 interface. Since binding of monomeric IgA to FcαRI can elicit an inhibitory signaling cascade in FcαRI-expressing immune cells, this interaction could result in a reduced immunogenicity of our vaccine candidate (36). However, FcαRI is not yet well characterized in pigs. Further research is thus needed to elucidate whether our constructs elicit FcαRI-mediated signaling in porcine immune cells and whether this synergizes with APN-mediated signaling.

In conclusion, the results presented here provide evidence for APN targeting as a promising new technology for delivery of vaccine antigens to the gut immune system and will contribute to the development of new and effective oral subunit vaccines. If the immunogenicity of FedF can be further improved, this could lead to the development of a novel subunit vaccine capable of protecting piglets against edema disease. Furthermore, as APN is a highly conserved protein, this vaccine delivery technology could be translated to other species as well, including humans.

Data availability statement

The raw data supporting the conclusions of this article will be made available by the authors, without undue reservation.

Ethics statement

The animal study was reviewed and approved by Ethical Committee of the Faculty of Veterinary Medicine of Ghent University.

Author contributions

BD and EC conceived the idea and designed the research. HV and HJ produced and purified the recombinant antibodies. HV performed the *in vivo* experiment. HV performed the data analysis together with BD and EC. HV wrote the manuscript with contributions from BD and EC. All authors reviewed the manuscript before submission. All authors contributed to the article and approved the submitted version.

Funding

This research was funded by grants from the Industrial Research Fund of Ghent University (F2019/IOF-Advanced/283), the Special Research Fund of Ghent University (BOF/STA/202009/021; BOF/24Y/2021/0044, BOF/BAS/2015/0029/01) and F.W.O-Vlaanderen (I005220N).

Acknowledgments

The authors would like to thank Jan Clement, Simon Brabant, Charlotte Helsmoortel and other colleagues of the laboratory of Immunology for their assistance during the *in vivo* experiment.

Conflict of interest

The authors declare that the research was conducted in the absence of any commercial or financial relationships that could be construed as a potential conflict of interest.

Publisher's note

reviewers. Any product that may be evaluated in this article, or claim that may be made by its manufacturer, is not guaranteed or endorsed by the publisher.

Supplementary material

The Supplementary Material for this article can be found online at: https://www.frontiersin.org/articles/10.3389/fimmu.2023.1192715/full#supplementary-material

SUPPLEMENTARY FIGURE 1
Purity of the porcine IgA-FedF fusion constructs. Coomassie staining (left) and BSA-specific western blot (right) of the vaccine candidate after ammonium sulphate precipitation and dialysis in PBS. DC: Precision Plus Protein Dual Color Standard (Bio-rad). MM: MagicMark™ XP Western Protein Standard (Thermo Fisher).

SUPPLEMENTARY FIGURE 2
In vitro villous adhesion assay. The average number of bacteria adhering to the brush border of the jejunal villi was calculated for each piglet after incubation with an F18-fimbriated STEC strain (F107/86). The dotted line indicates the susceptibility threshold (5 bacteria/250 µm villi). Numbers on the x-axis indicate the individual piglets.

SUPPLEMENTARY FIGURE 3
No pig IgA-specific IgG antibodies could be observed in the pig serum after immunization. A porcine IgA-specific ELISA was performed by coating a Maxisorp plate with a polyclonal anti-pig IgA antibody (10 µg/ml), followed by IgG-depleted pig serum (diluted to 10 µg/ml porcine IgA). The binding of the porcine IgA from the serum to the capture antibody was confirmed using an HRP-conjugated anti-pig IgA antibody. After blocking with BSA (1%), serum (1/10 dilution) from the different piglets (n = 8 per group) at 0 and 28 days post primary immunization (dppi) was incubated and detected with an HRP-conjugated anti-pig IgG antibody. The optical density (O.D.) was measured at 405nm after 60 min incubation with ABTS at 37°C. In between each incubation, three wash steps were performed with PBS + 0.2% Tween-20. Data is shown as the average ± standard deviation.

References

1. Van der Weken H, Cox E, Devriendt B. Advances in oral subunit vaccine design. *Vaccines* (2020) 9(1). doi: 10.3390/vaccines9010001

2. Moyle PM, Toth I. Modern subunit vaccines: development, components, and research opportunities. *ChemMedChem* (2013) 8(3):360–76. doi: 10.1002/cmdc.201200487

3. Devriendt B, De Geest BG, Goddeeris BM, Cox E. Crossing the barrier: targeting epithelial receptors for enhanced oral vaccine delivery. *J Controlled Release* (2012) 160 (3):431–9. doi: 10.1016/j.jconrel.2012.02.006

4. Ohno H, Hase K. Glycoprotein 2 (GP2): grabbing the FimH bacteria into m cells for mucosal immunity. *Gut Microbes* (2010) 1(6):407–10. doi: 10.4161/gmic.1.6.14078

5. Shima H, Watanabe T, Fukuda S, Fukuoka S, Ohara O, Ohno H. A novel mucosal vaccine targeting peyer's patch m cells induces protective antigen-specific IgA responses. *Int Immunol* (2014) 26(11):619–25. doi: 10.1093/intimm/dxu061

6. Yoshida M, Claypool SM, Wagner JS, Mizoguchi E, Mizoguchi A, Roopenian DC, et al. Human neonatal fc receptor mediates transport of IgG into luminal secretions for delivery of antigens to mucosal dendritic cells. *Immunity* (2004) 20(6):769–83. doi: 10.1016/j.immuni.2004.05.007

7. Ward ES, Ober RJ. Targeting FcRn to generate antibody-based therapeutics. *Trends Pharmacol Sci* (2018) 39(10):892–904. doi: 10.1016/j.tips.2018.07.007

8. Rath T, Baker K, Pyzik M, Blumberg RS. Regulation of immune responses by the neonatal fc receptor and its therapeutic implications. *Front Immunol* (2014) 5:664. doi: 10.3389/fimmu.2014.00664

9. Pyzik M, Kozicky LK, Gandhi AK, Blumberg RS. The therapeutic age of the neonatal fc receptor. *Nat Rev Immunol* (2023), 1–18. doi: 10.1038/s41577-022-00821-1

10. Corcos N, Culina S, Deligne C, Lavaud C, You S, Mallone R. Oral fc-coupled preproinsulin achieves systemic and thymic delivery through the neonatal fc receptor and partially delays autoimmune diabetes. *Front Immunol* (2021) 12:616215. doi: 10.3389/fimmu.2021.616215

11. Yang WT, Yang GL, Wang Q, Huang HB, Jiang YL, Shi CW, et al. Protective efficacy of fc targeting conserved influenza virus M2e antigen expressed by lactobacillus plantarum. *Antiviral Res* (2017) 138:9–21. doi: 10.1016/j.antiviral.2016.11.025

12. Shipp MA, Look AT. Hematopoietic differentiation antigens that are membrane-associated enzymes: cutting is the key! *Blood* (1993) 82(4):1052–70. doi: 10.1182/blood.V82.4.1052.1052

13. Kramer W, Girbig F, Corsiero D, Pfenninger A, Frick W, Jahne G, et al. (CD13) is a molecular target of the cholesterol absorption inhibitor ezetimibe in the enterocyte brush border membrane. *J Biol Chem* (2005) 280(2):1306–20. doi: 10.1074/jbc.M406309200

14. Larsen SL, Pedersen LO, Buus S, Stryhn A. T Cell responses affected by aminopeptidase n (CD13)-mediated trimming of major histocompatibility complex class II-bound peptides. *J Exp Med* (1996) 184(1):183–9. doi: 10.1084/jem.184.1.183

15. Van der Weken H, Sanz Garcia R, Sanders NN, Cox E, Devriendt B. Antibody-mediated targeting of antigens to intestinal aminopeptidase n elicits gut IgA responses in pigs. *Front Immunol* (2021) 12:753371. doi: 10.3389/fimmu.2021.753371

16. Melkebeek V, Rasschaert K, Bellot P, Tilleman K, Favoreel H, Deforce D, et al. A newly identified receptor for F4ac fimbriae, enhances the intestinal mucosal immune response. *Mucosal Immunol* (2012) 5(6):635–45. doi: 10.1038/mi.2012.37

17. Bakshi S, Sanz Garcia R, van der Weken H, Tharad A, Pandey S, Juarez P, et al. Evaluating single-domain antibodies as carriers for targeted vaccine delivery to the small intestinal epithelium. *J Controlled Release* (2020) 321:416–29. doi: 10.1016/j.jconrel.2020.01.033

18. Baert K, de Geest BG, de Rycke R, da Fonseca Antunes AB, de Greve H, Cox E, et al. Beta-glucan microparticles targeted to epithelial APN as oral antigen delivery system. *J Controlled Release* (2015) 220(Pt A):149–59. doi: 10.1016/j.jconrel.2015.10.025

19. Luppi A, Gibellini M, Gin T, Vangroenweghe F, Vandenbroucke V, Bauerfeind R, et al. Prevalence of virulence factors in enterotoxigenic escherichia coli isolated from pigs with post-weaning diarrhoea in Europe. *Porcine Health Management* (2016) 2:20. doi: 10.1186/s40813-016-0039-9

20. Hoelzer K, Bielke L, Blake DP, Cox E, Cutting SM, Devriendt B, et al. Vaccines as alternatives to antibiotics for food producing animals. part 2: new approaches and potential solutions. *Veterinary Res* (2018) 49(1):70. doi: 10.1186/s13567-018-0561-7

21. Hoelzer K, Bielke L, Blake DP, Cox E, Cutting SM, Devriendt B, et al. Vaccines as alternatives to antibiotics for food producing animals. part 1: challenges and needs. *Veterinary Res* (2018) 49(1):64. doi: 10.1186/s13567-018-0560-8

22. Nadeau E, Fairbrother JM, Zentek J, Belanger L, Tremblay D, Tremblay CL, et al. Efficacy of a single oral dose of a live bivalent e. coli vaccine against post-weaning diarrhea due to F4 and F18-positive enterotoxigenic e. coli. *Veterinary J (London England: 1997)* (2017) 226:32–9. doi: 10.1016/j.tvjl.2017.07.004

23. Sridhar S, Brokstad KA, Cox RJ. Influenza vaccination strategies: comparing inactivated and live attenuated influenza vaccines. *Vaccines* (2015) 3(2):373–89. doi: 10.3390/vaccines3020373

24. Pollard AJ, Bijker EM. A guide to vaccinology: from basic principles to new developments. *Nat Rev Immunol* (2021) 21(2):83–100. doi: 10.1038/s41577-020-00479-7

25. Van der Weken H, Cox E, Devriendt B. Rapid production of a chimeric antibody-antigen fusion protein based on 2A-peptide cleavage and green fluorescent protein expression in CHO cells. *mAbs* (2019) 11(3):559–68. doi: 10.1080/19420862.2019.1574531

26. Meijerink E, Fries R, Vogeli P, Masabanda J, Wigger G, Stricker C, et al. Two alpha(1,2) fucosyltransferase genes on porcine chromosome 6q11 are closely linked to the blood group inhibitor (S) and escherichia coli F18 receptor (ECF18R) loci. *Mamm Genome* (1997) 8(10):736–41. doi: 10.1007/s003359900556

27. Coddens A, Verdonck F, Tiels P, Rasschaert K, Goddeeris BM, Cox E. The age-dependent expression of the F18+ e. coli receptor on porcine gut epithelial cells is positively correlated with the presence of histo-blood group antigens. *Veterinary Microbiol* (2007) 122(3-4):332–41. doi: 10.1016/j.vetmic.2007.02.007

28. van Beers-Schreurs HM, Vellenga L, Wensing T, Breukink HJ. The pathogenesis of the post-weaning syndrome in weaned piglets: a review. *Veterinary Quarterly* (1992) 14(1):29–34. doi: 10.1080/01652176.1992.9694322

29. Lee SI, Ntakiyisumba E, Won G. Systematic review and network meta-analysis to compare vaccine effectiveness against porcine edema disease caused by shiga toxin-producing escherichia coli. *Sci Rep* (2022) 12(1):6460. doi: 10.1038/s41598-022-10439-x

30. Imberechts H, De Greve H, Lintermans P. The pathogenesis of edema disease in pigs. a review. *Veterinary Microbiol* (1992) 31(2-3):221–33. doi: 10.1016/0378-1135(92)90080-D

31. Casanova NA, Redondo LM, Dailoff GC, Arenas D, Fernandez Miyakawa ME. Overview of the role of shiga toxins in porcine edema disease pathogenesis. *Toxicon: Off J Int Soc Toxinol* (2018) 148:149–54. doi: 10.1016/j.toxicon.2018.04.019

32. Kato Y, Abbott RK, Freeman BL, Haupt S, Groschel B, Silva M, et al. Multifaceted effects of antigen valency on b cell response composition and differentiation in vivo. *Immunity* (2020) 53(3):548–63 e8. doi: 10.1016/j.immuni.2020.08.001

33. Lebens M, Terrinoni M, Karlsson SL, Larena M, Gustafsson-Hedberg T, Kallgard S, et al. Construction and preclinical evaluation of mmCT, a novel mutant cholera toxin adjuvant that can be efficiently produced in genetically manipulated vibrio cholerae. *Vaccine* (2016) 34(18):2121–8. doi: 10.1016/j.vaccine.2016.03.002

34. Aleyd E, Heineke MH, van Egmond M. The era of the immunoglobulin a fc receptor FcalphaRI; its function and potential as target in disease. *Immunol Rev* (2015) 268(1):123–38. doi: 10.1111/imr.12337

35. Monteiro RC, Van De Winkel JG. IgA fc receptors. *Annu Rev Immunol* (2003) 21:177–204. doi: 10.1146/annurev.immunol.21.120601.141011

36. Breedveld A, van Egmond M. IgA and FcalphaRI: pathological roles and therapeutic opportunities. *Front Immunol* (2019) 10:553. doi: 10.3389/fimmu.2019.00553

frontiers | Frontiers in Immunology

TYPE Mini Review
PUBLISHED 07 July 2023
DOI 10.3389/fimmu.2023.1171212

OPEN ACCESS

EDITED BY
Raúl Manzano Román,
University of Salamanca, Spain

REVIEWED BY
Selim Aslan,
Near East University, Cyprus
Dirk Werling,
Royal Veterinary College (RVC),
United Kingdom

*CORRESPONDENCE
Heather L. Wilson
heather.wilson@usask.ca

†These authors have contributed equally to this work

RECEIVED 21 February 2023
ACCEPTED 16 June 2023
PUBLISHED 07 July 2023

CITATION
Choudhary P, Magloire D, Hamonic G and Wilson HL (2023) Immune responses in the uterine mucosa: clues for vaccine development in pigs. *Front. Immunol.* 14:1171212. doi: 10.3389/fimmu.2023.1171212

Immune responses in the uterine mucosa: clues for vaccine development in pigs

Pooja Choudhary[1†], Donaldson Magloire[1,2†], Glenn Hamonic[1] and Heather L Wilson[1,2*]

[1]Vaccine and Infectious Disease Organization (VIDO), University of Saskatchewan, Saskatoon, SK, Canada, [2]Department of Veterinary Microbiology Sciences, Western College of Veterinary Medicine, University of Saskatchewan, Saskatoon, SK, Canada

The immune system in the upper reproductive tract (URT) protects against sexually transmitted pathogens, while at the same time providing immune tolerance responses against allogenic sperm and the developing fetus. The uterine environment is also responsive to hormonal variations during the estrus cycle, although the most likely timing of exposure to pathogens is during estrus and breeding when the cervix is semi-permissive. The goal for intrauterine immunization would be to induce local or systemic immunity and/or to promote colostral/lactogenic immunity that will passively protect suckling offspring. The developing fetus is not the vaccine target. This minireview article focuses on the immune response induced in the pig uterus (uterine body and uterine horns) with some comparative references to other livestock species, mice, and humans.

KEYWORDS

uterus, vaccine, adjuvants, fertility, pigs, livestock, intrauterine

1 Introduction

Unlike many other large livestock animals, pigs are not immobilized in headgates during handling; therefore, delivery of vaccines can be difficult and a potential safety hazard, especially in terms of the risk of needle-stick injuries (1). Before immunization can take place, the animals need to be snared or moved into crates, both of which require more than one person. Like other agriculture sectors, the pig industry is experiencing a labor shortage, and novel ideas to eradicate inefficiencies within the barns may help bridge these gaps. To that end, vaccines that can be administered without needles and at a time when animals are immobilized (without the need for multiple workers) would be well-received by the swine industry. Sows and gilts are bred during estrus when the cervix is semi-permissive and, upon being exposed to the boar or boar pheromones, they become temporarily rigid in preparation for mounting, referred to as lordosis (2). Because they are temporarily immobilized, the sows and gilts are safe to immunize and other barn personnel are not required to snare the animals, meaning that two tasks can be accomplished at once

(breeding and immunization) with reduced laborers. Further, because breeding takes place more than two times per year, the timing of intrauterine immunization is optimal for induction of immunity (3–5). Reports on the innate and adaptive immune response in the uterus support the hypothesis that the uterus may be amenable to an immune induction site, although care should be taken to avoid induction of non-tolerizing response to sperm and seminal fluid constituents.

2 Innate immune responses in the uterus and uterine horns

It has lately been appreciated that the uterus and uterine horns have their own microbiome (6). The gut microbiome in the sow can be modulated in response to antimicrobials, reproductive stages, feed and supplements, pathogen exposure as well as vaccines (reviewed in (7)). The impact of these factors on the sow uterine microbiome needs to be explored, as does the potential impact that an intrauterine vaccine may have on the microbiome of the uterus and other sites.

The uterine microenvironment is under immune surveillance and is reactive to foreign antigens (8). Sperm deposited in the uterus triggers a natural immune response, which serves both to clear the uterus of excess sperm (9, 10) as well to accommodate the embryo for implantation (11). Studies in livestock bred by AI showed that spermatozoa, seminal plasma, and extender trigger rapid and transient neutrophil infiltration into the lumen and an inflammatory response, complete with cytokine and chemokine induction (12–15). Studies in pigs show that semen extender and seminal plasma alone induced interleukin (IL)-10, transforming growth factor (TGF)-β, IL-8, and tumor necrosis factor (TNF)-α gene expression but that when combined with spermatozoa, the expression of these genes is reduced (16). Sperm has been shown to promote immune tolerance via signaling through Toll-like receptor (TLR) 4 (17, 18). Furthermore, seminal fluid antigens activate regulatory T cells in the uterus draining lymph node, which dampens the immune response in the uterus to tolerate the antigens present in the embryo (19).. Others show that semen extender triggers induction of granulocyte-macrophage colony-stimulating factor (GM-CSF) and a corresponding increase in major histocompatibility complex (MHC) class II-positive cells in the uterine lamina propria and directly basolateral to the epithelial layer (20). The extent to which a vaccine coupled with artificial insemination will influence the sperm and seminal fluid's role in evoking or dampening an immune response has not been fully elucidated.

Recruitment of antigen-presenting cells (APC) to the lumen or the uterine tissue may be key to an effective intrauterine (i.u.) vaccine that is delivered in combination with a semen extender. Boar semen combined with three adjuvants (poly I:C, host defense peptide, and polyphosphazene (Triple Adjuvant; TriAdj)) administered to the uterus was shown to trigger changes in localized gene expression and cellular recruitment *in vivo* and greatly increased the number of neutrophils in the uterine lumen (12, 21). These data suggest that sperm, semen, semen extender, and adjuvants may augment local immune response and, therefore, may influence the immune response to intrauterine vaccines. Our results in pigs have shown that vaccines coupled with sperm at the time of breeding does not affect reproduction, but the effect of multiple breedings/vaccinations should investigate whether anti-sperm antibodies do increase (22). Caution should be used to formulate the vaccine so that it does not trigger the induction of anti-sperm antibodies, which may cause infertility (23).

3 The uterus as an immune induction site

Intrauterine immunization is a novel approach and currently, published data have been limited to rodents and pigs. In mice, prior i.u. exposure to live *Chlamydia trachomatis* (Ct) generated protective immunity against subsequent challenge, suggesting that the uterus can act as an immune induction site (24, 25). Further, immunization with ultraviolet light (UV)-inactivated Ct (UV-Ct) complexed with charge-switching synthetic adjuvant biodegradable nanoparticles (cSAPs) elicited long-lived protection in conventional and humanized mice (24). Mice immunized with UV-Ct alone generated regulatory T cells and an accumulation of tolerogenic $CD11b^{-}CD103^{+}$ dendritic cells (DCs) that exacerbated subsequent Ct infection, whereas mice immunized with UV-Ct-cSAP exhibited elevated immunogenic uterine $CD11b^{+}CD103^{-}$ DCs that led to effector T cells seeding the uterine mucosa with resident memory T (T_{RM}) cells (24). These data suggest that the inclusion of mucosal adjuvants may be critically required for protective i.u. immunization.

The hormonal state may also impact the immune response as although DCs in the decidua of pregnant mice retain responsiveness to pro-inflammatory stimuli and migration capacity towards CCL21, these cells are prevented from trafficking to the draining lymph node (LN), possibly to promote T cell tolerance to fetal antigens (26). These data suggest that DCs may have region-specific or timing/hormone-specific responses. Understanding the mechanism of action of adjuvants and the cells they target should continue to be a research focus for i.u. vaccines.

Recent studies in pigs show that the uterus can act as a site of booster immunization and/or as an immune induction site. In a previous study, sows that had been immunized repeatedly with the Porcine ParvoShield L5E Swine Vaccine® (Elanco Animal Health) by the intramuscular (i.m.) route at each parity were bred with semen alone or semen plus BEI-inactivated porcine parvovirus (1×10^7 $TCID_{50}$ PPV (NADL-7) formulated with a combination adjuvant (TriAdj; host defense peptide, poly I:C, and polyphosphazene) (21). This vaccine was not spermicidal. Positive control sows received i.m. ParvoShield® vaccine as they entered farrowing crates. Serum antibody titres against viral protein 2 (VP2, one of the capsid proteins of PPV) were comparable between the positive control sows and sows immunized by the uterine route, suggesting that the uterus could act as a site of booster immunization to an inactivated virus (21). When sows were bred

with the immunogenic recombinant spike protein from a porcine epidemic diarrheal virus (rPEDVS) plus TriAdj adjuvants, the anti-PEDVS serum and uterine antibodies were low in the i.u.-vaccinated gilts (22). These data suggest that a single primary immunization delivered into the uterus may not be sufficient to evoke a systemic or mucosal humoral immune response (21). Importantly, there was no difference in the viable fetus/corpus luteum ratio after 30 days between i.u.-vaccinated and control sows, suggesting that the i.u. vaccines did not impact fetal development.

To assess whether multiple i.u. vaccines could trigger a robust immune response, gilts were bred with heat-inactivated extended semen containing rPEDVS formulated with TriAdj. The gilts returned to estrus after 21 days and they were rebred with the same inactivated semen and vaccine, suggesting that i.u. immunization did not impact hormonal cycling. When they returned to estrus again, they were bred with live semen plus the vaccine (22). Control gilts were administered semen alone at second estrus following common industrial breeding practices. Litter weights and the number of live to non-viable piglets were comparable, indicating that the three-times-administered i.u.-vaccine did not appear to impact fertility. The i.u.-vaccinated gilts showed significant PEDVS-specific serum, colostral, and uterine antibody titers, and low-level colostral PEDVS-neutralizing antibodies. Serum from piglets born from i.u immunized gilts showed increased antibody titers compared to control piglets (22), which showed that i.u vaccines can induce higher maternal antibodies. Piglets born to i.u.-vaccinated gilts received partial passive protection from PEDV infection 3 days after birth but eventually succumbed to the disease (22). Collectively, these data indicate that the porcine uterus could act as an immune induction site, but that more than one dose is needed, at least when TriAdj is used as the vaccine adjuvant (22). In a follow-up trial, the rPEDVS vaccine was formulated with polymeric poly-(lactide-co-glycolide) (PGLA)-nanoparticle (NP) including a muramyl dipeptide analog and a monophosphoryl lipid A (MPLA) analog as adjuvants (NP-PEDVS) (27). The gilts responded with significant induction of serum anti-PEDVS-IgG following the single dose after 30 days, suggesting that an NP vaccine may be suitable for primary i.u. vaccination. Collectively, these experiments indicate that the pig uterus can act as an immune inductive site when the vaccine is administered at breeding, but that the use of robust adjuvants (that are formulated to not be spermicidal) may be critical to vaccine efficacy. In addition to rodents and pigs, it would be interesting to see the results on other animals that breed via AI such as cattle and horses.

Intradermal (i.d.) vaccination is also an alternative to i.m. immunization which results have shown can induce a comparable or better immune response (28). In some instances, i.d. immunization requires needles administered using the Mantoux technique, which requires 5–15° injection angle into the skin going approx. 1 mm deep (29–31). This technique requires persons be trained and it can be difficult to use on a non-anesthetized animal (31, 32). Administration of i.d. vaccines using bifurcated needles or multipuncture devices can be complicated by uneven antigen delivery (33). In contrast, i.u. immunization takes advantage of breeding practices and does not require specialized skills from the administrator.

4 Mechanism of action

4.1 Uterine epithelial cell pattern recognition receptors

As in other mammals, the porcine uterus/uterine horn is lined with a single layer of simple columnar cells with tight junctions between the cells to control passage, and the tight junctions are regulated by the hormonal state, cytokines, growth factors, TLR agonists, and pathogens (34–36). The underlying endometrial layer has a superficial functional layer (*stratum functionale*) and a deeper basal layer (*stratum basale*) with glandular epithelial cells forming tubular glands that spiral into the tissue (37, 38). The endometrium undergoes changes in the branching of the glands and growth, including changes in endometrial thickness and epithelial cell height in response to the estrus cycle (37, 39, 40).

The epithelial and endometrial layer of the uterus expresses several pattern recognition receptors that may play a role in the uterine immune response. TLRs are membrane-spanning receptors on the uterine epithelial cell surface that identify the pathogen-associated molecular patterns (PAMPs) present in bacterial, fungal, and viral pathogens and initiate innate immune responses (41, 42). Analysis of mRNA expression levels performed on isolated and cultured pig primary uterine epithelial cells showed that TLRs 1-7 and 9, NOD1, NOD2, NLRP3, NLRP6, NLRX1, RIG1, MDA5, and LGP2 are expressed (43). Polarized primary uterine epithelial cells (UECs) stimulated with TLR3, TLR4, and TLR9 ligands showed induced secretion of IL-6, IL-13, and IL-10, respectively, indicating that these receptors were functional (43). Polarized uterine epithelial cells stimulated with a TLR3 agonist showed increased expression of interferon (IFN)-β, TNF-α, IL-8, CCL2, CCL3, CCL4, and CCL-20 (21). Further, laser-captured uterine epithelial cells obtained one day after being bred with semen plus an adjuvant cocktail containing a TLR3 agonist showed significantly increased CCL2, suggesting that pig uterine epithelial cells are responsive to immune stimuli (21). Immunohistofluorescence and immunofluorescence performed on pig uterine tissue and in polarized pig primary UECs indicated that TLR3 and TLR9 localizes to the apical cell surface, whereas TLR4 localizes to the intracellular space (43). Surface localization of TLR3 in pig uterine epithelial cells shows agreement with uterine epithelial cells in humans (44, 45) and rabbits (46); continued research in this area shows that the 'canonical' localization patterns of TLRs may not be conserved across the cell and/or tissue types and may also vary in response to stimulation, age, disease, or cellular environment (reviewed in (43)).

4.2 Immune cells in the uterine lumen and endothelium

Cells in the uterine lumen and endometrium are sensitive to changes in the hormonal environment. We limited the scope of this mini-review to the estrus cycle when the cervix may be permissive to vaccines. Immune cells in the endometrium are primarily

lymphocytes, with some macrophages and APCs and large numbers of neutrophils; these levels tend to be at their highest during estrus (38, 40). Macrophages, DCs, lymphocytes, and granulocytes migrate from the blood to subepithelial tissue where they may persist (20, 47). Neutrophils are found close to the basal lamina of the surface epithelium and the subepithelial capillaries at pre-estrus and estrus (48, 49). They migrate into the uterine lumen after breeding where they eliminate a large number of spermatozoa and microbes present in boar semen (47, 50) and they usually die after 24 hours (20).

Uterine APCs, such as macrophages and DCs, are present throughout the endometrium during estrus; however, at other stages of the estrus cycle, they are found deeper in the lamina propria and rarely reside directly below the surface epithelium (40, 51). In mice, macrophages can be identified by the expression of the cell surface F4/80 and can be positive or negative for the surface marker CD11c (52, 53).. Macrophages are the most abundant professional APC in the human uterus (54). DCS can be characterized into 3 major subsets: plasmacytoid DC (pDC), conventional DC1 (cDC1), and conventional DC2 (cDC2) populations based on cell-surface markers and transcription factors such as interferon regulatory factors 8 and 4 (IRF8 and IRF4) (55–57). Once DCs capture antigens, they become mature and migrate to lymphoid structures to present antigens to T cells (58). DCs in the uterus are characterized as having high levels of major histocompatibility complex class II. In mice, cDC1 cells in nonlymphoid tissue, such as the uterine tissue, can be either $CD103^+CD11b^-$ cDC1 and $CD11b^+$ cDC2 (59). $CD103^+$ cDC1 has two principal functions, i.e., priming $CD8^+$ cells by cross presentation and induction of tolerance (60). pDC1 cells mainly produce high type I IFN in response to viral infection (61) whereas $CD11b^+$ cDC2 drives the $CD4^+$ T helper 2 (TH2) and 17 (TH17) response (62). In pigs, subsets of DCs are identified and characterized as cDC1: $CD135^+CD14^-CD172a^{low}CADM1^+wCD11R1^+$ cells; cDC2: $CD135^+CD14^-CD172a^+CADM1^+CD115^+wCD11R1^+CD1^+$ cells; and pDCs: $CD4^+CD135^+CD172a^+CD123^+CD303^+$ (63).

In pigs, plasma cells are dispersed throughout the endometrium with a predominance of IgG-secreting plasma cells (38, 38). The most prevalent cell type at all stages of the estrus cycle is the $CD2^+$ cell (48) with $CD8^+$ cells being present more frequently than $CD4^+$ T cells in the surface epithelium compared to the $CD4^+$, and more $CD4^+$ cells than $CD8^+$ cells in the glandular connective tissue (51). In the connective tissue of the subepithelial layer, there is no significant effect of the estrus cycle stage on the numbers of $CD2^+$, $CD4^+$, and $CD8^+$ cells (49).

4.3 Antigen presentation

For an immune response to occur, APCs need to internalize the antigen, process it, and present it to T cells on MHCI or MHCII proteins (64, 65). The quality and direction of the adaptive response depends on how the APCs react to the adjuvant, leading to the secretion of select cytokines (66, 67).. In the human uterus, antigen presentation on MHC class II can be performed by professional APCs as well as uterine epithelial cells (68, 69). In contrast, in pigs, SLA-DRA gene expression was not detected in any uterine epithelial cells, indicating that pigs do not express the porcine equivalent of MHC class II (21). These data suggest that there are species-specific differences between the roles of epithelial cells in immune activation in the uterus and that pig uterine epithelial cells do not act as APCs.

The upper reproductive tract does not contain the mucosal-associated lymphoid tissue (MALT) thought to be critically required for the induction of an immune response (70). There is limited evidence that the pig's upper reproductive tract has lymphoid aggregates that may be acting as a limited MALT. One study showed that in 3 out of 6 sows studied, aggregations of lymphocytes were noted in the subepithelial connective tissue of the cervix (https://stud.epsilon.slu.se/12300/1/edstrom_k_171031.pdf). Another study referred to an unpublished observation that reported 50% of ancestral multiparous sows had a few small lymphocyte aggregations in the endometrium at weaning (71). Other studies show that lymphoid aggregates are present throughout the uterus, usually within the surface and in the glandular epithelium, and vary in size throughout the estrous cycle stages (72, 73). In the glandular epithelium, $CD4^+$ cells are absent, $CD8^+$ cells typically increase during estrus whereas $CD2^+$ cells are at most during estrus and early diestrus. On the surface epithelium, more $CD4^+$ are found over $CD8^+$ cells during estrous, whilst $CD2^+$ cells are in high numbers both during estrus and early diestrus (73).

The human uterus has lymphoid aggregates in the endometrial tissue at the basal and functional area of the uterus near the uterine epithelial glands (74). These aggregates are comprised of $CD19^+$ B cells surrounded by numerous (and primarily $CD8^+$) T cells and an outer layer of monocytes or macrophages (75, 76). The size of the lymphoid aggregates varies with the estrus cycle. It appears to be the largest during the secretory and proliferative phases; this is consistent with an increase in the immune cell trafficking into the endometrium, which may contribute to the larger lymphoid aggregate in the secretory phase (75, 77).

In the subepithelial stromal layer of the endometrium of the bovine uterus, isolated lymphoid nodules and aggregates predominantly comprised of clusters of B and T-lymphocytes have been reported (78, 79) (80). B lymphocytes were also observed as a small aggregate deep in the stroma or adjacent to blood vessels in the myometrial layer of the uterus, possibly recruited to the mucosal surfaces in response to the chemokines secreted during infection (81–83). These studies indicate there may be species-specific differences in how vaccines in the uterine lumen mediate the immune response, and/or it is possible that uterine vaccination would require transport of the vaccine across the epithelial barrier.

4.4 Transport of molecules across the epithelial barrier

Tight junctions between UECs limit the transport of molecules across the epithelial barrier. The predominant method for transporting macromolecules across an epithelial cell wall would be through pinocytosis, which involves transporting

macromolecules into or across the cell using vesicles. Pinocytosis is a form of endocytosis that is not receptor-mediated and is therefore non-specific. Pinocytosis involves the internalization of the plasma membrane to form a vesicle that contains extracellular fluid, and any molecules present in that fluid. Studies in other epithelial cell barriers such as in alveoli and the intestine have shown that pinocytosis occurs in a non-specific fashion and transports macromolecules across the epithelial cells at a rate proportional to their size (84) and that negatively charged nanoparticles are more efficiently transported (85). Although there is limited data on the mechanisms of pinocytosis by UECs and how the size or charge of particles impacts their transport, there is evidence of molecules being transported in a luminal to basolateral direction, which could be used by intrauterine vaccines (86).

Another mechanism of transport across the uterine epithelial cell barrier may include receptor-mediated transport using antibody transporters. For example, despite its name, neonatal Fc receptor (FcRN) is expressed by both porcine and human UECs into adulthood (87, 88). IgG can be bi-directionally transported between neutral environments through FcRN-mediated transport (89, 90). The transfer of IgG by FcRN in the human female reproductive tract has been confirmed (87). It is possible that by binding to the vaccine antigen, FcRN-IgG transportation could deliver the antigen and possibly the associated vaccine components across the epithelial wall. Further, polymeric immunoglobulin receptor (pIgR)-mediated transport for the secretion of sIgA has been well described and is known to be carried out by uterine epithelial cells (88), although IgA is not the predominant immunoglobulin secreted into the uterine lumen. Thus, antibodies bound by these receptors could transport coupled antigens across the epithelial barrier. Future studies should investigate where the vaccine components localize and are taken up by innate immune cells when they are formulated as soluble or particulate vaccines.

A summary of how intrauterine immunization can impact the pig industry and factors that may influence immune activation are presented in Table 1.

TABLE 1 Impact of intrauterine immunization.

Impact on industry		Factors that may influence immune activation
Positive attributes	Potential challenges	
•Needle-free •Safe to immunize during lordosis response •Coupling breeding with immunization reduces labor requirements	•Assess long-term impact on fertility •Must ensure sperm are not targeted and no negative effect on microbiome	•Uterine epithelial cell pattern recognition receptors •Hormonal changes in transport receptors, cell numbers, and cell localization •Site of immune activation is not yet clear. •Uterus has limited lymphoid aggregates instead of MALT •UECs do not present antigens to T cells

5 Discussion

The uterus is known to exhibit inflammatory responses and there is evidence that it can act as an immune induction site. Studies are needed to determine whether intrauterine vaccines trigger immune cell recruitment into the lumen, which is critical for induction of immunity, or whether the antigen traverses the uterine wall to trigger immunity. How the antigen traverses the uterine wall (i.e., via paracellular transport or transcytosis, uptake by dendritic cells extending dendrites into the lumen, etc.) and whether the antigen is presented to draining LNs or lymphoid aggregates should also be investigated. Once it is clear how the uterus acts as an immune induction site, vaccines can be formulated to exploit this mechanism of action. Coupling breeding with vaccination should reduce the number of personnel required for handling and would not require any special training, making it a potentially important new route of immunization for the pig industry. The effect of multiple rounds of i.u. immunization on sperm tolerance and the uterine microbiome must be investigated further, with each new vaccine formulation.

Author contributions

PC, DM, and HW researched and wrote the initial draft. All authors contributed to revising and reviewing the manuscript. Portions of this manuscript are also found in the Ph.D. thesis for GH, used with permission. All authors contributed to the article and approved the submitted version.

Funding

VIDO receives operational funding from the Government of Saskatchewan through Innovation Saskatchewan and the Ministry of Agriculture and from the Canada Foundation for Innovation through the Major Science Initiatives for its CL3 facility. Financial support was provided by a Natural Sciences and Engineering Research Council of Canada (NSERC) Discovery Grant to HW (No. RGPIN-2020-05891) and Saskatchewan Agriculture Development Fund to HW (No. 20210690). PC receives a MITACS Accelerate Industrial Postdoctoral Fellowship (No. SK-ISED).

Acknowledgments

This manuscript is published with the permission of the Director of VIDO as journal series #1014.

Conflict of interest

The authors declare that the research was conducted in the absence of any commercial or financial relationships that could be construed as a potential conflict of interest.

Publisher's note

References

1. Hafer AL, Langley RL, Morrow WEM. Occupational hazards reported by swine veterinarians in the united states. *J Swine Health Production* (1996) 4(3):128–41.

2. Dorries KM, Adkins-Regan E, Halpern BP. Sensitivity and behavioral responses to the pheromone androstenone are not mediated by the vomeronasal organ in domestic pigs. *Brain Behav Evol* (1997) 49(1):53–62. doi: 10.1159/000112981

3. McNamara KA, Sloter N L, Zas Rodriguez S L, Knox R V, Gall T J, Levis D G, et al. An analysis of survey data by size of the breeding herd for the reproductive management practices of north American sow farms. *J Anim Sci* (2013) 91(1):433–45.

4. Knox RV. Artificial insemination in pigs today. *Theriogenology* (2016) 85(1):83–93. doi: 10.1016/j.theriogenology.2015.07.009

5. Hernández-Caravaca I, Izquierdo-Rico MJ, Matás C, Carvajal JA, Vieira L, Abril D, et al. Reproductive performance and backflow study in cervical and post-cervical artificial insemination in sows. *Anim Reprod Sci* (2012) 136(1):14–22. doi: 10.1016/j.anireprosci.2012.10.007

6. Rampersaud R, Randis TM, Ratner AJ. Microbiota of the upper and lower genital tract. *Semin Fetal Neonatal Med* (2012) 17(1):51–7. doi: 10.1016/j.siny.2011.08.006

7. Monteiro MS, Poor AP, Muro BBD, Carnevale RF, Leal DF, Garbossa CAP, et al. The sow microbiome: current and future perspectives to maximize the productivity in swine herds. *J Swine Health Production* (2022) 30(4):238–250. doi: 10.54846/jshap/1277

8. Robertson SA. Control of the immunological environment of the uterus. *Rev Reprod* (2000) 5(3):164–74. doi: 10.1530/ror.0.0050164

9. Zambrano F, Poor AP, Muro BB.D, Carnevale RF, Leal DF, Garbossa CA.P, et al. Leukocytes coincubated with human sperm trigger classic neutrophil extracellular traps formation, reducing sperm motility. *Fertil Steril* (2016) 106(5):1053–1060.e1. doi: 10.1016/j.fertnstert.2016.06.005

10. Hong J, Dicker BL, Jayasinghe SN, Gregorio De F, Tian H, Han DY, et al. Strong inhibition of neutrophil-sperm interaction in cattle by selective phosphatidylinositol 3-kinase inhibitors. *Biol Reprod* (2017) 97(5):671–87. doi: 10.1093/biolre/iox121

11. Troedsson MH, Loset K, Alghamdi AM, Dahms B, Crabo BG. Interaction between equine semen and the endometrium: the inflammatory response to semen. *Anim Reprod Sci* (2001) 68(3-4):273–8. doi: 10.1016/S0378-4320(01)00164-6

12. Katila T. Post-mating inflammatory responses of the uterus. *Reprod Domest Anim* (2012) 47(s5):31–41. doi: 10.1111/j.1439-0531.2012.02120.x

13. Rozeboom KJ, Troedsson MH.T, Molitor TW, Crabo BG. The effect of spermatozoa and seminal plasma on leukocyte migration into the uterus of gilts. *J Anim Sci* (1999) 77(8):2201–6. doi: 10.2527/1999.7782201x

14. Marey MA, Yousef MS, Kowsar R, Hambruch N, Shimizu T, Pfarrer C, et al, et al. Local immune system in oviduct physiology and pathophysiology: attack or tolerance/ *Domest Anim Endocrinol* (2016) 56 Suppl:S204–11. doi: 10.1016/j.domaniend.2016.02.005

15. Hawk HW. Transport and fate of spermatozoa after insemination of cattle. *J Dairy Sci* (1987) 70(7):1487–503. doi: 10.3168/jds.S0022-0302(87)80173-X

16. Taylor U, Zerbe H, Seyfert H-M, Rath D, Baulain U, Langner KFA, et al. Porcine spermatozoa inhibit post-breeding cytokine induction in uterine epithelial cells in vivo. *Anim Reprod Sci* (2009) 115(1):279–89. doi: 10.1016/j.anireprosci.2008.11.019

17. Schjenken JE, Glynn DJ, Sharkey DJ, Robertson SA. TLR4 signaling is a major mediator of the female tract response to seminal fluid in mice. *Biol Reprod* (2015) 93 (3):68. doi: 10.1095/biolreprod.114.125740

18. Schjenken JE, Sharkey DJ, Green ES, Chan HY, Matias RA, Moldenhauer LM, et al. Sperm modulate uterine immune parameters relevant to embryo implantation and reproductive success in mice. *Commun Biol* (2021) 4(1):572. doi: 10.1038/s42003-021-02038-9

19. Guerin LR, Moldenhauer LM, Prins JR, Bromfield JJ, Hayball JD, Robertson SA. Seminal fluid regulates accumulation of FOXP3+ regulatory T cells in the preimplantation mouse uterus through expanding the FOXP3+ cell pool and CCL19-mediated Recruitment1. *Biol Reprod* (2011) 85(2):397–408. doi: 10.1095/biolreprod.110.088591

20. O'Leary S, Jasper M, Warnes G, Armstrong D, Robertson S. Seminal plasma regulates endometrial cytokine expression, leukocyte recruitment and embryo development in the pig. *Reproduction* (2004) 128:237–47. doi: 10.1530/rep.1.00160

21. Hamonic G, Pasternak JA, Ng SH, Fourie KR, Simko OM, Deluco B, et al. Assessment of immunological response and impacts on fertility following intrauterine vaccination delivered to swine in an artificial insemination dose. *Front Immunol* (2020) 11:1015. doi: 10.3389/fimmu.2020.01015

22. Choudhary P, Fourie KR, Ng S, Hamonic G, Bérubé N, Popowych Y, et al. Intrauterine immunizations trigger antigen-specific mucosal and systemic immunity in pigs and passive protection in suckling piglets. *Vaccine* (2021) 39(42):6322–32. doi: 10.1016/j.vaccine.2021.08.080

23. Tokuhiro K, Ikawa M, Benham AM, Okabe M. Protein disulfide isomerase homolog PDILT is required for quality control of sperm membrane protein ADAM3 and male fertility [corrected]. *Proc Natl Acad Sci U.S.A.* (2012) 109(10):3850–5. doi: 10.1073/pnas.1117963109

24. Stary G, Olive A, Radovic-Moreno AF, Gondek D, Alvarez D, Basto PA, et al. VACCINES. a mucosal vaccine against chlamydia trachomatis generates two waves of protective memory T cells. *Science* (2015) 348(6241):aaa8205.

25. Gondek DC, Olive AJ, Stary G, Starnbach MN. CD4+ T cells are necessary and sufficient to confer protection against chlamydia trachomatis infection in the murine upper genital tract. *J Immunol* (2012) 189(5):2441–9. doi: 10.4049/jimmunol.1103032

26. Collins MK, Tay CS, Erlebacher A. Dendritic cell entrapment within the pregnant uterus inhibits immune surveillance of the maternal/fetal interface in mice. *J Clin Invest* (2009) 119(7):2062–73. doi: 10.1172/JCI38714

27. Choudhary P, Tay CS, Erlebacher A. A single-dose intramuscular nanoparticle vaccine with or without prior intrauterine priming triggers specific uterine and colostral mucosal antibodies and systemic immunity in gilts but not passive protection for suckling piglets. *Front Vet Sci* (2022) 9:931232. doi: 10.3389/fvets.2022.931232

28. Louis L, Clark M, Wise MC, Glennie N, Wong A, Broderick K, et al. Intradermal synthetic DNA vaccination generates leishmania-specific T cells in the skin and protection against leishmania major. *Infect Immun* (2019) 87(8). doi: 10.1128/IAI.00227-19

29. Kim YC, Jarrahian C, Zehrung D, Mitragotri S, Prausnitz MR. Delivery systems for intradermal vaccination. *Curr Top Microbiol Immunol* (2012) 351:77–112. doi: 10.1007/82_2011_123

30. Mrsny RJ. Does an intradermal vaccination for monkeypox make sense? *AAPS J* (2022) 24(6):104. doi: 10.1208/s12248-022-00754-6

31. Tarnow K, King N. Intradermal injections: traditional bevel up versus bevel down. *Appl Nurs Res* (2004) 17(4):275–82. doi: 10.1016/S0897-1897(04)00079-5

32. Norman JJ, Gupta J, Patel SR, Park S, Jarrahian C, Zehrung D, et al. Reliability and accuracy of intradermal injection by mantoux technique, hypodermic needle adapter, and hollow microneedle in pigs. *Drug Delivery Transl Res* (2014) 4(2):126–30. doi: 10.1007/s13346-013-0184-5

33. Lambert PH, Laurent PE. Intradermal vaccine delivery: will new delivery systems transform vaccine administration? *Vaccine* (2008) 26(26):3197–208. doi: 10.1016/j.vaccine.2008.03.095

34. Ochiel DO, Fahey JV, Ghosh M, and Haddad SN, Wira CR. Innate immunity in the female reproductive tract: role of sex hormones in regulating uterine epithelial cell protection against pathogens. *Curr Womens Health Rev* (2008) 4(2):102–17. doi: 10.2174/157340408784246395

35. Capaldo CT, Nusrat A. Cytokine regulation of tight junctions. *Biochim Biophys Acta* (2009) 1788(4):864–71. doi: 10.1016/j.bbamem.2008.08.027

36. Fahey JV, Wright JA, Shen L, Smith JM, Ghosh M, Rossoll RM, et al. Estradiol selectively regulates innate immune function by polarized human uterine epithelial cells in culture. *Mucosal Immunol* (2008) 1(4):317–25. doi: 10.1038/mi.2008.20

37. Edstrom K. *The porcine cervix*. Uppsala: Swedish University of Agricultural Sciences (2009).

38. Hussein AM, Newby TJ, Bourne FJ. Immunohistochemical studies of the local immune system in the reproductive tract of the sow. *J Reprod Immunol* (1983) 5(1):1–15. doi: 10.1016/0165-0378(83)90016-5

39. Lorenzen E, Follmann F, Jungersen G, Agerholm JS. A review of the human vs. porcine female genital tract and associated immune system in the perspective of using minipigs as a model of human genital chlamydia infection. *Vet Res* (2015) 46:116–6. doi: 10.1186/s13567-015-0241-9

40. Kaeoket K, Persson E, Dalin AM. Corrigendum to "The sow endometrium at different stages of the oestrus cycle: studies on morphological changes and infiltration by cells of the immune system". *Anim Reprod Sci* (2002) 73(1):89–107. [Anim. Reprod. Sci. 65 (2001) 95–114]. doi: 10.1016/s0378-4320(00)00211-6

41. Akira S, Takeda K. Toll-like receptor signalling. *Nat Rev Immunol* (2004) 4 (7):499–511. doi: 10.1038/nri1391

42. Akira S, Hemmi H. Recognition of pathogen-associated molecular patterns by TLR family. *Immunol Lett* (2003) 85(2):85–95. doi: 10.1016/S0165-2478(02)00228-6

43. Hamonic G, Pasternak JA, Forsberg NM, Kaser T, Wilson HL. Expression of pattern recognition receptors in porcine uterine epithelial cells in vivo and in culture. *Vet Immunol Immunopathol* (2018) 202:1–10. doi: 10.1016/j.vetimm.2018.06.006

44. Schaefer TM, Fahey JV, Wright JA, Wira CR. Innate immunity in the human female reproductive tract: antiviral response of uterine epithelial cells to the TLR3 agonist Poly(I:C). *J Immunol* (2005) 174(2):992. doi: 10.4049/jimmunol.174.2.992

45. Hamonic G, Pasternak JA, Wilson HL. Recognizing conserved non-canonical localization patterns of toll-like receptors in tissues and across species. *Cell Tissue Res* (2018) 372(1):1–11. doi: 10.1007/s00441-017-2767-9

46. Pasternak JA, et al. Intrauterine delivery of subunit vaccines induces a systemic and mucosal immune response in rabbits. *Am J Reprod Immunol* (2017) 78(5):e12732. doi: 10.1111/aji.12732

47. Rozeboom KJ, Troedsson MH, Crabo BG. Characterization of uterine leukocyte infiltration in gilts after artificial insemination. *J Reprod Fertil* (1998) 114(2):195–9. doi: 10.1530/jrf.0.1140195

48. Bischof RJ, Lee CS, Brandon MR, Meeusen E. Inflammatory response in the pig uterus induced by seminal plasma. *J Reprod Immunol* (1994) 26(2):131–46. doi: 10.1016/0165-0378(94)90036-1

49. Kaeoket K, Persson E, Dalin AM. The sow endometrium at different stages of the oestrous cycle: studies on morphological changes and infiltration by cells of the immune system. *Anim Reprod Sci* (2001) 65(1-2):95–114. doi: 10.1016/S0378-4320(00)00211-6

50. Gączarzewicz D, Udała J, Piasecka M, Błaszczyk B, Stankiewicz T. Bacterial contamination of boar semen and its relationship to sperm quality preserved in commercial extender containing gentamicin sulfate. *Polish J Vet Sci* (2016) 19 (3):451–9. doi: 10.1515/pjvs-2016-0057

51. Kaeoket K, Persson E, Dalin AM. Corrigendum to "The sow endometrium at different stages of the oestrous cycle: studies on the distribution of CD2, CD4, CD8 and MHC class II expressing" cells. *Anim Reprod Sci* (2002) 73(1):109–19. [Anim. Reprod. Sci. 68 (2001) 99–109]. doi: 10.1016/s0378-4320(02)00126-4

52. Waddell LA, Lefevre L, Bush SJ, Raper A, Young R, Lisowski ZM, et al. ADGRE1 (EMR1, F4/80) is a rapidly-evolving gene expressed in mammalian monocyte-macrophages. *Front Immunol* (2018) 9:2246. doi: 10.3389/fimmu.2018.02246

53. Lu L, Kuroishi T, Tanaka Y, Furukawa M, Nochi T, Sugawara S. Differential expression of CD11c defines two types of tissue-resident macrophages with different origins in steady-state salivary glands. *Sci Rep* (2022) 12(1):931. doi: 10.1038/s41598-022-04941-5

54. Bulmer JN, Williams PJ, Lash GE. Immune cells in the placental bed. *Int J Dev Biol* (2010) 54(2-3):281–94. doi: 10.1387/ijdb.082763jb

55. Guilliams M, Ginhoux F, Jakubzick C, Naik SH, Onai N, Schraml BU, et al. Dendritic cells, monocytes and macrophages: a unified nomenclature based on ontogeny. *Nat Rev Immunol* (2014) 14(8):571–8. doi: 10.1038/nri3712

56. Granot T, Senda T, Carpenter DJ, Matsuoka N, Weiner J, Gordon CL, et al. Dendritic cells display subset and tissue-specific maturation dynamics over human life. *Immunity* (2017) 46(3):504–15. doi: 10.1016/j.immuni.2017.02.019

57. Collin M, Bigley V. Human dendritic cell subsets: an update. *Immunology* (2018) 154(1):3–20. doi: 10.1111/imm.12888

58. Steinman RM, Inaba K, Turley S, Pierre P, Mellman I. Antigen capture, processing, and presentation by dendritic cells: recent cell biological studies. *Hum Immunol* (1999) 60(7):562–7. doi: 10.1016/S0198-8859(99)00030-0

59. Merad M, Sathe P, Helft J, Miller J, Mortha A. The dendritic cell lineage: ontogeny and function of dendritic cells and their subsets in the steady state and the inflamed setting. *Annu Rev Immunol* (2013) 31:563–604. doi: 10.1146/annurev-immunol-020711-074950

60. Cao Q, Lu J, Li Q, Wang C, Wang XM, Lee VW, et al. CD103+ dendritic cells elicit CD8+ T cell responses to accelerate kidney injury in adriamycin nephropathy. *J Am Soc Nephrol* (2016) 27(5):1344–60. doi: 10.1681/ASN.2015030229

61. Summerfield A, Guzylack-Piriou L, Schaub A, Carrasco CP, Tâche V, Charley B, et al. Porcine peripheral blood dendritic cells and natural interferon-producing cells. *Immunology* (2003) 110(4):440–9. doi: 10.1111/j.1365-2567.2003.01755.x

62. Mayer JU, Demiri M, Agace WW, MacDonald AS, Svensson-Frej M, Milling SW, et al. Different populations of CD11b(+) dendritic cells drive Th2 responses in the small intestine and colon. *Nat Commun* (2017) 8:15820. doi: 10.1038/ncomms15820

63. Auray G, Keller I, Python S, Gerber M, Bruggmann R, Ruggli N, et al. Characterization and transcriptomic analysis of porcine blood conventional and plasmacytoid dendritic cells reveals striking species-specific differences. *J Immunol* (2016) 197(12):4791–806. doi: 10.4049/jimmunol.1600672

64. Ashwell JD, DeFranco AL, Paul WE, Schwartz RH. Antigen presentation by resting b cells. radiosensitivity of the antigen-presentation function and two distinct pathways of T cell activation. *J Exp Med* (1984) 159(3):881–905. doi: 10.1084/jem.159.3.881

65. Cruse JM, Lewis RE, Wang H eds. 7 - ANTIGEN PRESENTATION. In: *Immunology guidebook*. San Diego: Academic Press. p. 267–76.

66. Luckheeram RV, Zhou R, Verma AD, Xia B. CD4$^+$T cells: differentiation and functions. *Clin Dev Immunol 2012* (2012) p:925135. doi: 10.1155/2012/925135

67. Strutt TM, McKinstry KK, Swain SL. Control of innate immunity by memory CD4 T cells. *Adv Exp Med Biol* (2011) 780:57–68. doi: 10.1007/978-1-4419-5632-3_6

68. Prabhala RH, Wira CR. Sex hormone and IL-6 regulation of antigen presentation in the female reproductive tract mucosal tissues. *J Immunol* (1995) 155 (12):5566–73. doi: 10.4049/jimmunol.155.12.5566

69. Wira CR, Rossoll RM. Antigen-presenting cells in the female reproductive tract: influence of the estrous cycle on antigen presentation by uterine epithelial and stromal cells. *Endocrinology* (1995) 136(10):4526–34. doi: 10.1210/endo.136.10.7664673

70. Brandtzaeg P, Kiyono H, Pabst R, Russell MW. Terminology: nomenclature of mucosa-associated lymphoid tissue. *Mucosal Immunol* (2008) 1(1):31–7. doi: 10.1038/mi.2007.9

71. Dalin AM, Kaeoket K, Persson E. Immune cell infiltration of normal and impaired sow endometrium. *Anim Reprod Sci* (2004) 82-83:401–13. doi: 10.1016/j.anireprosci.2004.04.012

72. Bischof RJ, Brandon MR, Lee CS. Studies on the distribution of immune cells in the uteri of prepubertal and cycling gilts. *J Reprod Immunol* (1994) 26(2):111–29. doi: 10.1016/0165-0378(94)90035-3

73. Kaeoket K, Dalin AM, Magnusson U, Persson E. Corrigendum to "The sow endometrium at different stages of the oestrous cycle: studies on the distribution of CD2, CD4, CD8 and MHC class II expressing" cells. *Anim Reprod Sci* (2002) 73(1-2):109–19. doi: 10.1016/S0378-4320(02)00127-6

74. Khong TY. Immunohistologic study of the leukocytic infiltrate in maternal uterine tissues in normal and preeclamptic pregnancies at term. *Am J Reprod Immunol Microbiol* (1987) 15(1):1–8. doi: 10.1111/j.1600-0897.1987.tb00141.x

75. Yeaman GR, Guyre PM, Fanger MW, Collins JE, White HD, Rathbun W, et al. Unique CD8+ T cell-rich lymphoid aggregates in human uterine endometrium. *J Leukoc Biol* (1997) 61(4):427–35. doi: 10.1002/jlb.61.4.427

76. Mettler L, Jürgensen A, Volkov NI, Kulakov V, Parwaresch MR. Lmmuno histochemical profile of endometrium in patients with genital endometriosis. *Diagn Ther Endosc* (1997) 3(3):127–45. doi: 10.1155/DTE.3.127

77. Yeaman GR, Collins JE, Fanger MW, Wiram CR, Lydyard PM. CD8+ T cells in human uterine endometrial lymphoid aggregates: evidence for accumulation of cells by trafficking. *Immunology* (2001) 102(4):434–40. doi: 10.1046/j.1365-2567.2001.01199.x

78. Blazquez NB, Batten EH, Long SE, Perry GC. Histology and histochemistry of the bovine reproductive tract caudal to the cervix. part i. the vestibule and associated glands. *Br Vet J* (1987) 143(4):328–37. doi: 10.1016/0007-1935(87)90066-2

79. Corbeil LB, Munson L, Campero C, BonDurant RH. Bovine trichomoniasis as a model for development of vaccines against sexually-transmitted disease. *Am J Reprod Immunol* (2001) 45(5):310–9. doi: 10.1111/j.8755-8920.2001.450507.x

80. Corbeil LB, Campero CM, Rhyan JC, Anderson ML, Gershwin LJ, Agnew DW, et al. Uterine mast cells and immunoglobulin-e antibody responses during clearance of tritrichomonas foetus. *Vet Pathol* (2005) 42(3):282–90. doi: 10.1354/vp.42-3-282

81. Anderson ML, BonDurant RH, Corbeil RR, Corbeil LB. Immune and inflammatory responses to reproductive tract infection with tritrichomonas foetus in immunized and control heifers. *J Parasitol* (1996) 82(4):594–600. doi: 10.2307/3283783

82. Oliveira LJ, Mansourri-Attia N, Fahey AG, Browne J, Forde N, Roche JF, et al. Correction: characterization of the Th profile of the bovine endometrium during the oestrous cycle and early pregnancy. *PloS One* (2014) 9(1). doi: 10.1371/annotation/93d63399-0e71-4a25-a45c-311910ee6da5

83. Oliveira LJ, Mansourri-Attia N, Fahey AG, Browne J, Forde N, Roche JF, et al. Characterization of the Th profile of the bovine endometrium during the oestrous cycle and early pregnancy. *PloS One* (2013) 8(10):e75571. doi: 10.1371/journal.pone.0075571

84. Bertasoli B, Santos dos A, Paula R, Barbosa A, SIlva G, Jorge E, et al. Swine placenta and placentation. *Brazillian J Biol Sci* (2015) 2(4):199–207.

85. Bannunah AM, Vllasaliu D, Lord J, Stolnik S. Mechanisms of nanoparticle internalization and transport across an intestinal epithelial cell model: effect of size and surface charge. *Mol Pharmaceutics* (2014) 11(12):4363–73. doi: 10.1021/mp500439c

86. Leroy F, Van Hoeck J, Bogaert C. Hormonal control of pinocytosis in the uterine epithelium of the rat. *J Reprod Fertility* (1976) 47:59–62. doi: 10.1530/jrf.0.0470059

87. Li Z, Palaniyandi S, Zeng R, Tuo W, Roopenian DC, Zhu X, et al. Transfer of IgG in the female genital tract by MHC class I-related neonatal fc receptor (FcRn) confers protective immunity to vaginal infection. *Proc Natl Acad Sci United States America* (2011) 108(11):4388–93. doi: 10.1073/pnas.1012861108

88. Richardson J, Kaushic C, Wira C. Polymeric immunoglobulin (Ig) receptor production and IgA transcytosis in polarized primary cultures of mature rat uterine epithelial cells. *Biol Reprod* (1995) 53:488–98. doi: 10.1095/biolreprod53.3.488

89. Dickinson BL, Badizadegan K, Wu Z, Ahouse JC, Zhu X, Simister NE, et al. Bidirectional FcRn-dependent IgG transport in a polarized human intestinal epithelial cell line. *J Clin Invest* (1999) 104(7):903–11. doi: 10.1172/JCI6968

90. Rodewald R, Kraehenbuhl JP. Receptor-mediated transport of IgG. *J Cell Biol* (1984) 99(1 Pt 2):159s–64s. doi: 10.1083/jcb.99.1.159s

Frontiers in Immunology

Explores novel approaches and diagnoses to treat immune disorders.

The official journal of the International Union of Immunological Societies (IUIS) and the most cited in its field, leading the way for research across basic, translational and clinical immunology.

Discover the latest Research Topics

See more →

Frontiers

Avenue du Tribunal-Fédéral 34
1005 Lausanne, Switzerland
frontiersin.org

Contact us

+41 (0)21 510 17 00
frontiersin.org/about/contact